Molecular Cloning, Characterisation And Functional Expression Of Cyclic Nucleotide-Gated Ion Channel Genes Expressed In Sino-Atrial Node Region of Heart

Thesis submitted for the degree of
Doctor of Philosophy
at the
University of Leicester

by

Sukhinder Paul Singh Hundal BSc. (Hons.)

Department of Biochemistry
University of Leicester

September 1994

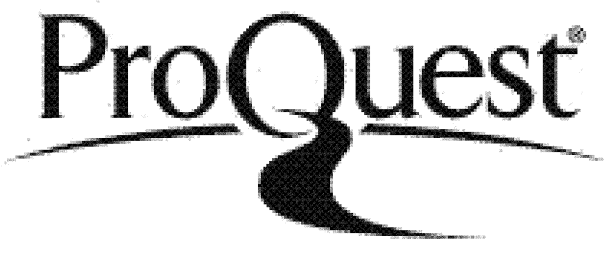

ProQuest LLC
789 East Eisenhower Parkway
P.O. Box 1346
Ann Arbor, MI 48106-1346

Abstract

Pacemaker cells of the mammalian sino-atrial node (SAN) contain a hyperpolarization-activated, non-specific cationic current, I_f which is an important component involved in the initiation and neurotransmitter-mediated control of cardiac rhythm. cAMP can directly modulate I_f by a mechanism independent of phosphorylation, demonstrating that cyclic nucleotide-sensitive ion channel genes are expressed within cardiac pacemaker cells.

Through a combination of library screening methods based on cross-hybridising cyclic nucleotide-gated channel probes and a PCR 'fingerprint' employing primers designed to sequences encoding an ion channel cyclic nucleotide-binding domain, partial cDNA clones were isolated from a prepared sino-atrial node regional-specific cDNA library, which were either homologues of previously identified ion channels shown to be expressed in sensory tissues or putative new channel clones. Isolate rscNGC 1 following retrieval of a full coding region by anchor-PCR, demonstrated 90.4% sequence identity to the α-subunit of the rod photoreceptor cGMP-gated channel. The PCR 'fingerprint' identified a SAN homologue of the olfactory neuron cAMP-gated channel within library aliquots. This was the first demonstration that two distinct cyclic nucleotide-gated ion channel genes were expressed in SAN region of heart. Heterologous expression of rscNGC 1 following micro-injection of capped cRNA in *Xenopus* oocytes, gave rise to cGMP-stimulated channel activity exhibiting electrophysiological properties similar to the characterised α-subunit of the rod photoreceptor cGMP-gated channel.

A reconstituted second messenger-pathway mediating endogenous receptor coupling to heterologously expressed cAMP-gated ion channels — shown to be present within native nodal tissue — was attempted within MEL cells. However, the absence of endogenous receptors positively-coupled to adenylyl cyclase within MEL cells, and the inability to functional characterise cAMP-stimulated cationic conductances via electrophysiological methods, prevented such studies. Thus demonstrating the inappropriateness of the MEL cell, as a heterologous system for studying receptor-mediated second messenger coupling to cNG channels.

Although cyclic nucleotide-gated ion channels are *obligatorily* coupled to intracellular signalling agonists commonly found in heart. they have yet to be described in functional terms within SAN or any other cardiac subregion. It is postulated that they may have a role in vasculature — underlying mechanisms of smooth muscle relaxation.

Acknowledgements

I would like to take this opportunity to thank the many people I have worked with over the course of my studies, especially the old ICI Joint Lab for their support and overall contribution to the 'madness' that once was.

I am very grateful to Matt Owen (Dept. of Physiology, University of Leeds) and Dr. John Quayle (Dept. of Physiology, University of Leicester) for their electrophysiological support.

I would like to thank Prof. W.J. Brammar for his guidance and for giving me the opportunity to study for a Ph.D.

A very special thankyou goes to Dr. Ed Conley for his immeasurable support, supervision and encouragement throughout the course of my post-graduate training — crass puns and all!

Abbreviations

ATP	Adenosine 5'-triphosphate
BSA	Bovine serum albumin
cAMP	Adenosine 3',5'-cyclic monophosphate
cDNA	Complementary DNA
cGMP	Guanosine 3',5'-cyclic monophosphate
cRNA	Complementary RNA
dATP	Deoxyadenosine 5'-triphosphate
dCTP	Deoxycytidine 5'-triphosphate
dGTP	Deoxyguanosine 5'-triphosphate
dTTP	Deoxythymidine 5'-triphosphate
DEPC	Diethyl pyrocarbonate
DNA	Deoxyribonucleic acid
DNase	Deoxyribonuclease I
DTT	Dithiothreitol
EDTA	Ethylenediaminetetraacetic acid
IAA	Isoamyl alcohol
IPTG	Isopropyl-β-D-thiogalactopyranoside
mRNA	Ribonucleic acid
PCR	Polymerase chain reaction
PEG	Polyethylene glycol
pfu	Plaque forming unit
RNA	Ribonucleic acid
RNase	Ribonuclease
RT-PCR	Reverse transcription-polymerase chain reaction
rUTP	Ribouridine 5'-triphosphate
SDS	Sodium dodecyl sulphate
SSC	Standard sodium citrate
UV	Ultra violet
v/v	volume/volume
X-gal	5 Bromo-4-chloro-3-indolyl-β-D-galactoside

Molecular Cloning, Characterisation And Functional Expression Of Cyclic Nucleotide-Gated Ion Channel Genes Expressed In Sino-Atrial Node Region of Heart

Accumulated Contents

Chapter 1

General Introduction

Chapter 2

Materials and Methods

2.1 Materials

2.2 Methods of sterilisation

2.3 Nucleic Acid Methods

Chapter 3

Isolation of a partial cDNA homologue of the retinal rod photoreceptor cyclic nucleotide-gated channel from a rabbit sino-atrial node specific cDNA library

Chapter 5

Searching for novel cyclic nucleotide-gated ion channel genes in the sino-atrial node

Chapter 1

General Introduction

Preface: Characterisation of pacemaker cyclic nucleotide-*sensitive* ion channels

The central objective of the work described within this thesis was the cloning and functional expression of ion channel molecules *sensitive* to intracellular fluxes of cyclic nucleotides, expressed in mammalian sino-atrial node tissue — the primary pacemaking region of the heart. This followed the demonstration that the cardiac channel underlying the 'pacemaker' current I_f was *directly* modulated by intracellular cAMP. These classes of molecules, form electrically-conductive pores whose gating i.e opening or closing — controlling the passive flow of ions across biological membranes, is directly regulated by the second messengers cAMP and cGMP. As such cyclic nucleotide-sensitive channels are *obligatorily* dependent upon a receptor-second messenger system for their activation. A further goal of this thesis was the study of receptor-ion channel coupling — mediated through diffusible cyclic nucleotide second messengers, within a heterologous system.

Part 1 The cyclic nucleotide-sensitive ion channel underlying the pacemaker current I_f

1.1 The importance of 'spontaneous' electrical activity in heart

Recordings of electrical activities in the sino-atrial node (SAN) demonstrates the voltage range and time course of the pacemaker potential (Figure 1.1). Pacemaker cells have electrical properties that are distinct from working i.e atrial and ventricular myocardial cells, as they display 'a spontaneous diastolic depolarisation' which initiates excitation of the heart [Irisawa and Hagiwara, 1991]. (The net influx of positive ions into a cell results in the intracellular potential becoming more positive, this is termed depolarisation, conversely, a net efflux of positive charges causes hyperpolarisation). During this phase the membrane voltage is driven from the maximum level of hyperpolarisation reached at the termination of an action potential, up to threshold triggering a faster

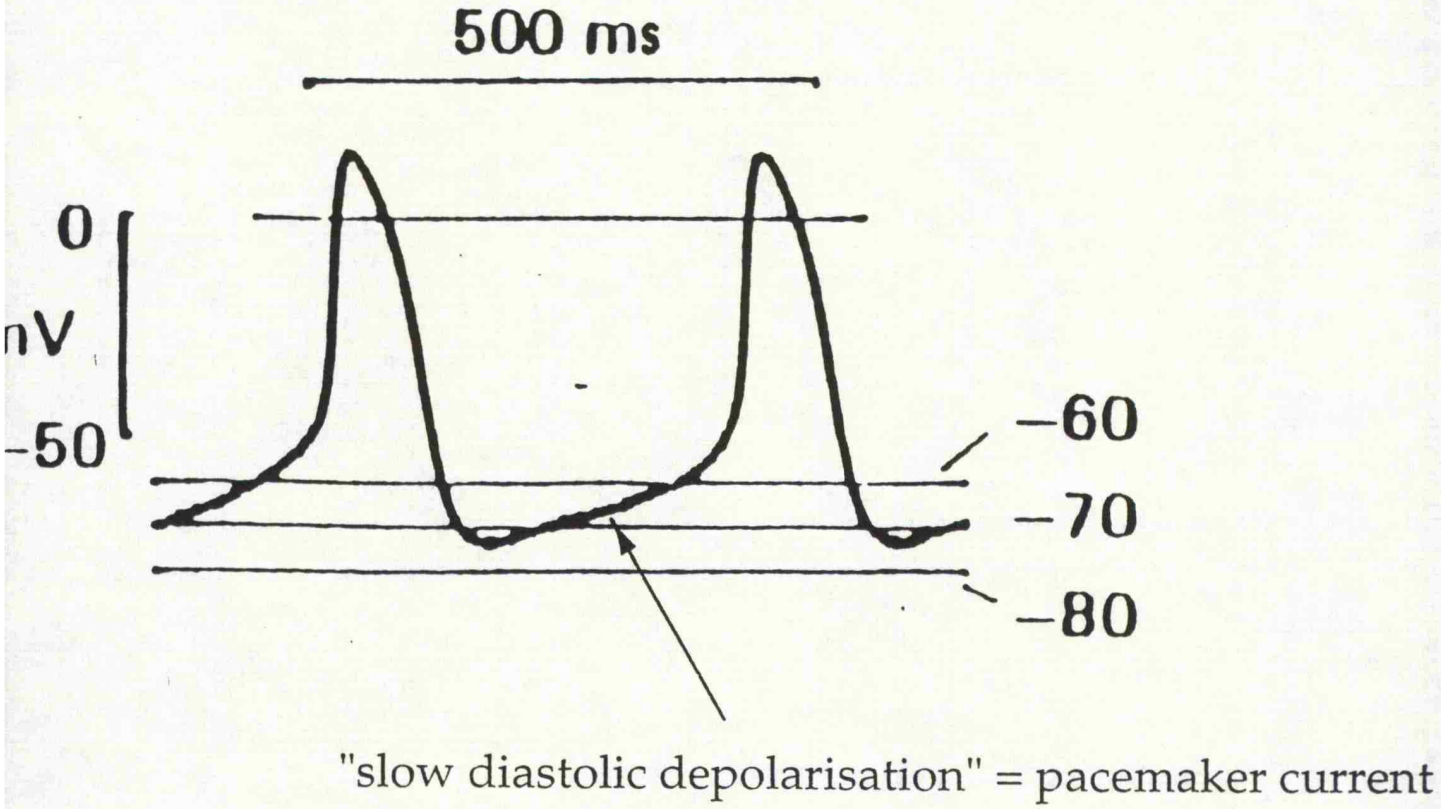

Figure 1.1 Recording of spontaneous activity in a typical mammalian sino-atrial node cell.

The spontaneous slow diastolic depolarisation (also referred to as the pacemaker potential) is indicated between -71 to -51 mV.
[From DiFrancesco, 1990].

systolic depolarisation, which is conducted to the surrounding atrial fibres through interconnecting gap junctions. Following the peak of the action potential, the membrane potential repolarises and the gradual depolarisation begins again [reviewed by Campbell *et al.*, 1992]. Hence pacemaker cells have been described to act as 'natural oscillators' [Rosen *et al.*, 1990], cycling between the different phases of depolarisation and repolarisation, and it is the slow diastolic depolarisation or pacemaker potential which provide these cells with the capacity for spontaneous rhythmic self-excitation.

1.2 Use of classical biophysical methods to study the ionic currents underlying spontaneous pacemaker activity at the single cell level

The extreme sensitivity of the patch clamp technique [Hamill *et al.*, 1981] and reviewed in Figure 1.2, has demonstrated that a hyperpolarisation-activated current termed I_f, may be involved in the initiation of the diastolic depolarisation phase and therefore allowing mammalian pacemaker cells to beat spontaneously. However, there still remains considerable controversy over I_f's overall contribution to the initiation of the pacemaker potential in mammalian cells [reviewed by Rasmusson *et al.*, 1990]. The present view is that SAN pacemaking is caused by the interaction of several currents, with no one current being exclusively responsible [Irisawa *et al.*, 1993].

1.2.1 *Characteristics of I_f*

I_f can be described as a non-specific, mixed cationic current carried by both Na^+ and K^+ ions under physiological conditions, which is activated upon hyperpolarisation [DiFrancesco, 1986(a)]. It is the only inward time-dependent component activated at voltages in the diastolic depolarisation range [DiFrancesco, 1991]. At the termination of an action potential, the membrane voltage becomes more negative than -40/-50mV and I_f will begin to activate. As I_f is inward at these voltages, its activation will promote a slow depolarising process that will last until threshold when a subsequent action potential is generated, at which stage I_f becomes inactivated.

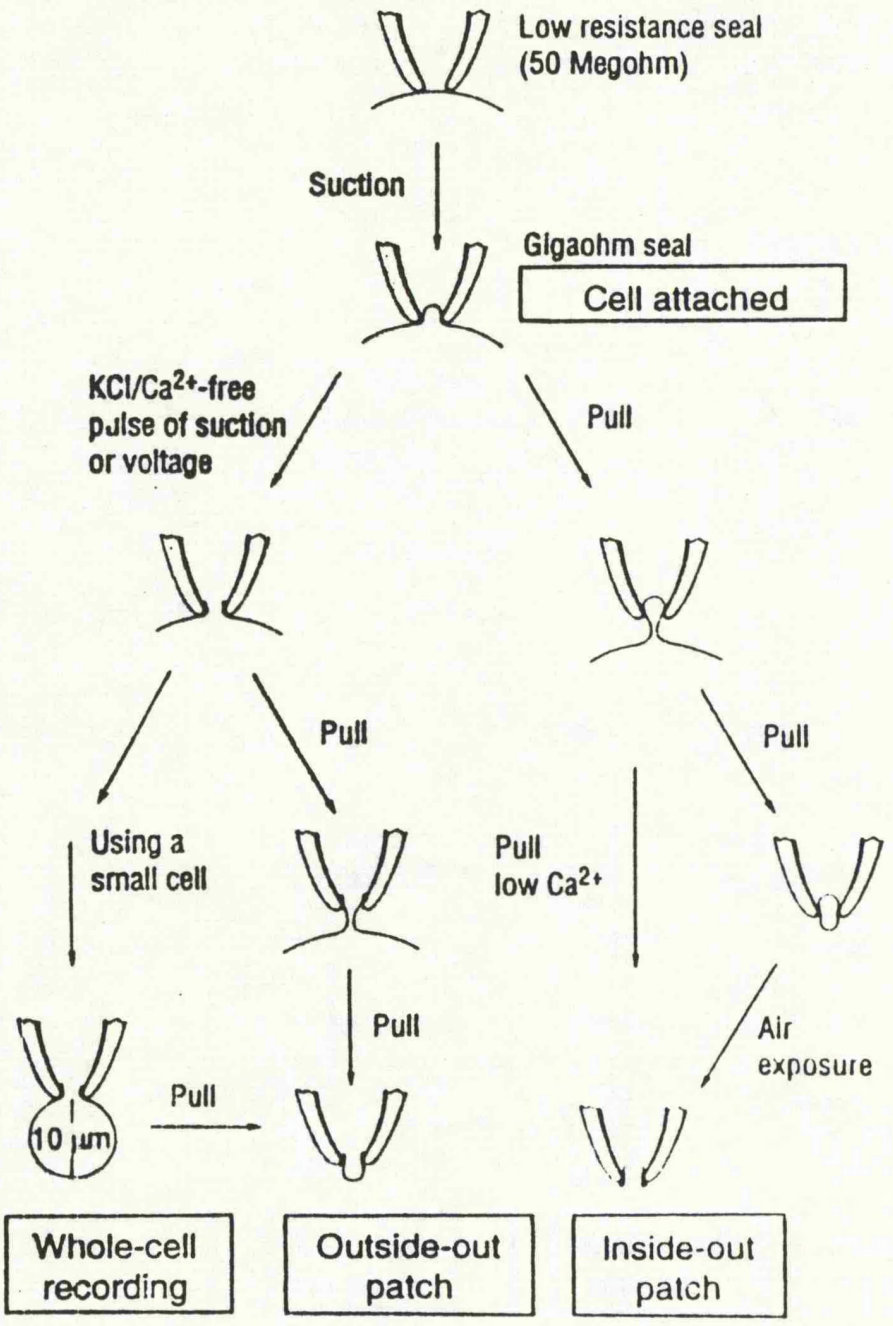

Figure 1.2 Schematic representation of the procedures that lead to the different patch-clamp configurations.

A 'gigohm' seal can be formed around a small patch of a cellular membrane containing an ion channel. A patch can be removed from cells by simply withdrawing the pipette, resulting in "excised patches", which are accessible for solution changes from both sides. Alternatively, a patch can be ruptured by a short pulse of suction or voltage, establishing an electrical connection between the measuring pipette and cell. This configuration is termed a "whole-cell recording".
[From Hamill *et al.*, 1984]

1.3 I_f is *directly* modulated by intracellular cAMP

cAMP was shown to activate I_f by a mechanism independent of phosphorylation, involving a *direct* interaction with the channels at their cytoplasmic side [DiFrancesco and Tortora, 1991]. I_f was recorded in cell-free inside-out macropatches excised from the membrane of isolated rabbit SAN myocytes. Under these conditions, perfusion with 100 μM cAMP resulted in I_f activation. This was not a result of phosphorylation by endogenous protein kinases because it could be reproduced both after removal of ATP and Mg^{2+} from the intracellular solution, and after the addition of a non-specific protein kinase inhibitor or of a specific protein kinase A inhibitor. The cAMP concentrations involved in the modulation of I_f gating were well within the range controlled under physiological conditions by adenylate cyclase i.e 0.2-5 μM in cardiac tissue [Teresaki and Brooker, 1977].

I_f channels are voltage-gated channels, in that a hyperpolarised membrane potential is required to gate the channels from closed to open, and that the direct binding of cAMP simply *modulates* the effect of membrane potential. In all cases, the *frequency* of channel openings is changed, whereas both the channel's unitary conductance and time of individual openings remain unchanged.

1.4 I_f is a key current involved in the regulation of pacemaker activity under *working concentrations* of neurotransmitters

Heart rate is increased by β-adrenergic effects of the transmitter noradrenaline and decreased by muscarinic cholinergic effects of the transmitter acetylcholine (ACh), released from cardiac sympathetic and vagus nerves respectively [Hutter and Trautwein, 1956]. This neural control of heart beat alters the *rate* of the diastolic depolarisation and simultaneously maintains both action potential upstroke and duration, so maintaining conditions for reliable propagation to adjacent atrial tissue.

Sympathetic control of working myocardial cells by beta-agonists which raise intracellular cAMP are known to increase both a L-type voltage-gated

calcium current $I_{Ca,L}$ and a delayed-rectifier potassium current I_k [Walsh *et al.*, 1988], while in SAN cells I_f is increased by isoproterenol [DiFrancesco, 1986(b)]. Parasympathetic control mediated through muscarinic cholinergic receptors has three reported effects on isolated SAN cells; (i) the activation of an inwardly-rectifying potassium current, $I_{k,ACh}$ [Sakmann *et al.*, 1983], (ii) reduction of $I_{Ca,L}$ [Brown and Denyer, 1988] and (iii) reduction of I_f [DiFrancesco and Tromba, 1988(a)]. Slowing of spontaneous activity of SAN pacemaker cells by acetylcholine was principally thought to arise as a consequence of acetylcholine-induced augmentation of K^+ permeability [Trautwein, 1981], and of a depression of the Ca^+ permeability [Shibat *et al.*, 1985; Egan and Noble, 1987]. However, DiFrancesco (1989), demonstrated that I_f represented the key mechanism by which physiological concentrations (up to 0.01 μM) of sympathetic and parasympathetic stimuli regulate via the diastolic depolarisation rate, the pacing frequency of SAN cells and thus heart rate.

1.5 Significance of direct activation of I_f by cAMP

Heterotrimeric guanine nucleotide-binding G proteins couple membrane autonomic neurotransmitter receptors to ionic channels. Briefly, G proteins are activated physiologically, when hormone-occupied receptors interact with the trimeric G protein and stimulate the exchange of bound GDP on the α-subunit for GTP. Upon binding GTP, the (α-GTP) subunit dissociates from the βγ subunits, whereupon the subunits activate multiple effector molecules i.e adenylate cyclase or ion channels. The activation of the α-subunit is terminated by GTP hydrolysis catalysed by the α-subunit and subsequent reassociation with the βγ subunits [for review see Gilman, 1987]. G proteins can couple receptors to ion channels by both: (i) membrane-delimited direct pathways, and (ii) cytoplasmic second messenger pathways (Figure 1.3).

1.5.1 Molecular mechanism of I_f regulation

Through different sets of receptors, adrenergic and cholinergic neurotransmitters act on the same membrane system adenylate cyclase to affect the intracellular cAMP concentration, the second messenger involved in I_f modulation. The mechanism underlying the control of

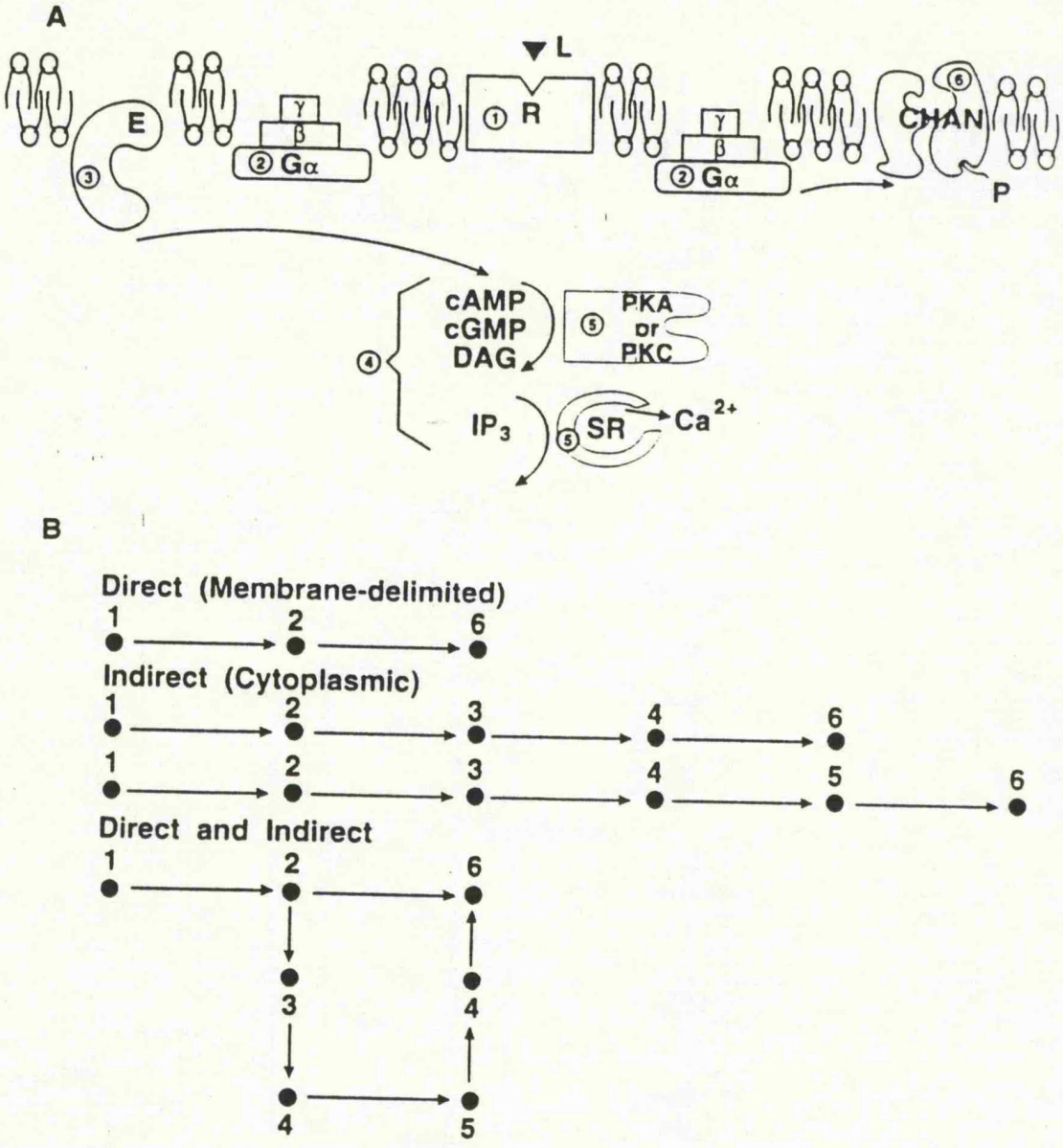

Figure 1.3 Molecular components involved in direct and indirect receptor-G protein-ionic channel pathways (a), and examples of three, five, six and seven component pathways (b).

1 = receptor (R); 2 = heterotrimeric (α,β,γ) guanine nucleotide-binding (G) protein; 3 and 4 = effectors such as adenylyl cyclase, cGMP phosphodiesterase, phospholipase C, and phospholipase A_2 and their second messenger products such as cAMP, cGMP, diacylglycerol (DAG) and inositol 1,4,5-triphosphate (IP_3); 5 = protein kinase A (PKA), or protein kinase C (PKC), or sarcoplasmic reticulum (SR); 6 = Membrane ion channel (Chan).
[From Brown, 1991]

intracellular cAMP concentrations are well characterised not only in SAN cells but in other cellular systems as well. β-adrenergic receptor stimulation increases cAMP synthesis by stimulating the catalytic activity of adenylate cyclase, which catalyses the synthesis of cAMP via Gs (stimulatory) species of G protein, whereas inhibition of adenylate cyclase by muscarinic ACh receptors involves the G_i (inhibitory) species of G protein. Thus β-agonists increase the cAMP level within the cell whereas ACh decreases cAMP levels. Unlike cardiac Ca^+ and K^+ channels which are modulated via cAMP through channel phosphorylation involving the activation of cAMP-dependent protein kinases [Osterieder *et al.*, 1982; Walsh and Kass, 1988], cAMP activates I_f by a mechanism *independent of phosphorylation*. The presence of this *direct* control of I_f channel gating provides a mechanism for *rapid* control of electrical signalling in response to changes in intracellular second messengers (Figure 1.4).

1.5.2 *Direct regulation of I_f by G proteins*

It has been suggested that muscarinic and β-adrenergic receptors are coupled directly to I_f by G proteins in a membrane-delimited manner [reviewed by Brown, 1991]. G proteins isolated from erythrocytes and preactivated with guanosine 5'-0-(3-thiotriphosphate), GTPγS, a poorly-hydrolysed GTP analogue, were shown to stimulate I_f currents from excised inside-out (I-O) membrane patches excised from SAN cells [Yatani *et al.*, 1990]. As noted by Hartzell (1988), one problem with these and other such studies was that native heart G proteins were not used, instead G proteins isolated from other species and tissues particularly human erythrocytes, were employed within the I-O membrane patch experiments. Conclusive evidence of such direct G protein-ion channel interaction will require co-reconstitution of both cloned G protein subunits and I_f ion channels in a defined lipid membrane. However, several observations rule in favour of a direct cAMP dependent mechanism being the main process by which neurotransmitters modulate I_f. For example, I_f can be controlled by procedures that alter the intracellular cAMP levels independently of the interaction with membrane receptors, such as direct stimulation of adenylate cyclase or inhibition of phosphodiesterases [DiFrancesco and Tromba, 1988(b)].

The pacemaker ion channel If is a voltage-gated channel whose gating is directly modulated by cAMP

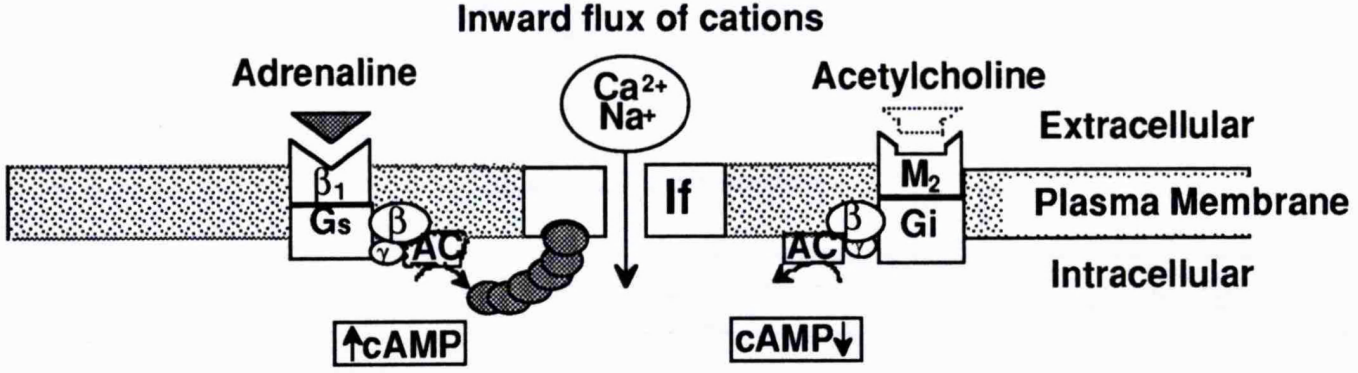

Fast (~ms) ± regulation

The direct interaction of cAMP with If provides a mechanism for rapid electrical signalling in response to small changes in the concentration of intracellular second messengers

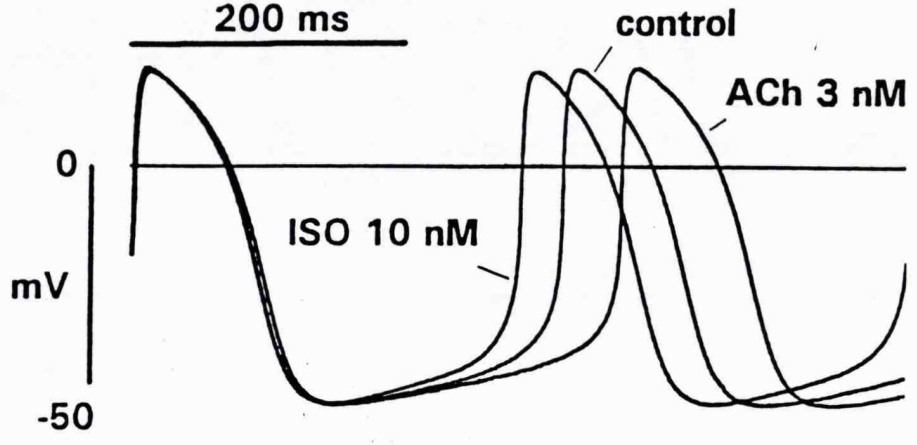

Figure 1.4 Beat-to-beat control of heart-rate in the cardiac pacemaker cell.

At physiological concentrations of neurotransmitters, I_f represents a key mechanism by which adrenaline (represented here by the β-adrenergic agonist, isoproterenol (ISO)) and acetylcholine (ACh) accelerate or slow respectively via the diastolic depolarisation rate, the pacing frequency of sino-atrial node cells and thus the heart rate.
This neurotransmitter regulation occurs via receptor (β_1, M_2)-G protein (Gs, Gi, βγ) coupled allosteric modulation of adenylyl cyclase (AC) — resulting in changes in the intracellular concentration of the second messenger cAMP, which is able to *directly* modulate I_f gating.

Part 2 Classes of Ion Channels

2.1 Ion channels can be classified into several superfamilies

Recent molecular genetic techniques have shown that ion channels can be divided into five distinct superfamilies; i) voltage/second messenger-gated channels, ii) inward-rectifier K^+ channels, iii) ligand-gated channels, iv) internal Ca^{2+} release channels, and v) ABC (ATP-binding cassette) transporters, which include the CFTR (cystic fibrosis transmembrane regulator) Cl^- channel and the multidrug resistance P-glycoprotein [Ranganathan, 1994].

2.1.1 *Classification of I_f*

Electrophysiological properties suggest that I_f channels do not easily fit into any of these families. Like the inward-rectifier class of ion channels, I_f channels open at negative potentials, close at positive potentials, and are blocked by Cs^+ and Rb^+ ions [DiFrancesco 1986(b)]. Like members of the cyclic nucleotide-gated ion channel family, they are non-selective for cations i.e permeable to Na^+, K^+ and Ca^{2+} ions, have a reversal potential near -20 mV and are directly regulated by cyclic nucleotides [DiFrancesco and Tortora, 1991]. Finally, in accordance with voltage-gated Na^+, Ca^{2+} and delayed rectifier K^+ channel families, I_f channels exhibit steeply voltage-dependent gating [DiFrancesco 1986(b)].

However the direct modulation of the voltage-dependence of I_f in SAN myocytes by cyclic nucleotides means that in purely 'regulatory' terms, I_f can be described as a cyclic nucleotide-*sensitive* channel.

2.2 The family of cyclic nucleotide-sensitive channels

The family of second messenger-sensitive channels are functionally heterogenous with respect to the control of channel activity by cAMP and cGMP. This family can be divided into those channels which *obligatorily*

require intracellular cyclic nucleotides to open, and those channels, such as I_f, which are modulated by cyclic nucleotides, i.e the ligand is not *mandatory* for channel opening.

2.2.1 *Cyclic nucleotide-gated (cNG) ion channels*

cNG channels have been well-characterised in vertebrate sensory cells, where they mediate *fast* responses to sensory stimuli. These channels, which include the cGMP-gated channel of rod photoreceptor [Kaupp *et al.*, 1989] and cone photoreceptor cells [Bönigk *et al.*, 1993], and the cAMP-gated channel of olfactory neurons [Dhallan *et al.*, 1990] are involved in mammalian visual and olfactory responses, respectively. cNG channels act as molecular switches that rapidly and cooperatively respond to small changes in the concentration of the respective cyclic nucleotide [Kaupp, 1991].

Recently, several further members of the cNG channel family have been cloned from various 'non-sensory' cells. A rabbit aorta cDNA clone, encoding a polypeptide highly homologous to that expressed in olfactory neurons has been isolated [Biel *et al.*, 1993], indicating that these cDNAs are derived from the same gene. cDNA clones whose coding regions are virtually identical to that of the cloned photoreceptor cNG channels have also been obtained from kidney [Ahmad *et al.*, 1992] and retinal ganglion cells [Ahmad *et al.*, 1994], suggesting that genes previously thought to be specific for photoreceptors or olfactory neurons are also expressed in such 'non-sensory' tissues. Identical cDNAs representing transcript products from a new cNG channel gene, have also been obtained from bovine testis [Weyand *et al.*, 1994] and kidney [Biel *et al.*, 1994]. Interestingly, Northern analysis and sequences amplified by the PCR demonstrated that this gene was also expressed in cardiac atrial and ventricular tissue [Biel *et al.*, 1994].

The physiological importance and specific cellular localisation of these 'non-sensory' cNG channels remain to be established. This family of cNG channels seems likely to expand further with future work as there is also considerable electrophysiological evidence for the existance of cNG channels in the pineal gland [Dryer and Henderson, 1991], retinal bipolar cells [Nawy and Jahr, 1990] and in the membrane of inner and outer hair

cells of the mammalian cochlear [Kolesnikov *et al.*, 1991]. The molecular identities of these channels have not been determined.

2.2.2 *Cyclic nucleotide-modulated channels*

It is likely that these channels belong to other generic families. It is noteworthy that the cloned non-mammalian potassium selective channels, *Drosophila ether-à-go-go* [Warmke *et al.*, 1991] and *Arabidopsis thaliana* AKT1 [Sentenac *et al.*, 1992], show considerable amino acid similarity to the above family of cNG channels (discussed below). The inner medullary collecting duct contains a cation channel whose open probability is reduced by cGMP, with part of the effect arising from a direct interaction between cGMP and the channel [Light *et al.*, 1990]. Whether this channel bears a relation to the cloned kidney cNG channel is not known. It is also yet to be determined whether the cAMP-activated potassium channel persistently activated in the *Drosophila dunce* mutant [Delgado *et al.*, 1991] also shares sequence homology to the cNG channel family.

A summary of the biological roles and electrophysiological characteristics of these cyclic nucleotide-sensitive channels is given in Table 1.1. For the reason that the sensory cNG channels represent the best characterised members of cyclic nucleotide-sensitive channels, the remaining part of this introduction will focus on their cloned cDNAs. I will concentrate on structural and functional features important for understanding the biological role of cNG channels, as key effector molecules in signal transduction pathways. cNG family members represent ideal probes in the cloning and identification of further cyclic nucleotide-sensitive channels, such as the molecular species giving rise to the pacemaker current I_f.

Table 1.1. Examples of Characterised Cyclic Nucleotide-Sensitive Channels.

References are given in the text.
[N.B $K_{1/2}$ refers to concentration of cyclic nucleotide resulting in half-maximal channel activation].

Source/Location of Cyclic Nucleotide-Sensitive Channel	Biological Function	Gating of Channel	Cyclic Nucleotide Specificity	Effect of Cyclic Nucleotide Binding	Ion Selectivity of Channel
Retinal rod photoreceptor cells	Phototransduction. Channel generates the light-evoked hyperpolarisation of retinal rods, lowering the rate of transmitter release from synaptic termini.	Directly and cooperatively gated by cGMP, shows no obvious voltage dependence under saturating cGMP concentrations.	$K_{1/2}$ cGMP~50 μM. cAMP insensitive.	Channel activation.	Cation non-selective.
Retinal cone photoreceptor cells	Phototransduction.	Directly gated by cGMP.	$K_{1/2}$ cGMP~75 μM. cAMP insensitive.	Channel activation.	Cation non-selective.
Olfactory sensory neurons	Olfactory signal transduction. Receptor binding of odourant molecules causes G protein-linked generation of cAMP resulting in channel activation leading to membrane depolarisation.	Directly gated by cyclic nucleotides.	$K_{1/2}$ cGMP~4 μM. $K_{1/2}$ cAMP~20 μM.	Channel activation.	Cation non-selective.
Aorta	The physiological importance of the channel is unclear.	Directly gated by cyclic nucleotides.	$K_{1/2}$ cGMP~2 μM. $K_{1/2}$ cAMP~60 μM.	Channel activation.	Cation non-selective.
Testis	The physiological importance of the channel is unclear, speculation of an involvment in the cGMP-signalling pathway that controls chemotaxis of vertebrate sperm.	Directly gated by cyclic nucleotides.	$K_{1/2}$ cGMP~8.3 μM. $K_{1/2}$ cAMP~1.5 mM.	Channel activation.	Cation non-selective.
Pineal gland	Phototransduction, light induces inhibition of melatonin secreation.	Directly gated by cGMP.	$K_{1/2}$ cGMP~10-50μM. cAMP insensitive.	Channel activation.	Cation non-selective.
Bipolar retinal cells	The neurotransmitter glutamate, by suppressing a cGMP-activated conductance induces membrane hyperpolarisation.	Directly gated by cGMP.	$K_{1/2}$ cGMP~20-60μM. cAMP insensitive.	Channel activation.	Cation non-selective.

Retinal ganglion cells	Nitric oxide released from amacrine cells activates a cGMP-gated cation conductance through the generation of cGMP via a soluble guanylate cyclase, to modulate ganglion cell activity.	Directly gated by cGMP.	Highly selective for cGMP over cAMP.	Channel activation.	Cation non-selective.
***Drosophila* larval muscle *dunce* mutant**	The physiological importance of the channel is unclear, but evidence indicates that it may contribute to the resting potential. The channel is found in the *Drosophila* mutant *dunce*, which is a single gene mutant showing poor levels of associative learning and rapid short-term memory loss. The mutant *dunce* lacks a form of phosphodiesterase leading to abnormally high intracellular cAMP levels.	Activated directly and reversibly by cAMP.	$K_{1/2}$ cAMP~50μM. cGMP did not activate the channel at micromolar concentrations.	Channel activation.	Potassium selective.
***Drosophila* larval muscle *ether à go-go (eag)* mutant**	The physiological importance of the channel is unclear, but the *eag* locus encodes a subunit that is common to all potassium channels resulting in altered potassium currents in excitable tissue. The mutants exhibit spontaneous, repetitive firing of action potentials in the motor axons of larval neuromuscular junction.	Voltage-gated ion channel that is directly modulated by cAMP.	2 mM cAMP, but not cGMP produces a significant increase in outward-current.	cAMP modulates the voltage-dependence of the *eag* current.	Permeable to both potassium and calcium ions.
***Arabidopsis* thaliana (AKT1)**	The physiological importance of the channel is unclear, however they are believed to be required for growth, osmoregulation, cell movement.	Strong voltage-dependence of gating.	Not determined.	Not determined.	Potassium selective.
M1 mouse cortical collecting duct cells.	The physiological importance of the channel is unclear. Biological role possibly in the initiation of diuresis and natriuresis.	Strong voltage-dependence of gating.	Highly selective for cGMP over cAMP.	Cytoplasmic application of 0.1mM cGMP *decreases* channel open probability by 27%.	Non-cation selective.
Mammalian sino-atrial node myocytes	The channel gives rise to an inward cationic current I_f on hyperpolarisation, which contributes to a slow diastolic depolarisation responsible for the initiation of a subsequent action potential.	Strong voltage-dependence of gating.	$K_{1/2}$ cAMP~0.2 μM. $K_{1/2}$ cGMP~8 μM.	cAMP directly modulates the channel.	Cation non-selective.
Mammalian cochlear hair cells	The physiological importance of the channel is unclear, but it rises the possibility that mechanotransduction might be mediated by cyclic-nucleotides.	Directly gated by cAMP.	Channel is only activated by cAMP.	Channel activation.	Cation non-selective.

Part 3 The family of cyclic nucleotide-gated channels

3.1 Structural features of cyclic nucleotide-gated channels

The rod photoreceptor and olfactory channel polypeptides are highly homologous. Both channels have been cloned and characterised and have open reading frames of 670-690 amino acids, encoding proteins of molecular weight 76-79 kDa. About 60% of the aligned sequences in the two polypeptides from bovine tissues, are occupied by identical amino acid residues, and an additional 14% are occupied by conserved residues. Their homologous amino acid sequences and similarity in function on expression suggest that cyclic nucleotide-gated channels belong to a family that are closely related, both genetically and structurally [Kaupp, 1991].

3.1.1 cNG channels belong to a large superfamily of voltage/second messenger-gated channels

Functionally, cNG channels belong to the class of ligand-gated ion channels because of their direct opening by a cyclic nucleotide ligand to a specific receptor site. A comparison of hydropathicity profiles of amino acid sequences of several polypeptides that form ligand-gated and voltage-gated channels are shown in Figure 1.5. As can be seen from these hydropathicity plots, the cyclic nucleotide-gated channels share no significant similarity to ligand-gated channels such as the nicotinic acetylcholine (nACh) receptor, instead they share sequence motifs with, and have been proposed to be a member of the same family that includes voltage-gated sodium, calcium and potassium channels [Jan and Jan, 1990].

Sequence similarity is generally taken as evidence of evolutionary homology. The cloning of membrane polypeptides AKT1 [Sentenac *et al.*, 1992] and *eag* [Warmke *et al.*, 1991] from *Arabidopsis thaliana* and *Drosophila*, which contain highly conserved S4 and pore-lining regions typical of the *Drosophila Shaker* family of voltage-gated potassium channels (see below), and cyclic nucleotide-binding domains highly homologous to cNG channels, supports a hypothesis of an ancient

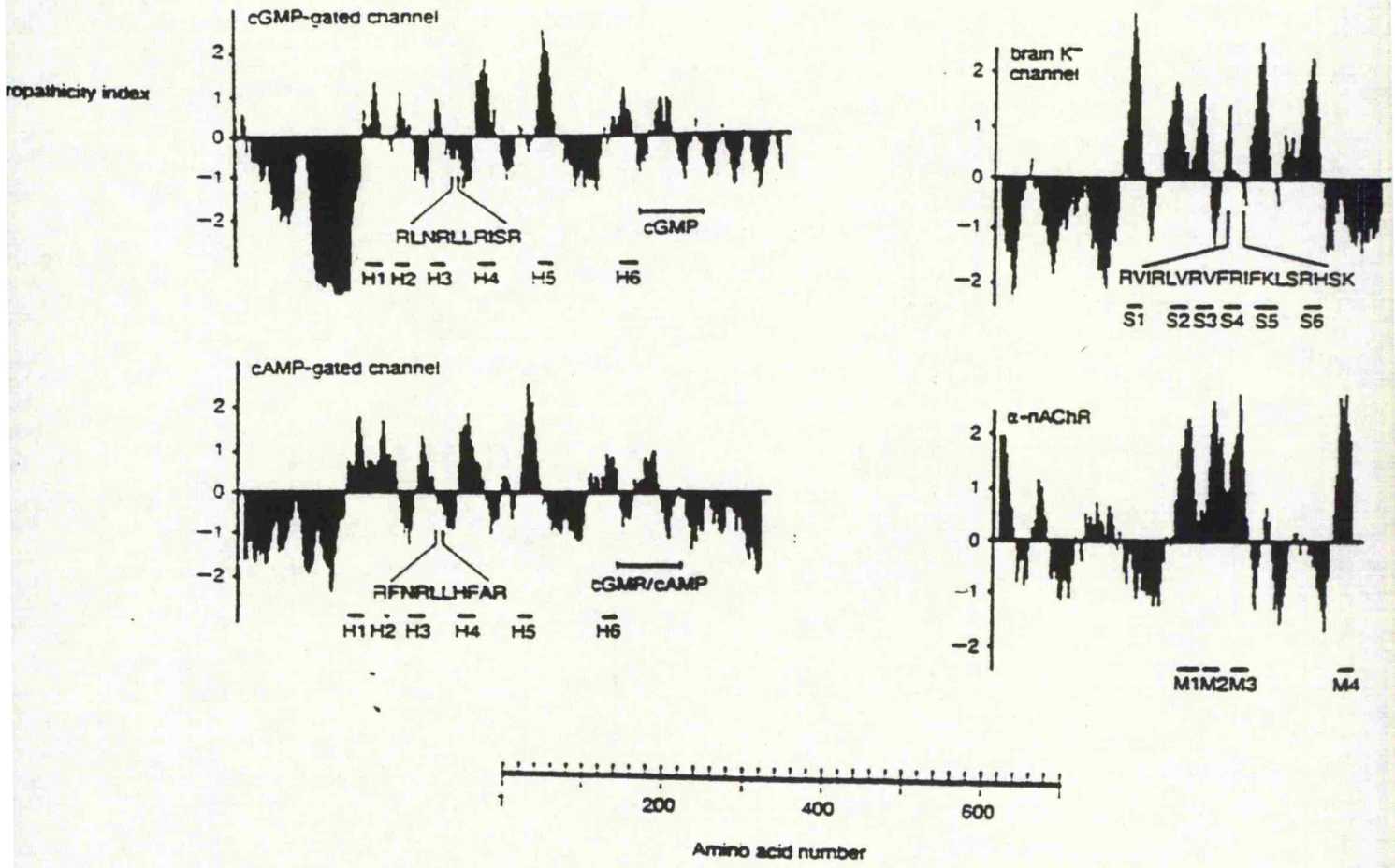

Figure 1.5 Hydropathicity plot of the amino acid sequence of several polypeptides that form ligand-gated and voltage-gated channels.

The averaged hydropathicity index of a nonadecapeptide composed of amino acid residues i-9 to 1+9 are plotted against the amino acid number i [Kyte and Doolittle, 1982]. The putative cyclic nucleotide-binding sites are indicated by horizontal bars and the putative transmembrane segments are indicated as H1-H6 , S1-S6 and M1-M4. The voltage sensor sequence motif and its location within the polypeptide are also shown. Amino acid sequence of the rod cGMP-gated channel [Kaupp *et al.*, 1989], cAMP-gated channel [Dhallan *et al.*, 1990], K^+ channel [Pongs *et al.*, 1988], and nicotinic acetylcholine receptor α-subunit (α-nAChR) [Noda *et al.*, 1983]. [From Kaupp, 1991].

common origin of voltage- and cyclic nucleotide-gated ion channels [Guy and Durell, 1991]. Indeed these classes of ion channels form a large superfamily of voltage/second messenger-gated channels, which also include a putative Ca^{2+}-activated K^+ channel *(Drosophila slow-poke slo gene)* [Atkinson *et al.*, 1991], a putative Ca^{2+} channel for phosphoinositide-mediated calcium entry (encoded by the *gene transient receptor potential trp*) [Hardie and Minke, 1992; Phillips *et al.*, 1992] and the plant K^+ channel/transporter KAT1 [Anderson *et al.*, 1992]. This sequence similarity between selected protein domains of the voltage-gated and second messenger-gated ion channel families is shown in Figure 1.6.

3.1.2 cNG and voltage-gated channels share two important functional motifs

cNG channels contain a sequence motif similar in nature to the S4 transmembrane domain of voltage-gated channels, which is thought to serve as a voltage-sensor [Numa, 1989]. Whereas the *Shaker* B voltage-gated potassium channel [Pongs *et al.*, 1988] contains 7 positively charged residues within this domain, cNG channels generally contain only 5 positively charged amino acids, and in addition 3 negatively charged residues (Figure 1.6). It has been suggested that the difference in the voltage-sensitive gating properties between these two classes of channels, may in part result from these sequence differences within S4 [Goulding *et al.*, 1992]. What then is the functional significance of this motif in cNG channels? It has been proposed that this S4 motif by acting as a generalised 'gating motif' may interact with the ligand-binding pocket sensing the presence of a bound ligand in cNG channels [Eismann *et al.*, 1993]. However this remains to be determined.

cNG channels also contain a domain homologous to the hydrophobic SS1-SS2 domain of voltage-gated channels which is thought to constitute the ion pore [reviewed by Imoto, 1993]. cNG channels however, are deficient in a tyrosine-glycine (YG) motif which is present in potassium selective channels (Figure 1.6), which has been demonstrated to be part of the selectivity filter of potassium channels [Heginbotham *et al.*, 1992]. cNG channels also contain an acidic glutamate residue adjacent to this YG motif which has been demonstrated to participate in the binding and control of calcium entry into the cell, as well as being important for the

S1/H1 Domain

eag (Ca/K)	I **L** L H Y C A F K **A I** W D W V I L C **L T**
plant (K)	F **L V** V L V V **Y** T **A** W V S **P** F E F G F **L**
cGMP-gated (cation)	G N T Y Y N W **L F C I** T **L P** V M Y N W **T**
Shaker (K)	**R** V **V** A I I S **V F** V **I** L **L** S I V I F C **L**
slo (K)	**R** K Y W C F L **L S** S **I** F T F L A G L **L** V

S2/H2 Domain

eag (Ca/K)	L **L** V V **D** S **I** V **D V I F F** I **D** I V L N **F** H **T**
plant (K)	**F F A I D I** I M T F F V G Y L D K **S** T Y **L** I
cGMP-gated (cation)	W **L A** F **D** Y **L S D V** V **Y** L L **D** M F **V R** T R **T**
Shaker (K)	**F F** L **I** E T **L** C I **I** W **F** T F E L T **V R F** L A
slo (K)	V **F** I L S **I** A **S** L **I I Y F** V **D** A S **S** E E V E

S3/H3 Domain

eag (Ca/K)	**S W F** I **I D L L S** C L **P Y** D **V** F N A F D R D
plant (K)	**S W** T L **L D L** V **S** T **I P** S E A A M R **I** S S Q
cGMP-gated (cation)	F Q **F** K **L D V L S** V **I P** D T L L Y I K F G W
Shaker (K)	V M N V **I D** I I A I **I P Y** F I T L A T V V A
slo (K)	I T Q Q **I D L** A F N **I** F F M **V** Y F F **I** R F I

S4 Domain

	*		*		*		*		*		*	
eag (Ca/K)	**F** S A **L** K **V** V **R L L R** L **G R** V V **R** K **L** D **R** Y L
plant (K)	**F** N M **L R L W R** L R **R V G** A L **F** A R **L** E K D R
cGMP-gated (cation)	Y P E I **R** L N **R** L **L R** I S **R** M **F** E F E Q **R** T E
Shaker (K)	L A I **L R V** I **R** L V **R V** F **R** I **F** K **L** S R H S K
slo (K)	I Y L D **R** T **W** I G **L R** F L **R** A L **R L** M T V P D

S5/H4 Domain

eag (Ca/K)	**L**	I	**L**	**L**	L	**C**	**F**	Y	M	L	**V**	A	**H**	**W**	L	**A**	**C**	I	W	**Y**	**S**	**I**
plant (K)	**C**	**A**	K	**L**	**V**	**C**	V	T	L	F	A	**V**	**H**	C	**A**	**A**	**C**	F	**Y**	**Y**	**L**	**I**
cGMP-gated (cation)	**I**	S	N	**L**	**V**	M	T	I	**I**	**I**	I	I	**H**	**W**	N	**A**	**C**	V	**Y**	F	**S**	**I**
Shaker (K)	**L**	G	**L**	**L**	I	F	**F**	L	F	**I**	G	**V**	V	L	F	S	S	A	V	**Y**	F	A
slo (K)	**L**	**A**	Q	**L**	**V**	S	I	F	**I**	S	**V**	W	L	T	**A**	**A**	G	**I**	I	H	**L**	L

SS1-SS2 Domain

eag (Ca/K)	**L**	**Y**	**F**	T	M	**T**	C	**M**	**T**	S	**V**	**G**	F	**G**	N	Y	A
plant (K)	M	**Y**	**W**	**S**	**I**	**T**	**T**	**L**	**T**	**T**	**V**	**G**	**Y**	**G**	**D**	L	H
cGMP-gated (cation)	**L**	**Y**	**W**	**S**	T	L	**T**	**L**	**T**	**T**	I	**G**			E	T	P
Shaker (K)	F	W	**W**	A	**V**	**V**	**T**	**M**	**T**	**T**	**V**	**G**	**Y**	**G**	**D**	M	T
slo (K)	V	**Y**	**F**	L	**I**	**V**	**T**	**M**	S	**T**	**V**	**G**	**Y**	**G**	**D**	V	Y

S6/H5 Domain

eag (Ca/K)	**T**	**F**	R	**L**	A	S	D	**G**	C	**L**	R	**A**	**L**	A	M	H	F	M	M	S	H	S
plant (K)	**I**	**Y**	M	**L**	**F**	N	**L**	**G**	**L**	T	A	Y	**L**	**I**	G	N	M	T	N	L	**V**	**V**
cGMP-gated (cation)	**I**	**F**	A	D	C	E	**A**	**G**	**L**	**L**	**V**	E	**L**	V	L	K	L	Q	**P**	Q	**V**	**Y**
Shaker (K)	**I**	V	G	S	L	C	**A**	I	A	**G**	**V**	L	T	**I**	**A**	L	P	V	**P**	V	**I**	**V**
slo (K)	**T**	**F**	L	V	**F**	F	**L**	L	V	**G**	L	A	M	F	**A**	S	S	I	**P**	E	**I**	I

Figure 1.6 Alignment of Members of the Superfamily of Voltage-Gated and Second Messenger-Gated Ion Channels.

The voltage-gated channels *Drosophila ether-à-go-go (eag)* [Warmke *et al.*, 1991], the plant *Arabidopsis thaliana* [Sentenac *et al.*, 1992] and a K^+ channel encoded by *Shaker* [Pongs *et al.*, 1988] are aligned to the second messenger-gated channels of the photoreceptor cGMP-gated cation channel [Kaupp *et al.*, 1989] and the Ca^{2+}-activated K^+ channel encoded by the *Drosophila* mutant *slow-poke* (slo) [Atkinson *et al.*, 1991]. Channel selectivity is indicated in brackets. Residues conserved in this alignment are indicated in boldface. The position of positively-charged amino acids in the S4 domain of *Shaker* are indicated by (*). [modified from Jan and Jan, 1992].

voltage-dependent block of cNG channels to millimolar concentrations of calcium and magnesium ions [Root *et al.*, 1993].

3.1.3 cNG and voltage-gated channel polypeptides share a similar molecular structure of six putative transmembrane domains

Voltage-gated channels share a basic domain arrangement that consists of a set of six potential membrane-spanning segments flanked by cytoplasmic hydrophilic sequences [reviewed by Hoshi and Zagotta, 1993]. Cyclic nucleotide-gated channels share this same basic arrangement. Whereas the S1-S6 and H5 arrangement is present in each of the four internal repeats of the voltage-gated sodium and calcium channel α-subunits [Catterall, 1988], it is present only once in voltage-gated potassium channel polypeptides, such as those encoded by the *Drosophila Shaker* gene [Papazian *et al.*, 1987; Kamb *et al.*, 1988; Pongs *et al.*, 1988] and vertebrate cyclic nucleotide-gated channels [Kaupp *et al.*, 1989].

Analysis of cloned cNG channel genes has shown the absence of a typical signal sequence, and hence the N-terminus has been assigned to the cytoplasmic face of the membrane [Kaupp *et al.*, 1989]. The cyclic nucleotide binding region comprising of 80 amino acids is found towards the carboxyl terminus and has also been assigned to the cytoplasmic side. Each polypeptide has a single cyclic nucleotide-binding site. The cytoplasmic location of both termini of the polypeptide, has been confirmed by immunohistochemical gold labeling [Molday *et al.*, 1991], [Cook *et al.*, 1989]. A proposed transmembrane topography of voltage/second messenger-gated channels is shown in Figure 1.7(a).

3.1.4 The C-terminal cyclic nucleotide-binding domain

The cyclic nucleotide-binding site of cNG channels comprising of 110 amino acid residues is located near the carboxy terminus (Figure 1.7(a)). In this region the amino acid sequence shows significant similarity to that of other cA/GMP binding proteins, namely the cGMP binding domains of cGMP-dependent protein kinase (cGK) [Takio *et al.*, 1984], and the homologous cAMP binding regions of the regulatory subunit of cAMP-dependent protein kinase (cAK) and the catabolite gene activator protein (CAP) of *E.coli.* [Weber *et al.*, 1989].

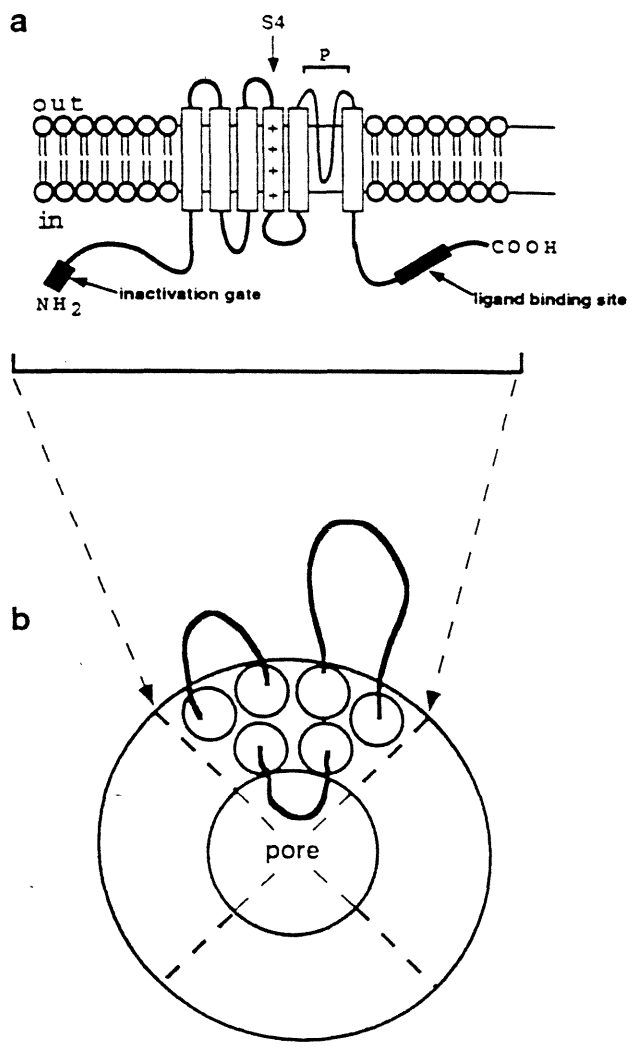

Figure 1.7 Schematic diagram showing structural features of the voltage-gated K^+ channel and second messenger-gated channel family.

(a) Each domain consists of six putative transmembrane segments (S1-S6), a putative voltage-sensing region in S4 — shown with charged residues, a P segment that forms part of the ion permeation pathway, and hydrophilic N and C termini located intracellularly with inactivation and ligand-binding motifs.
(b) Four such segments are thought to associate to form a functional channel with an aqueous pore that can support relatively large ionic fluxes. Diagram shows a schematic view of the channel from the extracellular side.

3.2 Electrophysiological properties of cNG channels

Classical biophysical methods have provided detailed functional analysis of cNG ion channel properties, including the conformational changes underlying activation and inactivation i.e regulated channel opening and closing, mechanisms of ionic selectivity and permeation, and specific interactions with pharmacological agents. The electrical properties of the rod photoreceptor cGMP-gated channel expressed heterologously in *Xenopus* oocytes by the injection of channel-specific mRNA derived from cloned cDNA are described in Table 1.2. cDNAs encoding the ~79 kDa polypeptide alone give rise to functional channels with properties largely similar to those of the native channel in the rod photoreceptor outer membrane [Kaupp *et al.*, 1989; Nizzari *et al.*, 1993].

3.3 Subunit stoichiometry and composition of the retinal rod cGMP-gated ion channel

The heterologously-expressed channel has a Hill coefficient *(n)* of 1.7-3.1, for channel activation by cGMP [Kaupp *et al.*, 1989]. A Hill coefficient ≥ 3 suggests that complete channel activation requires the co-operative binding of four or more molecules of cGMP to open. The rod cNG channel polypeptide contains only one cGMP-binding site per monomer indicating that the functional channel must be composed of four or more monomers. As cNG channels belong to the same superfamily as voltage-gated channels, one would expect that functional channels are formed by the assembly of four monomers to give a tetrameric complex (Figure 1.7(b)), as is the case for the family of potassium channels [MacKinnon, 1991]. This postulated tetrameric architecture for cNG channels has yet to be determined structurally.

3.3.1 cNG channels exist as a heteromultimeric complex

The cloning of a second (β)–subunit (hrcNGC-β) of the human rod cNG channel from a low stringency screen of a retinal rod cDNA library [Chen *et al.*, 1993] suggests that the rod channel is able to form hetero-oligomeric complexes. This β-subunit shows only ~30% overall sequence identity

Table 1.2 Electrophysiological Characterisitics of the Cloned Retinal Rod Photoreceptor cGMP-Gated Ion Channel (rcNGC-α) Expressed in *Xenopus* Oocytes.

Gating	Directly and co-operatively regulated by cGMP. $K_{1/2}$ for cGMP ~50 μM (cAMP does not activate the channel, even at ~1 mM) [Kaupp *et al.*, 1989]. Channel shows no obvious voltage dependence in inside-out patches excised from *Xenopus* oocytes in divalent cation-free symmetrical solutions and under saturating cGMP concentrations. Strong outward rectification is observed when the extracellular side of the membrane is exposed to physiological levels of Ca^{2+} and Mg^{2+} (~1 mM) and the intracellular solution contains no Ca^{2+} and Mg^{2+} [Kaupp *et al.*, 1989].
Selectivity	Poorly cation selective, being permeable to both monovalent and divalent cations. The ion permeability ratio for common monovalent cations Li^+, K^+, Rb^+, Cs^+ relative to relative to Na^+ are 1.1: 0.7: 0.5: 0.3 [Nizzari *et al.*, 1993]. Under physiological conditions ~70% of the inward current is carried by Na^+ ions, ~15% by Ca^{2+} ions and ~5% by Mg^{2+} ions [Yau and Baylor, 1989].
Open Channel Characteristics	Openings of native cGMP-activated channels typically consist of bursts lasting a few milliseconds; channel activity has a characteristic flickery nature [Torre *et al.*, 1992] Heterologous expression of the cloned rod channel gives rise to distinct rectangular single-channel currents [Kaupp *et al.*, 1989]. To emulate the native pattern of gating in a heterologous cell system, co-expression of cloned rod channels (hrcNGC-α) with another rod-specific protein (hrcNGC-β, possessing ~30% overall identity and expressed in rod outer segment) is required. Although the hrcNGC-β protein does <u>not</u> form channels by itself, upon co-expression it introduces rapid flickers to the channel openings (~1 ms openings) and endows the complex with a high sensitivity to the blocker L-*cis*-diltiazem, as characteristic of the native channel [Chen *et al.*, 1993].
Single-Channel Data (dependant on patch conditions such as the presence of divalent cations)	Single-channel conductance is 20-30 pS (in the absence of Ca^{2+} or Mg^{2+}) which decreases to ~ 0.1 pS (~100 fS) in the presence of divalent cations (with ~1 mM Ca^{2+} or Mg^{2+}) [Kaupp *et al.*, 1989]. Mean amplitudes of single-channel currents following heterologous expression were measured at between 2.38-2.48 ± ~ 0.2 pA in 100 mM KCl [Nizzari *et al.*, 1993].
Blockers i) voltage-dependent block	Depolarising voltages promote open channel blockage by divalent cations from the cytoplasmic side; the channel is permeable to these ions, and block occurs after the ions enter the channel. The blockage may result from occupation of one or more binding sites for which cations compete [Yau and Baylor, 1989].
ii) pharmacological	The ~79 kDa form of the protein is reversibly blocked to one-half maximal amplitude by the Ca^{2+} channel blocker L-*cis*-diltiazem (~40 μM); the ~63 kDa form is insensitive, and this may indicate that the cleaved domain comprises the binding site for the blocker [Eismann *et al.*, 1993]. Diltiazem block occurs in membrane suspensions and excised patches but <u>not</u> intact cells, which may reflect an altered phosphorylation state [Gorden *et al.*, 1992]. Intracellular diltiazem has been shown to block salamander rod channels in a voltage-dependent manner, consistent with its binding site being about half-way across the membrane field [Haynes, 1992].
Hill coefficient (n):	2.1 ± 0.6 at -80 mV for cGMP. A Hill coefficient of $n \geq 3$ suggests that complete channel activation requires the co-operative binding of at least four molecules of cGMP [Kaupp *et al.*, 1989].

with the previously cloned α–subunit and ~50% identity in the cyclic nucleotide-binding region. Expression of this β-subunit alone does not give rise to functional channels. However co-expression with the α–subunit introduced rapid flickery kinetics to channel openings and sensitivity to the blocker *L-cis* -diltiazem, that were characteristic of the native channel [Chen *et al.*, 1993]. Thus rod cNG channel like other ligand-gated ion channels exists as a heteromultimer, composed of several distinct but genetically related subunits.

3.4 Regulation of cNG channel ligand sensitivity

Cellular factors in addition to cGMP can control channel activity, and it has been demonstrated that cNG ion channels can be modulated by other second messenger molecules, regulatory proteins, and by phosphorylation *in situ*, which are able to convert the channel between its low and high ligand affinity states.

3.4.1 Modulation by intracellular calcium

Calcium has been shown to reduce the sensitivity of rod photoreceptor cNG channels by a calmodulin-dependent process [Hsu and Molday, 1993], raising the $K_{1/2}$ for cGMP from 19 μM to 33 μM cGMP. This increase in the apparent Michaelis constant for cGMP reduces the rate of cation influx into the rod outer segment by two- to six-fold. The regulation occurred at calcium concentrations of between 50 and 300 nM, which is thought to lie within the physiological range of free calcium *in vivo* [Kaupp and Koch, 1992]. Ca^{2+}-calmodulin was shown to reversibly bind to a 240 kDa polypeptide which is tightly associated with the 63 kDa channel and constitutes the cGMP-gated channel complex within photoreceptor membranes [Molday *et al.*, 1990]; modulation is then thought to result by allosteric interaction between the 63K and 240K proteins. The molecular identity of this 240K polypeptide has yet to be determined, but it does exhibit immunocross-reactivity with the α-subunit of red blood cell spectrin and brain fodrin, both of which are known to bind calmodulin [Molday *et al.*, 1990].

3.4.2 *Modulation by channel phosphorylation*

Phosphorylation was shown to modulate the photoreceptor cNG channel's sensitivity to cGMP [Gordon *et al.*, 1992]. Following patch excision, a spontaneous increase in the channel's apparent agonist affinity was exhibited, which was blocked by specific serine/threonine phosphatase inhibitors — indicating the involvement of an endogenous patch-associated protein phosphatase. The exogenous application of purified protein phosphatase 1 (PP-1) mimicked the action of the endogenous phosphatase, while protein phosphatase 2A (PP-2A) decreased the apparent agonist affinity. Thus there are potentially two phosphorylation sites on the channel and/or associated regulatory protein(s), that can modulate the ligand sensitivity of the channel to cGMP.

Such modulation of the rod cGMP-gated channel by cellular factors other than cGMP may account for the large variation in electrophysiological properties — $K_{1/2}$ for cGMP channel activation, differences in channel permeation and pharmacology, reported in studies comparing intact rods and excised patches [Yau and Baylor, 1989], as well as expressed channels [Nizzari *et al.*, 1993] compared with those *in situ* [Matthews and Watanabe, 1987].

Chapter 2

Materials and Methods

2.1 Materials

2.1.1 Chemicals

General laboratory chemicals were supplied by Fisons (Loughborough), BDH (Poole) or Sigma (Poole) unless otherwise stated and were of analytical grade or equivalent. Bacterial culture media were obtained from Difco (East Molesley) and animal cell culture media from Gibco BRL (Paisley). Radiolabelled nucleotides were supplied by Amersham International (Amersham). Millipore Super-Q® system (Millipore Corporation, Bedford) treated water was used for all solutions.

2.1.2 Enzymes and Proteins

Restriction endonucleases were purchased from Gibco BRL or New England Biolabs (*via* CP Laboratories, Bishop's Stortford). T4 polynucleotide kinase was supplied by Gibco BRL. DNA polymerase I (Klenow fragment) was supplied by either Amersham International or Gibco BRL. T4 DNA polymerase was obtained from New England Biolabs. T7 DNA polymerase and Sequenase™ (modified T7 DNA polymerase) were obtained from Pharmacia P-L Biochemicals (Milwaukee). *Taq* DNA polymerase was obtained from Boehringer Mannheim (Lewes), *Pfu Taq* DNA polymerase was obtained from Stratagene (San Diego). T4 DNA ligase was purchased from Gibco BRL and New England Biolabs. Avian Myeloblastosis Virus reverse transcriptase was obtained from Life Sciences Inc. (St. Petersberg). Proteinase K was purchased from Boehringer Mannheim (Lewes). RNase A (pancreatic RNase) and DNase I were obtained from Sigma. BSA (enzyme grade) was obtained from Gibco BRL. DNase-free RNase A and RNase-free DNase I were prepared by the methods described [Sambrook *et al.*, 1989].

™ , ® All registered trade marks are recognised as belonging to the company named.

2.1.3 Bacterial strains and culture conditions

Strains of *Escherichia coli* K12 used are given in Table 2.1.1. Bacteria were grown using the solid and liquid media given below.

Table 2.1.1 Bacterial Strains

Strain	Genotype	Reference
Epicurian Coli® SURE®	e14⁻(mcrA), Δ(mcrCB-hsdSMR-mrr)171, *sbc*C, *rec*B, *rec*J, *umu*C::Tn5(kan^r), *uvr*C, *sup*E44, *lac*, *gyr*A96, *rel*A1, *thi*-1, *end*A1 [F' *pro*AB, *lac*I^{q}ZΔM15, Tn*10*, (tet^r)]	[Greener, 1990]
DH5αF'	F' / *endA1, hsdR17* ($r_k^- m_k^+$) *supE44 thi-1 , recA1 , gyrA* (Nal^r) *rel*A1 *Δ(lacZYA-argF) U169 deoR* (ϕ80*dlac Δ(lacZ)M15)*	[Woodcock, 1989]

Solid media:

a). Luria agar (LA): tryptone, 1% (w/v); yeast extract, 0.5% (w/v); NaCl, 0.5% (w/v); agar, 1.5% (w/v).
b). BBL top agar: BBL trypticase, 1% (w/v); NaCl, 0.5% (w/v); agar, 0.8% (w/v).
c). NZY : NZ Amine (casein hydrolysate), 1% (w/v); NaCl, 0.5% (w/v); $MgSO_4 \cdot 7H_2O$, 0.2% (w/v); yeast extract, 0.5% (w/v); agar, 0.8% (w/v).

Liquid media:

a). Luria broth (LB): tryptone, 1% (w/v); yeast extract, 0.5% (w/v); NaCl, 0.5% (w/v).
b). 2xYT broth (2xYT): tryptone, 1.6% (w/v); yeast extract, 1% (w/v); NaCl, 0.5% (w/v).

2.1.4 Cloning vectors

The rabbit sino-atrial node cDNA library was constructed in Uni-ZAP™ XR vector (Stratagene Inc). Routine subcloning was performed in the vector pBluescript SK+®, which was purchased from Stratagene (San Diego).

2.2 Methods of sterilisation

Autoclaving: Autoclaves used to sterilise media and disposable plastic-ware were as follows: a Cabburn 8cu.ft. capacity autoclave (Cabburn Sterilisers, Shoeburyness) set to attain a temperature of 121°C for 30 minutes; a model ST19 portable electric autoclave (Dixon's surgical instruments, Wickford) set to attain a temperature of 121°C for 20 minutes.

Dry sterilisation: A B&T "Unitemp" sterilising cabinet (Laboratory thermal equipment, Oldham) was used to sterilise glass-ware. The cabinet was set to attain a temperature of 160°C for 6 hours.

Filter sterilisation: Small volumes (up to 50ml) were filter sterilised by passing through Acrodiscs (Gelman Sciences, Ann Arbor) with a pore size of 0.2mm. Larger volumes (50-500ml) were filter sterilised using Nalgene 0.2mm vacuum filter sterilising units (Nalgene, Rochester, New York).

™ , ® All registered trade marks are recognised as belonging to the company named.

2.3 Nucleic Acid Methods

2.3.1 Solutions Used During the Handling of Nucleic Acids

Ammonium acetate (5 M): 38.5 g of ammonium acetate was dissolved in 100 ml of Q water; following filter sterilisation, the solution was stored at room temperature.

Caesium Chloride (5.7 M): 96 g of caesium chloride (BRL, optical grade) was dissolved in 100 ml of 0.1M EDTA (pH 8), sterilised by autoclaving and stored at room temperature.

Calcium chloride (1 M): 21.9 g of calcium chloride.$6H_2O$ (BDH) was dissolved in 100 ml of Q water, sterilised by autoclaving and frozen in 10 ml aliquots at -20°C.

Chloroform/iso-amyl alcohol: 98% (v/v) chloroform (Fisons), 2% (v/v) iso-Amyl alcohol (Fisons) was prepared and stored at room temperature.

Citric acid (1 M): 4.2 g of citric acid (BDH) was dissolved in 20 ml of Q water, sterilised by filtration and stored at room tempertature.

DEPC treated Q water: 0.1% (v/v) DEPC was added to Q water. After shaking vigorously, the bottles of Q water were left overnight in a fume cupboard with loosened caps. The DEPC-treated Q water was then autoclaved and stored at room temperature.

dNTP solutions (2 mM): 20 µl of stock solutions of 100 mM dTTP, dCTP, dATP,dGTP (Pharmacia) were dissolved in 920 µl of Q water, and stored at -20°C.

DTT (1 M): 1.55 g of DDT (Sigma) was dissolved in a final volume of 10 ml of 10 mM sodium acetate (pH 5.6) and sterilised by filtration. 1 ml aliquots were stored at -20°C.

Ethidium bromide (10 mg and 5 mg/ml): Ethidium Bromide (Serva) was dissolved at the specified concentration in Q water and stored in opaque plastic bottles at room temperature.

Ethanol (100%, 80%, 70%): Ethanol (Fisons) was diluted as required with Q water and stored at -20°C.

Formamide, deionised (100%): Formamide (Fisons) was deionised using Amberlite" MB-3 ion exchange resin (Sigma), filtered through Whatman™ No.1 filter paper and stored in aliquots at -20°C.

Glycerol (45%): Glycerol (Fisons) was dissolved at a concentration of 45% (w/v) in Q water and filter sterilised. The solution was stored at room temperature.

HEPES (2 M, pH 6.6): 9.53 g of HEPES (Sigma) was dissolved in a final volume of 20 ml Q water after adjusting the pH to 6.6 with 5 M NaOH. After filter sterilisation, the solution was stored at 4°C.

HCl (0.25 M): 21.55 ml of concentrated HCl (Fisons) was added to 978.45 ml of Q water. The solution was stored at room temperature.

IPTG (100 mM): 238 mg of IPTG (Sigma) was dissolved in 10 ml of Q water and stored at -20°C.

λ Buffer: 6 mM Tris-HCl (pH 8); 10 mM $MgCl_2$ (Fisons), 100 mM NaCl (Fisons); 0.05% (w/v) gelatin (Fisons). Sterilised by autoclaving and stored at room temperature.

Magnesium chloride (1 M): 20.3 g of $MgCl_2.6H_2O$ was dissolved in 100 ml of Q water, sterilised by autoclaving and stored at room temperature.

Magnesium sulphate (1 M): 24.6 g of $MgSO_4.7H_2O$ (Fisons) was dissolved in 100 ml of Q water, sterilised by autoclaving and stored at room temperature.

Maltose (20%): 4 g of maltose (Sigma) was dissolved in 20 ml of Q water and filter sterilised. The solution was stored at 4°C.

MOPS buffer (10x): 0.2 M MOPS, 50 mM sodium acetate.$3H_2O$, 1 mM EDTA (pH 8). The pH was adjusted to 8 with NaOH prior to autoclaving. The solution was stored at room temperature.

PCI: 50% (v/v) phenol (Fisons), 48% (v/v) chloroform, 2% (v/v) iso-Amyl alcohol; equilibrated against 10 mM Tris-HCl (pH 8) and kept in the dark at 4°C.

Phenol (liquified): Liquified phenol containing 0.1% (w/v) 8-hydroxy-quinoline and equilibrated against 100 mM Tris (pH 7.6) was obtained from Fisons.

Sodium acetate, (3 M, pH 5.6): 40.8 g of sodium scetate.$3H_2O$ (Fisons) was dissolved in 100 ml of Q water, after adjusting the pH to 5.6 with glacial acetic acid. The solution was sterilised by autoclaving and stored at room temperature.

Sodium acetate, (1.1 M, pH 7): 14.96 g of sodium acetate.$3H_2O$ was dissolved in a final volume of 100 ml of Q water after the pH had been adjusted to 7. Following sterilisation by autoclaving, the solution was stored at room temperature.

Sodium chloride (4 M): 23.4 g of sodium chloride (Fisons) was dissolved in 100 ml of Q water and sterilised by autoclaving. The solution was then stored at room temperature.

SDS (10%): 50 g of SDS (Fisons) was dissolved in 500 ml of Q water and stored at room temperature.

Sodium hydrogen phosphate (0.5 M): 89 g of $Na_2HPO_4.2H_2O$ (Fisons) was dissolved in 1 L of Q water. After sterilising by autoclaving, the solution was stored at room temperature.

Sodium hydroxide (10 M): 200 g of sodium hydroxide (Fisons) was added slowly to 400 ml of Q water. After adjusting the volume to 500 ml, the solution was stored at room temperature.

Southern denaturation solution: 0.5 M NaOH, 1.5 M NaCl; autoclaved and stored at room temperature.

Southern neutralisation solution: 0.5 M Tris-HCl (pH 7.4), 3 M NaCl; autoclaved and stored at room temperature.

SSC (20x): 3 M NaCl, 0.3 M tri-sodium citrate (Fisons); pH adjusted to 7 with NaOH, autoclaved and stored at room temperature.

TAE (10x): 48.4 g of Trizma base (Sigma) and 20 ml of 0.5 M EDTA (pH 8) were dissolved in 1 litre of Q water after the pH had been adjusted to 7.5 with glacial acetic acid (Fisons).

TBE (10x): 108 g of Trizma base, 55 g of boric acid (Fisons) and 9.3 g of EDTA were dissolved in 1 litre of Q water.

TBE (0.5x) Acrylamide (6%) Urea: 50 ml of 10 x TBE, 430 g of urea (Serva) and 150 ml of 40% acrylamide were dissolved in 1 litre of Q water and stored in the dark at 4°C.

TBE (2.5x) Acrylamide (6%) Urea: 250 ml of 10 x TBE, 430 g of urea, 150 ml of 40% acrylamide, 50 g of sucrose (BRL) and 50 mg of bromophenol blue (Sigma) were dissolved in 1 litre of Q water and stored in the dark at 4°C.

TE: 10 mM Tris-HCl (pH 7.2), 1 mM EDTA (pH 8); autoclaved and stored at room temperature.

TLE: 20 ml of 1 M Tris-HCl (pH 9), 0.42 g of LiCl (Sigma), 5 ml of 500 mM EDTA (pH 8) and 1 ml of 10% SDS were dissolved in 100 ml of DEPC-treated Q water, sterilised by autoclaving and stored at room temperature.

Tris-HCl (1 M): 121.1 g of Trizma base was dissolved in 1 litre of Q water after adjusting the pH as required with concentrated HCl. Following sterilisation by autoclaving, the solution was stored at room temperature.

X-gal (20 mg/ml): 200 mg of X-gal (5-Bromo-4-Chloro-3-indolyl-β-D-galactoside) obtained from Novabiochem (Nottingham) was dissolved in 10 ml of dimethylformamide (Fisons) and stored in the dark at -20°C.

2.3.2 Oligonucleotides used

Synthetic oligonucleotides used during the course of this thesis are shown in Table 2.3.1 or described in the relevant sections.

Table 2.3.1 Synthetic oligonucleotides

Oligonucleotide Description	5'-3' sequence
Reverse Primer	AACAGCTATGACCATG
T3 Primer	ATTAACCCTCACTAAAG
KS Primer	CGAGGTCGACGGTATCG
SK Primer	TCTAGAACTAGTGGATC
M13-20 (Universal) Primer	GTAAAACGACGGCCAGT
T7 Primer	AATACGACTCACTATAG
*rsc*G-1	AGGTTCATCAAAACAGGC
*rsc*G-2	GTAATATGTGTTTCCTGAGGGATCA
*rsc*G-3	AGGCAGCAGTACTTGCCGGGT
*rsc*G-4	AGAAAGAGGAGACAAAGAAA
*rsc*G-5	ATAGTCTATCTTGTTGACATG
*rsc*G-6	TTTGAGTTCTTTCAGAACAA
*rsc*G-7	CCTGACGTTAATGATCCTGAA
*rsc*G-8	TGGACCAACAAAAAGACAGTT
*rsc*G-9	ATTCTTTAACATTAAAGGCAGC
*rsc*G-10	CCTAAAGATCTCGAAGAGAAG
*rsc*G-11	TCATCTCTTGAAGGAGCTGGA
*rsc*G-12	ACGGATATGGGAAAAGATATA
*rsc*G-13	GTTTGGATACAATTTTAAAAA
*rsc*G-14	TTGAAGTTACAGCCCCAAGTCTAT
*rsc*G-15	TCCAACATGAACGCAGCTAGG
cA-Pr 1	CCTGGAGATTATATTTGC
cA-Pr 2	CGTAAGGGGGACATTGGC

cA-Pr 2	CGTAAGGGGGACATTGGC
cA-Pr 3	AAGGAAATGTACATCATC
cA-Pr 4	TACGGATATTAGCAGTAC
cA-Pr 5	AGATCTGAGTAGCCCAGG
cA-Pr 6	TCCTTGGACAAGCAGAAG
A_{2a}-1	TCAGGACGTGGCTGCGAATGATCTT
A_{2a}-2	TGTCTACTTGCGGATCTTCCTA
A_{2a}-3	ACACTCTGGGCAAAAGAAGGTA

2.3.2 Sino-Atrial Node Tissue Preparation

3 grams of sino-atrial node tissue was collected by Dario Difrancesco (Department of Physiology and Biochemistry, University of Milan). The nodal preparation was taken from outbred adult male rabbits weighing about 2.4-2.7 kg. Tissue was isolated from sino-atrial nodal areas where I_f can be recorded by whole cell and patch clamp electrophysiological techniques. Briefly after removal of the whole heart, the atria were separated from ventricular tissue. The sinus node was exposed and isolated by opening the inferior and superior vena cava, during the fine dissection of sinus node, the cardiac tissue was continuously bathed in ice-cold Tyrode solution pH 7.4 (140 mM NaCl, 5.4 mM KCl, 1.8 mM $CaCl_2$, 0.5 mM $MgSO_4$, 5 mM HEPES and 10 mM glucose). During the dissection procedure care was taken to avoid contamination of the the sinus preparation with atrial tissue. The entire removal procedure took 10 minutes, before freezing the heart. After removal, the sinus node was put in a Dewar flask containing liquid nitrogen for instantaneous freezing. Each individual sinus preparation weighed approximately 0.1 g.

2.3.3 Purification of Genomic DNA from Tissues

Small pieces of rabbit tissue (obtained from adult NZW rabbits approximately 2-2.5 kg) were powdered under liquid nitrogen in a mortar and pestle. The powder was then added to 5 ml of SE buffer (150 mM NaCl; 100 mM EDTA, pH 8) plus 1/10 volume of 10% SDS and 1/40 volume of proteinase K (20 mg/ml) in Corex® (DuPont Scientific Instruments, Delaware) tubes, mixed gently and incubated overnight at 37°C. 1/2 volume of PCI was added and after mixing, the emulsion was

spun at 10,000 rpm in a HB-4 rotor (DuPont) within a Sorvall® RC-5B centrifuge (DuPont) for 2 minutes. The aqueous phase was transferred to a fresh tube and the phenol was re-extracted with 1/4 volume of SE. Both aqueous phases were pooled and 2 volumes of absolute ethanol (Fisons) was added. Upon mixing, a precipitate appeared which was pelleted by spinning for 10 minutes at 10,000 rpm in a HB-4 rotor. After drying, the pellet was resuspended in 500 µl of TE containing 100 µg/ml pancreatic RNase (DNase-free), transferred to a 1.5 ml microfuge tube and incubated at 37°C for 30 minutes. 250 µl of PCI was added, the phases mixed thoroughly and then separated by spinning at 13,000 rpm for 1 minute in an MSE microfuge (MSE Scientific Instruments, Crawley). 50 µl of 3M sodium acetate pH 5.6 was added, then 1 µl of absolute ethanol. The precipitate which formed on mixing was pelleted by spinning at 13,000 rpm for 20 minutes in a microfuge, washed with 70% ethanol and air-dried. The pellet was resuspended in 50-100 µl of TE or Q water and the nucleic acid concentration determined by spectrophotometric analysis.

2.3.4 Purification of Total RNA from Tissues

Total RNA was purified from whole tissues by either caesium chloride centrifugation [Glisin, 1974] or by acid guanidinium thiocyanate-phenol-chloroform extraction [Chomczynski *et al.*, 1987]. All solutions were prepared using DEPC-treated Q water and all vessels containing RNA were soaked in DEPC-treated Q water prior to use. The two methods used are described briefly below:

1). Caesium chloride centrifugation: Powdered tissues were prepared as described in section 2.3.3.2 above. Without thawing, the powder was transferred to 5 ml of TLE and phenol extracted twice. Both aqueous phases were pooled and subjected to caesium chloride pad (5.7 M CsCl) centrifugation at 25,000 rpm in a TST41:14 swing-out rotor (Sorvall®) in a Sorvall® OTD 50B ultracentrifuge (DuPont) for 18 hours at 25°C. The purified RNA was ethanol precipitated, resuspended in DEPC-treated Q water and stored at -70°C. The quantity and quality of the RNA was checked by spectrophotometric analysis and agarose gel electrophoresis respectively.

2). Guanidinium thiocyanate extraction: Tissue was homogenised on ice in 1ml of extraction buffer (4 M guanidium thiocyanate, 25 mM sodium citrate, pH 7, 0.5% sarcosyl, 0.1 M 2-mercaptoethanol) then extracted with phenol. The aqueous phase was precipitated twice with isopropanol (Fisons), washed with 70% ethanol, dried and resuspended in 0.5% SDS or DEPC-treated Q water. The quantity and quality of the RNA was checked by spectrophotometric analysis and agarose gel electrophoresis respectively.

2.3.5 Isolation of Poly (A)$^+$ mRNA

The following two methods were employed for the isolation of mRNA.

1). Oligo (dT) cellulose affinity chromatography. Total RNA extracted as described in 2.3.4 was redissolved in 0.5 ml of TE buffer. The RNA was heated at 65°C for 5 minutes, cooled on ice and 0.5 ml of 1 M NaCl was added prior to the addition to an oligo (dT)-cellulose Type 7 column (Pharmacia), pre-equilibrated according to the manufacturer's instructions. The column was washed with 5-10 bed volumes of application buffer (10 mM Tris-HCl (pH7.5), 1 mM EDTA, 0.5 M NaCl), 5 bed volumes of wash buffer (10 mM Tris-HCl (pH7.5), 1 mM EDTA, 0.1 M NaCl), and the RNA was eluted with 3 bed volumes of TE buffer and collected in 0.2 ml fractions. The fractions were pooled together and re-applied to a second column as above. The eluted poly (A)$^+$ mRNA was ethanol precipitated, resuspended in DEPC-treated Q water and stored at -70°C.

2). Fast lysis oligo (dT) selection method (FastTrack^{TM}, Invitrogen). Poly (A)$^+$ mRNA was isolated according to the manufacturer's instructions. Briefly 1 gram of tissue was homogenized in 15 ml of Lysis buffer using a Polytron (Status, Lucern), for 15-30 seconds. The lysate was incubated at 45°C for 30 minutes, and the NaCl concentration was adjusted to 0.5 M with 5 M NaCl, before the addition of one oligo (dT) cellulose tablet. After mixing at room temperature for 15 minutes, the oligo (dT) cellulose was pelleted, and washed in low salt buffer, before being resuspended in a final volume of 0.8 ml. The sample was pipetted into a spin-column and the poly (A)$^+$ mRNA was eluted in 400 µl of elution buffer, ethanol precipitated, resuspended in DEPC-treated Q water and stored at -70°C.

2.3.6 Large Scale Preparation of Plasmid DNA

Alkaline lysis and purification of DNA by the use of Qiagen™ columns (Hybaid, Teddington) was performed according to the manufacturer's instructions.

Subsequent to purification, the quantity and quality of the DNA was checked by spectrophotometric analysis and agarose gel electrophoresis respectively.

2.3.7 Small Scale Purification of Plasmid DNA

Isolation of plasmid DNA from 1-2 ml of bacterial culture was performed using the alkaline lysis method, essentially according to the method of Sambrook *et al.*, (1989).

2.3.8 Gel Electrophoresis

1). Agarose. Nucleic acids were separated by electrophoresis through horizontal agarose slab gels (Seakem HGT or NuSieve GTG; both purchased from Flowgen, Sittingbourne), which varied between 0.8 and 5% (w/v). Gels were made and run in either 1.0 x TAE (DNA) or 1 x MOPS (RNA) buffers. Ethidium bromide was added to the gel and buffer at 0.5 mg/ml for DNA gels to allow visualisation of the DNA when illuminated by ultraviolet light (254 nm wavelength). When a permanent record of a gel was required, the gel was photographed using a Polaroid MP4 land camera loaded with Polaroid type 667 black and white positive film (Polaroid, St. Albans). Markers used on agarose gels were as follows: λ DNA cleaved with *Bst*EII and *Hind*III; ϕX174 DNA cleaved with *Hae*III (BRL).

2). Polyacrylamide. Nucleic acids were separated by electrophoresis through vertical polyacrylamide gels of various percentages and types. 6% non-denaturing gels were used for purification of small DNA fragments, whilst 6% denaturing gels (0.5 x TBE) were used for separating the products of DNA sequencing reactions. All gels were run in TBE buffer of the same strength as that in the gel.

2.3.9 Restriction Enzyme Digestions and Southern (DNA) Blotting

Restriction endonucleases were used according to the manufacturers' instructions and incubated for sufficient time to attain complete digestion. 1/10 volume of loading buffer (20 mM EDTA, 50% (v/v) glycerol, 0.05% (w/v) bromophenol blue) was added and the sample loaded on an agarose gel together with a suitable size marker. After electrophoresis and photography, capillary transfer of the DNA to a nylon membrane (Hybond-N, Amersham) was performed essentially as described by Southern, (1975), using 20 x SSC as a transfer buffer. The filter was dried and the DNA cross-linked to the membrane by irradiation with ultraviolet light (254 nm).

2.3.10 Removal of Probes and Re-use of DNA Blots

Probe sequences were removed by incubating the filter in 0.4 M NaOH at 45°C for 30 minutes followed by incubation in 0.1 x SSC, 0.1% (w/v) SDS, 0.2 M Tris-HCl (pH 7.5) at 45°C for 30 minutes. After probe removal the filter was prehybridised and hybridised as normal.

2.3.11 Preparation of Probes

^{32}P radiolabelled probes were generated by two different methods:

1). Random priming method. The method used was that of Feinberg and Vogelstein, (1983). Labelling reactions were performed at either 37°C for 30 minutes or 20°C for 4-5 hours with 2 units of Klenow polymerase (Amersham). New preparations of DNA were checked for efficiency of radionucleotide incorporation as follows: 1 µl (approximately 1/100) of the probe mix was pipetted onto a 2 cm circle of DE81 paper (Whatman), dried and Cerenkov counted in a Tri-Carb® Minaxi-β 4000 series liquid scintillation counter (Packard Instruments, Downers Grove, Illinois). After washing off the unincorporated nucleoside triphosphate with 0.5 M Na_2HPO_4, the filter was dried and counted again. Typically 70-80% incorporation was seen, and probes with over 60% incorporation were used without further purification.

2). *In vitro* RNA transcription. High specific activity radiolabelled RNA probes (riboprobes) were generated by a modification of the procedure described by Melton *et al.*, (1984). All DNA templates used for the production of riboprobes were linearized with restriction endonucleases generating 5' protruding ends, followed by phenol extraction and ethanol precipitation. The following components (Promega) were mixed in order, in a final reaction volume of 20 µl: 4 µl of 5 x transcription buffer (200 mM Tris-HCl, pH7.5, 30 mM $MgCl_2$, 10 mM spermidine, 50 mM NaCl), 2 µl 100 mM DTT, 20 units rRNasin® ribonuclease inhibitor, 4 µl of 2.5 mM rATP, rGTP and rUTP, 2.4 µl 100 µM rCTP, 1 µg linearized template, 5 µl of [α-^{32}P]rUTP 50 mCi/ml (3000Ci/mmol) (Amersham) and 20 units of T7 RNA polymerase. The reaction was incubated for 2 hours at 37°C. The reaction products were analysed on a 3% NuSieve GTG agarose gel run at 45 volts for 3 hours, and the desired riboprobe fragment was excised, quantitated and melted before dilution in 20 ml of hybridisation buffer.

2.3.12 Preparation of ^{32}P Radiolabelled Markers and Analysis by Electrophoresis

Labelled DNA fragments used as size markers during gel electrophoresis were made essentially according to the method of Sambrook *et al.*, (1989), and run on a 1% Alkaline Agarose gel (0.8 g of agarose was melted in 72 mls of water to which 8mls of 10x Alkaline Buffer (0.3 M NaOH, 0.02 M EDTA) were added and the gel poured). The gel was run overnight in 1x Alkaline Buffer at 45 volts. The gel was dried and analysed autoradiographically.

2.3.13 Purification of DNA Fragments from Agarose gels

The method used is essentially that of McDonell *et al.*, (1977). Briefly, the desired fragment was excised from an agarose gel, placed inside dialysis tubing containing a small amount of 0.5 x TAE and electrophoresed at 10 V/cm for 15 minutes. The eluted DNA was then ethanol precipitated, dried and resuspended in a suitable volume of Q water.

2.3.14 Ligation of DNA Molecules and Transformation of Competent *E. coli* Cells

Ligations were performed using T4 DNA ligase at 15°C. Standard reactions were performed in a 10 µl volume with 10-100 ng of vector and an appropriate amount of insert to give a 1:1 molar ratio of vector:insert. Occasionally, greater amounts of insert were used (up to a 10-fold excess) without problem. For ligation of molecules containing cohesive ends, T4 DNA ligase from Gibco BRL at 0.1 unit/µl final concentration was used; incubations being for 4-24 hours. For ligation of molecules containing blunt ends, T4 DNA ligase from New England Biolabs at 200 units/µl (equivalent to 3 BRL units/µl) final concentration was used and incubations were for a minimum of 24 hours.

E. coli cells were made competent for the uptake of DNA and transformed by a variation of the method used by Mandel and Higa, (1970). Briefly, an overnight culture of bacteria was diluted 1:100 into 100 ml of fresh medium and grown until mid log phase (A_{550}= 0.3-0.6), chilled on ice for 10 minutes and centrifuged to pellet the cells. The cells were resuspended in 50 ml of 0.1 M $MgCl_2$ and pelleted again. The cells were resuspended in 25 ml of freshly diluted 0.1 M $CaCl_2$ and incubated on ice for 20 minutes, followed by pelleting. Finally, the cells were resuspended in 5 ml of 0.1 M $CaCl_2$ and kept on ice until required. For freezing competent cells, the final pellet was resuspended in 5 ml of 0.1 M $CaCl_2$ containing 12.5% (v/v) glycerol, snap frozen in a dry ice/ethanol bath and stored at -70°C. These cells were thawed on ice when required.

Transformation of competent cells was performed as follows: 95 µl of 1 x SSC and 5 µl of ligation reaction were added to 200 µl of competent cells. After mixing, the cells were incubated on ice for 45 minutes, subjected to heat shock at 45°C for 2 minutes then incubated on ice for 30 minutes. Subsequent steps depended on the type of DNA being transformed. For plasmid DNA, 1 ml of Luria broth was added to the cells which were then incubated at 37°C for 30 minutes prior to plating on Luria-plates containing 50mg/ml ampicillin. The plates were allowed to dry, inverted and incubated overnight at 37°C. If colour selection by use of the chromogenic substrate X-gal was being used, the plates also had 80 µl of

stock X-gal and 50 µl of stock IPTG spread on their surface before addition of bacteria.

2.3.15 Construction of the Rabbit Sino-Atrial Node cDNA Library

The sino-atrial node (SAN) oligo (dT)-primed cDNA library was constructed from 5 µg of SAN poly (A)$^+$mRNA, in a unidirectional λ ZAP II^{TM} vector according to the manufacturer's instructions (Stratagene). All ligations were done for an extended period of time 4°C for 1-2 days and ethanol precipitations were done overnight at -20°C. Briefly the mRNA was copied into hemi-methylated cDNA [Gubler and Hoffman, 1983] using an oligo $(dT)_{18}$ primer containing an integral 3' *Xho*I site, for priming first-strand synthesis with RNase H-free moloney murine leukaemia virus reverse transcriptase (M-MuLVRT). After second strand synthesis, using DNA polymerase I to nick-translate RNase H generated RNA fragments into second strand cDNA, and following phenol extraction and ethanol precipitation, the cDNA ends were blunted using T4 DNA polymerase in the presence of 2.5 mM dNTPs. Following another round of phenol extraction and ethanol precipitation, *Eco*RI adaptors were ligated onto the blunted cDNA ends. After heat-inactivation of the ligase, the *Eco*RI adaptors were phosphorylated with T4 polynucleotide kinase, and the kinase was heat-inactivated subsequent to *Xho*I digestion. The resultant cDNA was size-selected for inserts ≥ 0.5 kb on a Sephacryl S-400 column, phenol extracted and ethanol precipitated. 150 ng of the resuspended cDNA was ligated into 1µg of *Eco*RI/*Xho*I-digested and dephosphorylated Uni-ZAP XR^{TM} vector (Stratagene). Ligated DNA was packaged *in vitro* with Gigapack^{TM} II Gold packaging extract (Stratagene), according to the manufacturer's packaging instructions. The packaged ligation products were plated on the *E.coli* strain PLK-F' and the resultant primary cDNA library of recombinant plaques was of the order of 5×10^5 pfu/µg of arms. 2.5×10^5 recombinant phages were immediately amplified to make a large stable quantity of high titre stock of 10^9 pfu/ml. For short term storage, chloroform was added to a final volume of 0.3% (v/v) to the pooled stock of amplified library, and aliquots of 1.5mls were stored at 4°C. For longer term storage DMSO was added to a final concentration of 7% (v/v) and aliquoted samples of the amplified library were stored at -70°C.

2.3.16 Screening of the SAN cDNA Library

For both the primary and amplified library screens, recombinant phages were mixed with *E.coli* XL1-Blue cells and 0.65% BBL top agar and plated on NZY agar in 150-mm Petri dishes at an approximate density of 20,000 plaque forming units/plate, as described by the manufacturer's instructions (Stratagene). The plates were incubated at 37°C until lytic plaques started to form after approximately 5 hours and cooled overnight at 4°C to arrest phage replication. Phages from the lytic plaques were transferred onto duplicate, orientated nylon membranes (Hybond™-N, Amersham), according to the manufacturer's instructions. The membranes were air-dried and the DNA cross-linked to the membranes by irradiation with ultraviolet light (254 nm).

2.3.17 Hybridization and Washing Conditions

Replicate filters with recombinant phage DNA were hydridized with ^{32}P radiolabelled probe by the method of Church and Gilbert, (1984) at 55-60°C for 12 hours, in a Maxi 14 hydridisation oven with rotisserie (Hybaid). No pre-hybridisation was required. The filters were then washed with 3 x SSC at room temperature, then 42°C and then in 2 x SSC at 55°C overnight until background radioactivity on the filters as monitored with the hand held Geiger counter was low (10 c.p.s). With the primary cDNA library screen a final wash of 0.5 x SSC at 55°C overnight had to be done to achieve a low background signal. Filters were dried and exposed to Kodak X-Omat™ film with an intensifying screen at -70°C for 3 days.

2.3.18 Isolation of Hybridization-Positive Phages

Autoradiographic spots from the screening procedure that appeared on replicate membranes, identified areas of the original plate containing phage plaques of interest. Plaques of interest were isolated from the agar plate and transferred into a sterile microfuge tube containing 500 µl of λ buffer, vortexed, titrated, and subjected to a second round screen. Second round positives were plaque-purified and stored following standard procedures as described in Sambrook *et al.*, (1989). Inserts harbored in positive phage were excised by plasmid rescue of Bluescript SK-® after

superinfection with a R408 helper phage (Stratagene), following the manufacturer's instructions.

2.3.19 Extraction of Bacteriophage λ DNA

Phages from the amplified cDNA library were extracted by modification of the procedure as described in Sambrook *et al.*, (1989). Briefly EDTA was added to 1 ml of the library stock, to give a final concentration of 20mM. After the addition of proteinase K to a final concentration of 50 μg/ml and SDS to a final concentration of 0.5% (w/v), the sample was incubated for 1 hour at 56°C. Following phenol extraction the aqueous phase was ethanol precipitated and the phage DNA resuspended in 200 μl of TE.

2.3.20 Nucleic Acid Sequencing

Double-stranded plasmid DNA templates were prepared by alkaline-lysis plasmid DNA isolation as described in 2.3.6 and using Tip100 columns (Qiagen). DNA samples were adjusted in concentration to 250 ng/μl, based on the absorbance at 260 nm. Both DyeDeoxy™ Terminator and Dye Primer sequencing were preformed using the cycle sequencing procedure and the Cycle Sequencing Kits essentially as described by the supplier (ABI). The reactions were carried out using the PCR System 480 Thermal Cycler (Perkin Elmer-Cetus). The samples were electrophoresed on an ABI 373 automated DNA Sequencer. The primary sequence data was edited using the program package SeqEd™ 675 DNA Sequence Editor (ABI) on a Macintosh IIci.

2.3.21 Clone Characterisation and Analysis

Edited sequence data were analysed on a Macintosh IIcf computer using the sequence analysis software *MacVector*™ version 4.1 (International Biotechnologies, Inc, New Haven). Sequence comparisons were done against the latest releases of the DNA and Protein portions of the *Entrez:Sequences* database on CD-ROM (NCBI, Bethesda).

2.3.22 In Vitro Transcription for Expression in *Xenopus* Oocytes

Template DNAs (approximately 1 μg), linearized with restriction endonucleases generating 5' protruding ends, were treated with 1/10th of

the volume of Proteinase K (20 mg/ml) and incubated at 50°C for 1 hour, followed by phenol extraction and ethanol precipitation. 7-methyl-guanosine(5')-triphospho(5')guanosine (GpppG)-capped RNA was transcribed and purified using mMESSAGE mMACHINE™ (Ambion), with SP6 or T7 RNA polymerases, according to the manufacturer's instructions. The size and integrity of the transcribed RNA was confirmed by analysing one tenth of the transcription reaction on a 1.2% agarose gel, with RNA size markers (BRL). The mRNA was stored in sterile water at -70°C .

2.3.23 PCR methods

PCR was used for amplifying sequences from DNA/cDNA in several protocols. Amplifications were performed using a Perkin Elmer Cetus DNA thermal cycler. The 10 x buffer used was supplied with the *Taq* DNA polymerase (Boehringer Mannheim). Also cloned *Pfu* DNA polymerase (Stratagene) was used in some applications. The reaction volume was 100 µl containing 2.5 units of *Taq* polymerase, 250 mM dNTPs, 0.125% Tween and overlayed with 50 µl of mineral oil (Fisons). Primers were present at 0.2 pM and template DNA at 10-300 ng.

1). For amplification of genomic DNA sequences using two known primers, the reactions were set up according to the protocol supplied with the DNA thermal cycler and amplification performed using 30 cycles of: 94°C melt for 1 minute, anneal for 1 minute and extension at 72°C for 3 minutes. The final extension was for 10 minutes, followed by a 4°C soak. Annealing temperatures were usually 2-5°C below the calculated melting temperature of the oligonucleotide primers. Melting temperatures were determined by assigning a value of 2^{o}C to nucleotides A and T, and 4^{o}C for nucleotides C and G for each oligonucleotide primer.

2). Reverse transcription-PCR (RT-PCR). 1 µg of RNA was heated in 11 µl of RNase free H_2O to 56^{o}C for 3 minutes, quenched on ice and added to 2 µl 10x Reverse Transcription Buffer (100 mM Tris-HCl, 500 mM KCl, 1% Triton X-100) (Promega), 2 µl of 10 mM dNTPs, 0.5 units of rRNasin® Ribonuclease Inhibitor (Promega), 15 units of AMV Reverse Transcriptase (Promega) and 0.5 ug of oligo (dT) primer or 3' gene-specific primer in a final volume of 20 µl. This was incubated at 42^{o}C for 1 hour and 52^{o}C for

30 minutes and diluted to 100 µl in RNase free H_2O. Aliquots of 2-10 µl were generally taken for PCR as above, using 30-40 cycles.

3). 5'-AmpliFINDER™ RACE. 5'-AmpliFINDER™ RACE (Clontech) a modification of SLIC (single-strand ligation to single-stranded cDNA) [Dumas *et al.*, 1991] and the original RACE (rapid amplification of cDNA ends) [Frohman *et al.*, 1988] methods, was used to retrieve the 5' end of truncated cDNA clones, from 2 µg of SAN poly $(A)^+$ RNA as described by the manufacturer.

2.3.24 Cloning of PCR Products

PCR products were cloned into the following two vectors:

1). pT7Blue T-Vector (Novagen) as described by the manufacturer. This enabled RNA synthesis by *in vitro* transcription of cloned PCR products by T7 RNA Polymerase, following linearisation of the recombinant vector.

2). pUC18 *Sma*I/dephosphorylated vector (SureClone™, Pharmacia) as described by the manufacturer. This enabled the sequencing and characterisation of cloned PCR products.

2.4 *In Vitro* cell culture methods

2.4.1 Solutions used during the culture and transformation of animal cells

DMEM: DMEM (without sodium pyruvate, with 4500 mg/l glucose) was purchased from Gibco BRL and stored at 4°C. The medium was supplemented with 10% (v/v) FCS (Gibco BRL), 2 mM glutamine (Gibco BRL) and antibiotic (100 u/ml penicillin and 100 mg/ml streptomycin, Gibco BRL).

PBS (tissue culture): Dulbecco's modified PBS (without Mg^{2+} or Ca^{2+}) was prepared by dissolving ten tablets (ICN Flow) in 1000 ml of Q water. The PBS was dispensed (250 ml aliquots) into 500 ml tissue culture bottles (Gibco BRL). Following sterilisation by autoclaving, the solution was stored at room temperature.

Electroshock buffer for MEL-cells: Electroshock buffer for the electroporation of MEL-cells contained 140 mM NaCl, 25 mM HEPES pH 7.5 (correct pH obtained using 4 M NaOH) and 0.75 mM Na_2HPO_4. 500 ml aliquots of the buffer were filter sterilised. The final pH of the buffer was approximately pH 7.

Gene pulser cuvettes: Gene pulser cuvettes with a 0.4 cm electrode gap, for the electroporation of MEL cells, were obtained from Biorad.

Geneticin (G418): Geneticin (G418) powder was dissolved in Q water to a final concentration of 200 mg/ml (w/v) and stored as 1ml aliquots at -20°C.

Cell lines cultured *In Vitro* : MEL-C88 murine erythroleukaemia cells [Deisseroth *et al.*, 1978] were employed.

2.4.2 General Cell Culture

Cell manipulations were performed in a class II microbiological safety cabinet (Medical Air Technology Ltd., Manchester). Cells were routinely cultured in 10 ml of medium in 9cm Nunclon® (Gibco BRL) dishes. All mammalian cells were incubated at 37°C (5% CO_2 atmosphere) in a humidified incubator.

2.4.3 Subculturing and handling of cells

To concentrate MEL-cell lines (non-adherent cells), the medium containing cells was centrifuged in a sterile 10ml cone base plastic tube (Northern Media Supply Ltd., North humberside) for 5 minutes at 2000 rpm in a Heraeus Digifuge^{GL} (Heraeus Equipment Ltd., Brentwood). The medium was aspirated and the cells resuspended in a suitable volume of fresh medium. To subculture these cell-types, log-phase cells were diluted as required (up to one hundred-fold) into fresh medium in 9 cm dishes (10 ml per dish).

2.4.4 Cryogenic storage of cells

Cells from one 9 cm dish were pelleted as above and resuspended in 2 ml of medium containing 10% DMSO (Sigma, cell culture grade). 100ul aliquots were dispensed into 1.0 ml ampoules and cooled slowly to -196°C before storing in liquid nitrogen in a model LR40 cryostorage refrigerator (Jencons Scientific Ltd., Leighton Buzzard).

Growth of cells from frozen samples was performed as follows: a vial of frozen cells was placed in a water bath at the normal culture temperature of the cells until thawed. The cells were then transferred to 9 ml of culture medium in a 9 cm dish and incubated overnight. The following day, the medium was changed for fresh medium and incubation continued.

2.4.5 Transfection of MEL-cells

Expression constructs were linearized with a suitable restriction enzyme prior to electroporation. 1×10^7 MEL cells in logarithmic growth phase were washed twice with PBS and resuspended in 0.9ml of electroshock buffer before being mixed with 25 µg quantities of DNA containing expression constructs. The cell-DNA mixture was placed in a genepulser cuvette and electroporated in a Bio-Rad Gene Pulsar™ at 960 mF and 250 V in sterile electroshock buffer. Following electroporation, cells were diluted in fresh culture medium to 10^4 - 10^5 cells/ml; 24 hours later, G418 was added (final concentration 1 mg/ml) to select for transfectants. Semi-adherent colonies (at a size visible to the naked eye) appeared 10-14 days post-transfection, and were either pooled or grown in separate wells under G418 selection. Independently-propagated cell-lines were numbered and aliquots taken for storage in liquid nitrogen. Cells were pelleted in a bench-top centrifuge (~1500 rpm, 10 minutes) and gently resuspended in $1/10^{th}$ volume complete DMEM medium supplemented with 10% DMSO before slow freezing (200 µl aliquots) in liquid nitrogen vapour.

2.4.6 Induction of MEL-cells for expression studies

For expression studies, cells were thawed at 37°C, and 50 µl diluted into 10 ml complete DMEM medium. Exponential growth was maintained for a

minimum of four days prior to addition of DMSO (2%(v/v)) to induce differentiation and expression. Cells were suitable for electrophysiological analysis and luciferase activity assays between 0.5 to 5 days post-induction.

2.5 Luciferase assays

After transfection individual cell colonies were tested for inducible luciferase expression by plating 3 x 10^5-10^6 cells per well in 6-well tissue culture plates (Nunclon). After 20 h incubation at 37°C cells were stimulated for 5 h with 20 µM forskolin or appropriate agonist. After removal of the medium the cells were washed with PBS and assayed using the Promega Luciferase Assay System according to the manufacturer's instructions. Luciferase activity was measured on a Pharmacia Wallac 1410 (Sollentura, Sweden) liquid scintillation counter.

Chapter 3

Isolation of a Partial cDNA Homologue of the Retinal Rod Photoreceptor Cyclic Nucleotide-Gated Channel from a Rabbit Sino-Atrial Node Specific cDNA Library

3 Isolation of a pacemaker cNG channel-clone rscNGC 1

Introduction

DiFrancesco and Tortora (1991), demonstrated that within mammalian sino-atrial node (SAN) pacemaker cells, the non-specific cationic conductance I_f, could be *directly* modulated by intracellular levels of cyclic nucleotide second messengers. This raised the possibility that SAN pacemaker cells expressed molecules belonging to the family of cyclic nucleotide-*sensitive* channels. The initial objective of this thesis was to isolate cDNA clones encoding for such family members from a SAN-specific cDNA library.

A SAN-specific cDNA library was prepared from microdissected rabbit SAN according to electrophysiological criteria, so that the library clones were representative of those relevant to the physiology of that tissue. The library was designed so as to reflect 'faithfully' the abundance of gene transcripts in the original mRNA population, i.e the cDNA library was a non-biased representation of the mRNA population. It was predicted that cDNA clones encoding 'rare' or 'low-abundance' channel mRNAs, whose frequency of mRNA in the starting preparation was low, could prove difficult. Therefore the primary objectives of this thesis were; (i) the construction of a cDNA library whose size was sufficient to ensure that rare clones encoding for I_f were represented, (ii) the preparation of a high specific activity probe based on the olfactory cyclic nucleotide-*gated* (cNG) channel — which represented the best route to the molecular cloning of I_f, and (iii) the optimisation of cross-hybridising library screens, to identify and isolate pacemaker cyclic nucleotide-sensitive channel clones of interest.

3.1 Poly A+ mRNA preparation

Poly A+ mRNA was isolated directly from sino-atrial nodal preparations by a number of methods as described in Table 3.1. Of these the fast lysis oligo (dT) selection method (FastTrack, Invitrogen) enabled the isolation of large amounts of high quality mRNA/gram of cardiac tissue.

Table 3.1. Methods employed in the isolation of poly A+ mRNA.

Cardiac Tissue	Poly A+ mRNA Isolation Method	Quantity of Poly A+ mRNA obtained /g of tissue
Young (8 week old) male NZW rabbit (weighing 1.5 kg)	1) FastTrack system. 2) Total RNA isolation by guanidinium isothiocyanate extraction followed by cesium chloride ultracentrifugaton [Chirgwin *et al.*, 1979] and subsequent isolation of poly A+ mRNA by oligo (dT) cellulose affinity chromatography.	33 µg/g 9 µg/g
Adult male rabbit (weighing 2.4-2.7 kg)	1) FastTrack.	5 µg/g

From 1 gram of sino-atrial nodal tissue (approximately 10 seperate nodes, 3 mm in diameter) 5 µg of poly A+ mRNA was obtained. An aliquot of the mRNA was fractionated by electrophoresis on a 1.2% agarose gel and stained with ethidium bromide to check the integrity of the mRNA. This demonstrated a smear of RNA running from 0.5-4.0 kb (as compared to the DNA marker λ/*Hind*III), with the bulk of the mRNA lying between 1.5-2.0 kb. The yield of 5 µg of nodal poly A+ mRNA from adult rabbits, contrasted with the 33 µg obtained from whole cardiac tissue of young rabbits. This six-fold difference could be accounted for by differing levels

of overall transcription, reflecting the relative rates of protein turnover between the respective preparations.

3.2 Construction of the sino-atrial node cDNA library

A unidirectional rabbit sino-atrial node cDNA library was constructed in the Uni-ZAP^{TM} XR vector (Stratagene), from 5 μg of nodal poly A$^+$ mRNA.

The quality and quantity of first and second stand cDNA was analysed by following the incorporation of [α-^{32}P] dATP into synthesized cDNA, by running in parallel a small 'pilot' reaction. The synthesized radioactive cDNA was analysed by electrophoresis through an alkaline 1% agarose gel, which demonstrated a broad distribution of synthesized cDNA molecules. First-strand cDNA molecules ranged in size from approximately 0.5-6.0 kb, with the majority of the material between 1 and 2 kb. Second-strand cDNA made by self-priming ranged in size from approximately 0.5-9 kb (Figure 3.1(a)).

The quantity of the first and second strand cDNA synthesized was determined by following the incorporation of [α-^{32}P] dATP into the synthesized cDNA by scintillation counting. A total of 1.2 μg of first strand cDNA was synthesized from the starting 5.2 μg of poly A$^+$ mRNA, indicating that the efficiency of reverse transcription was of the order of 20%. Approximately 200 ng of this first-strand cDNA was reserved for analysis by PCR amplification (as described in Section 3.5). A total of 1 μg of second strand cDNA was synthesized, demonstrating that the efficiency of second strand synthesis by replacement synthesis was of the order of 85%.

The cDNA was fractionated through a Sephacryl S-400 spin column (Pharmacia) following *Eco*RI linker addition and *Xho*I digestion, in order to remove unligated linker prior to vector ligation, and to select for cDNA species greater than 400 nucleotides in size. The eluted cDNA pool was collected in the first fraction following separation and analysed on a alkaline 1% agarose gel (Figure 3.1(b)). This pool of cDNA was of size

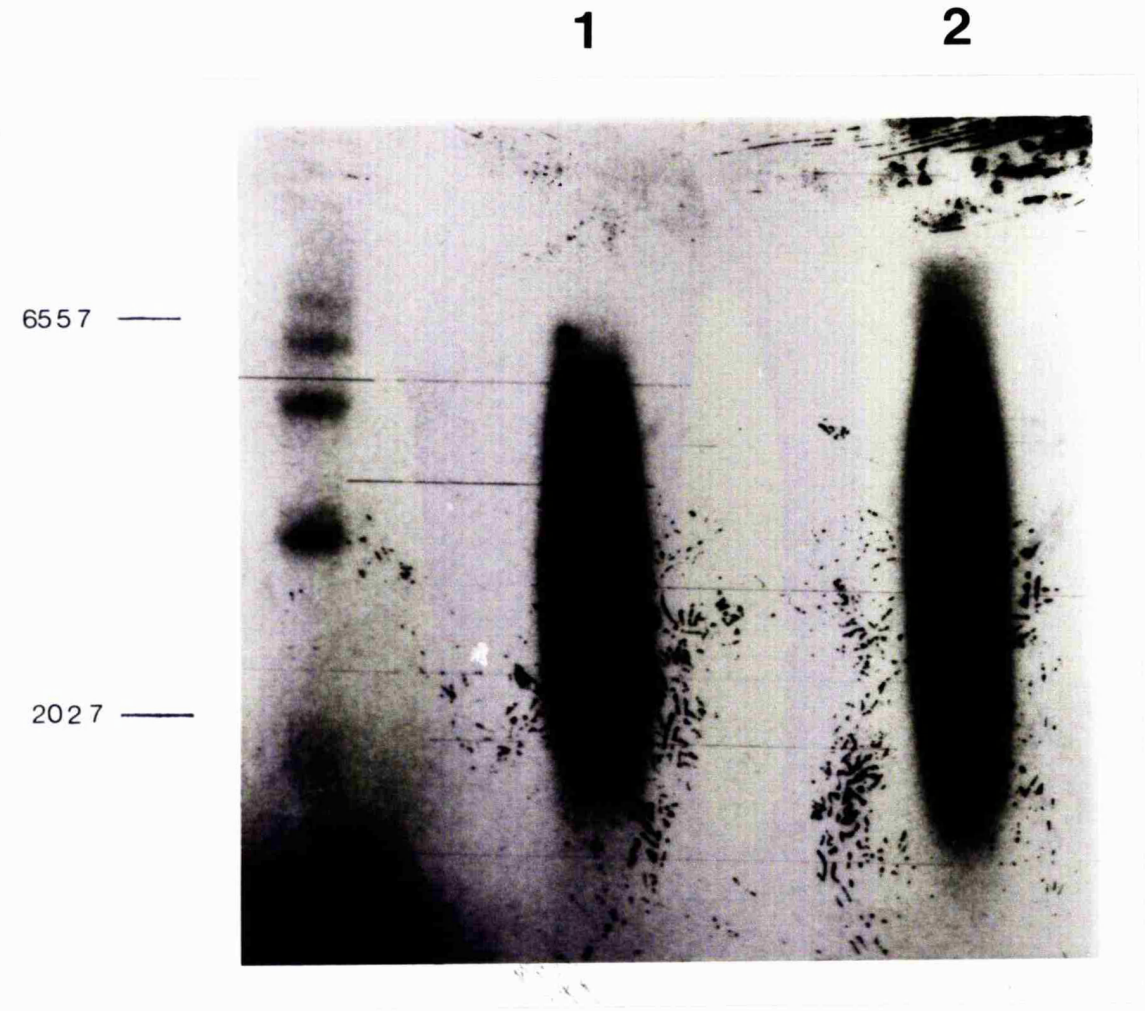

Figure 3.1(a) Analysis of [α-^{32}P] dATP labelled SAN first and second strand cDNA synthesized from 5 µg of poly A$^+$ RNA by electrophoresis through an alkaline 1% agarose gel.

Markers [α-^{32}P] end-labelled λ DNA/*Hind*III molecular size.
Lane 1: First-strand cDNA.
Lane 2: Second-strand cDNA.

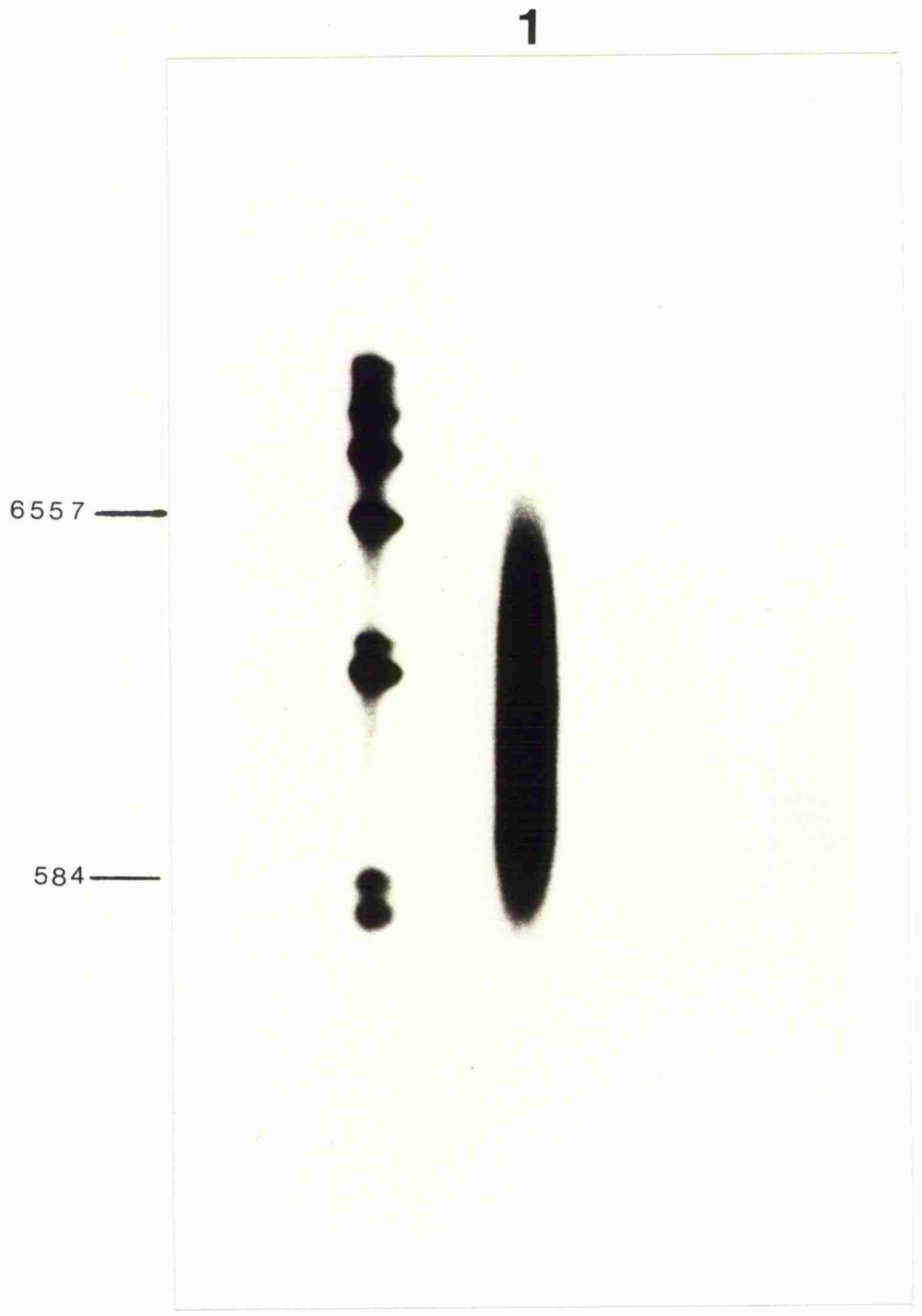

Figure 3.1(b) Analysis of the eluant fractions collected after separation on a Sephacryl S-400 column.

Molecular size markers shown (in base pairs) are [α-^{32}P] end-labelled λ DNA/*Hind*III

Lane 1: First collected fraction.

0.5-4.0 kb and of approximate concentration 50 ng/µl, as judged by an ethidium bromide plate assay. Approximately 150 ng of cDNA was ligated into 1 µg of *Eco*RI/*Xho*I digested Uni-ZAP XR dephoshorylated vector. The ligation mix was packaged *in vitro* and the number of recombinant phages was of the order of 5×10^5 pfu/µg of arms. The total number of recombinant phages possible from the primary sino-atrial node cDNA library was approximately 2×10^6 pfus. The library was immediately amplified to make a large stable quantity of high titre stock of 10^9 pfu/ml.

Ten randomly picked recombinant phages from the primary and the amplified library were excised *in vivo*. Plasmid DNA was prepared from the resulting colonies and digested with the restriction enzymes *Eco*RI and *Xho*I in order to analyse the size of cDNA inserts. Inserts ranged from 0.7-2.2 kb, with a mean insert size of 1.3 kb. This compared favourably with the average size of the mRNA population of approximately 1.8 kb extracted from most types of mammalian cells [Sambrook *et al.*, 1989]. Of the 10 phages analysed from the primary library 6 contained cDNA inserts which were released on *Eco*RI/*Xho*I digestion, whereas all 10 from the amplified library contained inserts. The specifications of the prepared unidirectional λ–ZAP ™ XR rabbit SAN cDNA library are summarised below.

Total number of recombinant phages in primary cDNA library	2×10^6
Titre of amplified library	10^9 pfu/ml
cDNA insert ratio (sample of 10)	primary library 60 % amplified library 100%
Range of cDNA insert size (sample of 10)	primary library 0.7-2.2 kb amplified library 0.7-2.0 kb
Average cDNA insert size	primary library 1.3 kb amplified library 1.3 kb

3.3 Design of cNG channel and β_1, M_2 receptor subtype PCR primers

A pair of PCR primers 'diagnostic' for cyclic nucleotide-gated ion channels were designed to regions of sequence similarity between the published bovine rod photoreceptor and rat olfactory cNG channels [Kaupp *et al.*, 1989; Dhallan *et al.*, 1990], identified by a Pustell DNA matrix comparison using the *MacVector*™ sequence analysis software. This matrix analysis is a variation of the simple dotplot method, where the residues of one sequence are placed along the X-axis of a two dimensional graph and the residues of the other are written along the Y-axis. By placing a 'dot' at each *x,y* coordinate where the residues of the two sequences are identical, regions of similarity are displayed as diagonal dotted lines.

Conserved sequences were identified at the nucleotide level from residues 700-1800 bp of the bovine photoreceptor cGMP-gated channel to residues 600-1700 bp of the rat olfactory cAMP-gated channel (Figure 3.2). From this analysis two PCR primers were designed *roc*A-1 and 2 to the H4 transmembrane and the C-terminal cyclic nucleotide-binding domains (Figure 3.3). These primers encompassed the cyclic nucleotide-binding domain which would be expected to be conserved, amongst the class of cyclic nucleotide-sensitive channels.

PCR primer sets were also designed to cardiac β_1-adrenergic and M_2 muscarinic receptor subtypes — thought likely to modulate nodal cAMP-regulated ion channels such as I_f through G protein-coupled adenylyl cylase pathways. Primers again were designed to conserved regions of these receptor subtypes using the *MacVector* Pustell DNA matrix comparison and are shown in Table 3.2. The third cytoplasmic loop region of the β_1 and M_2 receptors were chosen for the design of sense PCR primers, as their is a great degree of sequence divergence between the various receptor subtypes in this region, which has been suggested to underlie their capacity for differential coupling to distinct biochemical effectors [Nathanson, 1987].

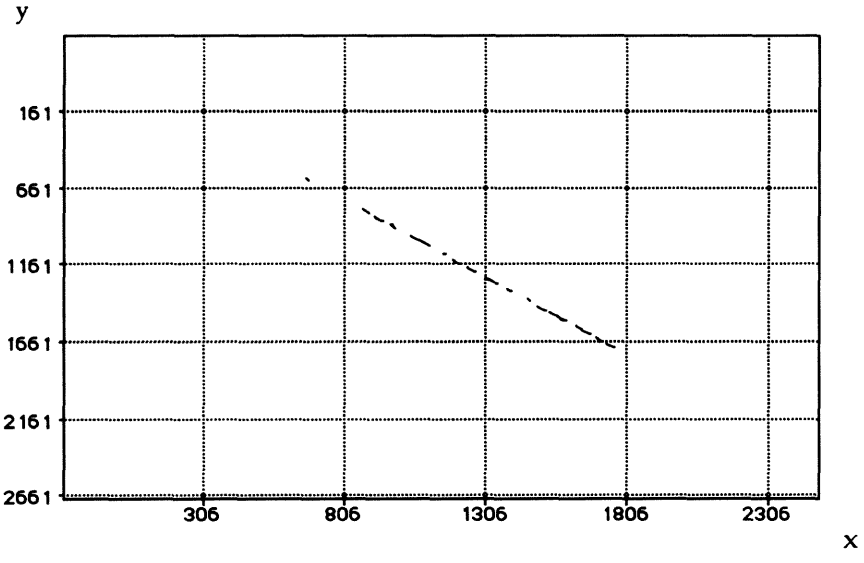

Figure 3.2 A Pustell DNA alignment of the sensory cNG channels.

The bovine rod photoreceptor cGMP-gated channel (x-axis) [Kaupp *et al.*, 1989] has been aligned to the rat olfactory neuron cAMP-gated channel (y-axis) [Dhallan *et al.*, 1990], using a DNA database matrix. Numbers along the axis represent positions of nucleic acid residues in the respective sequences.

Method
A scoring matrix was chosen which scored the DNA alignment as follows;
+4 for a match, -2 for a mismatch, -12 for an indel (insertion or deletion), and -4 to extend an existing indel. A hash value (k-tuple or k-tup), a measure of how long an exact match must be found between two sequences before an attempt to score and align the matching regions is made, was set to a 6-base match. The jump parameter was set such that the hash value represented both the number of bases in a row that must match perfectly and the number of triplets in a row whose first base must match perfectly. The window size was set to 30 nucleotides. A minimum percentage score of 65% was used such that windows whose score equalled or exceeded this were saved.

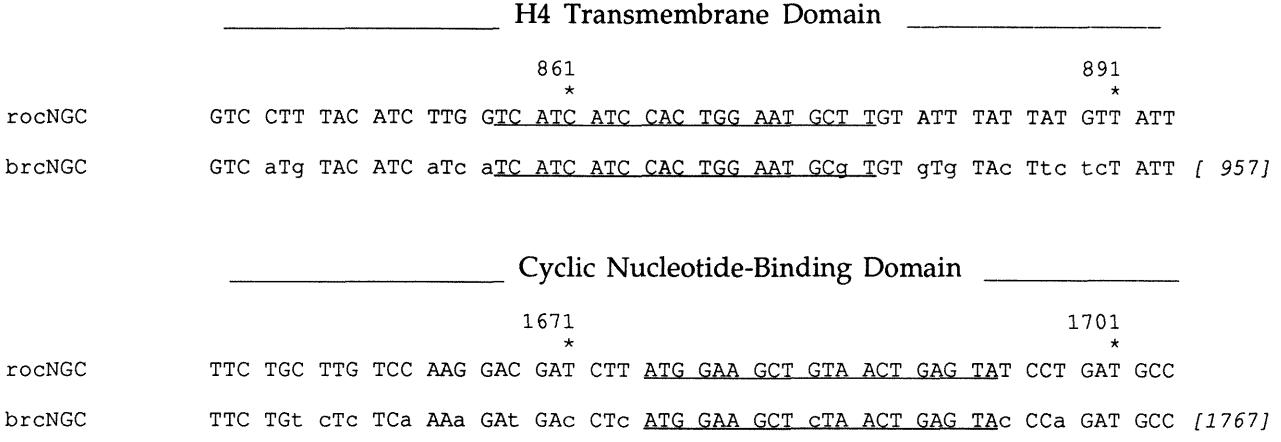

The cNG channel PCR primers chosen were as follows;

*roc*A-1	*5′ TCA TCA TCC ACT GGA ATG CTT 3′*	*Sense*
*roc*A-2	*5′ TAC TCA GTT ACA GCT TCC AT 3′*	*Anti-sense*

which correspond to sequences of the rat olfactory cAMP-gated channel.

Figure 3.3. Regions of the Rat Olfactory cAMP-Gated Ion Channel to which the PCR Primers were designed.

Underlined sequences represent the primer binding sites. Nucleotide similarities and differences between the rat olfactory (rocNGC) [Dhallan *et al.*, 1990] and bovine rod (brcNG) [Kaupp *et al.*, 1989] cyclic nucleotide-gated channels are indicated by upper and lower case letters respectively. Putative functional domains are indicated by lines above the sequence and numbers of the nucleotide residues are given both above and to the right of the respective sequences.

Receptor Subtype	Primer Sequence	Location of Primers	Expected size of PCR product
Muscarinic M_2	5' AAGGACAAGAAGGAGCCT 3' *sense*	Designed to nucleotide positions 655-673 of the third cytoplasmic loop.	
	5' GTTCTTATAATGACACATGAG 3' *antisense*	Designed to nucleotide positions 1364-1385 at the C terminal end.	730 bp
Adrenergic β_1	5' CAGGTGAAGAAGATCGACAG 3' *sense*	Designed to nucleotide positions 764-785 of the third cytoplasmic loop.	
	5' CGGCTCGTCCAGGCTCGA 3' *antisense*	Designed to nucleotide positions 1380-1398 at the C terminal end	634 bp
	5' GTTCTTATAATGACACATGAG 3' *antisense*	Designed to nucleotide positions 1501-1522 of the 3'untranslated region.	758 bp

Table 3.2 Design of PCR primers specific for muscarinic M_2 and adrenergic β_1 receptor subtypes.

Primer sequences shown are those found conserved amongst porcine and rat cardiac muscarinic M_2 receptor subtypes [Peralta *et al.*, 1987; Bonner *et al.*, 1987], and human and rat adrenergic β_1 [Frielle *et al.*, 1987; Gocayne *et al.*, 1987] receptor subtypes.

3.4 PCR amplification of rabbit cNG channel, β_1-adrenergic and M_2-muscarinic receptor sequences from genomic sources

To generate probes for screening the rabbit sino-atrial node cDNA library, for the presence of cyclic nucleotide-sensitive channel clones and their appropriate interacting receptors, the above set of primer pairs were used in PCR amplification of genomic DNA sources. A 830 bp PCR product was obtained with the cNG channel primers on the panel of genomic DNA (Figure 3.4), as would be expected if the cognate gene contained no introns within the amplified region. PCR products were repeatedly unattainable using the β_1-adrenergic receptor primers on any of the panel of genomic DNAs, despite synthesis of a new set of primers. It has been reported that the coding region for both mouse and rat β_1-adrenergic receptors do not contain introns [Shimomura and Terada, 1990; Jasper *et al.*, unpublished], so the reasons for the failure to generate PCR products remain unclear. An expected band of 730 bp was obtained from both rabbit and human genomic DNA with the M_2 receptor subtype primers. However with the rat genomic DNA sample, a single distinct PCR product was not obtained, instead a series of spurious bands were obtained. This probably reflected mispriming during amplification, as a result of species differences in sequence — the M_2 receptor subtype primers were designed to conserved regions found between porcine and human sequences.

3.5 PCR analysis of SAN poly A^+ mRNA and first-strand cDNA demonstrated the expression of a cNG channel and a M_2 receptor subtype within the pacemaker region

0.5 µg of SAN poly A^+ mRNA treated with RQ1 DNase (Promega) was reverse-transcribed using 0.5 µg of the 3' antisense *roc*A-2 and M_2 primers respectively. PCR amplification was performed using the respective primer pairs for 40 cycles and the PCR products were analysed on a 1.2% agarose gel (Figure 3.5(a)). The RT-PCR did not yield distinct PCR products, instead extraneous amplified products possibly due to spurious priming gave a smeared band. Empirically it was found that the choice of the 3' antisense primer as priming both reverse transcription and PCR amplification leads to this observed effect.

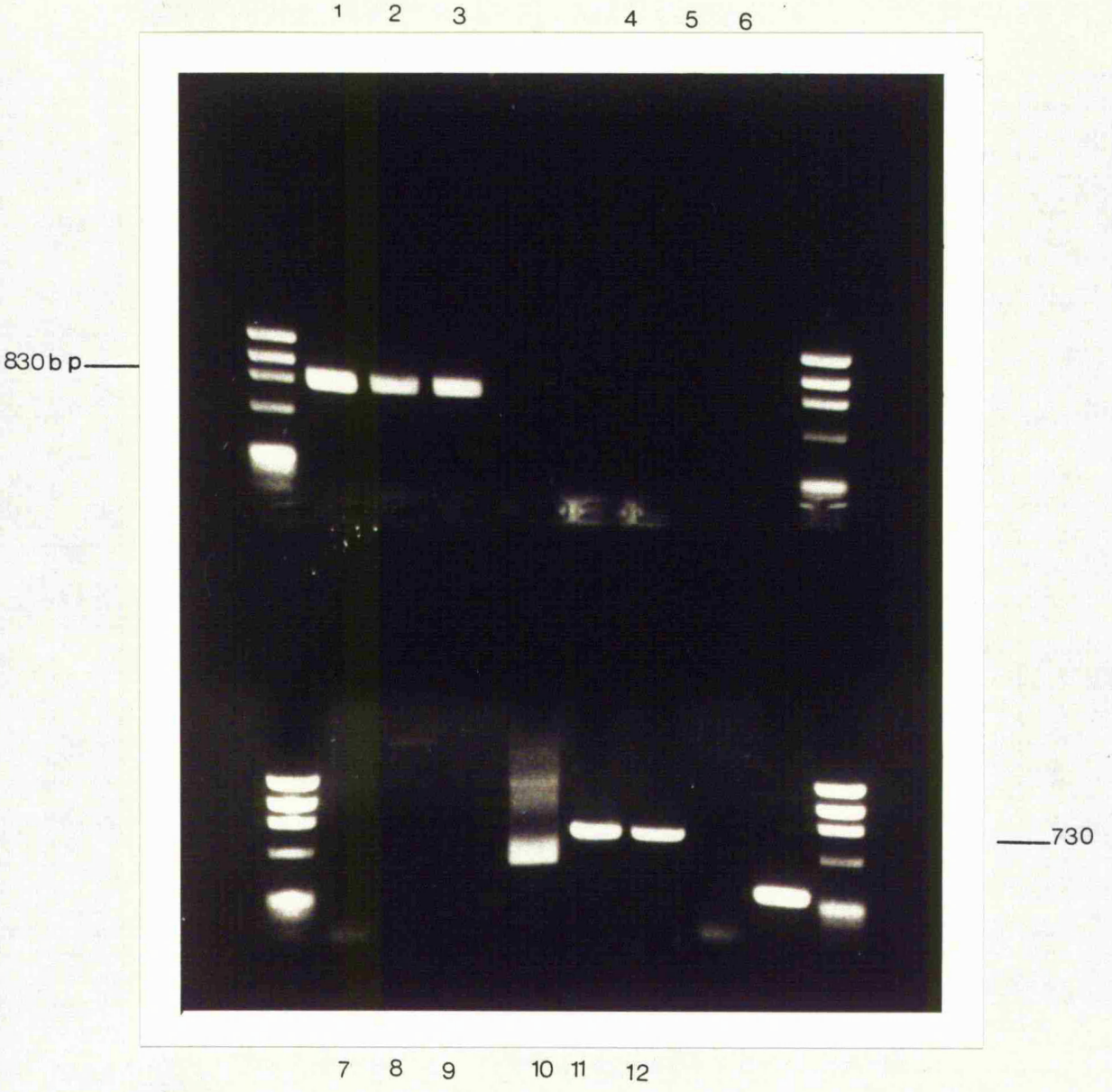

Figure 3.4 PCR amplification of cNG channel, β_1-adrenergic and M_2-muscarinic receptor sequences from genomic sources.

Lane 1, 2 and 3: 50 ng of rat, rabbit and human genomic DNA amplified with cNG channel *roc*A1 and 2 primers.
Lane 4, 5 and 6: 50 ng of rat, rabbit and human genomic DNA amplified with first set of β_1-adrenergic primers.
Lane 7, 8 and 9: 50 ng of rat, rabbit and human genomic DNA amplified with second set of β_1-adrenergic receptor primers.
Lane 10, 11 and 12: 50 ng of rat, rabbit and human genomic DNA amplified with M_2-muscarinic receptor primers.
Molecular size markers shown (in base pairs) ϕX174/*Hae*III .

Samples were amplified for 30 cycles, and a portion of the reaction product was electrophoresed on a 1.2% ethidium bromide-stained agarose gel.

Approximately 120 ng of oligo (dT) primed first-strand cDNA used in the construction of the rabbit sino-atrial node cDNA library, was analysed for the expression of cNG channels and M_2 receptor subtypes by PCR. PCR products of the predicted size were obtained from the SAN cDNA for both the cNG channel and M_2 receptor subtype primer pairs following analysis on a 1.2% agarose gel (Figure 3.5(b)). Similar PCR products were also obtained from whole rabbit heart cDNA.

The RT-PCR study demonstrated that a member of the family of cNG channels was expressed in the SAN region, together with a M_2 receptor subtype which may functional interact with the channel through a second-messenger pathway *in situ*. However, this study was unable to identify the molecular nature of the cNG channel expressed within the sinus node.

3.6 Cloning and characterisation of the 830 bp cNG channel PCR product from rabbit genomic DNA

The 830 bp cNG channel PCR product obtained by amplification from rabbit genomic DNA, was electroeluted following separation on a 1.2% agarose gel and subcloned into *Eco*RV site (containing single T-nucleotide overhangs) of pT7 Blue T-vector (Novagen) (Figure 3.6(a)). This vector was chosen because it contained a T7 promoter upstream of the multiple cloning region, allowing RNA synthesis by *in vitro* transcription. After transformation, blue/white selection was used to isolate 10 white recombinants. A diagnostic *Eco*RI digest was used to identify the relative orientation of the 830 bp cNG channel PCR product in the pT7 Blue T-vector, as cNG channel cDNAs contain an internal *Eco*RI site approximately 600 bp within the 830 bp PCR product. Those recombinants containing an insert whose orientation was such that transcription from the T7 promoter would produce 'sense' RNA, were then sequenced from both termini employing T7 promoter and pUC/M13 reverse primers (sequences given in Materials and Methods). Sequencing confirmed that the 830 bp PCR product was a rabbit equivalent of the olfactory cAMP-gated channel previously described by Dhallan *et al* (1990), from olfactory neurons.

Figure 3.5(a) PCR analysis of SAN poly A^+ mRNA for the expression of a cNG channel and a M_2 receptor subtype within the pacemaker region.

Lane 1: First-strand cDNA primed with the M_2 receptor subtype antisense primer, before amplification with M_2 primer pairs. Annealing temperature 50°C.
Lane 2: First-strand cDNA primed with the cNG channel *roc*A-2 primer, before amplification with *roc*A-1 and 2 primer pairs. Annealing temperature 50°C.
Lane 3: as lane 1 but annealing temperature 55°C.
Lane 4: as lane 2 but annealing temperature 55°C.
Lane 5: Negative control, amplification with *roc*A-1 and 2 primer pairs using 0.1 μg of SAN poly A^+ mRNA as template.
Lane 6: Positive control for amplification, 50 ng of rabbit genomic DNA amplified with *roc*A-1 and 2 primer pairs.

Samples were amplified for 40 cycles, and a portion of the reaction product was electrophoresed on a 1.2% ethidium bromide-stained agarose gel. Molecular size markers shown (in base pairs) are ϕX174/*Hae*III.

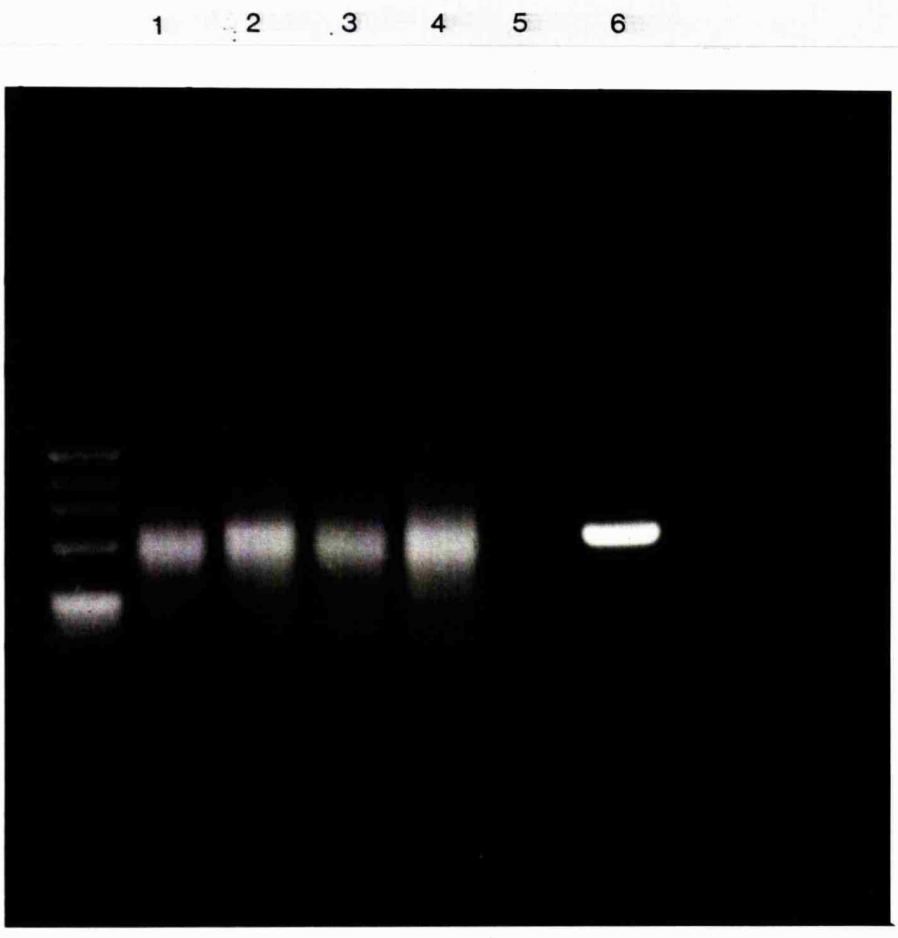

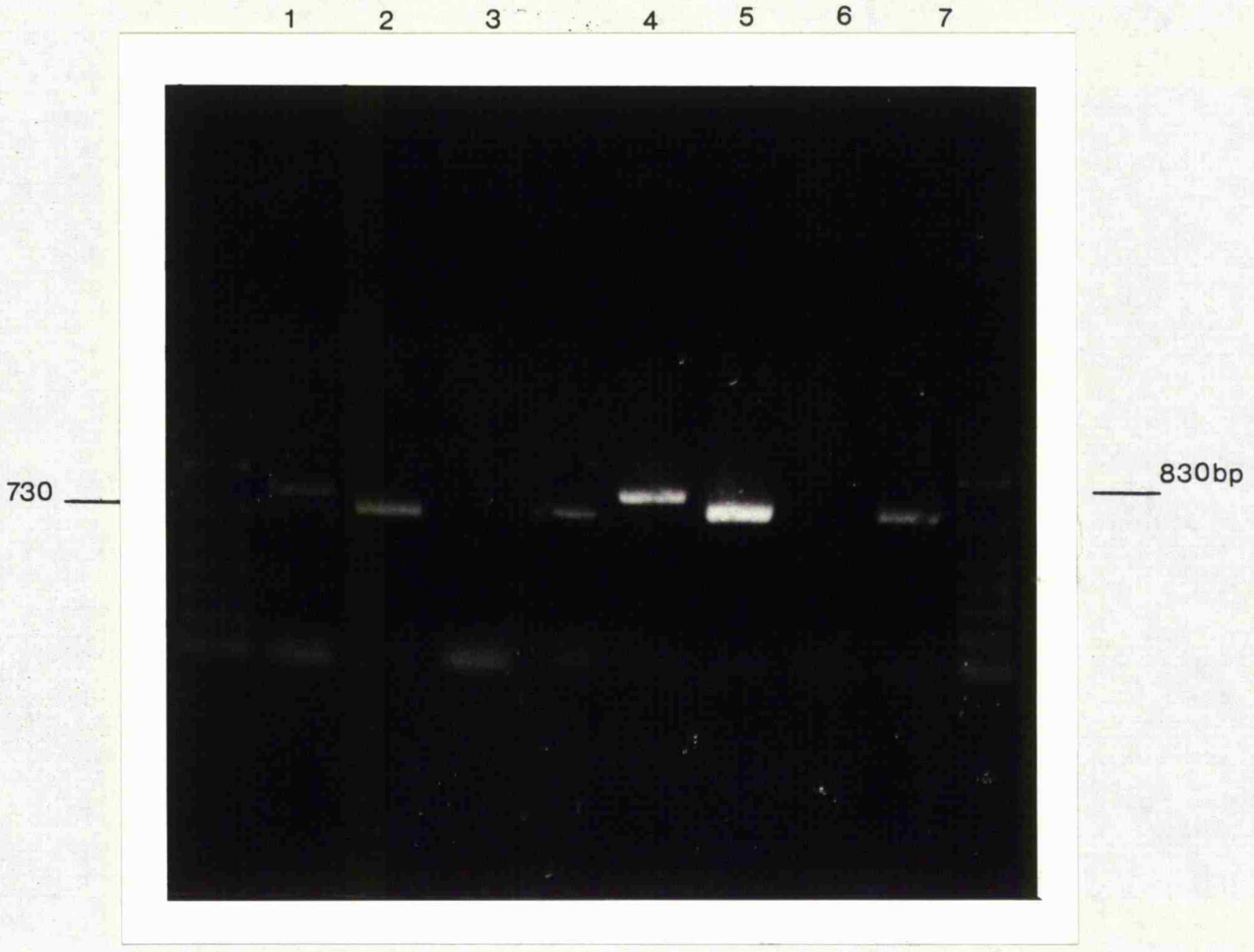

Figure 3.5(b) PCR analysis of SAN library first-strand cDNA demonstrated the expression of a cNG channel and a M_2 receptor subtype within the pacemaker region.

Lane 1: 30 ng of oligo dT-primed SAN cDNA amplified with *roc*A-1 and 2 primer pairs. Annealing temperature 55 °C.
Lane 2: 30 ng of oligo dT-primed SAN cDNA amplified with M_2 receptor subtype primer pairs. Annealing temperature 50 °C.
Lane 4 and 5: Positive controls for amplification 50 ng of rabbit genomic DNA amplified with *roc*A-1 and 2, and M_2 receptor subtype primer pairs. Annealing temperature 50 °C.
Lane 7 : 50 ng of oligo dT-primed whole heart cDNA amplified with M_2 receptor subtype primer pairs. Annealing temperature 50 °C.
Lane 3 and 6. Negative controls. Amplification of both oligo dT-primed SAN and whole heart cDNA with *roc*A-1 and 2 primer pairs. Annealing temperature 55 °C.

Samples were amplified for 40 cycles, and a portion of the reaction product was electrophoresed on a 1.2% ethidium bromide-stained agarose gel. Molecular size markers shown (in base pairs) are ϕX174/*Hae*III.

The PCR product encompassing the following functional domains (Figure 3.6(a)); the S5 transmembrane, H5 putative pore region, S6 transmembrane and the C-terminal cyclic nucleotide-binding domain, represented the best approach for a cross-hybridising screen of the sino-atrial node cDNA library — both for the presence of other cNG channel family members and for the molecular species giving rise to the current I_f, which shares properties of a non-specific cationic conductance and direct cAMP binding in common with cNG channels.

3.7 Preparation of the rabbit cAMP-gated channel probe

Two approaches were used in the synthesis of a high-specific activity cAMP-gated channel probe for screening the SAN cDNA library.

The synthesis of a radiolabelled DNA probe using random hexamers was essentially performed according to the method of Feinberg and Vogelstein (1983). Approximately 200 ng of the 830 bp rabbit cAMP-gated channel PCR product was used as a template to synthesize the radiolabelled probe with [α-^{32}P] dCTP. After separation of the unincorporated dNTPs by centrifugation through a column of Sephadex G-50, a small aliquot of the radiolabelled probe was analysed by electrophoresis on a 1% alkaline agarose gel (Figure 3.7). This demonstrated that the majority of the labelled fragments were less than 500 nucleotides in length. It was reasoned that this could decrease the sensitivity and success of a low stringency cross-hybridisation library screen for low abundance target cNG channel sequences. Approximately 3 x 10^5 pfu lifted and fixed in duplicate to Hybond-N (Amersham) nylon membranes, were screened with the random hexamer primed probe. Putative positives whose hybridising signals were significantly above background were not obtained, following an overnight hybridisation and low stringency wash (as described in Section 3.8).

To increase the sensitivity of the differential hybridisation screen a radiolabelled RNA probe was synthesized. These 'riboprobes' have the advantage of being full-length, and the absence of a complementary strand eliminates the formation of nonproductive hybrids composed of

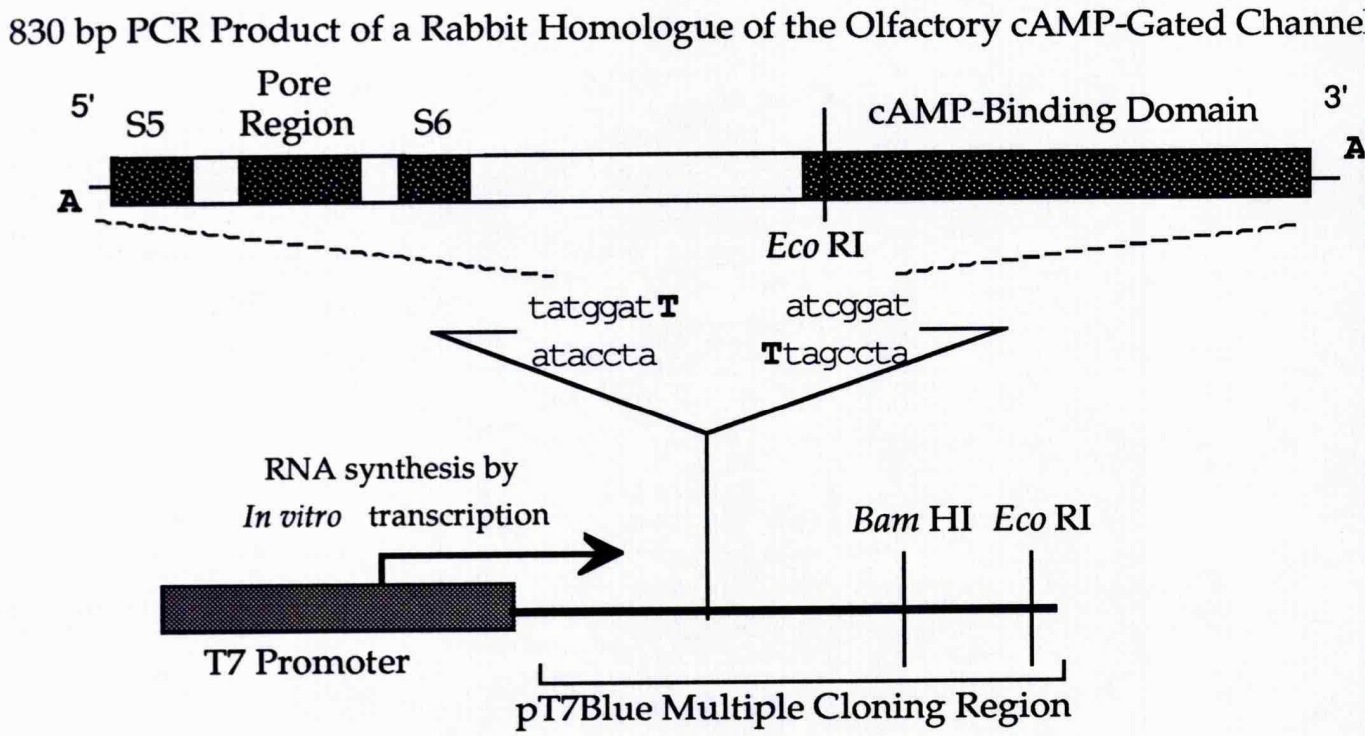

Figure 3.6(a) Schematic diagram representing the cloning of the 830 bp rabbit cAMP-gated channel (830-rcAGC) PCR product into the pT7 vector, downstream of the T7 promoter. Important functional domains of the 830-rcAGC PCR product are indicated.

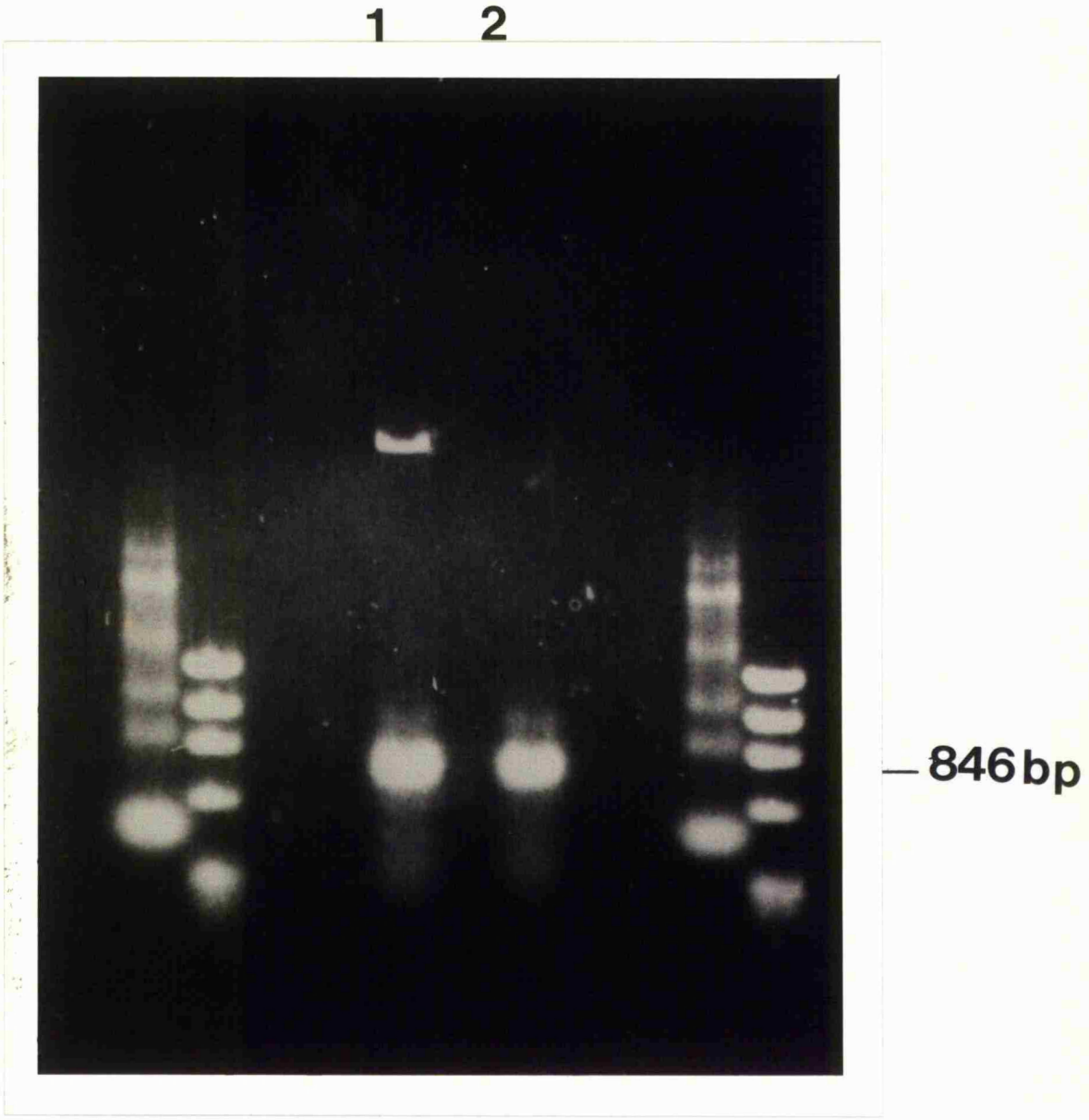

Figure 3.6(b) Generation of 'cold' cRNA for the 846-rcAGC PCR product by *in vitro* transcription using the T7 RNA polymerase promoter.

Lane 1: 2 µl of cold cRNA prior to DNase I treatment.
Lane 2: 2 µl of cold cRNA following DNase I treatment and phenol'chloroform extraction.

1 µg of RNA molecular size marker (0.24-9.5 kb) are shown.

Analysis of the products by agarose gel electrophoresis on a 1.2% gel.

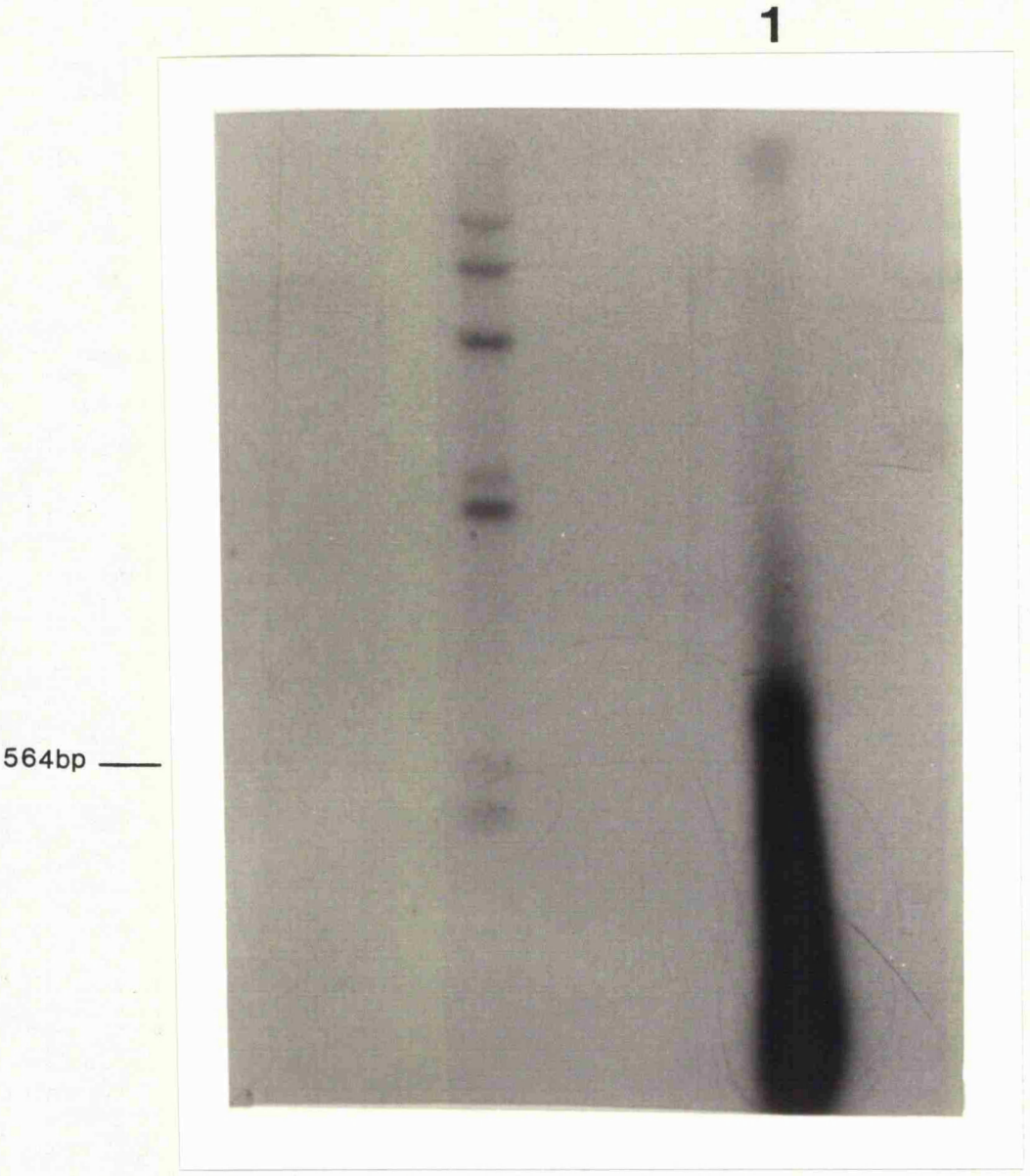

Figure 3.7 Analysis of the [α-^{32}P] dCTP-labelled random hexamer-primed 846-rcAGC probe, by electrophoresis on a 1% alkaline agarose gel.

Lane 1: 2 µl of random hexamer-primed radiolabelling reaction.

Molecular size markers shown (in base pairs) [α–^{32}P] end-labelled λ DNA/*Hind*III.

reannealed probe. These properties increase the likelihood of retrieving rare clones from tissue-specific cDNA libraries [Sambrook *et al.*, 1989].

The 830 bp rabbit cAMP-gated channel (830-rcAGC) PCR product/pT7 Blue T-vector template was prepared for *in vitro* transcription, by digesting 10 µg of Qiagen purified recombinant plasmid to completion with *Bam*HI (an aliquot of the linearised template was analysed on a 1.2% agarose gel to ensure complete digestion). After digestion, the template was Proteinase K treated, phenol/chloroform extracted and following ethanol precipitation, resuspended in DEPC-treated water at a concentration of 0.5 µg/µl.

In vitro transcription was performed 'cold', i.e in the absence of radiolabel to ensure that RNA synthesis was taking place, using T7 RNA polymerase. Analysis of the products by agarose gel electrophoresis on a 1.2% gel (Figure 3.6(b)), demonstrated that the linearised template was producing large quantities of cRNA of the expected size (approximately 800 bp) for the 830-rcAGC PCR product.

The method used for the *in vitro* synthesis of radiolabelled RNA probes of high-specific activity, was essentially a modification of the procedure described by Melton *et al* (1984). A radiolabelled 830-rcAGC probe was synthesized essentially as for the 'cold' reaction, but in the presence of a final concentration of 12 µM of cold rUTP. The proportion of radioactive [α-^{32}P] rUTP incorporated into the riboprobe was quantitated by adsorption onto a DE-81 filter, which demonstrated that ≥ 90% incorporation of the label was taking place. RNA probes of specific activity 0.8-2.5 x 10^8 cpm/µg were routinely synthesized by *in vitro* transcription.

3.8 Screening of the rabbit sino-atrial node cDNA library for the presence of cyclic nucleotide-sensitive channel clones, by nucleic acid hybridisation

Approximately 1.5 x 10^6 pfus from the amplified library were plated with host SURE cells and 0.65% BBL top agar onto 60 x 140 mm NZY plates to give a plaque density of approximately 25,000 plaques/plate. After incubating for 7 hours at 37°C to allow the plaques to grow to a pin-prick

size, the plates were stored overnight at 4°C. 'Plaque lifts' were done in duplicate using Hybond-N (Amersham) nylon membranes, each membrane was oriented by placing 5 asymmetric pinpricks around the membranes edge. Duplicated filters were then denatured, neutralized and UV-crosslinked prior to screening.

The replicate filters were hybridised according to the method of Church and Gilbert (1984). The melting temperature (T_m) — the temperature at which hybrids of the 846 bp-rcAGC RNA probe and its complementary DNA target sequence are 50% dissociated, was estimated by the equation of Casey and Davidson (1977). This gave a calculated Tm of 76°C for the RNA: DNA hybrid in Church and Gilbert buffer. Hames and Higgins (1985), have suggested that for the detection of *distantly*-related members of a family of sequences, the hybridisation should be at a 'relaxed criterion'. The hybridisation was therefore carried out overnight at a temperature of 55°C, which was 15-20°C below the T_m, in order to optimise the rate of annealing of the probe to such distantly-related targets. The volume of the hybridisation solution was kept as low as possible (approximately 25 mls) to enhance the kinetics of nucleic acid reassociation, and to minimize non-specific irreversible binding to the filter approximately 50 ng of ^{32}P-labelled riboprobe/ml of hybridisation buffer was used.

To detect cross-hybridising (closely and distantly-related) sequences the following low stringency washes were performed until background radioactivity on the filters, as monitored with a hand held Geiger counter was below 10 counts per second;

3.0 x SSC, 0.1% SDS at 37°C for 30 minutes,
2.5 x SSC, 0.1% SDS at 45°C for 30 minutes,
and 2.0 x SSC, 0.1% SDS at 55°C overnight.

(This final overnight wash increased the signal: noise ratio making it easier to detect genuine hybridising clones.)

After the final wash, excess buffer was removed from the membrane before wrapping the membrane in Saran Wrap to prevent it from drying

out and exposed to Kodak X-Omat film with an intensifying screen at -70°C for 3 days.

3.9 Isolation of 6-positively hybridising clones

The high plaque density of the primary screen prevented the isolation of single hybridising plaques. Areas of the original master plates containing positive plaques were picked, titrated, and plated out at a density of about 100 plaques per 9 cm diameter plates. Duplicate filters from each plate were screened as above. The specificity of the library screen was analysed by including membranes containing both positive (the pT7-Blue vector harbouring the 846 bp rcAGC-PCR product) and negative (pT7-Blue and pSK- Bluescript vectors without inserts) controls (Figure 3.8(a)). Six clones (numbered rscNGC 1-6 in decreasing order of signal intensity), whose signals were above background noise and duplicated on both membranes were isolated to homogeneity from the second round differential screen. The strength of the signal to noise ratio varied for each individual hybridising clone (Figures 3.8(b) and (c)). Clone rscNGC 1 gave the strongest signal in the differential screen under the low stringency wash conditions (Figure 3.8(c)). Interestingly the duplicated signal was lost by increasing the stringency of the final wash to 0.5 x SSC, 0.1% SDS at 55°C for 2 hours. This suggested that clone rscNGC 1 although possibly related in sequence to the cAMP-gated channel probe, however was not a SAN homologue of the channel.

3.10 Characterisation of clones rscNGC 1-6 by partial sequence analysis

Colonies containing double-stranded recombinant pBluescript phagemids for each rscNGC clone were obtained by *in vivo* excision. Plasmid DNA for restriction analysis and sequencing was prepared by Qiagen purification. The size of the cDNA inserts contained within the clones was determined by agarose gel electrophoresis following a *Eco*RI/*Xho*I double digest and are shown overleaf.

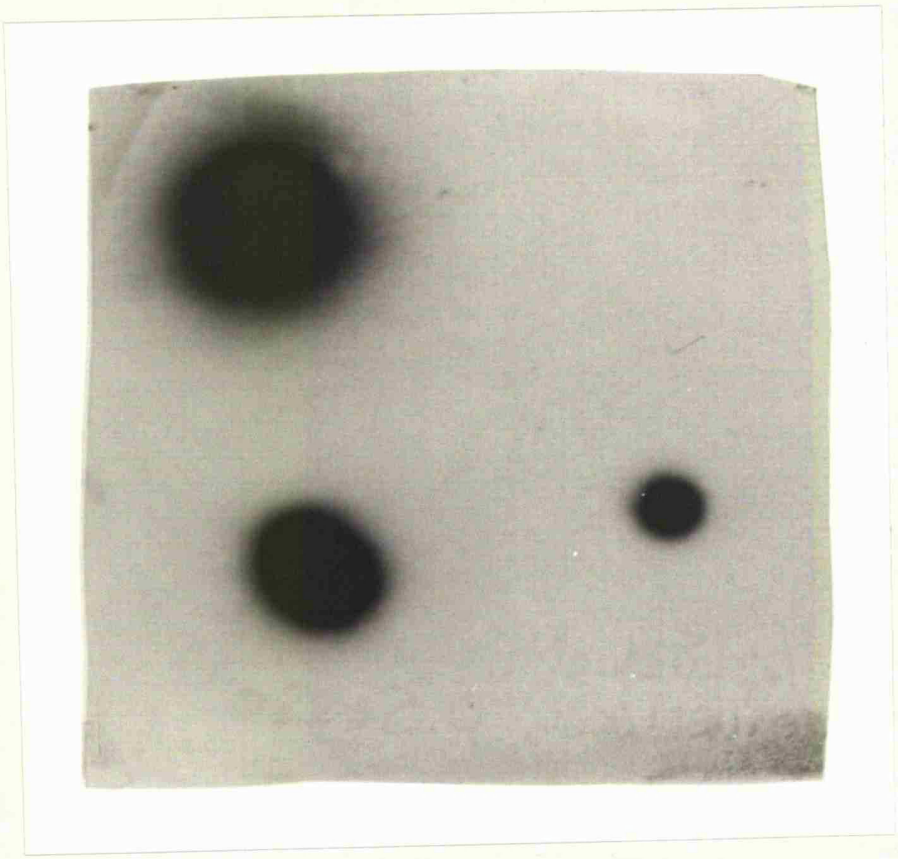

Figure 3.8 Typical hybridisation signals obtained following the second-round low-stringency library screen.

(a) Control filter.
(a) and (b) represent 50 and 20 ng of the recombinant 846 bp rcAGC-PCR product/pT7-Blue vector.
(c) 50 ng pT7-Blue vector.
(d) 50 ng pSK- Bluescript vector.

(b) Example of a typical duplicate filter obtained from the second-round library screen.

(c) The strongly hybridising isolate rscNGC 1 whose signal was duplicated on both filters is indicated.

Final stringency wash of 2.0 x SSC, 0.1% SDS at 55°C overnight. Filters shown were exposed to Kodak X-Omat film with an intensifying screen at -70°C for 3 days.

(b)

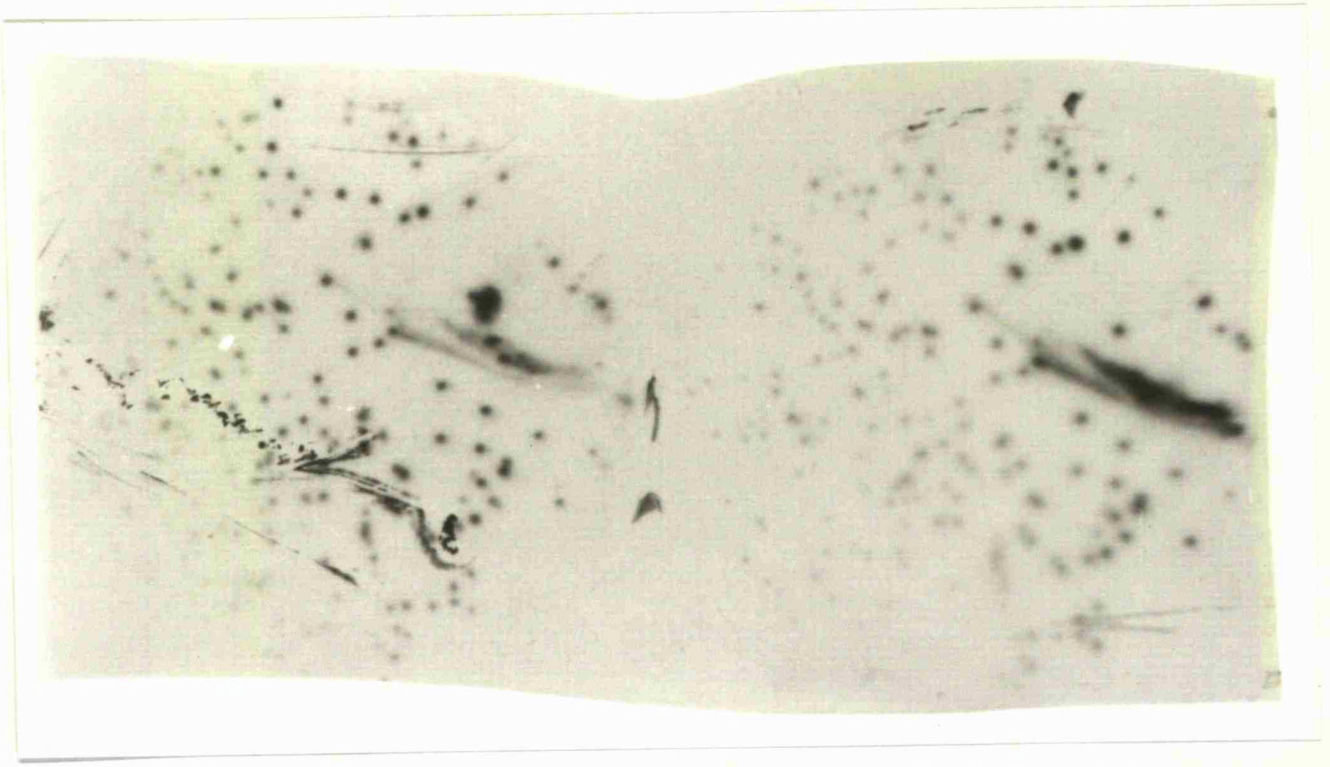

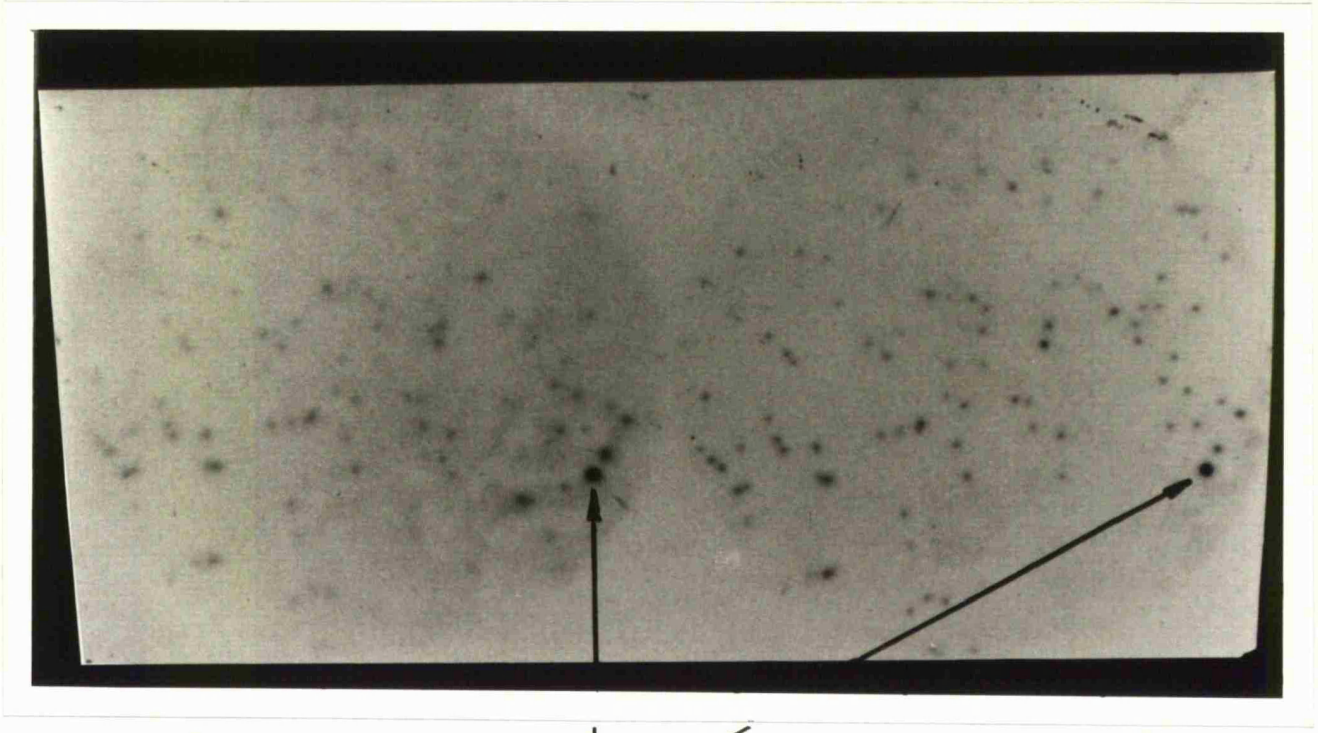

(c)

Isolate rscNGC 1
(Duplicated Signal)

rscNGC Clone Number	Size of cDNA Insert (kb)
1	2.2
2	1.7
3	0.6
4	1.3
5	0.7
6	0.5

Both 5' (employing the T3 primer) and 3' (employing the T7 primer) sequence information was obtained for each clone. 5' sequencing was likely to yield protein coding information and thus provide a clue as to what functional class the cDNA clone may belong to, whereas 3' sequencing (upstream of the poly A tail) served as an internal control for the redundancy of the clones. 3' sequencing demonstrated that each rscNGC clone was derived from a seperate gene transcript.

The 350-400 bp of nucleic acid sequence obtained from the 5' end of each clone was used to search the *Entrez: Sequences* database (release 7.0) distributed by NCBI using the *MacVector*^{TM} sequence analysis software. A Lipman-Pearson DNA library search subroutine was used to screen the database of sequences.

Clone rscNGC 1 showed striking homology at the nucleic acid level to the protein coding and 3' untranslated regions of the cGMP-gated non-specific cationic channel (hrcNGC 1) expressed in the plasma membrane of human vertebrate rod photoreceptors [Dhallan *et al.*, 1992] (Figure 3.9). At the amino-acid level the partial rabbit sequence showed 86% identity to hrcNGC 1. It was concluded that a rabbit *homologue* of the cGMP-gated retinal rod photoreceptor channel gene was expressed in the highly localised region of heart used for the construction of the original cDNA library. This was the first direct evidence to suggest that a cGMP-gated ion channel was expressed in the sino-atrial node (pacemaking) region of the heart. A graphical representation of the alignment of the 5' sequence of clone rscNGC 1 to hrcNGC 1 (Figure 3.10) demonstrated that the 2.1 kb rscNGC 1 clone was truncated at the 5' end, as 3' sequence information had shown the presence of a poly A tail preceeded by 350 bp of

```
hrcNGC 1                    ATT GCC ATT TTT AAT GTG AAC AAC AGC AGC AAT AAG GAC CAG GAA [291]
Clone rcNGC 1               ____________________________________.. ..t ..c ... ... ..a ...

hrcNGC 1          CCA GAG GAA AAA AAG AAA AAG AAA AAA GAA AAG AAG AGC AAG TCA GAT GAT AAA [345]
Clone rcNGC 1     .a. a.a ... ... ... ... ... ... ... ... ... ... ... ..a ... ... ... ...

hrcNGC 1          AAC GAA AAT AAA AAC GAC CCA GAG AAG AAA AAG AAG AAA AAG GAC AAA GAG AAG [399]
                                                              gga
                                                               |
Clone rcNGC 1     ..t ... ... ... ..g ..t t.. ... ... ... ... ... ... ..a ..g ... ... ...

hrcNGC 1          AAA AAG AAA GAG GAG AAA AGC AAA GAT AAG AAA GAA CAC CAC AAG AAA GAA GTT [453]
Clone rcNGC 1     ... ... ... ... ... .c. .ag ... ..a ... ... ... g.g g.g ... ... ... ..c

hrcNGC 1          GTG GTT ATT GAT CCC TCG GGA AAC ACA TAT TAC AAC TGG CTG TTT TGC ATC ACA [507]
Clone rcNGC 1     a.. a.. ... ... ... ..a ... ... ... ... ... ... ... ... ... ..t ... ..t

hrcNGC 1          TTA CCT GTT ATG TAC AAC TGG ACA ATG GTT ATT GCC AGA GCA TGT TTT GAT GAA [561]
Clone rcNGC 1     ... ... ..g ... ... ... ... ..t ... a.. ... ..a ... ..c ... ... ... ...

hrcNGC 1          CTT CAA TCT GAT TAC CTA GAA TAT TGG CTC ATT TTG GAT TAC GTA TCA GAC ATA [615]
Clone rcNGC 1     ... ... ... ... ... ... ... ... ... ... ... .gt ..c ... t.g ... ..t ...

hrcNGC 1          GTC TAT TTA ATC GAT ATG TTT GTA CGA ACA AGG ACA GGT TAC CTA GAA CAA GGA [669]
Clone rcNGC 1     ... ... c.t g.t ..c ... ... ... ... ... c.. ... ... ... ... ...
```

Figure 3.9. Sequence alignment of the sino-atrial node clone rcNGC 1 with the human retinal rod photoreceptor cGMP-gated channel (hrcNGC 1) [Dhallan *et al.*, 1992].

Dots represent nucleotide identities and lower case letters represent nucleotide mismatches to the hrcNGC 1 sequence. Clone rscNGC 1 contains three additional nucleotides as compared to the human channel; these are represented in italics above the sequence. Nucleotide positions are numbered in *parentheses* to the right of the sequence.

Method The Lipman-Pearson search routine was employed to scan the sequences for matches using a fast technique known as hashing. The hash size was set to six, so that only exact matches of six residues were recognised to be a 'hit'. Hits were scored using matrix which assigned the following scores for the query DNA sequence; +4 for a match, -2 for a mismatch, -12 for an indel (insertion or deletion), -4 to extend an existing indel, until a significant region of mismatch was encountered. This gave the initial match score. The final alignment step, inserted gaps in the alignment as necessary to improve the score, only if the initial score exceeded a calculated cut-off score. This optimised score was the score of the best *local* alignment of the matched region of the library sequence and the query sequence. The search was programmed to retain the best 100 matching sequences.

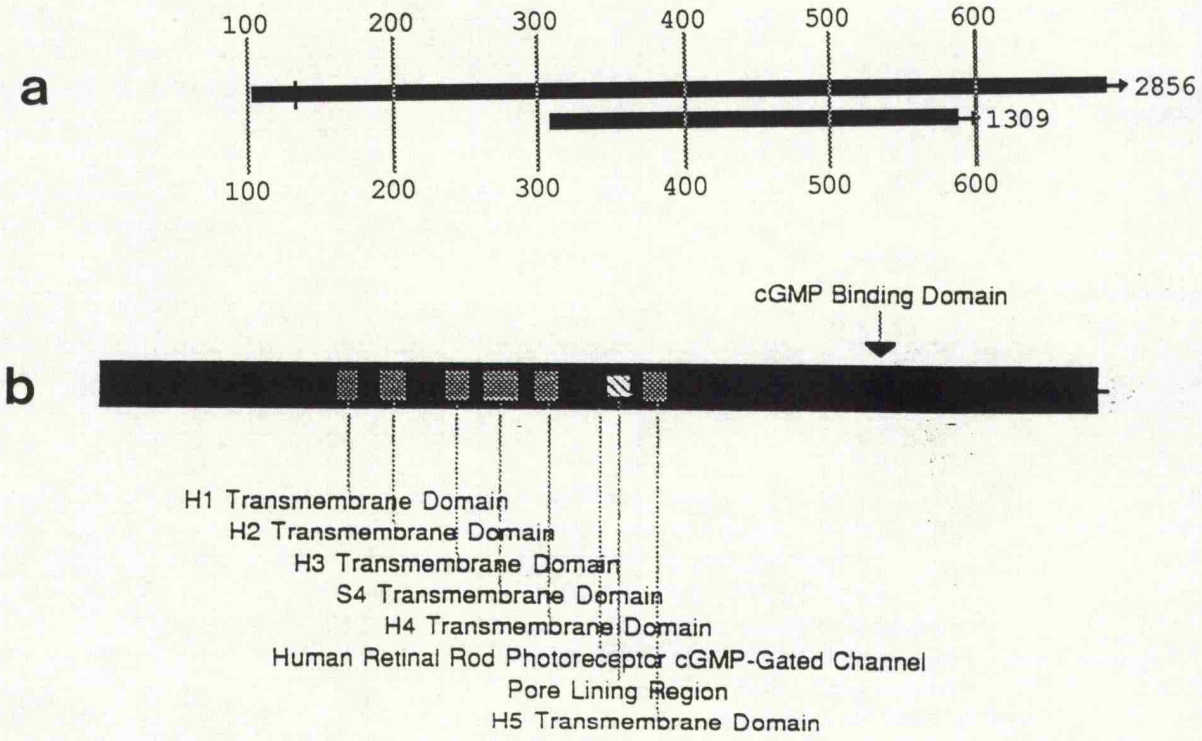

Figure 3.10 A Horizontal map, showing the alignment of the 5' sequence of isolate rscNGC 1 (a) to the human rod photoreceptor cGMP-gated channel (hrcNGC)[Dhallan *et al.*, 1992] (b). Also shown is the alignment of the 846rcA-PCR product used to generate the riboprobe in the cross-hybridising SAN cDNA library screen. Matching regions are represented by bars. Important functional domains of hrcNGC are shown.

untranslated sequence. The truncated clone lacked approximately 290 bp of protein coding sequence, representing the cytoplasmic amino terminus of the cGMP-gated channel.

Clones rscNGC 4 and 5 showed significant homologies to genes encoded by mouse and rat mitochondrial genomes. The 1.3 kb rscNGC 4 clone was identified as a rabbit equivalent of the mitochondrial gene for NADH-dehydrogenase. The 0.7 kb rscNGC 5 clone was identified as being a rabbit equivalent of the mouse mitochondrial genome which encodes a hydrophobic protein that acts as a maternally-transmitted histocompatibility antigen, in one of the reading frames [Loveland *et al.*, 1990].

Analysis of both 5' and 3' sequence information for clones rscNGC 2,3 and 6 failed to show any significant homologies to the current nucleic acid entries in release 7 of *Entrez: Sequences* database. Matches of possible functional relevance obtained from the best 100 matching sequences, are listed in Table 3.3. There appeared to be some weak stretches of sequence homology to both voltage- and ligand-gated ion channels at the nucleotide level. A histogram analysis of the scores was computed according to Lipman and Pearson parameters. Scores that lie more than 10 standard deviations from the mean are classified as being 'significant', greater than 6 standard deviations 'probably' significant, greater than 3 standard deviations 'possibly' significant, with those less than 3 standard deviations as being 'unlikely' to have any significance. The optimum scores obtained for the these clone matches suggest that they fall into the 'possible' significance category. Two of the clones also showed homology to cAMP and cGMP phosphodiesterases (PDEs). These cyclic nucleotide PDEs possess non-catalytic cyclic nucleotide-binding domains that show no detectable amino acid sequence similarity to those of the bacterial cAMP-regulated catabolite gene activator (CAP)-related proteins, which include cNG channels [Shabb and Corbin, 1992]. Thus the rscNGC clones 3 and 6 would not be expected to show significant sequence homology to the ligand binding domain of cNG channel family members.

Table 3.3. Analysis of the *'possible'* significant matches obtained with clones rscNGC 2, 3 and 6.

rscNGC Clone	Length of Score Region (bp)	Maximum Possible Score	Highest Optimum Score	Matches of Relevance Description	Optimum Score	Rank Position
2	580	2124	406	Rat GABA-A receptor alpha-4 subunit gene	366	36
3	561	1916	338	Rat cAMP phosphodiesterase mRNA, complete codons	338	1
				Mouse nicotinic acetylcholine receptor epsilon subunit	292	54
6	553	2080	508	Human DNA for cGMP phosphodiesterase (exons 4-22)	356	25
				Rat GABA-A receptor alpha-6 subunit gene	356	27
				Human voltage-dependent calcium channel beta-1 subunit	336	82

The length of score region defines the size of the rscNGC clone query sequence used in the database search. Maximum possible score is the score obtained for 100% identity of a rscNGC clone to an existing sequence. Highest optimum score is the score for the best local alignment of a matched region of a database entry to a rscNGC clone. Rank position represents the overall place of a 'hit" in the best 100 matched scores. The current *Entrez: Sequences* database release 7 contains 143,579 entries.

Discussion

The first two objectives of this thesis had been met, namely; i) the construction of a SAN specific cDNA library containing reasonably sized cDNA clones of low abundance mRNAs and ii) the retrieval of a nodal channel clone whose gating was directly *dependent* on intracellular cyclic nucleotide molecules, through optimisation of a low stringency differential library screen. This consisted of using a radiolabelled RNA probe-incorporating important cNG channel functional domains, and carrying out a 'relaxed-criterion' hybridisation and low stringency wash.

The isolation of clone rscNGC 1 confirmed the early results obtained by PCR analysis of library first-strand cDNA, that an ion channel belonging to the family of sensory cNG channels was expressed within SAN tissue. This finding is intriguing for two reasons. First there have been no previous reports of a role for such a channel in the SAN region or indeed any cardiac subregion. Secondly, the cyclic nucleotide sensitivity of clone rscNGC 1 necessitates the coupling of appropriate receptors/second messenger systems to gate the channel in the heart; these are unlikely to be related to those types co-expressed in the photoreceptor. I shall return to this theme in Chapter 6. It is expected that the possession of a cyclic nucleotide-binding site in clone rscNGC 1 provides a mechanism for *rapid* activation by cardiac second messenger systems.

Clone rscNGC 1 was unlikely to encode for a cyclic nucleotide-*sensitive* channel molecule having characteristics of the current I_f. In purely electrophysiological terms cNG channels share several characteristics in common with those underlying the current I_f. However a principal difference exists between the two, namely cNG channels are directly and co-operatively *gated* by the binding of cyclic nucleotide molecules to an intracellular domain of the channel, whilst I_f is a *voltage-gated* current where the effect of direct binding of cyclic nucleotides is to *modulate* the voltage sensitivity of the current. This initial work does not exclude the possibility that within the SAN cDNA library there exists further, novel

distantly-related members of the class of cyclic nucleotide-sensitive channels, with characteristics as described by DiFrancesco for the current I_f.

The human retinal rod photoreceptor cGMP-gated channel gene has been cloned and characterised [Dhallan *et al.*, 1992] and contains a transcription unit of 40 kb encompassing 10 exons, of which exons 3-10 form the coding region of the channel. The carboxyl two-thirds of the protein was encoded by exon 10 and the remaining amino terminal third of the channel was encoded by exons 3-9. The presence of several potential splice sites raises the possibility of a sinus node tissue specific splice variant. The existing 5' sequence data obtained for clone rscNGC 1, encompassing exons 6-9, has yet to reveal a nodal-specific splice variant.

The remaining five characterised rscNGC clones 2-6 fall into two categories; i) those that do not share any strong nucleic acid sequence homology to previously-characterised molecules, including ion channels, and ii) those that appeared to be rabbit equivalents of mitochondrial genes.

From the differential library screen these clones could be described as *weak* hybridising positives, as their signals were marginally above background. Although the three uncharacterised clones could encode for novel protein molecules, they were unlikely to represent distantly-related members of the class of cyclic nucleotide-sensitive channels, and were therefore not characterised further.

Chapter 4

Molecular and Functional Characterisation of Clone rscNGC 1 A Sino-Atrial Node Cyclic Nucleotide-Gated Channel

Introduction

Low stringency differential screening of the SAN cDNA library had resulted in the isolation of a nodal homologue of the photoreceptor cGMP-gated channel — clone rscNGC 1. Whether the partial clone rscNGC 1, through alternative splicing, exhibited unique structural and electrophysiological properties distinct from the photoreceptor cGMP-gated ion channel (discussed in Chapter 1), could only be addressed following retrieval of the 5' sequence predicted to encode the cytoplasmic N-terminus. The full coding region was necessary, both for the study of the molecular structure of clone rscNGC 1 and for functional expression — leading to complete electrophysiological characterisation. The isolation of truncated 5' regions is not unusual in cyclic nucleotide-gated channel (cNG) cDNAs, as partial clones for retinal rod [Dhallan *et al.*, 1992] and cone [Bönigk *et al.*, 1993] photoreceptor cGMP-gated channels were also previously isolated from oligo (dT)-primed cDNA libraries. This common truncation point might arise from secondary structure instability within the 5' end of the messenger RNA molecule, which would be predicted to obstruct the procession of reverse transcriptase along the entire gene transcript.

As discussed in Chapter 3, the human cGMP-gated ion channel gene has been characterised [Dhallan *et al.*, 1992]. The gene consisted of at least 10 exons and was shown to be located to chromosome 4, with a transcription unit of greater than 40 kb in length. The large exon 10 encodes the carboxyl-terminal portion (approximately two-thirds of the protein), whereas seven small exons encode the amino-terminal portion of the channel. The gene organisation is shown in Figure 4.1. The large number of introns interrupting the amino-terminus of the channel protein, dictated that the 5' protein coding sequence of clone rscNGC 1 could not be retrieved from genomic DNA sources. Furthermore retrieval of a cDNA was not expected to be straight forward, as isolation of a single clone representing a homologue of the rod cGMP-gated channel from 1.5 million recombinants of the SAN regional-specific library, and the observation of low-level signals in Northern hybridisation studies from

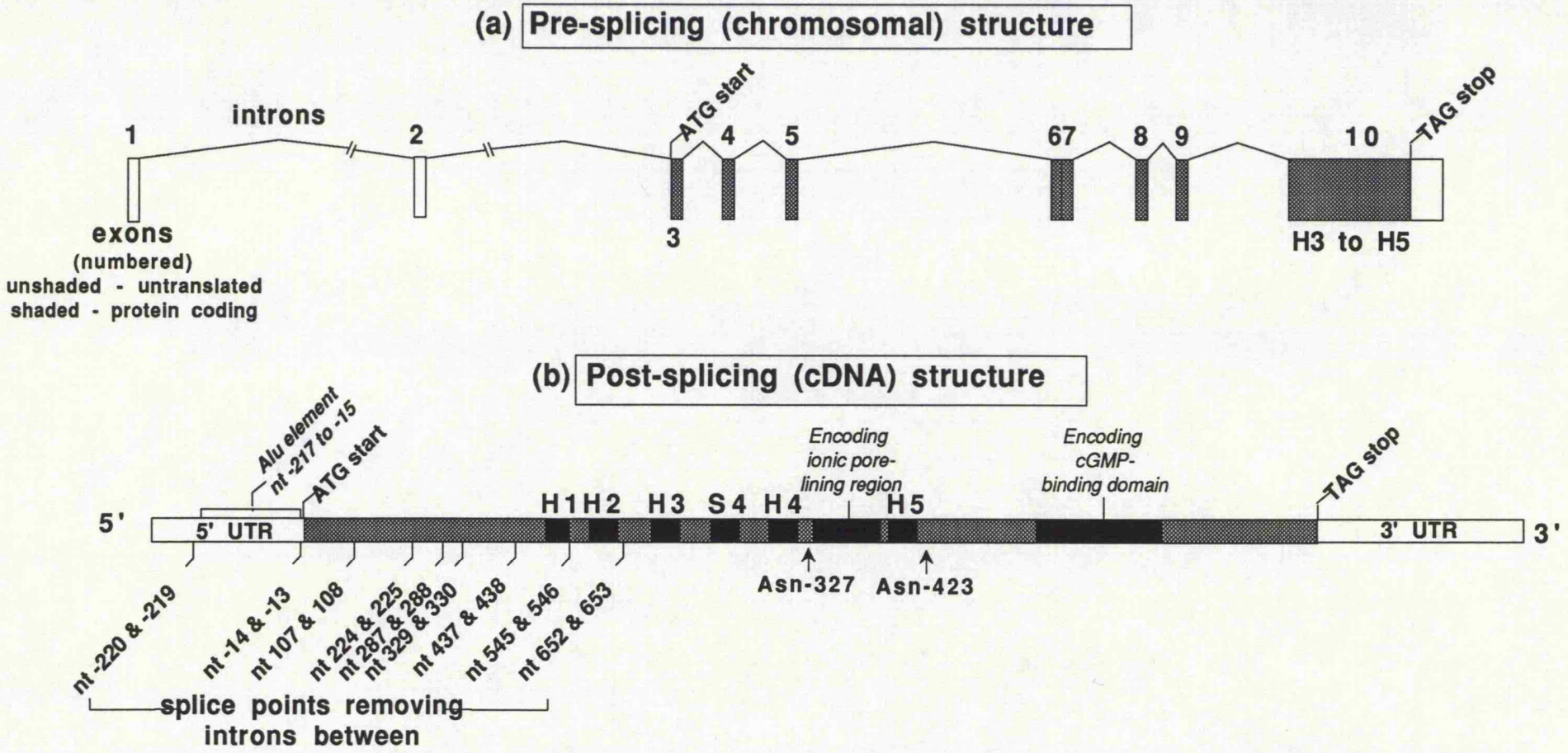

Figure 4.1 Human cGMP-gated channel gene structure.

The gene encompasses 10 exons shown in (a), the large exon 10 encodes the C-terminal two-thirds (457 aa) of the protein, whereas seven exons encode the amino-terminal one-third (229 aa). The sequences at each exon-intron boundary conform to consensus splice junction sequences. The nucleotide position of the intron splice points are numbered relative to the initiating ATG and are shown in *italics* in (b). Exon numbering is tentative, based on exon 1 containing the most 5' proximal sequences found in the cDNA [Dhallan et al., 1992]. Important functional domains of the cNG channel product are indicated above the final cDNA structure. Putative glycosylation sites (Asn) are shown, numbered according to amino acid position. 5' and 3' UTR represent 5' and 3' untranslated regions of the final cDNA.

vasculature [Biel *et al.*, 1993], confirmed the low abundance nature of cNG channel mRNA in heterogeneous multicellular preparations. As a consequence, the best route for retrieval of a 'full-length' protein coding sequence for clone rscNGC 1 was via direct amplification using PCR, which would circumvent the significant problem of low abundance.

4.1 PCR analysis of amplified cDNA library extracts for the presence of rscNGC 1 clones containing 5' sequences

4.1.1 Generation of PCR products by amplification employing a 'conserved' sense primer

PCR amplification methods were employed on 1 µl aliquots of the amplified library stock (~10^6 recombinants), to determine whether the library contained rscNGC 1 equivalent cDNA clones with longer 5' sequences. Amplification employing sense pBluescript reverse and T3 primers — located 5' to cloned cDNA inserts, and a rscNGC 1 clone-specific antisense primer *rsc*G-1, complementary to the first transmembrane domain H1 (see Materials and Methods for sequences), at first failed to produce homogenous PCR products from the sampled library stock. In a number of separate trials 'smear' products were repeatedly obtained on agarose gels.

As an alternative approach, available cDNA sequence information for human [Dhallan *et al.*, 1992], bovine [Kaupp *et al.*, 1989] and mouse [Pittler *et al.*, 1992] retinal rod photoreceptor cGMP-gated ion channels (rcNGC), was used to design a consensus ATG translation initiation sense primer (cATG-ts) (Table 4.1). This consisted of a 23-base sequence following the initiating methionine, encoding the first 7 codons of the rcNGC family. 5' to this sequence, a 12-base ribosome binding sequence was incorporated. This sequence has been shown to be important for the initiation of translation [Kozak, 1991].

In order to increase the efficiency of cDNA library screening by PCR amplification, an aliquot of recombinant Uni-ZAP XR λ Library was deproteinised and resuspended in TE buffer. This increased the number of putative targets by a factor of 25. PCR amplification, employing 1 µl of the

Table 4.1 Design of the concensus cATG-ts primer.

Table shows an alignment of the first seven codons encoding for retinal rod photoreceptor cDNA clones from human, mouse and bovine (references given in the text). The Kozak sequence is shown in italics, with the initiating methionine for concensus cATG-ts primer underlined. Identical and non-conserved nucleotides to the concensus sequence are represented by upper and lower case characters, repectively.

	Kozak Sequence	Alignment of the initiating start codon
Conserved ATG translation initiation primer (cATG-ts)	*GCC GCC GCC*	*ATG* AAG AAA AAT ATT ATC AAT AC Met Lys Lys Asn Ile Ile Asn Thr
Human rcNGC	*CC*	*ATG* AAG AAc AAT ATT ATC AAT AC
Mouse rcNGC	*CC*	*ATG* AAG AAc AAT ATT ATC AAT AC
Bovine rcNGC	*CC*	*ATG* AAG AAA gtg ATT ATC AAT AC

λ preparation as template, was carried out using the cATG-ts sense primer and the antisense primer *rsc*G-1 (Figure 4.2(a)).

At this stage the expected PCR product (of the of the order of ~ 650 bp) was not obtained following analysis of the products by agarose gel electrophoresis (Figure 4.2(b)). However amplification employing the cAMP-gated channel primer pairs *roc*A-1 and 2 (described in Chapter 3) gave rise to expected 846 bp products, using 1μl volumes of the λ preparation and 'neat' amplified cDNA library stock as templates. These bands were not due to any genomic DNA contamination of the library, as PCR amplification using verified opsin primers failed to produce bands of the expected size (Figure 4.2(b)). The results suggested that the integrity of the phage DNA obtained from the λ preparation had been maintained, and that the failure to retrieve PCR products carrying the 5' protein-coding region of the rscNGC 1 clone, was either due to an absence of authentic targets within the library or possibly to poor PCR primer design.

A modified antisense rscNGC 1 clone-specific primer *rsc*G-2, upstream of primer *rsc*G-1 (Figure 4.2(a)), whose T_m (~ 64°C) and length (25-nucleotides) were similar to primer cATG-ts (T_m~62°C) was designed, for optimisation of the PCR screen (see Materials and Methods for sequence). 40 cycle PCRs using 1 μl of the λ preparation of the library as template, were performed. Instead of an expected size of 350 bp (as predicted if the primary transcript encoding rscNGC 1 was spliced in an identical manner to that of the retinal rod transcript), two prominent smaller PCR products were obtained, of size 150 and 170 bp (see Figure 4.2(c)). It was thought that these products, could represent alternative 5' transcripts of clone rscNGC 1, created by differential mRNA splicing.

4.1.2 Characterisation of 150 and 170bp PCR products

The two smaller PCR products were successively subcloned — following blunting and kinasing, into a *Sma*I digested, dephosphorylated pUC 18 plasmid. Sequencing employing the universal primer (see Materials and Methods for sequence), generated 3' sequence information for both clones. The 170 bp PCR product displayed no sequence similarity at all to clone rscNGC 1 or to any other previously-isolated rcNGC proteins, although weak sequence similarity was shared with the 3' end of the rat olfactory

Figure 4.2 PCR amplification screen of the amplified SAN cDNA library for rscNGC 1-equivalent cDNA clones carrying 5' coding sequence.

(a) A diagramatic representation of the 5' gene structure of the human rod photoreceptor cGMP-gated channel (hrcNGC 1), demonstrating the cognate target sequences for the PCR primers cATG-ts, *rsc*G-1 and 2. Shown are the PCR products that would be obtained from the SAN amplified library stock, if clone rscNGC 1 was differentially spliced analogous to that of hrcNGC 1.

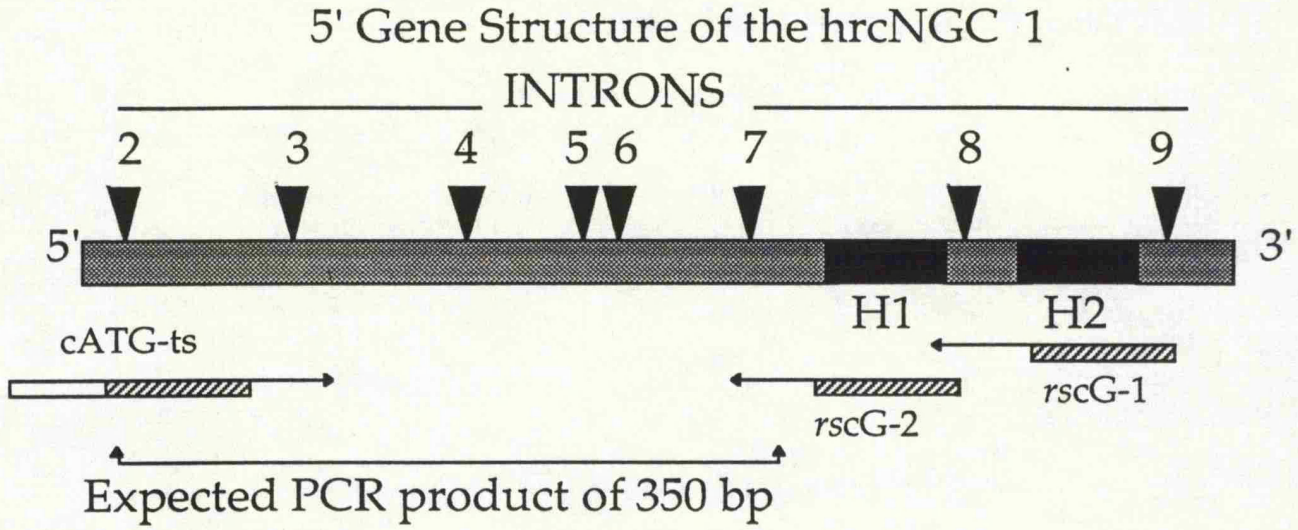

(b)

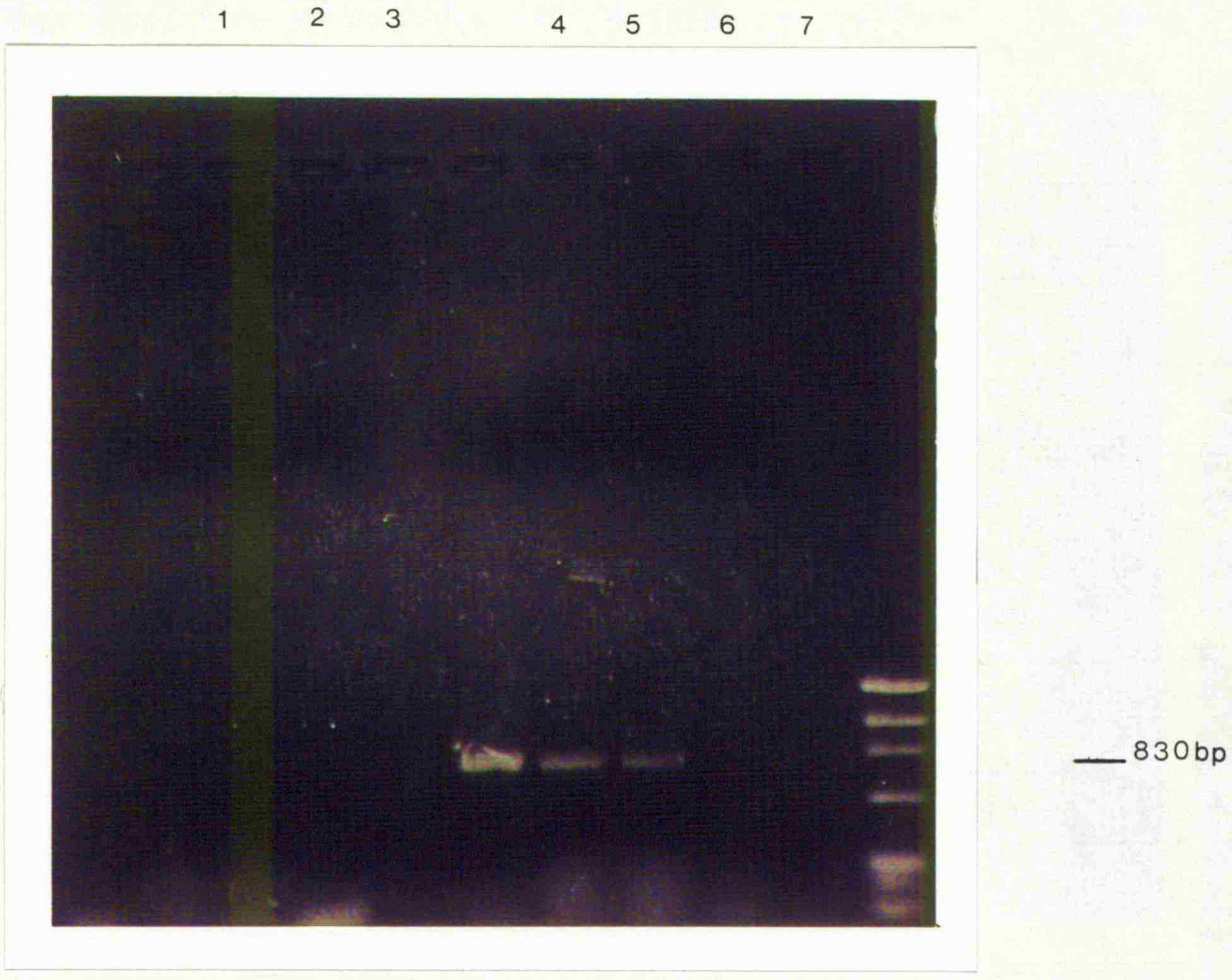

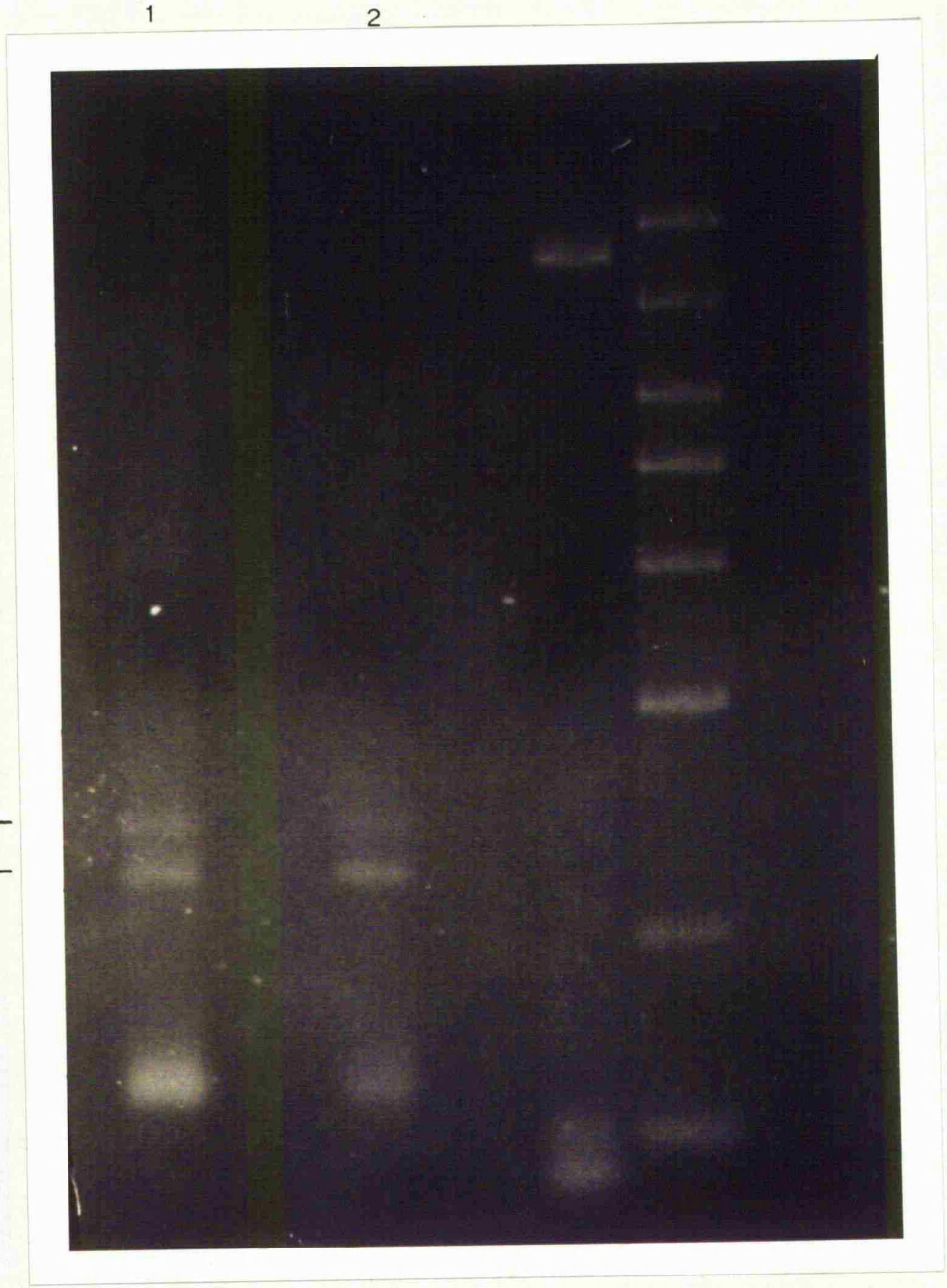

(b) Lane 1: 1 µl of λ preparation as template with cATG-ts and *rsc*G-1 as primers. Annealing temperature (AT) of 50°C. Lane 2: As Lane 1 but amplification at an AT of 55°C. Lane 3: 1 µl of λ preparation as template with opsin primers. AT 50°C. Lane 4: 1 µl of λ preparation as template with *roc*A1 and 2 primers. AT of 50°C. Lane 5: As Lane 4 but amplification at an AT of 55°C. Lane 6: 1 µl of neat cDNA library as template with *roc*A1 and 2 primers. AT of 50°C. Lane 7: Negative control. No template with *roc*A1 and 2 primers. AT of 50°C. Molecular size markers shown (in base pairs) ϕX 174/*Hae*III DNA.

(c) Lane 1: 1 µl of λ preparation as template with cATG-ts and *rsc*G-2 as primers. AT of 55°C. Lane 2: As Lane 1 but amplification at an AT of 58°C. Lane 3: Positive control. 1 µl of λ preparation as template with *roc*A1 and 2 primers. AT of 55°C. Molecular size markers shown (50-1000 bp) PCR size markers.
Samples were amplified for 40 cycles, and a portion of the reaction product was electrophoresed on a 1.8% ethidium bromide-stained agarose gel.

cAMP-gated channel (Figure 4.3(a)). The 150 bp PCR product did show sequence homology to the 5' end of clone rscNGC 1 (Figure 4.3(b)). The sequence of the antisense PCR primer *rs*cG-2 can clearly be seen at the 3' end of this PCR product. However, the sequence at the 5' end shows considerable divergence to that of clone rscNGC 1, such that their is no obvious similarity. The possibility that this sequence divergence was due to alternative exon usage was eliminated by a comparison with the human hrcNGC gene which revealed the presence of an intron further upstream of this divergent region.

These 'spurious' PCR products were probably a result of mismatch annealing of primers to nontarget sequences. Their smaller size as compared to the expected target size of 350 bp, probably resulted in more efficient amplification over a 40-cycle PCR. Such large number of cycles were required due to the extremely low abundance nature of cNG channel transcripts, making the isolation of their corresponding cDNAs difficult.

4.2 Retrieval of the 5' end of clone rscNGC 1 from native atrial tissue by 'anchor-PCR'

4.2.1 Approach

The 5' protein coding region of clone rscNGC 1 was retrieved from a rabbit atrial poly A^+ mRNA preparation, essentially by an 'anchor-PCR' method termed 5'-AmpliFINDER RACE (Clontech). This technique, a combination of SLIC (single-strand ligation to single-stranded cDNA) [Dumas *et al.*, 1991] and the original RACE (rapid amplification of cDNA ends) [Frohman *et al.*, 1988], allowed the generation of 5' upstream sequence for clone rscNGC 1, from which the protein coding region was retrieved by sequential PCR amplifications.

The following set of 'nested' antisense primers were designed to clone rscNGC 1; GSP-1 to prime cDNA synthesis and GSP-2 which annealed to the putative H1 transmembrane domain upstream from GSP-1 for PCR amplification (the sequences of these and other primers used in the anchor-PCR are shown in Figure 4.4). A nested primer was designed for PCR amplification in order to increase the specificity of the amplification

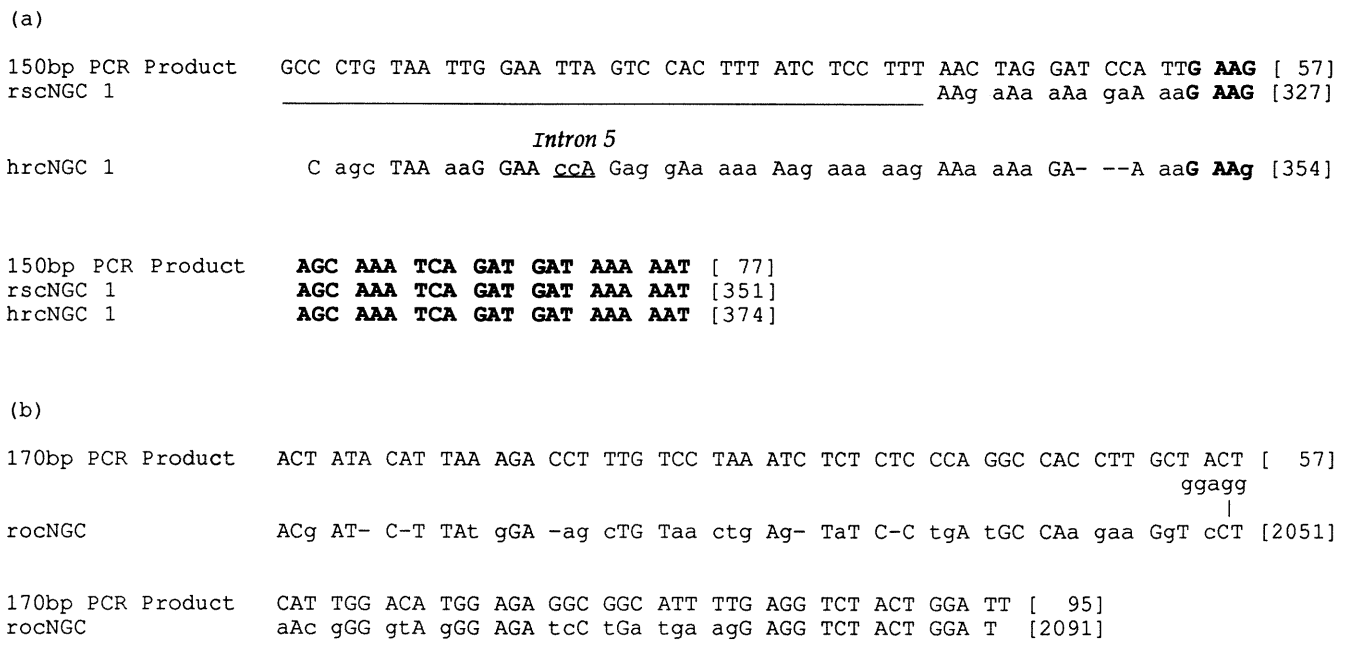

Figure 4.3 Characterisation of the 3' sequence of the 150 bp (a) and 170 bp (b) PCR products by sequence similarity searches.

Alignments are shown to the human rod photoreceptor cGMP-gated channel (hrcNGC 1) [Dhallan *et al.*, 1992] and to the rat olfactory cAMP-gated channel (rocNGC) [Dhallan *et al.*, 1990]. Nucleotide identities and mismatches to the PCR products are shown in upper and lower case letters respectively. Sequence of the antisense primer *rsc*G-2 is shown in bold face and the position of intron 5 in the hrcNGC 1 gene is underlined and shown in italics, in (a). Hyphens have been introduced for optimal alignment. Position of nucleotide residues are shown in *parentheses* to the right of the sequence.

Method of similarity search was the same as that described in Figure 3.9.

reaction. Both primers were designed so that their lengths, GC composition and there approximate T_m values were similar to those of a sense anchor primer sequence (Figure 4.4). Furthermore GSP-2 was designed specifically to the H1 domain of clone rscNGC 1, because within that region there existed a unique restriction enzyme site for *Bsu*36I. This would permit (at a latter stage) the construction of a full-length cDNA representing the complete protein coding region for clone rscNGC-1.

Due to the limiting amount of rabbit sino-atrial node tissue, 2 μg of poly A^+ mRNA extracted from the upper right atrial subregions of rabbit heart was used as template for first strand cDNA synthesis. Previous work using reverse transcription-PCR had demonstrated the expression of the cGMP-gated ion channel within the atrial tissue surrounding the sinus node [C.F Ratcliffe, unpublished], and as a result such channel transcripts would be expected to be present within the extracted poly A^+ mRNA population.

4.2.2 *Anchor RACE failed to produce homogenous PCR products*

The strategy used in the retrieval of the 5' protein-coding sequence of clone rscNGC 1 is illustrated in Figure 4.5. GSP-1 was used to prime synthesis of first-strand cDNA from the atrial poly A^+ mRNA by reverse transcriptase. A single-stranded anchor was directly ligated to the 3'-end of the first strand cDNA by using T4 RNA ligase — avoiding homopolymeric tailing as described in the original RACE technique [Frohman *et al.*, 1988]. Following anchor ligation, an aliquot of the cDNA was used as a template for PCR amplification using the complementary anchor primer and nested GSP-2 primer. 35-cycle amplification was performed at annealing temperatures of 60 and 62°C — which were ~2-4°C below the predicted T_ms of the above primers. This mediated approach which included i) limiting amplification to the desired product using the nested PCR strategy, and ii) increasing specificity of amplification by allowing primer annealing and extension to be carried out at high temperatures, was predicted to produce homogeneous products by reducing non-specific primer extension. However, analysis of the PCR products (Figure 4.6(a)), revealed a smear of heterogeneous products at an annealing temperature of 60°C, from which two very faint bands could be seen at approximately 450 and 700 bp. No products were obtained by amplification at 62°C.

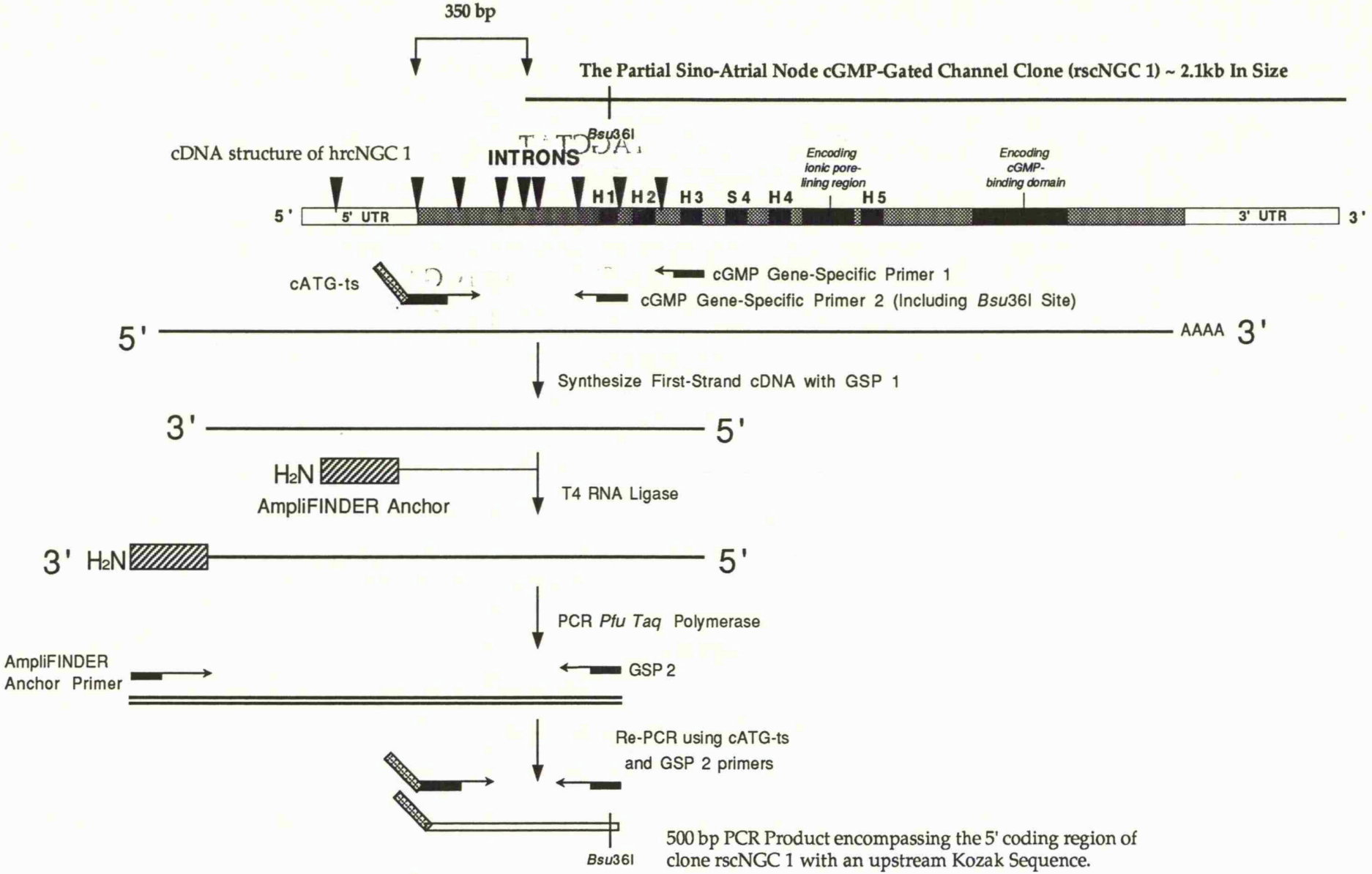

Figure 4.5 Diagrammatic representation of anchor-PCR retrieval of the 5' coding region of clone rscNGC 1.
Diagram illustrates the individual steps employed in the retrieval of the 5' coding region of clone rscNGC 1.
The human retinal rod photoreceptor cGMP-gated channel (hrcNGC 1) is shown. Positions of important functional domains, and intron/exon boundaries are marked.

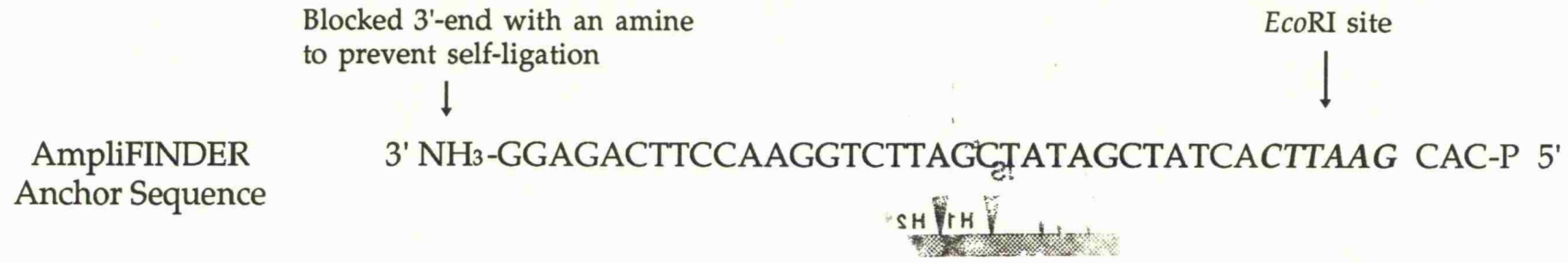

Anchor primer sequence

5'-CCTCTGAAGGTTCCAGAATCGATAG-3'

25 mer : 48% GC content : Tm ~ 74 C

Clone rscNGC 1 specific primer 1
(GSP-1)
for cDNA synthesis

5'-AGGTTCATCAAAACAGGCTCTTGCA-3'

25 mer : 44% GC Content : Tm~ 72 C

*Bsu*36I site

Clone rscNGC 1 specific primer 2
(GSP-2)
for PCR amplification

5'-GTAATATGTGTTT*CCTGAGG* GATCA-3'

25 mer 40% GC content Tm~ 70 C

Figure 4.4 Primers designed for 5'AmpliFINDER RACE

Reducing the annealing temperature from 60 to 54°C by increments of 2°C and decreasing the number of cycles to 30 also failed to increase the resolution of these PCR products. These 450 and 700 bp products which could have represented 5' upstream sequences of rscNGC 1, were unable to be isolated to homogeneity. The integrity of the technique was confirmed by the amplification of a 480 bp PCR product representing the 5' end of the 4.7 kb human transferrin receptor mRNA (a moderate to low abundance message), from 2 μg of human placental polyA$^+$ mRNA (Figure 4.6(a)).

4.2.3 Retrieval of the 5' end by subsequent amplification with primer cATG-ts

Following this first round of amplification, an aliquot of the products at the annealing temperature of 60°C was taken as template for re-amplification using the cATG-ts primer and the original GSP-2 primer. This cATG-ts primer 'nested' within the sense anchor primer used in the first round of amplification. 30-cycle PCR was performed at annealing temperatures of 52 and 60°C. A single amplified cDNA product of the predicted size ~500 bp (as expected from the previously cloned cNG cDNA sequences) was generated at the annealing temperature of 55°C (Figure 4.6(b)). This approach had the advantage that spurious target sequences that were produced during the first round of amplification can not be subsequently amplified. A similar sized PCR product was also obtained by performing a 35-cycle amplification using 0.5 μl aliquots of the GSP-1 primed first-strand cDNA as template, and directly employing the cATG-ts and GSP-2 PCR primers.

4.2.4 Is rscNGC 1 differentially spliced?

The 500 bp PCR product was gel-isolated and subcloned into a *Sma*I digested, dephosphorylated pUC 18 plasmid following. The identity of the PCR product was verified by complete sequencing using the universal primer, which demonstrated that the product encoded the 5' open reading frame of clone rscNGC 1 (Figure 4.7). From the sequence alignment it can clearly be deduced that the primary transcript giving rise to clone rscNGC 1 does not undergo differential splicing, and that the cardiac homologue of the cGMP-gated channel has overall similarity to the channel expressed in retinal rod photoreceptor cells. Therefore, it appeared unlikely that a

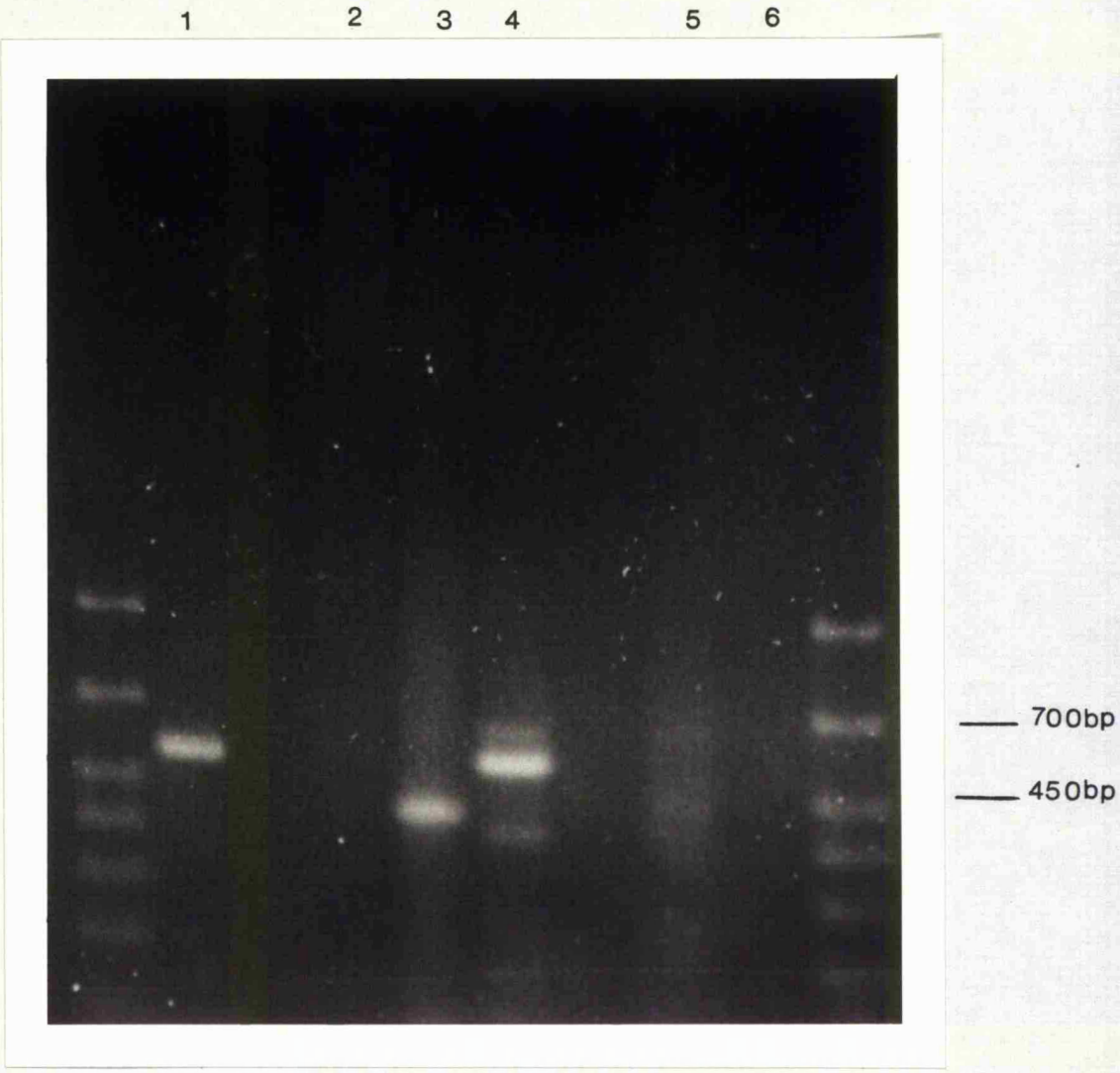

Figure 4.6(a) and (b) Anchor RACE for the retrieval of the 5' end of clone rscNGC 1

(a) Lane 1 and 8: ϕX174/*Hae*III molecular size markers. Lane 2: Positive PCR control 50 ng genomic DNA amplified with *roc*-A 1 and 2 primers. Annealing temperature 62°C. Lane 3: 0.5 µl of first-strand GSP-1 primed cDNA amplified with anchor primer and GSP-2. Annealing temperature 62°C. Lane 4: Positive anchor RACE control, human transferrin receptor. Annealing temperature 60°C. Lane 5: as lane 2 but annealing temperature 60°C. Lane 6: as lane 3 but annealing temperature 60°C. Lane 7: Negative PCR control as lane 6 but without template.

Samples were amplified for 35 cycles, and a portion of the reaction product was electrophoresed on a 2.0% ethidium bromide-stained agarose gel.

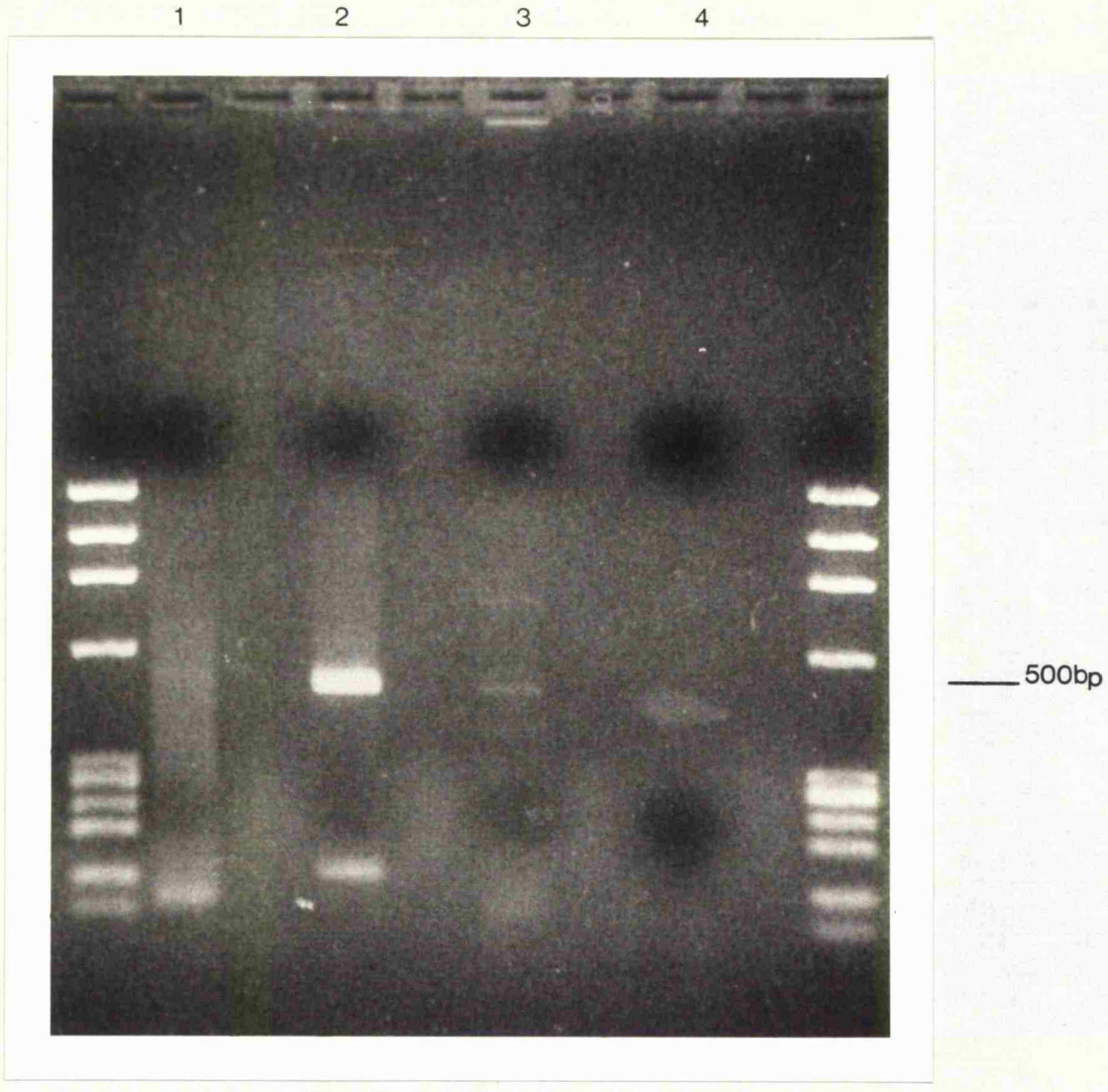

(b) Lane 1, 2 and 3: 1 µl of products from the 60°C anchor RACE reaction were re-amplified using cATG-ts and GSP-2 primers at 60, 55 and 52°C respectively. Lane 4: Negative control for PCR amplification as lane 3 but without template.

Molecular size markers shown (in base pairs) are ϕX174/*Hae*III

Samples were amplified for 35 cycles, and a portion of the reaction product was electrophoresed on a 2.0% ethidium bromide-stained agarose gel.

```
                                                                30
                                                                 *
Clone rscNGC 1  GCC GCC GCC ATG AAG AAA AAT ATT ATC AAT ACA CGG CGC ACC TTT ATA AAC ATT
Human rcNGC     _________.. ... ... ..c ... ... ... ... ... .a. .ag t.t ... g.. .c. ..g

                     60                                                 90
                      *                                                 *
Clone rscNGC 1  CCC AAT GTG ATT GCT CCA GAT ATT GAA AAG GAA ATA AGA AGG ATG GAA AAT GGA
Human rcNGC     ... ... ... ... .ta ... ... ... ... ... ... ... c.. ... ... ... ... ...

                          Intron 3                                          150
                             |                                               *
Clone rscNGC 1  GCA TGC AGC TCC TTT TCT GAA GAT GAT GAC AGT GCC TCT GTA TCT GAA GAG TCA
Human rcNGC     ... ... ... ... ... ... ..g ... ... ... ... ... .a. ac. ... ... ..a ...

                                      180                                       210
                                       *                                         *
Clone rscNGC 1  GAA AAT GAA AGC CTG CAC ACA AGG GGT TCC TTT GGA GAT AAC TCA CAC AGA AGG
Human rcNGC     ..g ... ... .a. .ct ..t g.. ... ... ... ... a.t t.. ..g ... .t. ... .a.

                                   Intron 4   240                                  270
                                      |        *                                   *
Clone rscNGC 1  GAA GGA CCA CCG CAG AGG CAG CAG TAC TTG CCG GGT ACC ATG GCA CTT TTC AAC
Human rcNGC     .g. ... ... t.a ... ... g.. ... ... c.. ..t ... g.. ..t ..c a.. ..t ..t

                                            Intron 5
                                               |
Clone rscNGC 1  ATT AAC AAC AGC AGT AAC AAG GAC CAA GAA CAA AAA GAA AAA AAG AAA AAG AAA
Human rcNGC     g.g ... ... ... ..c ..t ... ... ..g ... .c. g.g ... ... ... ... ... ...

                     330          Intron 6                    360
                      *              |                         *
Clone rscNGC 1  AAA GAA AAG AAG AGC AAA TCA GAT GAT AAA AAT GAA AAT AAA AAG GAT TCA GAG
Human rcNGC     ... ... ... ... ... ..g ... ... ... ... ..c ... ... ... ..c ..c c.. ...

                               390                                        Intron 7
                                *                                            |
Clone rscNGC 1  AAG AAA AAG AAG AAG GAA AAA GAG AAA GAG AAG AAA AAG AAA GAG GAG ACA AAG
Human rcNGC     ... ... ... ... ..- --. ..g ..c ... ... ... ... ... ... ... ... .a. .gc

                                      450                                       480
                                       *                                         *
Clone rscNGC 1  AAA GAA AAG AAA GAA GAG GAG AAG AAA GAA GTC ATG ATT ATT GAT CCC TCA GGA
Human rcNGC     ... ..t ... ... ... c.c c.c ... ... ... ..t g.. g.. ... ... ... ..g ...


Clone rscNGC 1  AAC ACA TAT TAC
Human rcNGC     ... ... ... ...
```

Figure 4.7 Sequence alignment of the 5' protein coding region of clone rscNGC 1 with the human retinal rod photoreceptor cGMP-gated channel (rcNGC 1) [Dhallan *et al.*, 1992].

Dots represent nucleotide identities and lower case letters represent nucleotide mismatches to the rscNGC 1 sequence. Intron positions are indicated by underlined sequence. Clone rscNGC 1 contains three additional nucleotides as compared to the human channel and these are marked by hypens. The sequences of the aATG-ts and GSP-1 primers are indicated in italics. Nucleotide positions are numbered from the translation initiator codon ATG and are indicated above the sequence.

tissue-specific spliced cNG channel variant, was expressed within the sinus node region.

4.3 Construction of a full-length open reading frame

The entire protein coding region of rscNGC 1 was contained within two separate DNA fragments of size 500 bp and 2.1 kb representing the respective 5' and 3' ends of the cDNA. These two partial DNA fragments contained a 180 bp overlap. Both fragments shared an unique restriction enzyme site for *Bsu*36I at nucleotide position 482. Additionally, two unique sites for *Xba*I and *Pst*I were found in the polylinkers 5' of both fragments.

A recombinant carrying the complete coding sequence was constructed as follows. The 500 bp 5' fragment was removed from the pUC 18 vector by both *Xba*I/*Bsu*36 I and *Pst*I/*Bsu*36I double digests. The recombinant pBluescript SK+ construct carrying the 2.1 kb 3' fragment was also prepared by *Xba*I/*Bsu*36 I and *Pst*I/*Bsu*36I double-digests. Subsequent ligation of the 500 bp fragments into the prepared recombinant pBluescript plasmid and transformation into DH5α *E.Coli* competent cells, continually failed to produce colonies following selection on ampicillin-agar plates. One possible explanation for this phenomenon could have been due to 'leaky' expression from the *lac* promoter, resulting in an in-frame fusion protein consisting of rscNGC 1 and the β-galactosidase gene product which may have been toxic to the cell.

An alternative approach was to construct the full coding sequence in the vector pBluescript KS+, whose multiple cloning site was oriented in a direction opposite to that found in the SK+ vector thereby preventing the production of such in-frame fusion products. Both the 500 bp fragment (excised by a *Pst*I/*Bsu*36I double digest from pUC 18) and the 2.1 kb fragment (excised by a *Bsu*36I/*Xho*I double digest from pBluescript SK+), were purified and concentrated by electroelution following separation by agarose gel electrophoresis. The fragments were ligated simultaneously into a pre-digested *Pst*I/*Xho*I pBluescript KS+ vector. Following transformation of DH5α *E.Coli* competent cells, blue/white selection was used to isolate putative recombinant colonies. Diagnostic *Xho*I/*Xba*I

double digests demonstrated that two of the white colonies obtained, contained a 2.5 kb insert representing the full coding sequence of rscNGC 1.

4.4 Sequence analysis of the entire reconstructed rscNGC 1 and delineation of functional domains

Double-stranded sequencing of rscNGC 1 was performed on both strands, by a gene-walking strategy using a cycle sequencing procedure employing dye-deoxy terminators (ABI). The gene-specific primers *rsc*G 3-15 designed for sequencing are described in Table 2.3.1 of the Materials and Methods.

The complete cDNA sequence and predicted translation product of rscNGC 1 are shown in Figure 4.8. The cDNA sequence of 2524 bp, contains an open reading frame of 2067 nucleotides and a 3' untranslated region of 457 nucleotides. The polyadenylation signal AATAAA (nucleotides 2482-2487) can be found 16 bp upstream of the poly (dA) tract consisting of 21 nucleotides.

4.4.1 rscNGC 1 shares sequence and structural identity to the rod α-subunit of the cGMP-gated channel

The open reading frame of rscNGC 1 would be predicted to encode a channel polypeptide 689 amino acids in length. The calculated molecular mass (including the initiating methionine) of rscNGC 1 is approximately 79,690 daltons. An alignment of the deduced amino acid sequence of rscNGC 1 to the human rod photoreceptor and two other genes encoding for cyclic nucleotide-gated channel polypeptides, is shown in Figure 4.9. Between the human rod α-subunit of the cGMP-gated channel and rscNGC 1, 90.4% (4.8%) of the aligned positions are occupied by identical or conserved (in parentheses) residues. The percentage of sequence similarity between rscNGC 1 and the β-subunit of the cGMP-gated channel is 35% (9%) and between the rabbit aorta cyclic nucleotide-gated channel is 60% (14%). This demonstrates that rscNGC 1 is a homologue of the α-subunit, which forms part of the retinal rod photoreceptor cGMP-gated ion channel complex.

```
GCC GCC GCC ATG AAG AAA AAT ATT ATC AAT ACA CGG CGC ACC TTT ATA [  39]
            Met Lys Lys Asn Ile Ile Asn Thr Arg Arg Thr Phe Ile

AAC ATT CCC AAT GTG ATT GCT CCA GAT ATT GAA AAG GAA ATA AGA AGG [  87]
Asn Ile Pro Asn Val Ile Ala Pro Asp Ile Glu Lys Glu Ile Arg Arg

ATG GAA AAT GGG GCA TGC AGC TCC TTT TCT GAA GAT GAT GAC AGT GCC [ 135]
Met Glu Asn Gly Ala Cys Ser Ser Phe Ser Glu Asp Asp Asp Ser Ala

TCT GTA TCT GAA GAG TCA GAA AAT GAA AGC CTG CAC ACA AGG GGT TCC [ 183]
Ser Val Ser Glu Glu Ser Glu Asn Glu Ser Leu His Thr Arg Gly Ser

TTT GGA GAT AAC TCA CAC AGA AGG GAA GGT CCA CCG CAG AGG CAG CAG [ 231]
Phe Gly Asp Asn Ser His Arg Arg Glu Gly Pro Pro Gln Arg Gln Gln

TAC TTG CCG GGT ACC ATG GCA CTT TTC AAC ATT AAC AAC AGC AGT AAC [ 279]
Tyr Leu Pro Gly Thr Met Ala Leu Phe Asn Ile Asn Asn Ser Ser Asn

AAG GAC CAA GAA CAA AAA GAA AAA AAG AAA AAG AAA AAA GAA AAG AAG [ 327]
Lys Asp Gln Glu Gln Lys Glu Lys Lys Lys Lys Lys Lys Glu Lys Lys

AGC AAA TCA GAT GAT AAA AAT GAA AAT AAA AAG GAT CCA GAG AAG AAA [ 375]
Ser Lys Ser Asp Asp Lys Asn Glu Asn Lys Lys Asp Pro Glu Lys Lys

AAG AAG AAG GAA AAA GAG AAA GAG AAG AAA AAG AAA GAG GAG ACA AAG [ 423]
Lys Lys Lys Glu Lys Glu Lys Glu Lys Lys Lys Lys Glu Glu Thr Lys

AAA GAA AAG AAA GAA GAG GAG AAG AAA GAA GTC ATG ATT ATT GAT CCC [ 471]
Lys Glu Lys Lys Glu Glu Glu Lys Lys Glu Val Met Ile Ile Asp Pro

TCA GGA AAC ACA TAT TAC AAC TGG CTG TTT TGT ATC ACT TTA CCT GTG [ 519]
Ser Gly Asn Thr Tyr Tyr Asn Trp Leu Phe Cys Ile Thr Leu Pro Val

ATG TAC AAC TGG ACT ATG ATT ATT GCA AGA GCC TGT TTT GAT GAA CTC [ 567]
Met Tyr Asn Trp Thr Met Ile Ile Ala Arg Ala Cys Phe Asp Glu Leu

CAA TCT GAT TAC CTA GAA TAT TGG CTC ATT GGG GAC TAC TTG TCA GAT [ 615]
Gln Ser Asp Tyr Leu Glu Tyr Trp Leu Ile Gly Asp Tyr Leu Ser Asp

ATA GTC TAT CTT GTT GAC ATG TTT GTA CGA ACA CGG ACA GGT TAC CTA [ 663]
Ile Val Tyr Leu Val Asp Met Phe Val Arg Thr Arg Thr Gly Tyr Leu

GAA CAA GGA CTG CTG GTG AAG GAA GAG CGC AAA CTC ATA GAA AAA TAT [ 711]
Glu Gln Gly Leu Leu Val Lys Glu Glu Arg Lys Leu Ile Glu Lys Tyr

AAA TCG AAT TTG CAG TTT AAA CTT GAT GTT CTG TCA GTG GTA CCA ACT [ 759]
Lys Ser Asn Leu Gln Phe Lys Leu Asp Val Leu Ser Val Val Pro Thr

GAT CTG CTG TAT TTT AAG TTG GGG TGG AAC TAT CCA GAA ATC AGA TTA [ 807]
Asp Leu Leu Tyr Phe Lys Leu Gly Trp Asn Tyr Pro Glu Ile Arg Leu

AAC AGG CTG TTA AGG ATC TCT CGT ATG TTT GAG TTC TTT CAG AGA ACA [ 855]
Asn Arg Leu Leu Arg Ile Ser Arg Met Phe Glu Phe Phe Gln Arg Thr

GAA ACG AGG ACA AAC TAC CCA AAC ATC TAC AGA ATT TCT AAT CTT GTC [ 903]
Glu Thr Arg Thr Asn Tyr Pro Asn Ile Tyr Arg Ile Ser Asn Leu Val

ATG TAT ATT GTC ATC ATT ATC CAC TGG AAT GCA TGT GTG TAC TAC TCT [ 951]
Met Tyr Ile Val Ile Ile Ile His Trp Asn Ala Cys Val Tyr Tyr Ser

ATT TCG AAA GCT ATT GGA TTT GGA AAT GAT GCA TGG GTA TAC CCT GAC [ 999]
Ile Ser Lys Ala Ile Gly Phe Gly Asn Asp Ala Trp Val Tyr Pro Asp
```

```
GTT AAT GAT CCT GAA TTT GGT CGT TTG GCT AGA AAA TAT GTC TAC AGT [1047]
Val Asn Asp Pro Glu Phe Gly Arg Leu Ala Arg Lys Tyr Val Tyr Ser

CTG TAT TGG TCT ACA CTG ACT CTG ACT ACC ATT GGT GAA ACA CCA CCT [1095]
Leu Tyr Trp Ser Thr Leu Thr Leu Thr Thr Ile Gly Glu Thr Pro Pro

CCT GTG CTG GAT TCT GAG TAT GTC TTT GTG GTG GTT GAC TTC TTA ATT [1143]
Pro Val Leu Asp Ser Glu Tyr Val Phe Val Val Val Asp Phe Leu Ile

GGA GTG TTA ATT TTT GCT ACC ATT GTT GGT AAT ATA GGT TCT ATG ATT [1191]
Gly Val Leu Ile Phe Ala Thr Ile Val Gly Asn Ile Gly Ser Met Ile

TCC AAC ATG AAC GCA GCT AGG GCA GAA TTT CAG GCA AGA GTC GAC GCT [1239]
Ser Asn Met Asn Ala Ala Arg Ala Glu Phe Gln Ala Arg Val Asp Ala

ATC AAG CAA TAC ATG AAT TTC CGC AAC GTA AGC AAG GAT ATG GAA AAG [1287]
Ile Lys Gln Tyr Met Asn Phe Arg Asn Val Ser Lys Asp Met Glu Lys

AGA GTT ATT AAG TGG TTT GAC TAT CTG TGG ACC AAC AAA AAG ACA GTT [1335]
Arg Val Ile Lys Trp Phe Asp Tyr Leu Trp Thr Asn Lys Lys Thr Val

GAT GAA AAA GAA GTC TTG AAG TAT CTA CCT GAT AAA CTG AGA GCA GAA [1383]
Asp Glu Lys Glu Val Leu Lys Tyr Leu Pro Asp Lys Leu Arg Ala Glu

ATC GCC ATC AAT GTT CAC TTA GAC ACA TTA AAA AAG GTG CGC ATT TTT [1431]
Ile Ala Ile Asn Val His Leu Asp Thr Leu Lys Lys Val Arg Ile Phe

GCT GAC TGT GAA GCA GGT CTG TTG GTG GAA TTG GTC TTG AAG TTA CAG [1479]
Ala Asp Cys Glu Ala Gly Leu Leu Val Glu Leu Val Leu Lys Leu Gln

CCC CAA GTC TAT AGT CCT GGA GAT TAT ATT TGC AAG AAA GGG GAT ATT [1527]
Pro Gln Val Tyr Ser Pro Gly Asp Tyr Ile Cys Lys Lys Gly Asp Ile

GGC CGA GAG ATG TAC ATC ATC AAG GAA GGC AAA CTC GCT GTG GTG GCA [1575]
Gly Arg Glu Met Tyr Ile Ile Lys Glu Gly Lys Leu Ala Val Val Ala

GAT GAT GGA ATC ACT CAG TTT GTG GTG CTG AGT GAT GGC AGC TAC TAT [1623]
Asp Asp Gly Ile Thr Gln Phe Val Val Leu Ser Asp Gly Ser Tyr Tyr

GGT GAG ATC AGC ATT CTT AAC ATT AAA GGC AGC AAA GCT GGC AAT CGA [1671]
Gly Glu Ile Ser Ile Leu Asn Ile Lys Gly Ser Lys Ala Gly Asn Arg

AGA ACA GCC AAT ATT AAA AGT ATT GGC TAT TCA GAT CTG TTC TGT CTC [1719]
Arg Thr Ala Asn Ile Lys Ser Ile Gly Tyr Ser Asp Leu Phe Cys Leu

TCA CAA GAT GAC CTC ATG GAG GCT CTA ACT GAG TAC CCG GAT GCC AAA [1767]
Ser Gln Asp Asp Leu Met Glu Ala Leu Thr Glu Tyr Pro Asp Ala Lys

ACA ATG CTG GAA GAG AAA GGG AAG CAG ATC TTG ATG AAG GAC GGC CTG [1815]
Thr Met Leu Glu Glu Lys Gly Lys Gln Ile Leu Met Lys Asp Gly Leu

CTG GAT GTG AAC ATT GCA AAC GCT GGC AGT GAC CCT AAA GAT CTC GAA [1863]
Leu Asp Val Asn Ile Ala Asn Ala Gly Ser Asp Pro Lys Asp Leu Glu

GAG AAG GTT GCT CGA ATG GAG GGC TCG GTA GAT CTC ATC CAA ACG AGG [1911]
Glu Lys Val Ala Arg Met Glu Gly Ser Val Asp Leu Ile Gln Thr Arg

TTT GCC CGG ATC CTG GCT GAG TAT GAG TCC ATG CAG CGG AAA CTG AAG [1959]
Phe Ala Arg Ile Leu Ala Glu Tyr Glu Ser Met Gln Arg Lys Leu Lys

CAA AGA TTG ACC AAG GTG GAG AAA TTT CTG AAA CCA CTT ATT GAG ACA [2007]
Gln Arg Leu Thr Lys Val Glu Lys Phe Leu Lys Pro Leu Ile Glu Thr
```

```
GAA TTT TCA TCT CTT GAA GGA GCT GGA GTA GAA AGT GGG CCC ACA GAC [2055]
Glu Phe Ser Ser Leu Glu Gly Ala Gly Val Glu Ser Gly Pro Thr Asp

TCT ACA CAG GAT TGA AGA GCT TGT CAC TGA CAG GGC TAT GTC TCA TTA [2103]
Ser Thr Gln Asp

TCC TTT TAA TCA TGT GAG TAA AGT TTA CTG TCA TTT GGA AGA AGA TGA [2151]

AGA CAC AGC TAG GAA TTT TTC TCA AAA GCA GCA TGT GCT TTG GGC ACT [2199]

GCA CAA GGC CTA CAC ACC CTC TGT GGG GTA CTG GAA TGC AAG AAC AAT [2247]

CCT ATT GTG GGA TTT TTC ATA ACG GAT ATG GGA AAA GAT ATA ACT GAT [2295]

CAA TCT GTC TGC ATC TGT ATC TTC CAA TTT TTC CAC ATG TTC CTT GTA [2343]

TGC AAT AAC CTT TAT AAA AGC ACA AGT ATA TCT CAC CTT CAG ACT ATT [2391]

TGC ACT GTT GAG GCC TAA GAT ATA TTA AGA CTA ACA GGG AAC TAT CAT [2439]

GTA CGT TGT GTT TGG ATA CAA TTT TAA AAA GAA TTA GAA TAC AAT AAA [2487]

GTA AAC ATG ATT ATG CAA AAA AAA AAA AAA AAA AAA A               [2524]
```

Figure 4.8 Complete cDNA and protein sequence of rscNGC 1

Nucleotide numbering starts with A of the translation initiator codon ATG and is shown to the right in parentheses. The polyadenylation signal is shown underlined.

```
                                20                  40                  60
                                 *                   *                   *
Rabbit scNGC 1 MKKNIIINTRRTFINIPNVIA PDIEKEIRRMENGACSSFSE DDDSASVSEESENESLHTRG
Human rcNGC-α  ..n.....qqs.vtm....v ..................... .....yt.......np.a..
Rabbit acNGC   -------------------- -------------------- --------------------
Human rcNGC-β  -------------------- -------------------- --------------------

                                80                  100                 120
                                 *                   *                   *
Rabbit scNGC 1 SFGDNSHRREGPPQRQQYLP GTMALFNINNSSNKDQEQKE KKKKKKEKKSKSDDKNENKK
Human rcNGC-α  ..syk.l.kg..s..e.... .ai.i..v.........pe. ...................n
Rabbit acNGC   -------------------- -------------------- -----r.eearp.sfl.rfr
Human rcNGC-β  -------------------- -------------------- --------------------

                                                                  ____H1____
                                140                 160                 180
                                 *                   *                   *
Rabbit scNGC 1 DPEKKKKKEKEKEKKKKEET KKEKKEEEKKEVMIIDPSGN TYYNWLFCITLPVMYNWTMI
Human rcNGC-α  ........-.d........k s.d...hh....vv...... ...................v
Rabbit acNGC   g..lqtvttqqgdg.gdkdg -dg.gtkk.f.lfvl..a.d w..r...v.am..l...cll
Human rcNGC-β  -------------------- --------------...lt  m.vl...fvvmawnw..-l.

__              _________H2_______                                  ____
                                200                 220                 240
                                 *                   *                   *
Rabbit scNGC 1 IARACFDELQSDYLEYWLIG DYLSDIVYLVDMFVRTRTGY LEQGLLVKEERKLIEKYKSN
Human rcNGC-α  ...................l ..v......i.......... ..........l...n.....
Rabbit acNGC   v.....sd..rg.flv..vl ..f..v..ia.l.i.l...f ........dpk..rdn.iht
Human rcNGC-β  pv.wa.pyqtp.nihh..lm ...c.li.fl.it.q..lqf vrg.diitdkkdmrnn.lks

        ________H3_____          _______S4_______                 _______
                                260                 280                 300
                                 *                   *                   *
Rabbit scNGC 1 LQFKLDVLSVVPTDLLYFKL GWNYPEIRLNRLLRISRMFE FFQRTETRTNYPNIYRISNL
Human rcNGC-α  .........li......... ..............f..... ..............f.....
Rabbit acNGC   .......a.ii....i..av .ihn..l.f....hfa.... ..d......s....f.....
Human rcNGC-β  rr..m.l..ll.l.f..l.v .-vn.ll..p.c.kymaf.. .ns.l.silskayv..virt

        ______H4_______                                     _____PORE_____
                                320                 340                 360
                                 *                   *                   *
Rabbit scNGC-1 VMYIVIIIHWNACVYYSISK AIGFGNDAWVYPDVNDPEFG RLARKYVYSLYWSTLTLTTI
Human rcNGC-α  ..............f..... .......t.....i...... ...................
Rabbit acNGC   .l..lv.......i..a... s....v.t....nit...y. y...e.i.c...........
Human rcNGC-β  ta.llysl.l.s.l..wa.a yq.l.sth...dg.gns-y- -i-.c.-.--f-avk..i..

        ______          _________H5________
                                380                 400                 420
                                 *                   *                   *
Rabbit scNGC 1 GETPPPVLDSEYVFVVVDFL IGVLIFATIVGNIGSMISNM NAARAEFQARVDAIKQYMNF
Human rcNGC-α  .......r........... ..................... .........i.......h.
Rabbit acNGC   .......k.e..l..if... ...........v....... ..t......ki..v.h..q.
Human rcNGC-β  .gl.d.ktlf.i..qllnyf t..fa.svmi.qmrdvvgaa t.gqtyyrscm.stvk....
```

```
                                  440                 460                 480
                                   *                   *                   *
Rabbit scNGC 1 RNVSKDMEKRVIKWFDYLWT NKKTVDEKEVLKYLPDKLRA EIAINVHLDTLKKVRIFADC
Human rcNGC-α  .................... .................... ....................
Rabbit acNGC   .k...e..ak.......... .......r....n..a.... ........s........q..
Human rcNGC-β  ykip.svqn..kt.ye.t.h sqgml..s.lmvq....m.l dl..d.nynivs..al.qg.


                                  500                 520                 540
                                   *                   *                   *
Rabbit scNGC 1 EAGLLVELVLKLQPQVYSPG DYICKKGDIGREMYIIKEGK LAVVADDGITQFVVLSDGSY
Human rcNGC-α  .................... .................... ........v..........t
Rabbit acNGC   ............r...f... ....r.....k......... ........v..yal..a..c
Human rcNGC-β  drqmifdmlkr.rsv..l.n ..v....e........qa.q vq.lgg..ksvl.t.ka..v

                        Cyclic Nucleotide-Binding Domain
                      560                 580                 600
                       *                   *                   *
Rabbit scNGC 1 YGEISILNIKGSKAGNRRTA NIKSIGYSDLFCLSQDDLME ALTEYPDAKTMLEEKGKQIL
Human rcNGC-α  f.................. .............k..... ....................
Rabbit acNGC   f............m..... ..r.l.........k..... .v.......kv...r.re..
Human rcNGC-β  f....l.av-.--g..... .vvah.ftn..i.dkk..n. i.vh..esqkl.rk.arrm.


                                  620                 640                 660
                                   *                   *                   *
Rabbit scNGC 1 MKDGLLDVNIANAGSDPKDL EEKVARMEGSVDLIQTRFAR ILAEYESMQRKLKQRLTKVE
Human rcNGC-α  .......l........... ....t........l...... .........q..........
Rabbit acNGC   ..e....e.eva.smev-.v q..lkql.tnmetly...g. l....tga.q.....i.vl.
Human rcNGC-β  p.eeksvlilppragt..lf naal.-.t.kmggkgakggk -..hlrarlke.aa-.eaaa


                                  680
                                   *
Rabbit scNGC 1 KFLKPLIETEFSSLEGAGVE SGPTDSTQD
Human rcNGC-α  .......d.....i..pws. ...i...
Rabbit acNGC   vkm.qnt.ddyl.-d.mn-s pe.aaae.
Human rcNGC-β  .-hee.v.qak..qdvk.-. e.saapd.h
```

Figure 4.9 Alignment of the amino acid sequence of rscNGC 1 with the human rod α-subunit (rcNGC-α) [Dhallan *et al.*, 1992], rabbit aorta (acNGC) [Biel *et al.*, 1993] and the human rod β-subunit (rcNGC-β) [Chen *et al.*, 1993] cNG channels.

Amino acid residues are shown in one-letter code and are numbered beginning with the initiating methionine. Dots and lower case letters indicate identical and non-conservative exchanges with rscNGC 1. Dashes symbolise gaps, which have been introduced into the sequences for optimal alignment. Positions of potential functional domains are indicated by lines above rscNGC 1 sequence:
H1-H5 = hydrophobic segments which might represent transmembrane segments; S4 = voltage sensor motif; pore = putative pore region; and cyclic nucleotide-binding domain.

A hydrophilicity plot of the rscNGC 1 polypeptide identified six putative hydrophobic regions which might represent transmembrane segments (Figure 4.10(a)). Like the human rod α-subunit, the rscNGC 1 polypeptide lacks a typical hydrophobic signal sequence, suggesting that the N-terminus would be expected to be located towards the cytoplasmic side. The proposed transmembrane topography of rscNGC 1 in accordance with other cNG channel family members [Eismann *et al.*, 1993] is shown in Figure 4.10(b).

A charged N-terminal domain of 160 amino acids is followed by the central core region of 240 amino acids, containing six putative transmembrane domains. In terms of amino acid conservation between the retinal rod and sino-atrial node α-subunits, H5 is perfectly conserved and H1 has only one minor substitution (Figure 4.9). H2-4 have several, mostly conservative substitutions which do not perturb runs of residues in these hydrophobic domains. The transmembrane domains H2, H3 and H5 contain 1-3 mostly negative charges, all of which are perfectly conserved between rod photoreceptor and SAN channel homologues. An 80 amino acid stretch of charged residues links the putative transmembrane regions with an intracellular C-terminal region. It is known from previous studies that this (partially-hydrophobic) domain forms the cytoplasmic ligand-binding pocket (discussed later).

4.4.2 Structural features of the N-terminal domain

The 160 amino acid intracellular N-terminal domain of rscNGC 1 represents a region of significant diversity amongst the various cloned cNG channel α-subunit homologues (Figure 4.11). As these subunits are products of the same gene, the observed differences in primary sequence can be accounted for by species variation. Additionally, this N-terminal domain shares very little sequence similarity amongst individual cNG channel genes, and thus represents a specific 'sequence tag' for family members.

A distinctive feature of the N-terminal domain of rscNGC 1 is the presence of a highly charged segment (~ 50 residues long) prior to the putative first transmembrane domain H1, consisting of 30 lysines (no arginines) and 18 glutamic/aspartic acid residues (Figure 4.11). This

(a)

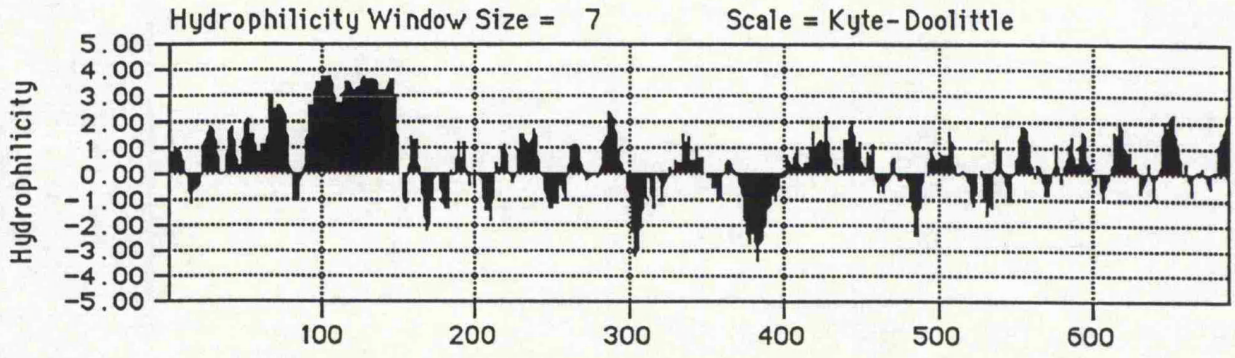

(b)

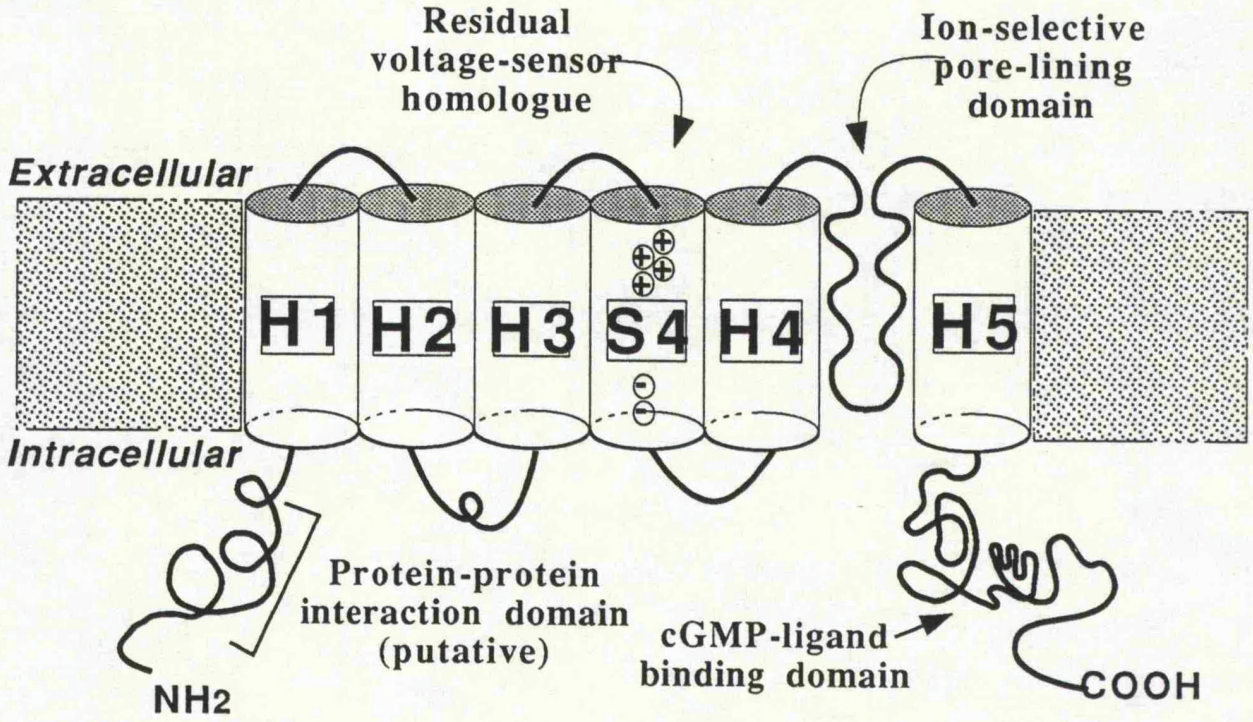

Figure 4.10 Hydrophilicity (a) and proposed transmembrane topography (b) of rscNGC 1

(a) The average hydrophilicity index of a heptad peptide composed of amino acid residues i-7 and i+7 was plotted against amino acid number i. Positive values donote hydrophilic regions which may be exposed on the outside of the molecule, whereas negative values indicate hydrophobic regions.

(b) The six putative transmembrane segments of a rscNGC 1 monomer are indicated by linearly displayed cylinders numbered H1-H5. Domains of functional relevance are labelled. + and - indicate the charge of amino acid residues in the S4 motif.

```
                              20                  40                  60
                               *                   *                   *
rscNGC 1     MKKNIINTRRTFINIPNVIA PDIEKEIRRMENGACSSFSE DDDSASVSEESENESLHTRG
hrcNGC-α     ..n.....qqs.vtm....v ..................... .....yt.......np.a..
brcNGC-α     ...v....whs.v.....vg ..v....t...........d ......mf....t.np.a.d
mrcNGC-α     ..t.....whs.v......v .a.................- ...ng.l.......--d--s

cccNGC       -------------------- -------------------- ------------------ -
btcNGC       ------------etsselq eg.am.t.glaesrq...ts qgptrlsrliislrawsa.-
racNGC       i.a.gkdes..rsrpqsaad d.tss.lq.laemdapqqrr ggfrri.rlvgvirqwan.-
hrcNGC-β     -------------------- -------------------- ------------------ -

                                  co or post-translational      _____ Hydrophilic
                                   proteolytic cleavage
                              80                  100                 120
                               *                   *                   *
rscNGC 1     SFGDNSHRREGPPQRQQYLP GTMALFNINNSSNKDQEQKE KKKKKKEKKSKSDDKNENKK
hrcNGC-α     ..syk.l.kg..s..e.... .ai.i..v.........pe. ...................n
brcNGC-α     ..rs.t.gsgq.s..e.... .ai....v......e..p.. ..........p........
mrcNGC-α     f.rs..yk.r..s..e.h.. .......v.........p.. ..........a.....-i.

cccNGC       -------------------- --l.r..v.f.n.tnedk.. e..ev..e.-.-ee.k.e..
btcNGC       hlhqedq.pdsfle.--frg aelqevssre.hvqnvgsq. ppdrgrsawplarnntntcn
racNGC       n.reeea.pdsfle.--frg pelqtvttqqgdg.gdkdgd g.gt..--------------
hrcNGC-β     -------------------- -------------------- --------------------

             Domain_____________________

                              140                 160
                               *                   *
rscNGC 1     DPEKKKKKEKEKEKKKKEET KKEKKEEEKKEVMIIDPSGN TY
hrcNGC-α     ........-.d........k s.d...hh....vv...... ..
brcNGC-α     ..........d.d......k g.d.........vv...... ..
mrcNGC-α     ..................k t...........vv...... ..

cccNGC       e-...dd.kdd.kdd..dd- ..--...q....fv....s. --
btcNGC       ns..dd.ak..-..e....k .en....k..dsvvm...s. --
racNGC       -------------------- -------------------- --
hrcNGC-β     -------------..arrml rsnn.pk.e.s.l.lp.rag .-
```

Figure 4.11 Sequence alignment of the N-terminal domain of rscNGC 1 with cloned cNG channels.

Human (h), bovine (b) and mouse (m) rod photoreceptor α-subunits (rcNGC-α) [Dhallan *et al.*, 1992; Kaupp *et al.*, 1989; Pittler *et al.*, 1992], chicken cone (cccNGC) [Bönigk *et al.*, 1993], bovine testis (btcNGC) [Weyand *et al.*, 1994], rabbit aorta (racNGC) [Biel *et al.*, 1993] and human rod photoreceptor β–subunit (hrcNGC-β) [Chen *et al.*, 1993] cyclic nucleotide-gated channels. Amino acid residues are shown in one-letter code and are numbered beginning with the initiating methionine above the sequence. Dots indicate identical residues, whereas lower case letters represent non-conservatively exchanged amino acid residues with respect to rscNGC 1. Dashes indicate gaps, which have been introduced into the sequences for optimal alignment. Position of the hydrophilic domain is indicated by a line above the rscNGC 1 sequence. Also shown in italics is the co/post-translational proteolytic cleavage site between serine residues 91 and 92 which are underlined.

hydrophilic segment of rscNGC 1 is highly conserved amongst the various cloned cNG channel α-subunit homologues. However, the hydrophilic region is much shorter, and only contains 20 charged residues in the olfactory/aorta, testis and cone channels, and is completely absent from the rod β-subunit. To date, no other sequenced ligand or voltage-gated channels contain a region of similar hydrophilicity.

4.4.3 *The S4 transmembrane domain — a remnant of a voltage-sensor domain*

rscNGC 1 in common with over cNG family members shares sequence motifs and structural elements in common with the class of voltage-gated ion channels, in particular to potassium-selective channels (discussed in Chapter 1). rscNGC 1 contains a sequence motif between H3 and H4 similar in nature to the S4 transmembrane domain of voltage-gated channels which is thought to serve as a voltage-sensor [Numa, 1989]. A sequence alignment of the S4 domain of rscNGC 1 with that of other cNG channel family members demonstrates a hydrophobic stretch of amino acids interrupted by arginine or lysine at every third residue (Figure 4.12(a)). Whereas the *Shaker* B voltage-gated potassium channel [Pongs *et al.*, 1988] contains 7 positively charged residues within this domain, rscNGC 1 in common with other cNG channels has only 5 positively charged amino acids, and in addition contains 3 negatively charged residues.

4.4.4 *The pore-lining domain*

rscNGC 1 also contains a domain homologous to the hydrophobic SS1-SS2 domain of voltage-gated channels which lies between the transmembrane domains H4 and H5, and is thought to constitute the ion pore [reviewed by Imoto, 1993]. A sequence alignment of this region (Figure 4.12(b)) demonstrates that rscNGC 1 in common with other cNG channels are deficient in the YG motif which as discussed in Chapter 1 is part of the selectivity filter of potassium channels. rscNGC 1 also contains the invariant glutamate residue adjacent to this YG motif which controls calcium influx and cation voltage-dependent block (discussed in Chapter 1).

(a)

	aa																										aa
			+			+			+			+			+			+	+		+					
Shaker B K^+ CHANNEL	348-	I	L	R	V	I	R	L	V	R	V	F	R	I	F	K	L	S	R	H	S	K					-368
RABBIT SAN CLONE rscNGC 1	266-	E	I	R	L	N	R	L	L	R	I	S	R	M	F	E	F	F	Q	R	T	E					-288
HUMAN ROD cNG α-subunit	267-	E	I	R	L	N	R	L	L	R	I	S	R	M	F	E	F	F	Q	R	T	E					-287
CHICKEN CONE cNG	314-	E	L	R	F	N	R	L	L	R	I	A	R	L	F	E	F	F	D	R	T	E					-334
RABBIT AORTA cNG	244-	E	V	R	F	N	R	L	L	H	F	A	R	M	F	E	F	F	D	R	T	E					-264
HUMAN ROD cNG β-subunit	132-	L	L	R	L	P	R	C	L	K	Y	M	A	F	F	E	F	N	S	R	L	E					-152
BOVINE TESTIS cNG	291-	E	L	R	F	N	R	L	L	K	L	A	R	L	F	E	F	F	D	R	T	E					-311

Distribution of net positive: ☐ and negative: ▒ amino acids in the S4 motif region of cNG channels

(b)

	aa																										aa
Shaker B K^+ CHANNEL	418-	P	D	A	F	W	W	A	V	V	T	M	T	T	V	G	Y	G	D	M	T	P	V	G			-440
RABBIT SAN CLONE rscNGC 1	347-	V	Y	S	L	Y	W	S	T	L	T	L	T	T	I	G	-	-	E	T	P	P	P	V			-367
HUMAN ROD cNG α-subunit	348-	V	Y	S	L	Y	W	S	T	L	T	L	T	T	I	G	-	-	E	T	P	P	P	V			-368
CHICKEN CONE cNG	395-	I	Y	S	L	Y	W	S	T	L	T	L	T	T	I	G	-	-	E	T	P	P	P	V			-415
RABBIT AORTA cNG	345-	V	Y	C	F	Y	W	S	T	L	T	L	T	T	I	G	-	-	E	M	P	P	P	V			-365
HUMAN ROD cNG β-subunit	205-	I	R	C	Y	Y	F	A	V	K	T	L	I	T	I	G	-	-	G	L	P	D	P	K			-225
BOVINE TESTIS cNG	371-	I	Y	S	L	Y	W	S	T	L	T	L	T	T	I	G	-	-	E	T	P	P	P	V			-391

Figure 4.12 Sequence alignment of the S4 motif (a) and the putative pore (SS1-SS2) region (b) of rscNGC 1 with the voltage-gated *Shaker* B potassium channel [Pongs *et al.*, 1988], human rod photoreceptor α and β-subunits [Dhallan *et al.*, 1992; Chen *et al.*, 1993], chicken cone [Bönigk *et al.*, 1993], rabbit aorta [Biel *et al.*, 1993] and bovine testis [Weyand *et al.*, 1994] cyclic nucleotide-gated channels. Distribution of charge within the S4 domain is indicated by the boxed residues in (a). Numbers of individual amino acid residues are shown to both the right and left of the sequence alignments.

4.4.5 *The cyclic nucleotide-ligand binding domain*

The cyclic nucleotide-binding site of rscNGC 1 comprising of 110 amino acid residues is located near the carboxy terminus of the protein. In this region the amino acid sequence of rscNGC 1 shows significant similarity to that of other cA/GMP binding proteins, namely the cGMP binding domains of cGMP-dependent protein kinase (cGK) [Takio *et al.*, 1984], and the homologous cAMP binding regions of the regulatory subunit of cAMP-dependent protein kinase (cAK) and the catabolite gene activator protein (CAP) of *E.coli.* [Weber *et al.*, 1989]. A sequence alignment of the ligand binding domain of rscNGC 1 to other cyclic nucleotide-binding polypeptides demonstrates that rscNGC 1 like the retinal rod photoreceptor cNG channels contains a cyclic nucleotide binding site that is structurally more similar to cGMP- than to cAMP-binding proteins (Figure 4.13).

The alignment of the putative cGMP-binding domain of rscNGC 1 with that of cGMP-dependent protein kinases (cG-PK) — which contain two tandem cGMP-binding domains, reveals that 25 amino acid residues out of the 110 that make up the binding pocket are identical and 29 represent conservative substitutions. Whereas the dimeric cG-PK molecule is co-operatively stimulated by the binding of two cGMP molecules per monomer, this analysis suggests that rscNGC 1 should bind only one ligand molecule per monomer. Many of the invariant residues that form the hydrophobic binding pocket and interact with cyclic nucleotides in the CAP protein for which the three-dimensional structure is available [McKay and Steitz, 1981; Weber and Steitz, 1987], are conserved among rscNGC 1. In particular, the 3 glycine residues (positions 508, 520 and 543) essential for the correct folding of the ligand-binding pocket, and the glutamate and arginine residues (positions 544 and 559) predicted to interact with the exocyclic oxygen atoms at the phosphodiester bond and the 2'-OH group of the ribose ring [Kumar and Weber, 1992], are highly conserved.

A threonine (T) residue has been shown to be invariant in the two cGMP-binding domains of all cGKs but is exchanged for an alanine (A) residue in 23 of 24 cAMP-binding sites in cAK [Weber *et al.*, 1989]. By site-directed

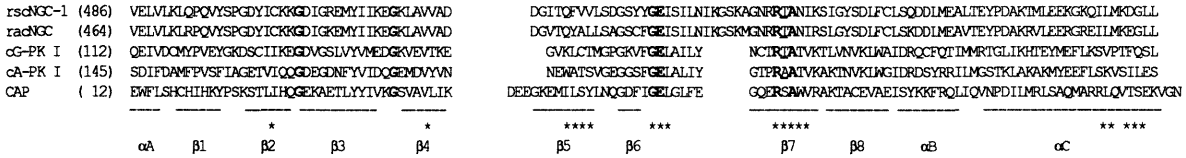

Figure 4.13 Primary and predicted secondary structural features of the cyclic nucleotide-binding domain of rscNGC 1.

The location of gaps conform to the alignments of Weber *et al.*, (1989). Regions of predicted secondary structure, α-helices and β-sheets in CAP [Shabb and Corbin, 1992] are indicated by bars beneath the alignment. Positions of residues that line the CAP cAMP-binding pocket are marked (*). Invariant residues are highlighted in bold type. The threonine/alanine residues that are important for the discrimination of cyclic nucleotides are underlined. Position of amino acid residues are shown in *parentheses* to the left of the sequences. Rabbit aorta cNG channel (racNGC) [Biel *et al.*, 1993, bovine cA/GMP-dependent protein kinases domain I (cA/G-PK I) [Takio *et al.*, 1984] and bacterial cAMP-regulated catabolite gene activator protein (CAP) [Weber *et al.*, 1987].

mutagenesis it has been shown that the A/T difference provides the structural basis defining cyclic nucleotide specificity in cNG channels [Altenhofen *et al.*, 1991]. rscNGC 1 like all cloned cNG channel proteins, contains a T residue at this particular position (560) and would thus be expected to exhibit a greater affinity for cGMP over cAMP when functionally expressed.

4.4.6 Presence of phosphorylation and glycosylation consensus sequences and motifs

The polypeptide sequence of rscNGC 1 was analysed for known consensus sequences and motifs. The amino acid sequence does not contain consensus motifs for phosphorylation by cGMP- or cAMP-dependent protein kinases. Also rscNGC 1 lacked a consensus motif for phosphorylation by protein kinase C.

Five potential sites for N-linked glycosylation (N-X-S/T; Hubbard and Ivatt, 1981) were identified at asparagine residues 53, 89, 90, 176 and 422 in rscNGC 1. Because of the proposed transmembrane topography of rscNGC 1, only residue 422 is located extracellularly and is of likely significance. The bovine rod channel has previously been shown to contain at least one carbohydrate chain that could be removed by treatment with glycopeptidase F [Wohlfart *et al.*, 1989]. It is not known however, if these sequences are functionally important. It has been shown that N-glycosylation although not necessary for the assembly of heterologous Torpedo nicotinic acetylcholine receptor subunits, is important for their efficient incorporation into the plasma membrane [Sumikawa and Miledi 1989]. Whether rscNGC 1 is glycosylated *in situ* and whether this modification is also important for channel activity, remains to be established.

4.5 Construction of Δ92-rscNGC 1 to investigate the *functional consequences* of N-terminal processing

4.5.1 In situ proteolytic cleavage of retinal photoreceptor cNG channels

Immunochemical studies have shown that both the retinal rod [Molday *et al.*, 1989] and cone [Bönigk *et al.*, 1993] photoreceptor cNG channels undergo a *cell-specific* co or post-translational cleavage of the N-terminus prior or during the incorporation of the channel into the plasma membrane. This truncated polypeptide represents the mature form of the native channel [Molday *et al.*, 1989]. The proteolytic cleavage has been demonstrated to occur between two serine residues, found at amino acid positions 91 and 92 (Figure 4.11). Cleavage of this N-terminal 92-amino acid segment does not occur, when retinal cNG channels are heterologously expressed in either COS-1 mammalian cells [Bönigk *et al.*, 1993] or *Xenopus* oocytes [Kaupp *et al.*, 1989]. The 78-kDa 'full-length' channel when expressed in *Xenopus* oocytes, exhibited functional channel properties which are for the most part, similar to those observed *in situ* [Kaupp *et al.*, 1989]. It remains to be established whether cleavage of the N-terminus of rscNGC 1 also occurs in native tissues, or whether such processing is specific for retinal photoreceptor cells.

4.5.2 What is the functional role of the N-terminus prior to posttranslational processing?

The N-terminal domain of *Shaker* potassium channels has previously been shown to be play an important role, both in channel inactivation [Hoshi *et al.*, 1990] and for the specificity of channel polypeptide interaction in subunit assembly [Li *et al.*, 1992]. It is possible that the 160 amino acid N-terminus of rscNGC 1 and all cNG channels could also determine co-assembly of monomeric subunits into both homo and heteromeric complexes, prior to channel processing and plasma membrane incorporation. However, a sequence similarity search of the N-terminus of rscNGC 1 against the protein information resource (PIR) portion of the *Entrez: Sequences* database (release 6), employing search methods based on measures of local sequence similarity failed to reveal any significant 'instructive' similarity to *Shaker* potassium channels or other protein

families. The potential importance of this region is also 'accentuated' by the observation that several exons encode for the 160 amino acid domain, raising the possibility that differential splicing may give rise to distinct electrophysiological properties.

It was important to address the question of whether; (i) the N-terminus of rscNGC 1 determines the formation of functional homo and heteromeric complexes?, and (ii) if so what structural element specifies subunit assembly? To address these questions a truncated rscNGC 1 channel was constructed Δ92-rscNGC 1, lacking precisely the 92 amino acids which become proteolytically processed *in situ*. It was reasoned that the use of electrophysiological techniques, would provide a sensitive 'assay' for assembly of Δ92-rscNGC 1 into functional homo and heteromeric complexes, following heterologous expression and co-expression with the human rod photoreceptor cNG channel β-subunit (hrcNGC-β). As discussed in Chapter 1, hrcNGC-β functions as a modulatory subunit forming heteromeric complexes with the rod photoreceptor cNG channel α-subunit hrcNGC-α [Chen *et al.*, 1993]. As rscNGC 1 is a nodal homologue of hrcNGC-α, it was reasoned that the β-subunit would form analogous heteromultimers exhibiting similar modulatory effects on the kinetics of channel gating.

4.5.3 Construction of Δ92-rscNGC 1

Δ92-rscNGC 1 was constructed by a recombinant PCR strategy, summarised in Figure 4.14(a). A 74 bp sense PCR primer was synthesized containing the following features; a 6 bp GC clamp, a consensus Kozak sequence (CCACCATG) [Kozak, 1991], followed by the nucleotide sequence encoding amino acid residues 92 to 100 of hrcNGC-α and 25 bp of sequence complementary to the 5' end of the partial rscNGC 1 clone. Nucleotide sequences of hrcNGC-α were employed, as at the time of primer synthesis the 5' coding sequence of clone rscNGC 1 had not been retrieved. The 25 bp antisense PCR primer was complementary to the putative H1 transmembrane domain of rscNGC 1, and contained the unique *Bsu*36I restriction site. A 30 cycle PCR amplification yielded a 235 bp product at annealing temperatures of 60 and 65°C (Figure 4.14(b)). The PCR product was gel isolated and cloned into the *Sma*I site of pUC 18. The identity of the PCR product was verified by sequencing using the universal primer.

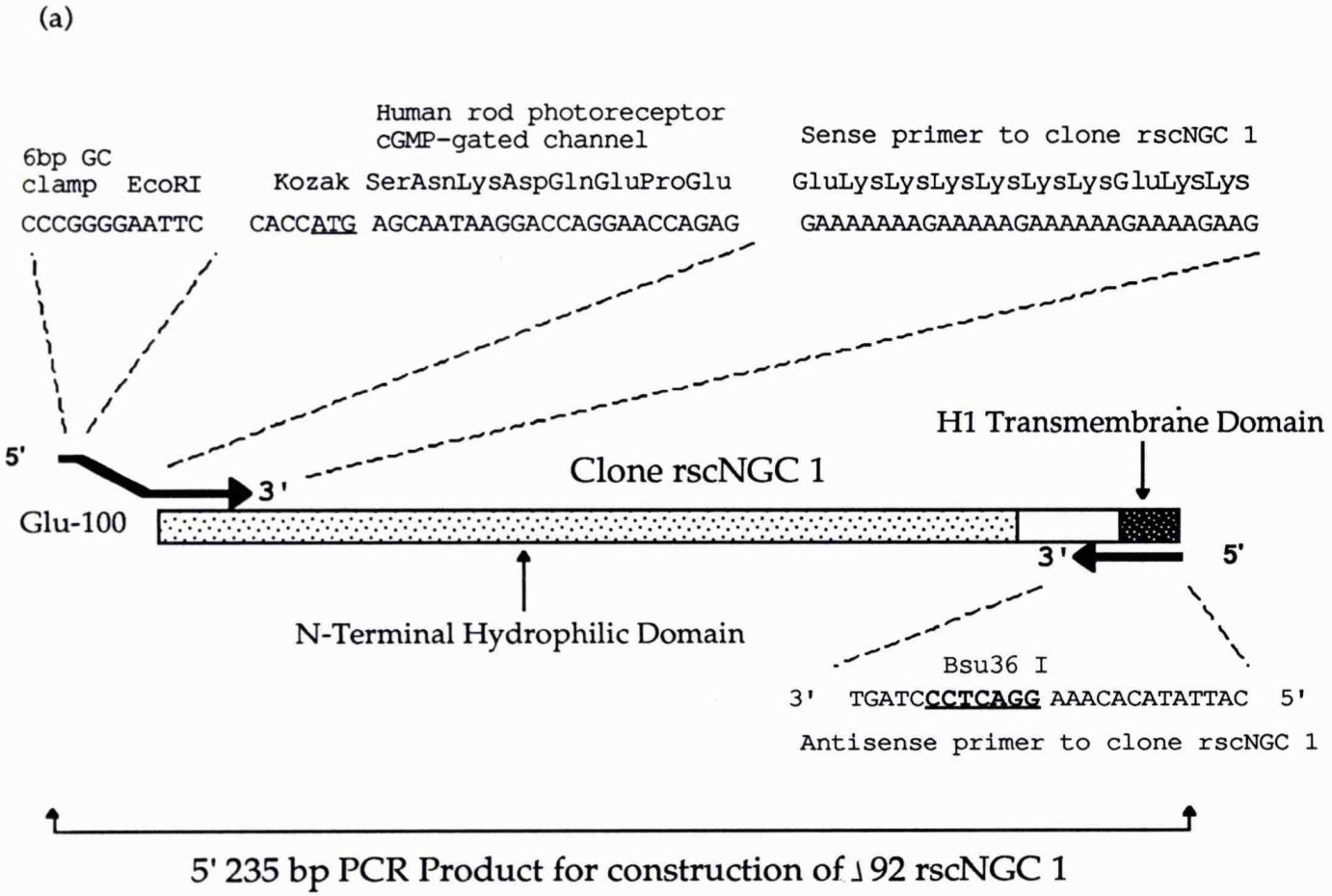

Figure 4.14(a) Schematic diagram outlining the strategy employed in the construction of Δ92-rscNGC 1

The compositions of the 72 bp sense and antisense primers are shown.

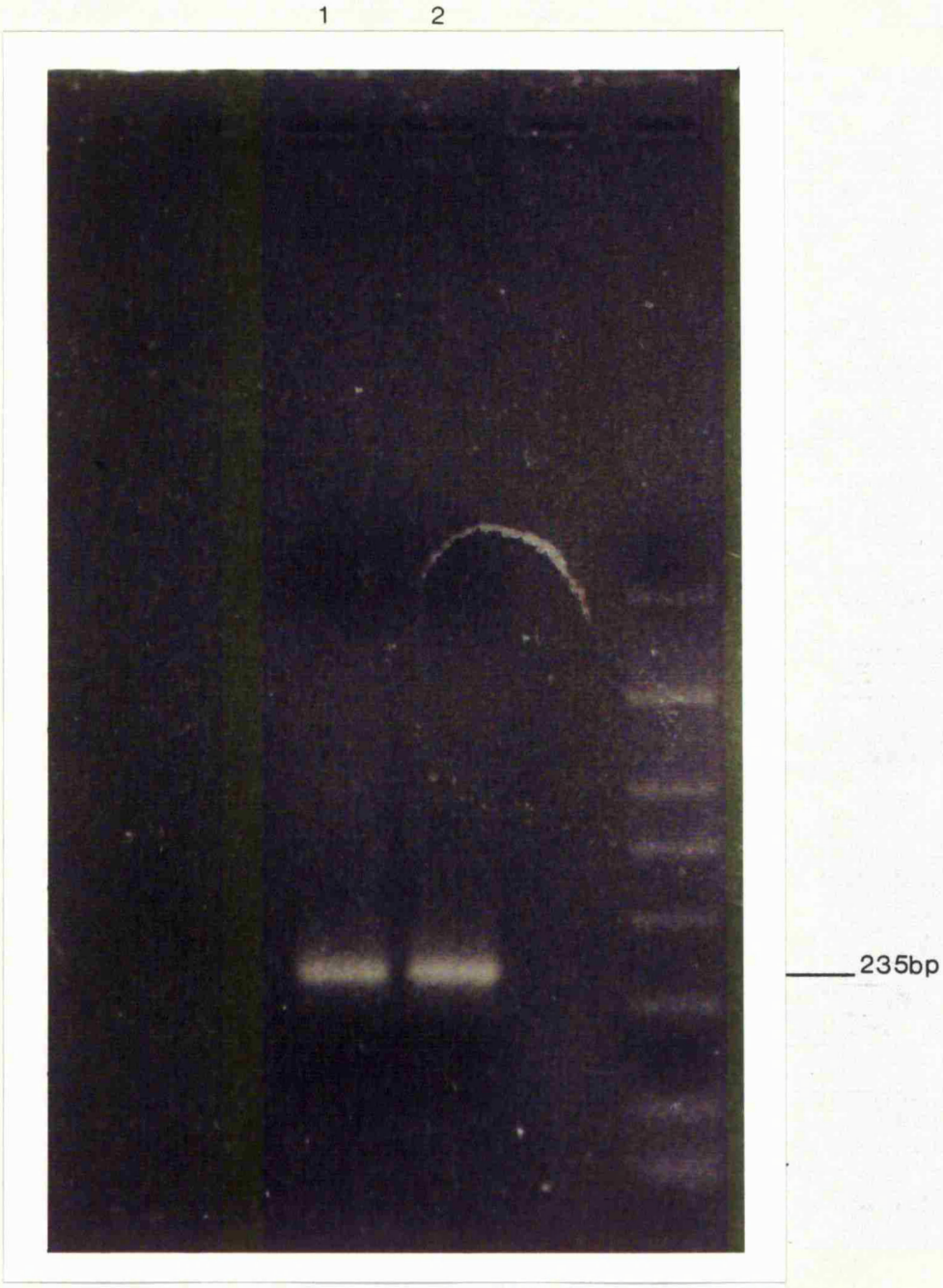

Figure 4.14(b) The 235 bp PCR product incorporating the Ser-92 processed 5' end.

Lane 1 and 2: 30 cycle PCR amplification employing 50 ng of the truncated clone rscNGC 1 as template at annealing temperatures of 60 and 65°C respectively. Molecular size markers shown (50-1000 bp) PCR markers.

A recombinant clone carrying the complete Δ92-rscNGC 1 sequence was constructed in pBluescript KS+ using overlapping restriction enzyme sites for *Bsu*36I and *Pst*I (Figure 4.15).

4.6 Heterologous expression of clone rscNGC 1 in *Xenopus* oocytes

Since the early 1980's, *Xenopus laevis* oocytes have been used extensively for the heterologous expression and accurate analysis of the discrete biological activities of a number of neurotransmitter receptors and ion channels [reviewed by Soreq and Seidman, 1992]. Oocytes have the following advantages in respect to the study of heterologous expressed ion channel molecules; i) the ability to process, assemble and insert oligomeric complexes into the plasma membrane, generating biological activities characteristic of the native molecules, and ii) their large size allows detailed functional analysis of channel activity by a variety of electrophysiological techniques.

4.6.1 Preparation of capped cRNA for cytoplasmic microinjection

cRNA transcripts for rscNGC 1 and Δ92-rscNGC 1 constructs were prepared for expression analysis in *Xenopus* oocytes by *in vitro* transcription using T7 RNA polymerase in the presence of the 5' cap analog dinucleotide 7-methylguanosine(5') triphospho(5')guanosine ($m^7G(5')ppp(5')G$ (0.5mM)), following linearisation of purified recombinant plasmids with *Xho* I (Figure 4.15). The 5' cap structure is believed to increase RNA stability and efficiency of expression of transcribed RNA in oocytes [Swanson and Folander, 1992].

Capped cRNA transcripts were also prepared for α and β-subunits of the human rod photoreceptor cNG channel (hrcNGC) as follows; i) hrcNGC–α kindly provided by Dr. R.S Dhallan (Dept. of Biomedical Engineering, John Hopkins University School of Medicine, Baltimore, Maryland. U.S.A) as a cDNA in the vector pBluescript KS+, was re-cloned in pBluescript SK+ using *Eco*RI and *Hind*III, prior to linearisation with *Xho*I and cRNA synthesis by *invitro* transcription using T7 RNA polymerase, and ii) rcNGC–β kindly provided by Dr. T-Y Chen (Dept. of Neuroscience, John Hopkins University School of Medicine, Baltimore, Maryland.

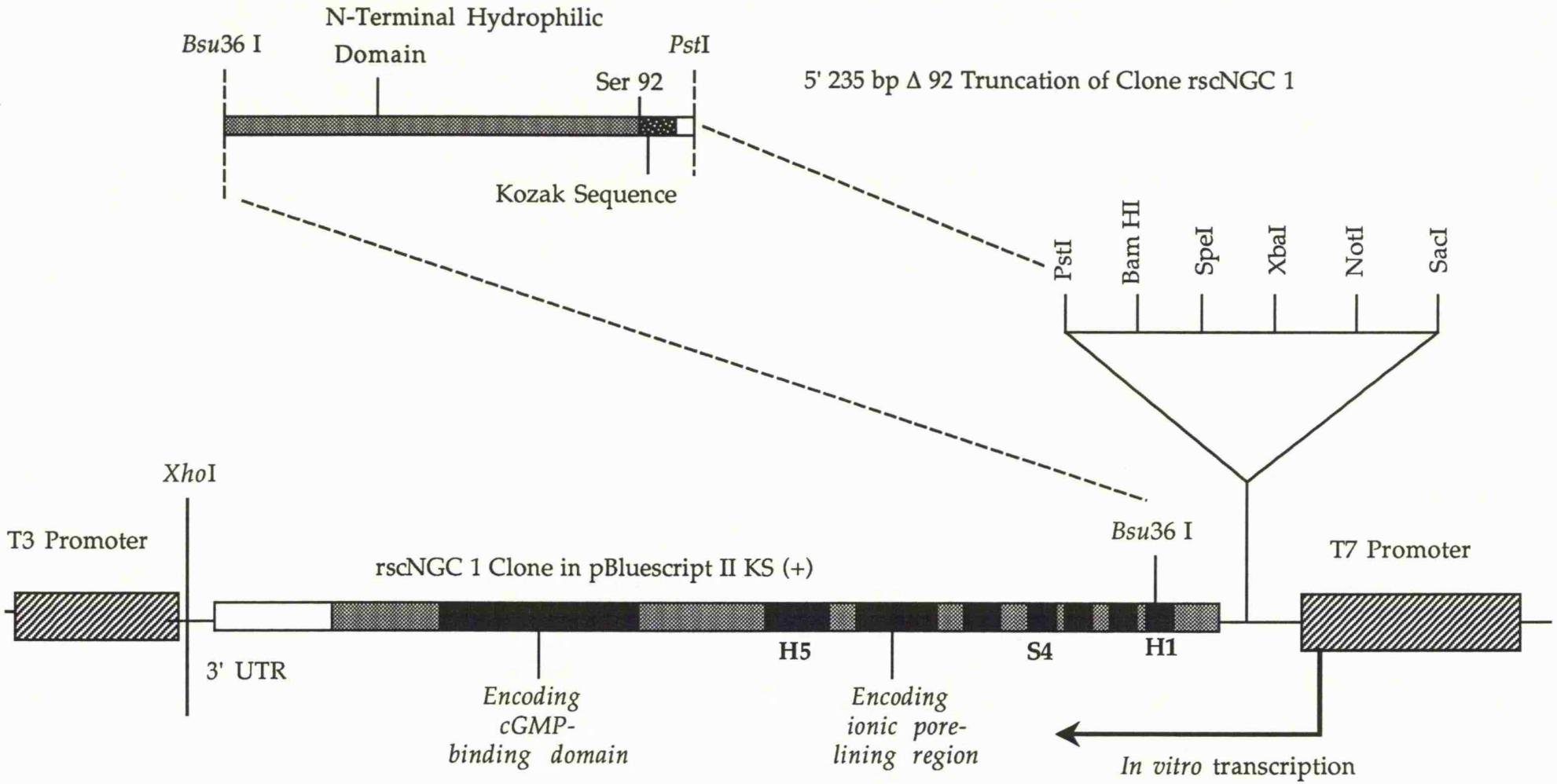

Figure 4.15 Construction of Δ 92-rscNGC 1 in pBluescript II KS+.

The 5' 235 bp product was removed from the pUC 18 vector by a *Pst*I/*Bsu*36I double digest and ligated into the prepared *Pst*I/*Bsu*36I recombinant rscNGC 1/pBluescript KS+ construct replacing the native N-terminus. cRNA was prepared by *In vitro* transcription following *Xho*I digestion.

U.S.A) as a cDNA in the vector pCIS was linearised with *Xba*I, and cRNA was synthesized by *in vitro* transcription using SP6 RNA polymerase. As hrcNGC–α has previously been heterologously expressed [Dhallan *et al.*, 1992], it served as a positive control for functional studies.

Aliquots of the *in vitro* transcription reactions (~1 μg of cRNA) were denatured, and analysed for integrity of synthesized RNA (Figure 4.16(a) and (b)). The product of each transcription reaction consisted of a single prominent species of RNA consistent with the size predicted from the nucleotide structure.

4.6.2 Expression of rscNGC 1 'assayed' by electrophysiological methods

rscNGC 1 channel-specific cRNA gave rise to 8-Br-cGMP-stimulated channel activity in three excised patches from 2 different cells after injection into *Xenopus* oocytes (Figure 4.17). No such responses to 8-Br-cGMP were detected in mock-injected oocytes. 8-Br-cGMP was used as it is a membrane permeable and hydrolysis-resistant analogue of cGMP. The different configurations of the patch clamp used within this investigation are described in Chapter 1.

The macropatch recording (Figure 4.17(a)) demonstrated that the cGMP-activated current was reversible i.e returned to baseline following 8-Br-cGMP 'wash-out', and its amplitude remained constant for several seconds, suggesting that the channel does not desensitize or inactivate in the presence of the cGMP analogue. Maximal currents of 20 pA at saturating 8-Br-cGMP concentrations (500 μM) were significantly smaller than previously observed (2-5 nA) for the heterologously expressed bovine rod cNG channel [Kaupp *et al.*, 1989].

To characterise the 8-Br-cGMP-stimulated current further, single channel currents obtained from patches containing only 1 ionic channel were recorded in the absence of divalent cations and at a low (5 μM) 8-Br-cGMP concentration. These revealed well resolved transitions between the open and closed state (Figure 4.17(b)). Distribution of open times appeared to have more than 1 mode, (some openings were very brief lasting on the order of 1 msec while other openings were extremely long, lasting several tens of msec), with an average open time of approximately 100

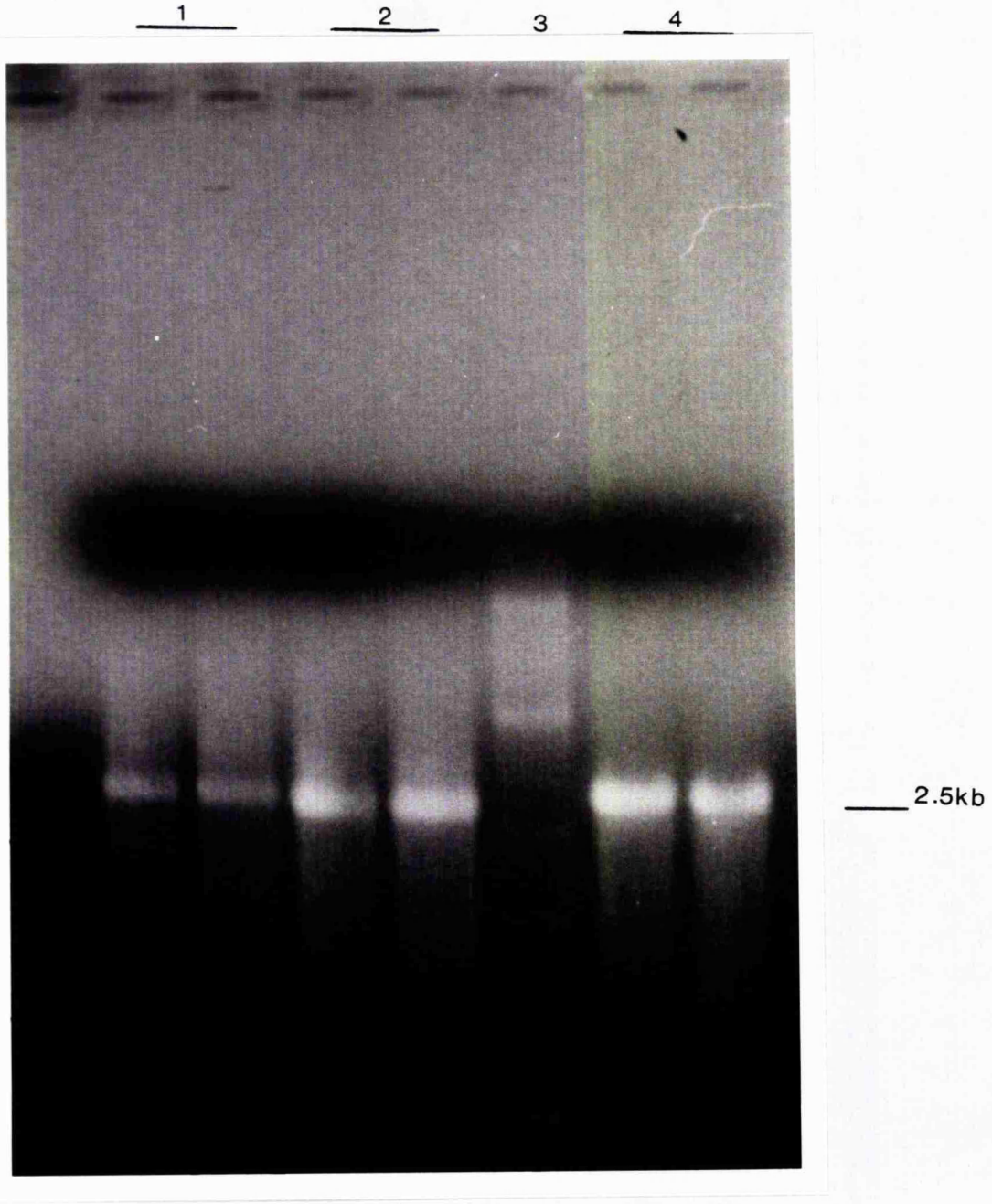

Figure 4.16 *In vitro* transcription of cRNA for (a) 'full-length' cNG channels and (b) processed Δ92-rscNGC 1

(a) Lane 1: 1 ul of *in vitro* transcription reaction using rscNGC 1/*Xho*I linearized as template. Lane 2: 1 ul of *in vitro* transcription reaction using hrcNGC-α/*Xho*I linearized as template. Lane 4: 1 ul of *in vitro* transcription reaction using hrcNGC-β/*Xha*I linearized as template. Lane 3: 1 μg of RNA (0.24-9.60 kb) molecular size markers.

Samples were analysed on an ethidium bromide-stained 1.2% agarose gel.

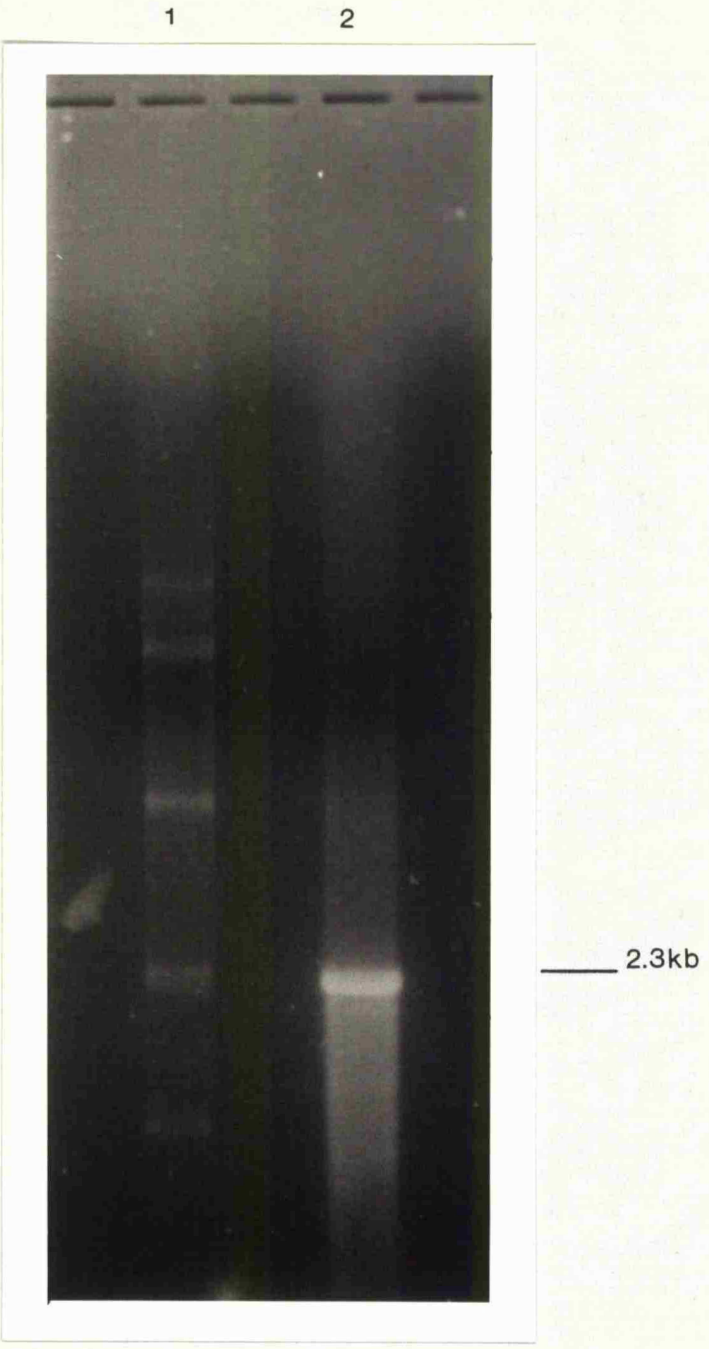

(b) Lane 1: 1 µg of RNA (0.24-9.60 kb) molecular size markers.
Lane 2: 1 ul of *in vitro* transcription reaction using Δ92-rscNGC 1/*Xho*I linearized as template.

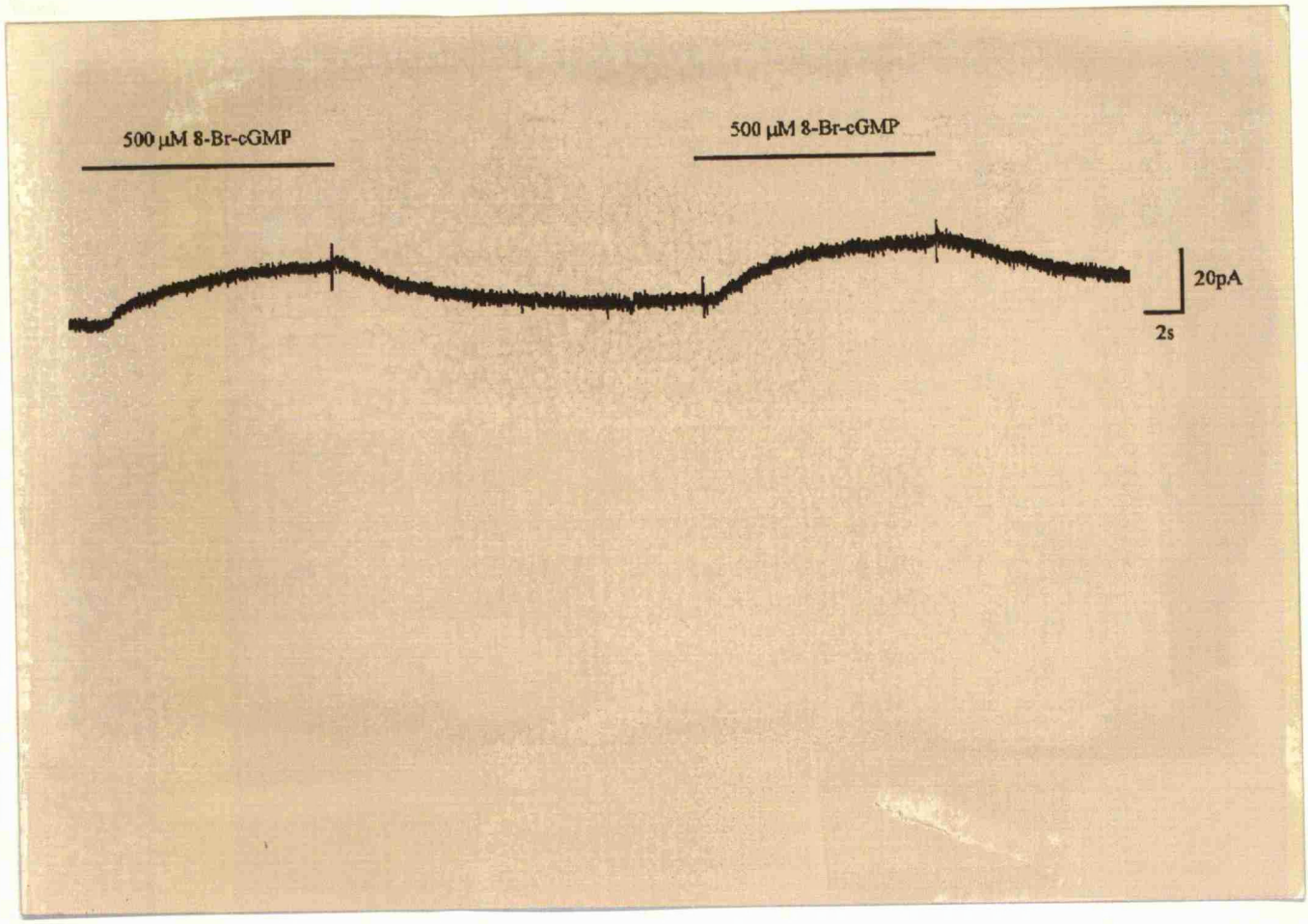

Figure 4.17 Properties of the cGMP-gated channel expressed in *Xenopus* oocytes injected with cRNA derived from rscNGC 1.

(a) Recording of rscNGC 1 from an inside-out macropatch at a holding potential of +60mV. 500 µM 8-Br-cGMP was applied during the period indicated by the bars. All recordings were made in symmetrical patch and bathing solutions of 100 mM KCl, 10 mM HEPES and 10 mM EGTA, pH 7.2.

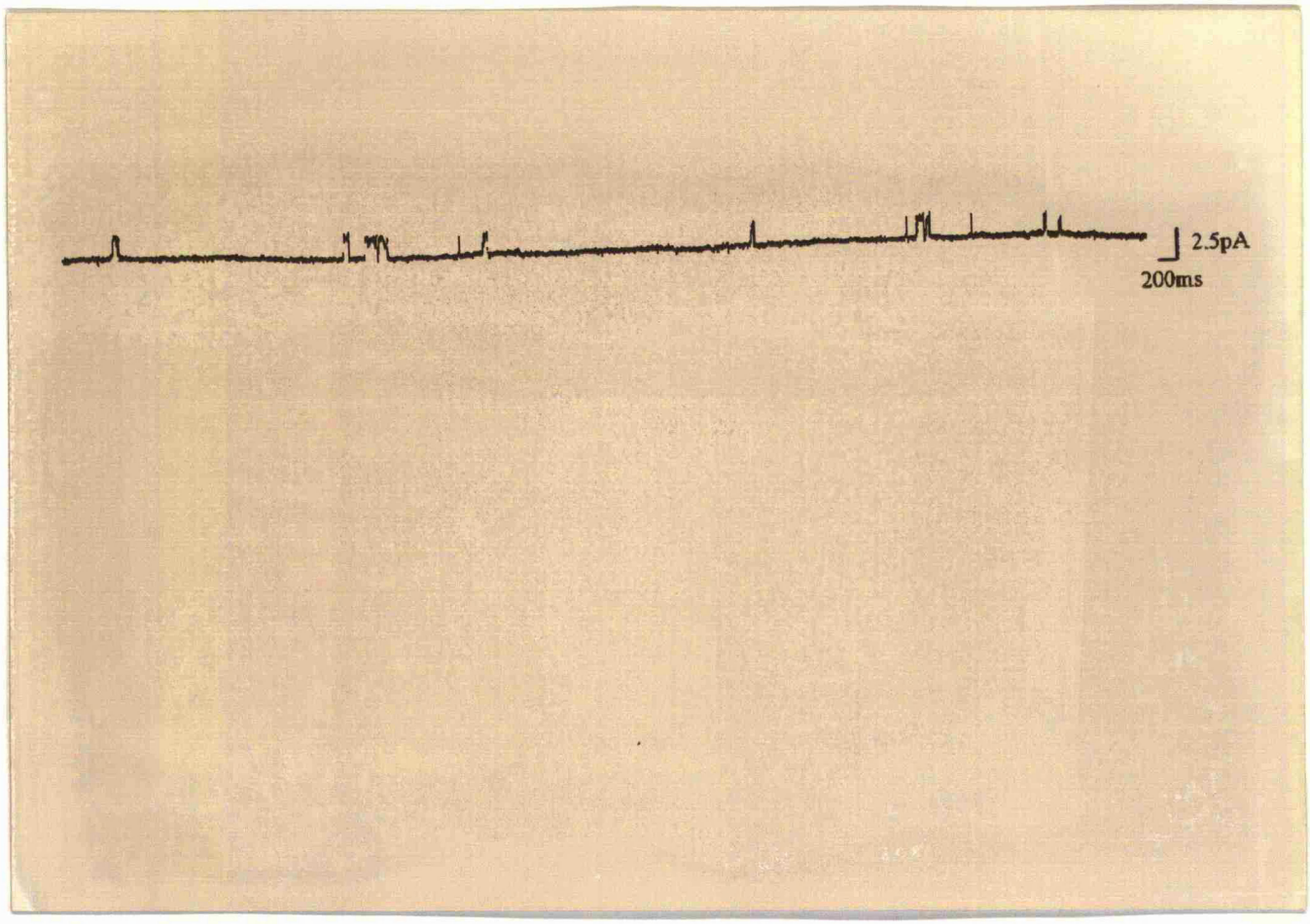

(b) Single channel recordings of rscNGC 1 from an inside out macropatch at a holding potential of +60 mV. 5 μM 8-Br-cGMP was applied during the whole period shown. Outward currents shown as upward deflection. All recordings were made in symmetrical patch and bathing solutions of 100 mM KCl, 10 mM HEPES and 10 mM EGTA, pH 7.2. (C) and (O) closed and open states respectively.

Method

cRNA was injected into Stage V and VI defolliculated *Xenopus laevis* oocytes (cRNA concentration 0.3 μg/μl; average volume injected per oocyte ~ 50 nl). Macroscopic and single-channel current measurements on excised inside-out patches were made after incubation of injected oocytes for 2-5 days, followed by removal of vitelline membrane.

milliseconds. The mean rscNGC 1 current amplitude in 100 mM KCl was 2 pA, which was very similar to that observed for the bovine rod cNG channel [Kaupp *et al.*, 1989].

4.6,3 'Loss' of functional expression

Following the initial characterisation of cGMP-activated currents for rscNGC 1, subsequent electrophysiological measurements failed to detect functional currents. Similar problems were encountered with hrcNGC-α specific-cRNA, which was used as a positive control for the expression and functional characterisation of cyclic nucleotide-gated channels within oocytes. The lack of functional expression was attributed to seasonal variations in the effectiveness of the oocyte as an heterologous expression system. Consequently further functional studies with Δ92-rscNGC 1 and hrcNGC-β could not be done.

Discussion

Sequence characterisation demonstrated that rscNGC 1 represented a SAN *homologue* of the rod photoreceptor cGMP-gated channel α–subunit (rcNGC-α). Although the N-terminal sequence of rscNGC 1 does not represent the native transcript, the cATG-ts primer employed in the anchor PCR retrieval of a full coding sequence encodes a peptide MKKNIINT which is highly conserved amongst cloned rcNGC-α subunits. It is hypothesised that the native SAN transcript would also encode such a sequence. It was reasoned that rscNGC 1 in common with other rcNGC-α subunits would adopt a similar transmembrane topography, which is proposed to consist of six transmembrane domains with intracellular N and C-terminal domains. This results in the 110 amino acid cyclic nucleotide-binding domain adopting an intracellular position, one which is necessary to function as a ligand 'pocket'. Like other characterised rcNGC-α subunits, rscNGC 1 shared sequence motifs i.e a S4 voltage sensor and a hydrophobic SS1-SS2 putative pore, in common with voltage-gated K^+ channels. The similarity in transmembrane topography and the conservation of key functional motifs

within the core of cNG channels, suggest that cNG and K^+ channels share a common ancestor [Jan and Jan, 1990].

rscNGC 1 homologues are encoded by a complex transcription unit raising the possibility that diverse channel proteins could be generated through alternative splicing. This has been shown to occur for the *Shaker* gene locus in *Drosophila*, which is composed of 21 exons that can alternatively be spliced to generate at least five distinct transcripts — increasing the functional heterogeneity of K^+ channels [Schwarz *et al.*, 1998]. However, differentially spliced variants of rscNGC 1 were not found within SAN tissue using anchor PCR. A Northern blot hybridisation was not attempted, as it was predicted that the limiting amount of SAN-derived poly A^+ mRNA would have made the detection of low abundance rscNGC 1 RNA transcripts difficult. Alternative splicing has been shown to remove exon 8 (encoding part of the putative first transmembrane domain, H1 see Figure 4.1), in a subset of transcripts within the human retina, producing an internal in-frame deletion of 36 codons. When expressed in a human embryonic kidney cell line this spliced variant, unlike the full-length cDNA did not produce functional channels [Dhallan *et al.*, 1992].

cNG channels are not only *directly* gated by intracellular signalling agonists, they are also targets for modulatory effects by *indirect* phosphorylation-dependent pathways. As discussed in Chapter 1 such pathways are known to regulate ligand affinity. However, the primary sequence of rscNGC 1 does not contain consensus motifs for phosphorylation. Although not excluding the possibility, this suggests that modulation of native rscNGC 1 activity by direct phosphorylation, does not seem to be physiologically important.

Oocyte micro-injection of rscNGC 1-specific cRNA elicited the expression of 8-Br-cGMP-activated currents, which could be assayed using the patch-clamp technique. Single-channel recordings demonstrated that rscNGC 1 exhibited similar characteristics to those observed for the heterologously expressed bovine rod cNG channel — reviewed in Chapter 1. These included distinct open-close transitions, which differ from the 'flickery' kinetics of channel openings in native rod outer segments [Kaupp *et al.*, 1989]. The lack of native channel recordings in SAN tissue preparations

prevents a systematic comparison to heterologously expressed rscNGC 1 currents. The small maximal current amplitude in inside-out oocyte macropatches and low success rate of detecting rscNGC 1 channel activity, indicates that the channel density is at least an order of magnitude lower than for the heterologously expressed bovine rod cNG channel. This was not a result of poor cRNA integrity, as oocyte micro-injection of capped cRNA prepared for the voltage-gated potassium channel-Raw 3, in an identical manner to rscNGC 1, gave rise to functional currents indistinguishable to those previously described [Rettig *et al.*, 1992]. This implied that properties inherent in the micro-injected cRNA were responsible for the observed low-level expression of rscNGC 1. This raises the possibility that the addition of 5' and 3' untranslated sequences of an RNA that is known to be efficiently translated in oocytes, such as the *Xenopus* β-globin transcript may in future enhance the levels of rscNGC 1 expression.

The seasonal variations in the 'quality' of oocytes prevented studies on Δ92-rscNGC 1. Such structure-function studies are vital in determining the contribution of the N-terminus to overall rscNGC 1 activity. The native 63-kDa 'processed' polypeptide i.e lacking the N-terminal 92 amino acids, has been purified from rod outer segments and functionally reconstituted into lipid membranes [Cook *et al.*, 1987]. This gives rise to the possibility that Δ92-rscNGC 1 may indeed form functional homomultimers following heterologous expression. However, it does not address whether such a mutated construct can modulate the sensitivity and selectivity for cyclic nucleotides, in an analogous manner to the reported N-terminal 'ball' of voltage-dependent K^+ channels — which has been shown to mediate inactivation by interacting with a region on the cytoplasmic face of K^+ channels [Hoshi *et al.*, 1990]. The main purpose of this study however, was to investigate whether the processed N-terminal polypeptide determined the formation of heteromultimers, by following possible co-assembly of Δ92-rscNGC 1 with the *modulatory* rod β-subunit (hrcNGC-β) using electrophysiological methods. It is anticipated that future studies with Δ92-rscNGC 1 may reveal that the N-terminal domain of rscNGC 1, in an analogous manner to voltage-dependent K^+ channels [Li *et al.*, 1992], determines the specificity of subunit co-assembly into heteromultimers.

Chapter 5

Searching for Novel Cyclic Nucleotide-Gated Ion Channel Genes In the Sino-Atrial Node

Introduction

Since the cloning of the first cyclic nucleotide-gated (cNG) ion channel gene in 1989 [Kaupp *et al.*, 1989], techniques of molecular cloning has revealed a growing family of cNG ion channel genes — to date 5 distinct genes have been cloned and functionally expressed. Conventional techniques of molecular biology have demonstrated the expression of these gene products in vasculature [Biel *et al.*, 1993], kidney [Biel *et al.*, 1994] and testicular tissue [Weyand *et al.*, 1994], as well as in the sensory tissues — retinal rod and cone photoreceptors and olfactory neurons [reviewed by Eismann *et al.*, 1993]. Thus, the tissue distribution of this class of channel proteins appears to be broad, rather than restricted to photoreceptor/olfactory tissue as first supposed [Ludwig *et al.*, 1990].

The demonstration that the native retinal rod photoreceptor cNG channel exists as an heteromultimeric structure containing at least two distinct subunits [Chen *et al.*, 1993], has raised the possibility that the other family members may also exist as heteromeric complexes. For example, comparisons of the ligand sensitivities of the native and cloned olfactory cNG channels show that they differ by 10- to 30-fold [Dhallan *et al.*, 1990]. It has been suggested that this discrepancy is dependent on additional unidentified subunits or factors which are required to reconstitute all the properties of the native channel. The notion of a heteromultimeric structure for cNG channels is consistent with the case for ligand-gated channels in general, such as those activated by neurotransmitters [reviewed by Barnard, 1992]. This combinatorial assembly of different cNG channel subunits to form heteromultimeric complexes, provides a means to increase the functional diversity of cyclic nucleotide-gated channels.

Could rscNGC 1 exist as a heteromultimer in situ?

Chapter 4 showed that the heterologous expression of the SAN homologue of the photoreceptor cGMP-gated channel (rscNGC 1) led to electrophysiological properties similar to those described for the expressed rod photoreceptor α-subunit (rcNGC-α) [Kaupp *et al.*, 1989]. These properties of rcNGC-α however, differed from those observed for the

photoreceptor channel *in situ*, where the co-expression of an additional cNG channel molecule, a β-subunit was required to reproduce electrophysiological characteristics of the native channel [Chen *et al.*, 1993]. This raised the possibility that like the human photoreceptor channel α-subunit, rscNGC 1 may also exist as a heteromultimeric complex in sino-atrial node regions of the heart. However, this is difficult to confirm or refute when recordings of the native nodal cNG channel have not been performed.

In an attempt to isolate further members of the cNG ion channel family which may or may not form heteromultimeric complexes with rscNGC 1, the sino-atrial node cDNA library was rescreened. The isolation and subsequent co-expression of such molecules with rscNGC 1, may be required for 'stable' heterologous expression.

5.1 Expression of a cAMP-gated channel homologue in sino-atrial nodal tissue

The original screening of 1.5 x 10^6 recombinant clones by nucleic acid hybridisaton had isolated a single cNG channel family member, isolate rscNGC 1, suggesting that such channel clones were of low abundance in the library. Prior to repeated low stringency cross-hybridisation screens for additional nodal cNG channel family homologues, a PCR screen was performed. It was reasoned that PCR screening would offer the best route to determine whether such related cNG channel sequences were represented in the amplified cDNA library, as large number of effective clones could be screened in a single reaction.

To determine if nodal homologues existed for the cNG channel gene product expressed in olfactory and aorta tissues, a *nested* set of PCR primers were designed to the published rat olfactory channel sequence [Dhallan *et al.*, 1989]. It was reasoned that sequences encoding the cyclic-nucleotide-binding domain were likely to be conserved between rat and rabbit, and so three sense (cA-Pr1-3) and antisense primers (cA-Pr4-6) annealing within this domain were designed (sequences are given in Materials and Methods), as shown in Figure 5.1(a). The cyclic nucleotide-binding domain because of its essential functional role, represented a

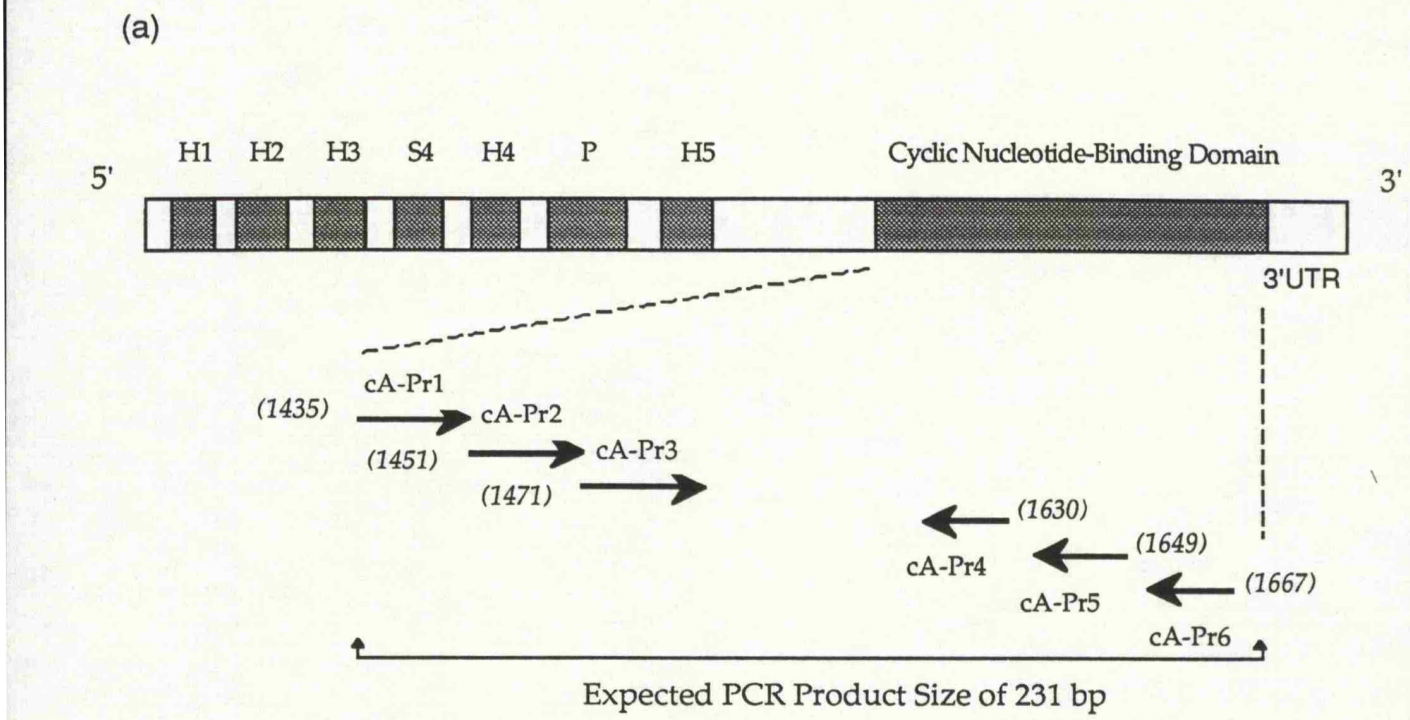

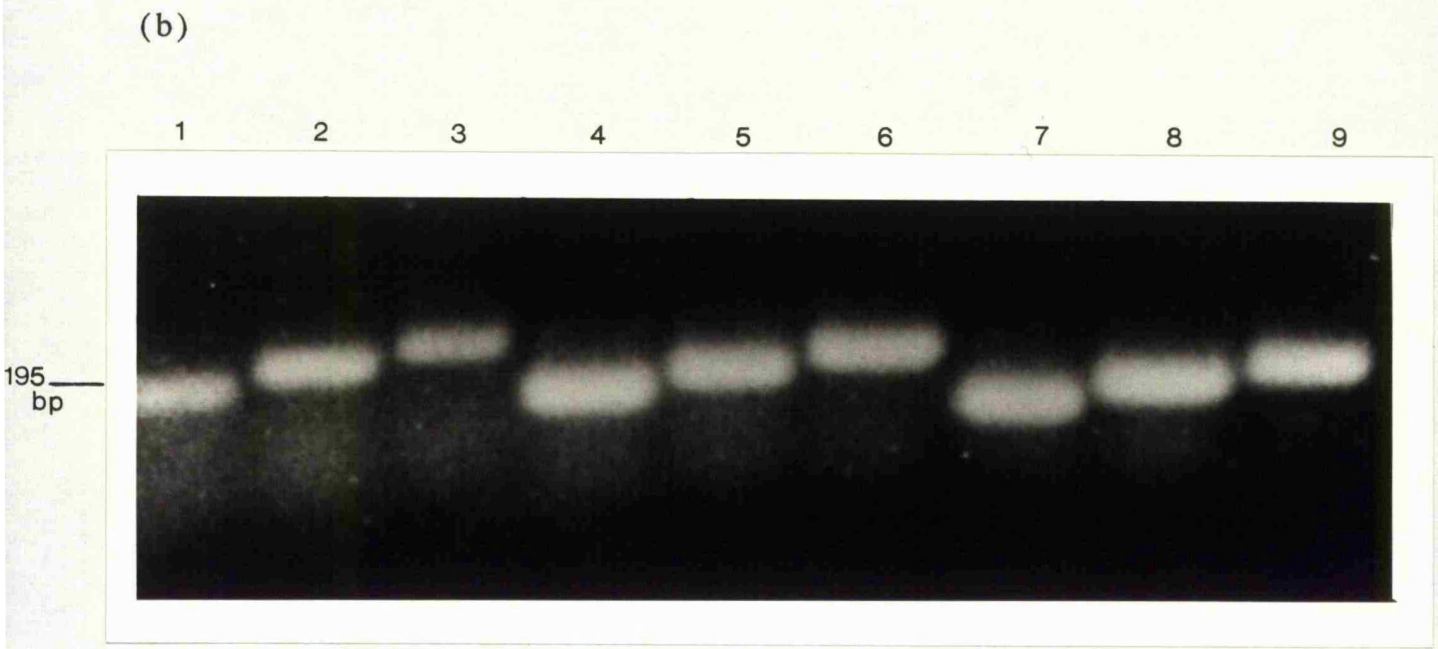

Figure 5.1 Multiplex PCR 'fingerprinting' demonstrating a cAMP-gated channel sequen in cDNA derived from the rabbit SAN tissue.

1 µl aliquots of the purified λ phage DNA was used as template. Samples were amplifie for 30 cycles at an annealing temperature of 50°C, and a portion of the reaction product v electrophoresed on a 1.2% ethidium bromide-stained agarose gel.

Lane 1: cA-Pr1/cA-Pr4. Lane 2: cA-Pr1/cA-Pr5. Lane 3: cA-Pr1/cA-Pr6.
Lane 4: cA-Pr2/cA-Pr4. Lane 5: cA-Pr2/cA-Pr5. Lane 6: cA-Pr2/cA-Pr6.
Lane 7: cA-Pr3/cA-Pr4. Lane 8: cA-Pr3/cA-Pr5. Lane 9: cA-Pr3/cA-Pr6.

diagnostic 'sequence-tag' for cNG channels. A 30 cycle amplification, using λ phage DNA as template (purified from aliquots of the amplified library representing 20 million recombinant clones), resulted in amplified bands of the expected size for all primer pair combinations (Figure 5.1(b)). Since only one of the primer pairs (cA-Pr2/cA-Pr5) was able to amplify a band from the previously isolated rscNGC 1, the PCR 'fingerprint' clearly demonstrated the expression of a distinct cAMP-gated channel in the sino-atrial node regional library.

This demonstrated that the initial sino-atrial node library contained cDNA clones for at least two distinct cNG channel genes, which had been previously thought to be expressed solely in photoreceptor and olfactory sensory tissues. This result gave good grounds to perform a further library screen for novel cNG channel genes.

5.2 Rescreen of the nodal cDNA library for additional cNG channel family genes

To isolate additional cNG channel clones which may be present within the nodal library, a further low stringency hybridisation screen was performed. The remaining 350 ng of sino-atrial node cDNA was ligated into *Eco*RI/*Xho*I digested Uni-ZAP XR dephosphorylated vector and packaged as previously described (Section 3.3). The resulting primary cDNA library contained of the order of 7.5×10^5 recombinant plaques. Due to the predicted low abundance of cNG channel clones within the amplified library (and the additional problems of preferential amplification of certain clones resulting in a biased cDNA population) it was considered necessary to screen a primary made cDNA library.

A [α-^{32}P] rUTP RNA probe of high specific activity could not be obtained despite several attempts, using the truncated 2.1 kb rscNGC 1 clone as template following *Xho*I linearisation. The large size of the template, required concentrations of cold rUTP for full-length transcription which decreased the overall incorporation of the radiolabel into the final transcript. To circumvent this problem, a random hexamer-primed probe, of specific activity 6×10^8 cpm/μg was synthesized and used in the primary library screen. The truncated rscNGC 1 clone was used for synthesis of the

probe as it lacked the N-terminal cytoplasmic domain, whose sequence is highly variable among individual cNG channels, but contained the core region which shows the highest conservation amongst individual cNG channel gene family members.

Method of screening and isolation of plaques (replicated on duplicate filters), was as previously described (Section 3.9 and 3.10). In total, forty clones that hybridised at low (2.0 x SSC, 0.1% SDS at 55°C overnight) but not at high stringency (0.5 x SSC, 0.1% SDS at 65°C overnight) were isolated to homogeneity by plaque purification from the second round screen. It was reasoned that these clones possibly shared regions of sequence similarity to rscNGC 1 and therefore, might represent new cNG channel members.

5.3 Characterisation of isolated cDNA clones by partial 'single-pass' sequencing

Following *in vivo* excision of each of the 40 individually-purified cDNA clones, double-stranded DNA templates were sequenced by the cycle sequencing protocol using dye-labelled primers on a 373A DNA Sequencer (Applied Biosystems). Clones were characterised by partial 5' and 3' sequencing. Sequences were aligned against the *Entrez: Sequences* database (release 7) and sequence similarity searches using the *MacVector*^{TM} sequence analysis software were performed as previously described (Section 3.10). Partial sequence generated from the M13 reverse sequencing primer produced of the order of 350-400 bp of usable 5' protein coding sequence for each clone. This enabled preliminary characterisation, following similarity searches against the nucleic acid database of *Entrez: Sequences* . It has been previously demonstrated that sufficient information is contained within 150 to 400 bases of a nucleotide sequence from one sequencing run for preliminary identification, and assignment of cDNAs to a gene family based on sequence similarity [Adams *et al.*, 1991].

This initial characterisation demonstrated that 48% of the clones (19 out of a total of 40) displayed variable nucleic acid identity to sequences already found in the database (Table 5.1).

Match Category of Isolated cDNAs	Number of Clones	Percentage of Total
No database match	19	47.5
Database match		
Non-mitochondrial genes	11	27.5
Mitochondrial genes	8	20.0
Clones which failed to *in vivo* excise	2	5.0
Total	40	

Table 5.1 Categories of cDNAs obtained from the primary SAN cDNA library following screening with the truncated clone rscNGC 1. Matches were determined by manual review of database searches of *Entrez: Sequences*.

Of the database matches, 8 of the isolates represented mitochondrial genes and the remaining 11 encoded for other nuclear genes (Table 5.2). These clones were grouped into broad functional categories in case this revealed a conserved motif of possible functional importance. Two clones matched partial cDNA sequences cloned from human atrial and skeletal muscle cDNA libraries, whose complete characterisation and biological functions remain to be determined.

Interestingly, of these 19 characterised clones, 12 represented matches to integral plasma membrane or to mitochondrial proteins, expressed in the inner mitochondrial membrane. This may be explained by the nature of the random hexamer primed rscNGC 1 probe, which would be expected to contain labelled fragments encoding putative membrane spanning α-helices. Generally, under low stringency hybridisation and wash

(a)

Functional Category	SAN Clone Nos	Putative Identification	Accession Number	Match Length (bp)	Percentage Identity
Cytoskeletal and Structural Proteins	9A	Human β-spectrin	M96803	333	91
	24B	Human cardiac α-myosin heavy chain	Z20656	272	59
Metabolic Enzymes	7A	Porcine lipoprotein lipase	X62984	357	83
	9B	Rabbit elongation factor EF-1	X62245	227	95
	25	Human spermidine/spermine N1-acetyltransferase	Z14136	186	84
Cell-Surface Proteins	10A	Human melanoma-associated antigen ME491	D00874	235	84
	10B	Human lysosomal membrane glycoprotein CD63	M58485	301	81
	24BA	Mouse membrane-associated protein (IC47)	L16953	249	85
Transporter	16A	Rabbit smooth muscle sarcoplasmic calcium ATPase	X02814	264	96
Unclassified	16B	Partial cDNA sequence clone HABA46. Source human atrial cDNA library	Z25905	369	82
	19B	Partial cDNA sequence, clone 09B09. Source human skeletal muscle cDNA library.	Z19257	152	93

(b)

SAN Clone Nos	Putative Identification	Accession Number	Match Length (bp)	Percentage Identity
4A and 6C	ND1 subunit of NADH-CoQ reductase complex	V00654	385	84
6A	ND4 subunit of NADH-CoQ reductase complex	V00654	364	86
8A	Rabbit blastocyst protein 4 mRNA, complete cds.	L04689	342	97
18A	Cytochrome b subunit of CoQ-cytochrome C reductase complex	X54172	374	92
20	Mus domesticus hydrophobic protein mRNA sequence.	L07095	339	82
25BA	ATPase subunit 6	J01394	394	87
29A	Cytochrome C oxidase subunit 1	V00654	321	81

Table 5.2 Sino-atrial node clones, showing significant nucleic acid sequence identity to (a) nuclear and (b) mitochondrial encoded genes.

Clones are listed with the sequence matched, the match length in nucleotides and percent identity of the alignment. Matches to nuclear encoded genes have been grouped into broad functional categories. Method of database searching was as previously described in Chapter 3.

conditions, signals significantly above background can be obtained for classes of molecules sharing 'islands of homology' to the probe — in this case multiple membrane spanning molecules.

19 clones showed no significant nucleic acid similarities to previously sequenced genes, and therefore represent new, previously uncharacterised cDNAs. Two of the clones failed to excise *in vivo* and were further investigated for the presence of an integral cyclic nucleotide-binding domain as found in cNG channel family members by PCR analysis. Since products were not obtained employing PCR primers *roc*A-1 and 2 (designed to conserved regions of the sensory cNG channels as described in Section 3.3) it was unlikely that these clones represented cg channel family members, and were discarded.

5.4 SAN cDNA clones not displaying database similarity

The majority of the partial cDNA sequences when compared against the nucleic acid database did not show any significant sequence similarity to published entries and appear to be derived from previously unidentified genes. These sequences may represent unknown gene families, or distantly-related, branches of known families. While within this group most cDNAs represent previously-unsequenced genes, the proportion that encode fundamentally new proteins are likely to be much smaller [Adams *et al.*, 1991].

Table 5.3 lists a selection of putative hits whose relative homology score ranked in the 100 best sequence alignments. All matches were ranked according to their optimum scores based upon measures of *local* sequence similarity. Many or all of the sequences within this group share local similarity to "excitability" proteins, such as ion channels, receptors, and ion pumps found in biological membranes [Lester, 1988]. Percentage values of nucleotide identity to such excitability molecules ranged from 45-50%, following the introduction of indels (insertions or deletions) and gaps for optimal alignment.

Clone	Length of Score Region (bp)	Maximum Possible Score	Matches to 'Excitability' Proteins Description	Optimum Score	Percentage Identity	Rank Position
03	461	2356	Chicken (Na+,K+)-ATPase-beta-2 subunit mRNA.	408	45.4	48
06B	453	2044	***B taurus RNA for cGMP-gated channel from retinal rod photoreceptor***	***360***	***45.7***	***18***
08B	426	1980	S.pombe sod2 gene for putative Na+/H+ antiporter Angiotensin receptor [turkeys, adrenal glands, mRNA] Bovine mRNA for endothelin receptor Opossum parathyroid hormone receptor mRNA,	362 350 342 338	44.6 44.2 43.7 43.2	22 46 68 83
12	484	2368	Human insulin receptor (allele 2) gene, exons 14, 15, 16 and 17.	450	43.4	70
14	421	1828	Rat mRNA for metabotropic glutamate receptor Human gamma-aminobutyric acid-A (GABA-A) receptor beta-1 subunit	322 314	49.3 47.1	42 60
15	470	2344	Rabbit cardiac muscle Ca2+ release channel	400	50.9	71
18B	411	1884	Sodium-glucose cotransporter homolog [human, kidney cortex] Human potassium channel (HPCN1) mRNA	386 324	44.7 42.2	2 88

20A/ 20B	444	1992	Mouse cystic fibrosis transmembrane conductance regulator (CFTR) gene, exon 10.	341	43.8	21
24BD	413	1956	Human gamma-aminobutyric acid-A (GABA-A) receptor beta-1 subunit	394	52.0	20
25BC	479	2188	***B.taurus RNA for cGMP-gated channel from retinal rod photoreceptor***	***392***	***53.2***	***18***
			Human cGMP-gated cation channel protein mRNA	***388***	***52.4***	***24***
			Human voltage-gated sodium channel mRNA	***378***	***52.1***	***43***
27	449	2444	Mouse mRNA for glutamate receptor channel subunit epsilon 3.	378	46.7	73

Table 5.3 Table of uncharacterised clones showing similarities to excitability proteins.

The length of score region defines the size of the clone query sequence used in the database search. Maximum possible score are the scores obtained for 100% identity of a clone to an existing sequence. Highest optimum score represents the score for the best local alignment of a matched region of a database entry to a clone. Rank position represents the overall place of a 'hit' in the best 100 matched scores. The current *Entrez: Sequences* database release 7 contains 143,579 entries. Matches to cNG channel genes are indicated in bold italics. Methods employed in the database searches were as previously described in Chapter 3.

5.4.1 *Clones sharing local sequence similarity to cNG channel genes*

Of particular interest were the cDNA clones 6B and 25BC which shared interrupted homology to genes encoding for retinal rod photoreceptor cNG ion channels. However, closer analysis demonstrated that clone 25BC shared a stronger match to the antisense than sense strand of the rod cNG channel and therefore was not of functional importance.

An optimal alignment of clone 6B to genes encoding the α and β–subunits of the human rod photoreceptor cNG channels, demonstrated that this isolate shared over 50% nucleotide identity to the 5'end of the α–subunit, encompassing the putative H1 transmembrane domain. The strongest nucleotide similarity existed in the polyadenylate region encoding the N-terminal lysine-rich hydrophilic domain. This raised the possibility that clone 6B could contain a similarly charged domain to that found in α-subunits of cNG channel family members. The overall similarity to the β-subunit of the human retinal rod cNG was considerably less.

5.5 Further characterisation of the 'cNG channel' homologue clone 6B

5.5.1 *Verification of sequence homology at the nucleic acid level*

The similarity of clone 6B to mammalian sequences encoding subunits of the cNG channel complex expressed in retinal rod photoreceptor cells, raised the possibility that the clone might represent a new cNG channel subunit.

The 1.8 kb clone 6B was characterised further by sequencing using a primer-walking strategy employing dye terminators. At each stage of characterisation the updated sequence information for 6B was searched against the nucleic acid database. As primer walking continued, the original similarity to cNG channel genes was lost. However, sequence similarities did remain intact at the nucleic acid level to other 'excitability' proteins, and in particular to other members of the voltage/second messenger-gated channel superfamily. This further suggested that clone 6B could represent a distantly-related member of this gene superfamily.

5.5.2 *Characterisation at the protein level identifies a polypeptide motif*

The observed distant evolutionary relationship to the voltage/second messenger-gated channel superfamily could have been merely coincidental at the nucleotide sequence level. To allow more sensitive sequence similarity searching, the 3 forward frames of clone 6B-1058 bp were translated. Open reading frames (ORF) longer than 50 amino acids were found only in the first reading frame. The deduced amino acid sequence was aligned to the protein identification resource (PIR) of *Entrez: Sequences* (Release 7) using a Wilbur-Lipman sequence similarity search subroutine. Both pam 250 and pam 250S amino acid substitution models were used for scoring similarities between peptide sequences. The pam 250S matrix matched amino acids according to the properties of their side chains allowing for conservative substitutions within an alignment, whereas the pam 250 matrix matched sequences according to amino acid identity. The value of such peptide similarity searching is in the use of primary structure conservation through evolution in the identification of known domains and motifs, enabling possible functional classification.

Clone 6B-ORF 1 (translated in the first open reading frame), showed sequence similarity to the N-terminal 89 kDa domain of human erythrocyte ankyrin, which is composed of a repeated 33-amino acid sequence motif [Lux *et al.*, 1990]. An alignment of 6B-ORF 1 with the erythrocyte ankyrin consensus sequence [Lux *et al.*, 1990], demonstrated the presence of a domain between residues 71-268 consisting of six imperfect repeats of 32-33 amino acids (Figure 5.2). These repeats have been shown to facilitate the binding of several integral membrane proteins, such as voltage-dependent sodium channels [Srinivasan *et al.*, 1988] and the (Na^+/K^+)-ATPase [Koob *et al.*, 1988] to the underlying cytoskeleton — maintaining polarisation within the membrane.

Due to the large degree of sequence redundancy in the PIR database, the best five alignment scores for clone 6B-ORF 1 were to erythrocyte and brain ankyrin gene products. However, these 'ankyrin-like' repeats are also found in a number of additional protein sequences from distinct multigene families. Of particular interest was the similarity that clone

Ankyrin Consensus Sequence

- G - T P L H - A A - - - - - - - - V - - L L - - G A - - - - - D -

Clone 6B-ORF 1

71-103	v d v p r f l k A A l e n k l a d V e k f L s d q n x p d v c D e
104-136	y k r T a L H r A c l e g h l a i V e k L m e a G A q i e f r D x
137-169	l e s T a i H w x c r g g n l e v x k l x x n k G A e i s a r D k
170-202	l l s T a L H v g v r t g h y e c a e x L i a c e x d l n a k D r
203-235	e G d T P L H d A v r l n r y x m i r x L i m x G A d l t i k n x
236-268	a G k T P m d l v l n w q n g t k a x f d x l k e e f l q n l s h

Figure 5.2 Comparison of aligned ankyrin-like repeats of clone 6B-ORF 1 with the ankyrin consensus sequence [Lux *et al.*, 1990].

A hyphen (-) in the ankyrin sequence marks a position where no consensus exists.
Identical residues to the consensus ankyrin sequence are indicated by underlined uppercase letters.
X represents codons for which an amino acid residue could not be assigned. The first and last amino acids of each repeat are indicated to the left of the sequence.

6B-ORF 1 showed to the high-affinity potassium transporter AKT1 from the plant *Arabidopsis thaliana* (Figure 5.3). The match to AKT1 extended from amino acids 485 to 748 a region that also contains six imperfect 'ankyrin-like' repeating sequences of 32-33 amino acids [Sentenac *et al.*, 1992]. This region is found towards the C-terminus of the transporter outside the core region encompassing six putative membrane-spanning domains. Interestingly, a match to another related potassium transporter (KAT1) from the same species of plants was found. However unlike AKT1, the transporter KAT1 does not contain an 'ankyrin-like' motif [Anderson *et al.*, 1992].

Over a match region of 277 amino acids, clone 6B-ORF 1 showed 40.1% amino acid sequence similarity (22.6% identity) to AKT1 and over a region of 46 amino acids, 41.9% similarity (18.6% identity) to KAT1. Both AKT1 and KAT1 share extensive amino acid sequence identity to one another, and they represent members of a multigene K^+ channel family in higher plants [Sussman, 1992]. As previously mentioned (Section 1.6) AKT1 and KAT1 share amino acid similarity (~20% overall sequence identity) to the superfamily of voltage/second messenger-gated ion channels. Of particular significance is the presence of an integral cyclic nucleotide-binding domain in AKT1, highly homologous to that found in cNG channel genes [Sentenac *et al.*, 1992]. This binding site is found in the cytoplasmic C-terminal domain upstream of the ankyrin-related sequence. It is currently unknown whether the 838 amino acid protein encoded by AKT1 mediates passive or active K^+ transport, which can be modulated by intracellular cyclic nucleotide second messengers.

5.5.3 Possible 'nature' of clone 6B

Clone 6B represents a novel isolate from the sinus node. Translation in the first open reading frame identified a domain containing six tandem 'ankyrin-like' repeats. Clone 6B shared sequence similarity with the plant potassium transpoter AKT 1 — a member of the voltage/second messenger-gated channel superfamily, which raises the possibility that clone 6B could be 'channel-like' in nature.

```
6B-ORF 1   PAHHVSLAEQ QWEREKQREA ELKKKKLEQR SKLENLEDLE IIIQLKKRKK YRKTKVPVAK EPEPEIITEP [ 70]
Ankyrin                             iqak tK-ngLspih maaQ-gdhld cvrlllqyda Eid-dItldh [338]
AKT 1                                     mnNL--Lq hlkemndpvm -tnvlleien mlargkmdlP [519]

                              1                                  2

6B-ORF 1   VDVPRFLKAA LENKLADVEK FLSDQNXPDV CDEYKRTALH RACLEGHLAI VEKLMEAGAQ IEFRDXLEST [140]
Ankyrin    ltplhvaahc ghhrvAkV-- lLdkgakPns ralngfTpLH iACkknHvrv mElLlktGAs Idavtesglt [406]
AKT 1      lnlc-F-aAi rEddLl-lhq lLkrgldPne sDnngRTpLH iAaskGtLnc VllLlEyhAd pncRDa-Egs [585]

                         3                                  4

6B-ORF 1   AIHWXCRGGN LEVXKLXXNK GAEISARDKL LSTALHVGVR TGHYECAEXL IACEXDLNAK DREGDTPLHD [210]
Ankyrin    plHvasfmGh LpivKnllqr GAspnvsnvk veTpLHmaaR aGHtEvAkyL lqnkakvNAK akddqTPLHc [476]
AKT 1      vplWeameGh ekVvKvlleh GstIdA-gdv -ghfactaae qGnlkllkei vlhggDvtrp rRtGtsaLHt [654]
KAT 1                                                            Ldvt nptsDTaLmD [549]

                    5                                  6

6B-ORF 1   AVRLNRYXMI RXLIMXGADL TIKNXAGKTP MDLVLNWQNG TKAXFDXLKE EFLQNLSHXY VLRKXDSFIS [280]
Ankyrin    AaRightnMv klLlennAnp nlattAGhTP lh-iaaregh vetvlalLek E                     [526]
AKT 1      AVceenieMv kyLleqGADv nkqdmhGwTP rDLa-e-QqG hedikalfrE k-Lhe-rrvh ietsssvpIl [720]
KAT 1      AihkedteMv kk-Ilkeqki e-rakverssse                                         [577]


6B-ORF 1   NCSTGIFGGX XLXTRATEPR XPVFFQTWF [310]
AKT 1      ktgirflGrf tsepnirpas reVsFrir  [748]
```

Figure 5.3 Sequence alignment of clone 6B-ORF 1 with ankyrin and plant transporters.

Human erythrocyte ankyrin [Lux *et al.*, 1990], and *Arabidopsis thaliana* K^+ transporters AKT1 and KAT1 [Sentenac *et al.*, 1992; Anderson *et al.*, 1992]. Amino acid gaps (marked by hyphens) introduced for maximal alignments. Position of the 6 'ankyrin-like' repeats are numbered and indicated above the sequence for 6B-ORF 1. Amino acid identities and mismatches to clone 6B -ORF1 are represented by upper and lower case letters respectively. Position of amino acid residues are marked in *parentheses* to the right of the alignments.

Method

Sequences were aligned using a Wilbur-Lipman sequence similarity search subroutine with a pam250 scoring matrix.

Discussion

A homologue of a cAMP-gated channel was demonstrated to be expressed in sino-atrial node tissue, by a PCR 'fingerprint' from aliquots of library cDNA. Because olfactory neurons employ cAMP as a second messenger this channel has been described as a cAMP-gated ion channel, although it is activated more potently by cGMP [Dhallan *et al.*, 1990]. By conventional molecular techniques it has been demonstrated that two distinct cNG ion channel genes previously thought to be restricted to photoreceptor and olfactory tissue, are expressed within sino-atrial tissue. A sequence highly homologous to the rat olfactory channel has also been recently cloned from mouse heart RNA [Ruiz *et al.*, 1993]. The expression of such a channel in cardiac subregions has also been confirmed, using RT-PCR studies [Biel *et al.*, 1993]. Neither work was able to localise the channel to a specific tissue or cell type. These results suggest that the olfactory channel homologue as well as being expressed within sino-atrial nodal tissue, is also found within other cardiac subregions. Because cAMP-gated channels require intracellular agonists to be activated, they are likely to be *obligatorily* coupled to cardiac receptor systems. However, they have yet to be described in functional terms within SAN, or any other cardiac subregion.

By the design of a series of oligonucleotide primers to the entire protein coding region of the published rat sequence, it was demonstrated by PCR on genomic DNA that the gene for the rabbit cAMP-gated channel homologue lacked introns in the coding region [E.C Conley, unpublished observations]. Although there may exist introns in both 5' and 3' untranslated sequences, the gene structure for cAMP-gated channels is clearly less complex than that for homologues of the rscNGC 1 channel, which as described in Chapter 4 contains several introns within the coding region.

The demonstration that two distinct cNG channels are expressed in SAN tissue raises the possibility that they could functionally co-assemble within native tissue, leading to the formation of unique heteromultimeric

complexes. However, evidence to support such a hypothesis whether *in situ*, or in the use of the cloned cDNAs for heterologous co-expression studies, is yet unavailable. Because of the heterogeneous nature of nodal pacemaker tissue, such *in situ* studies will require the use of immunocytochemical techniques to determine whether both channels are indeed expressed in a single cell type.

Native retinal rod photoreceptor cNG channels exist as a hetero-multimeric complex composed of separate α and β-subunits [Chen *et al.*, 1993]. This raised the possibility that there existed a similar subunit within the sino-atrial node, that could form functional heteromers with rscNGC 1. Re-screening of the nodal specific cDNA library under low stringency for the presence of new cNG channel clones resulted in the isolation of 39 putative positives, of which 18 represented previously characterised genes. However, the majority of the cDNA sequences when compared against the nucleic acid database appeared to correspond to previously unidentified genes, although regions of local sequence similarities were found to 'excitability' proteins raising the possibility that signalling proteins maybe major constituents of this unknown cDNA population. These sequences were not further analysed as regions of sequence similarity were not found to cNG channel genes. Additionally, the problem of frame-shift sequencing errors which would be predicted to affect the accuracy of the conceptual translation, may have prevented the identification of homologues, particularly distantly-related ones.

cDNA clone 6B, whose 5' protein coding sequence shared nucleic acid similarity to known members of the family of cNG channels, was further characterised. The generation of a total of 1.5 kb of sequence of which over 1 kb represented protein-coding information, allowed a more complete characterisation of this clone. Conceptual translation in all three reading frames, identified a polypeptide likely to form the native protein. Subsequent sequence similarity searching of a peptide database identified a region containing six tandem 'ankyrin-like' repeats. Of particular interest, clone 6B shared sequence similarity to two members of a multigene K^+ channel family in higher plants — one of which also contains an integral 'ankyrin-like' motif.

What is clone 6B?

It has been postulated that proteins bearing multiple ankyrin-like repeats are highly likely to be associated with receptors and the cytoskeleton [Lux *et al.*, 1990]. This implies that clone 6B would have the ability to interact with cytoskeletal elements or with subunits of regulatory proteins, and therefore could be of particular functional importance in cellular signalling. Grouping clone 6B as a putative cell-surface 'channel-like' molecule is based on local sequence similarity to two high-affinity potassium transporters AKT1 and KAT1 from the plant *Arabidopsis thaliana*. This similarity raises the *possibility* that clone 6B could represent a new, distantly-related member of the superfamily of voltage/second-messenger gated ion channels.

A number of further approaches do exist for pursuing the function of this new, previously uncharacterised nodal gene. These include complete sequencing and functional expression of the protein product, chromosome mapping, tissue distribution studies and immunological characterisation. Complete identification can only take place following retrieval of the complete open-reading frame. Clone 6B appeared to be a partial cDNA sequence of 1.8 kb in size, as a translational initiation ATG site surrounded by a ribosome-binding consensus sequence could not be found in the 5' region of the clone. The clone did however appear to have an intact 3' untranslated region as demonstrated by the presence of a poly A^+ tail. Thus in order to obtain full-length clones for complete characterisation and expression studies, retrieval of the 5' protein-coding region will be necessary, possibly by anchor-PCR methods as discussed in Section 4.2.

The low stringency library screen was specifically designed to identify new members of the cNG channel family which *may* form heteromultimeric complexes with rscNGC 1 — so why were such clones not retrieved from the library? The principle reason is likely to be the extremely low abundance nature of native cNG channels transcripts. As 'unprocessed' tissue-specific cDNA libraries can only reflect the abundance of gene transcripts in the original mRNA population, this makes the potential cloning and isolation of new cNG channels extremely difficult.

Chapter 6

MEL Cells As A Heterologous Expression System For Studying The Coupling Of Cyclic Nucleotide-Gated Channels To Second Messenger Systems

Introduction

A number of G protein-coupled second-messenger pathways involving closely-related families of signalling components have been described, all of which have been found to underlie physiological responses involving ionic channels [reviewed by Brown, 1991]. Cyclic nucleotide-gated (cNG) ion channels are *obligatorily* coupled to the intracellular second messengers cAMP and cGMP, providing a mechanism for rapid electrical signalling. For this channel family, the pathways found in vertebrate photoreceptor cells and olfactory sensory neurons are the best characterised. Retinal rod and cone photoreceptor cells respond to light with a membrane hyperpolarisation, due to closure of intrinsic membrane cGMP-gated ion channels. Light activates a G protein-mediated signalling cascade that leads to the activation of a cGMP phosphodiesterase, which by hydrolysing cytoplasmic cGMP molecules results in channel closure. In sensory neurons of the olfactory epithelium, odorants lead to the rapid stimulation of adenylyl cyclase and an elevation in intracellular cAMP through G protein-coupled receptors, which in turn directly activates the olfactory cNG ion channel resulting in membrane depolarisation.

The demonstration that sino-atrial nodal tissue express two distinct cNG ion channels (this thesis) raised an important question: what receptor-mediated intracellular second-messenger systems were coupled to these channels *in situ*? The SAN region of the heart can be described as a 'control centre' due to its rich innervation by both sympathetic and parasympathetic nerves, whose neurotransmitters have well documented effects on the intracellular levels of cyclic nucleotides following receptor stimulation [Hartzell, 1988]. Thus it is feasible that nodal cNG ion channels are coupled to adrenergic/cholinergic mediated second-messenger pathways *in situ*. The aim of the present work was to follow the functional coupling between receptor-mediated second messenger pathways and cNG channel components in a heterologous system. The reconstitution of such a defined channel-second messenger system *in vitro* , is an important step in understanding the functional significance of cNG channels within non-sensory signal transduction pathways. Murine

erythroleukaemia (MEL) cells were chosen as the model heterologous system as they were expected to contain a number of G protein-coupled second messenger signalling pathways, and due to their relative electrical 'quiescence', can support the functional analysis of expressed ion channels [Shelton *et al.*, 1993].

By the heterologous expression of a cAMP-gated ion channel cDNA — whose gene was shown to be expressed within sino-atrial nodal regions of the heart by a PCR 'fingerprint' (Section 5.1), it was both feasible and attractive to attempt the stable reconstitution of cNG channel activation through a receptor-mediated second messenger pathway. Such heterologous coupling would be reliant on extracellular agonists for the activation of endogenous MEL cell receptors. This is can be described as five element signalling pathway, with information flowing from G protein-coupled agonist occupied receptors to cNG ion channels, through activation of adenylyl cyclase (Figure 1.3). It was reasoned that the resultant increase in the intracellular concentration of cAMP would *open* the heterologously expressed cAMP-gated ion channel. Such channel activation would lead to an increase in membrane conductance — due to the influx of sodium and calcium ions. The measurement of this non-selective cationic current would form the basis of a sensitive electrophysiological assay for the functional reconstitution via an indirect (cytoplasmic second-messenger) pathway of receptor-cNG channel coupling.

The characterisation of the precise mechanism and kinetics of such agonist-activated electrophysiological responses within MEL cells, would provide a prototype system for the future study of a variety of intracellular ligand-gated ion channels.

The LCR/MEL gene activation system for the expression of heterologous proteins.

The LCR/MEL gene activation system allows the high-level expression of a range of heterologous proteins in erthyroid-specific cells such as MEL cells, using vectors containing sequence elements from the human β-globin locus control region (LCR). The LCR has been shown to directly influence the specific activation of β-globin genes in erythroid cells and is

characterised by the presence of four DNAse I-hypersensitive (HS) sites [Grosveld *et al.*, 1987]. These are specific to the chromatin of erythroid cells and enable the formation of a transcriptionally-competent locus. The LCR has the ability to confer on a gene linked *in cis* erythroid-specific expression which is independent of its site of integration, and directly proportional to gene copy number, when stably introduced in erythroid cells [Collis *et al.*, 1990].

Murine erythroleukaemia (MEL) cells [Friend *et al.*, 1971] are erythroid progenitor cells which have been transformed by the Friend virus complex and are arrested at the pro-erythroid stage of development. However, upon treatment with various chemical agents, including dimethyl sulfoxide (DMSO), MEL cells can be induced to undergo a pattern of terminal erythroid differentiation which closely mimics the analogous process *in vivo,* including the high level synthesis of globin proteins [Kabat *et al.*, 1975]. The human β-globin LCR sequences have been shown to be fully functional in MEL cells [Blom van Assendelft *et al.*, 1989].

The LCR/MEL gene-activation system has been previously used in the stable electrophysiological expression of a number of heterologous cDNAs, encoding both homomultimeric voltage- [Shelton *et al.*, 1993] and inward rectifying G protein-gated ($I_{k,ACh}$) [Jacobson *et al.*, unpubl. data], K^+ channel proteins.

6.1 LCR-mediated gene-activation of a luciferase reporter gene in MEL cells

To characterise the MEL cell for endogenous G protein-coupled receptors which could activate adenylyl cyclase, a reporter construct containing the firefly *Photinus pyralis* luciferase gene was to be used. The initial work focused on whether reliable, quantitative luciferase responses could be obtained from MEL cells in culture, using a luciferase reporter gene under the control of LCR gene-activation elements. In addition this study provided a quantitative analysis of the LCR/MEL system for expression of heterologous molecules.

6.1.1 *Production of stable μLCR-Luciferase/MEL clonal cell lines*

The vector μLCR-RSV-Luciferase was kindly provided by Dr. M. Antoniou (National Institute for Medical Research, Mill Hill, London. U.K). The 14.8 kb vector (Figure 6.1), incorporates a LCR 'microlocus' upstream of the firefly luciferase gene under the control of a RSV promoter, a partial *Nar*I-thymidine kinase-neomycin resistance gene conferring G418 resistance upon transformation into MEL cells and an ampicillin resistance gene. The 6.5 kb LCR microlocus encompasses four erythroid cell-specific DNase I hypersensitive sites.

Following a large-scale preparation, 50 μg of Qiagen purified μLCR-RSV-Luciferase plasmid was digested to completion with *Pvu*I prior to electroporation into MEL cells and selection of stable G418-resistant clonal cell lines.

6.1.2 *Induction of de novo luciferase activity following LCR activation*

Three independent clonal cell lines μLCR/*luc* 2, 4 and 5 were analysed for measurement of basal luciferase activity, to assess the expression activity of the integrated construct prior to DMSO-induction of MEL cell differentiation (Figure 6.2(a)), which demonstrated a heterogeneous clonal population in respect to luciferase activity. Clonal cell line μLCR/*luc* 4 showed no significant luciferase activity above basal levels. Both clonal cell lines μLCR/*luc* 2 and 5 showed considerable levels of luciferase activity, of the order 10^3 fold higher than basal levels prior to induction (Figure 6.2(a)). This 'leaky' expression may have been due to integration of the expression unit into local 'transcriptionally active' sites within the host genome, which could have driven expression of the luciferase gene from the RSV promoter.

DMSO was added to a final concentration of 2% (v/v) to induce terminal MEL cell differentiation and microlocus LCR-mediated expression of the luciferase gene. Following 4 days of induction, the differentiated cells were harvested and assayed for luciferase activity. Clonal cell line μLCR/*luc* 4 showed no luciferase activity following induction, suggesting that the LCR-expression unit may have undergone a deleterious rearrangement in the

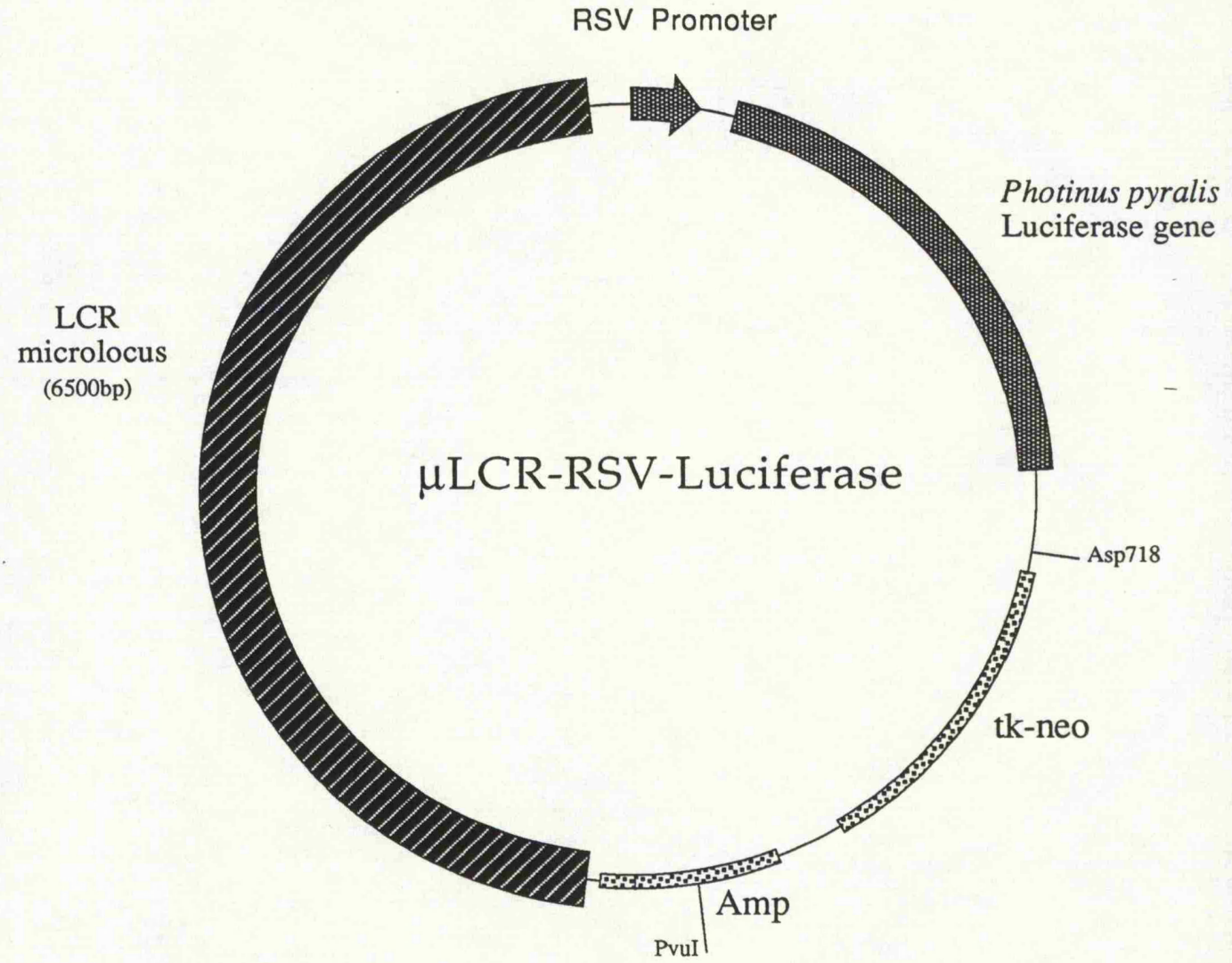

Figure 6.1 Schematic representation of the μLCR-RSV-Luciferase vector.

The 6.5 kB LCR microlocus [Talbot *et al.*, 1989] drives the *Photinus pyralis* Luciferass gene under the transcriptional control of the Rous Sarcoma virus long terminal repeat promoter (RSV) [De Wet *et al.*, 1987] and the neomycin-resistance gene (neo) under the control of the herpes simplex virus thymidine kinase (tk) promoter. Location of restriction enzyme sites are indicated; positions are represented by nucleotide residues shown in *parentheses*.

Abbreviations: Amp: β-lactamase.

host genome following transfection (Figure 6.2(b)). Clonal cell lines μLCR/*luc* 2 and 5 demonstrated a marked increase in the level of luciferase activity following induction. 1 in 10 serial dilutions of test samples revealed that luciferase activity could be quantitated upto 5 x 10^8 total counts per minute/10^6 MEL cells. This represented a 1400-2500 fold LCR-mediated increase in the heterologous expression of the luciferase gene within MEL cells.

This initial study demonstrated the feasibility to quantitatively measure luciferase activity within MEL cells. More importantly, the demonstration that the LCR/MEL system resulted in a 200-fold increase in the expression of the heterologous luciferase protein suggested that high-level expression of cNG channel molecules, necessary for reconstitution of a functional receptor-channel pathway, should be possible.

In separate studies conducted by Dr O.Gandelman and Prof P. Cobbold (Dept. Human Anatomy and Cell Biology, University of Liverpool), clonal cell line μLCR/*luc* 2 because of its intensity of luciferase luminescence, has been used in single cell measurements of intracellular ATP concentrations.

6.2 Production and characterisation of 'cAMP-responsive' pADneo2-C6-BGL/MEL clonal cell lines

A cellular screening system was used to characterise MEL cells for the expression of endogenous receptors coupling to the cAMP signal transduction pathway. Coupling was measured via transcriptional activation of the firefly luciferase gene, following the stable transformation of MEL cells with a reporter plasmid containing the luciferase gene under the transcriptional control of multiple cAMP responsive elements (CRE). A number of molecules involved in this regulatory pathway have been identified [Montiminy *et al.*, 1990]. Briefly, intracellular cAMP signalling cascades result in the stimulation and nuclear translocation of the cAMP-dependent protein kinase (PKA), which activates a homodimeric transcriptional activator CRE-binding protein (CREB) by phosphorylation. Phosphorylated CREB by binding to *cis*-regulatory CRE elements mediates transcriptional activation.

(a) *Luciferase Activity Pre-Induction (2%(v/v) DMSO)*

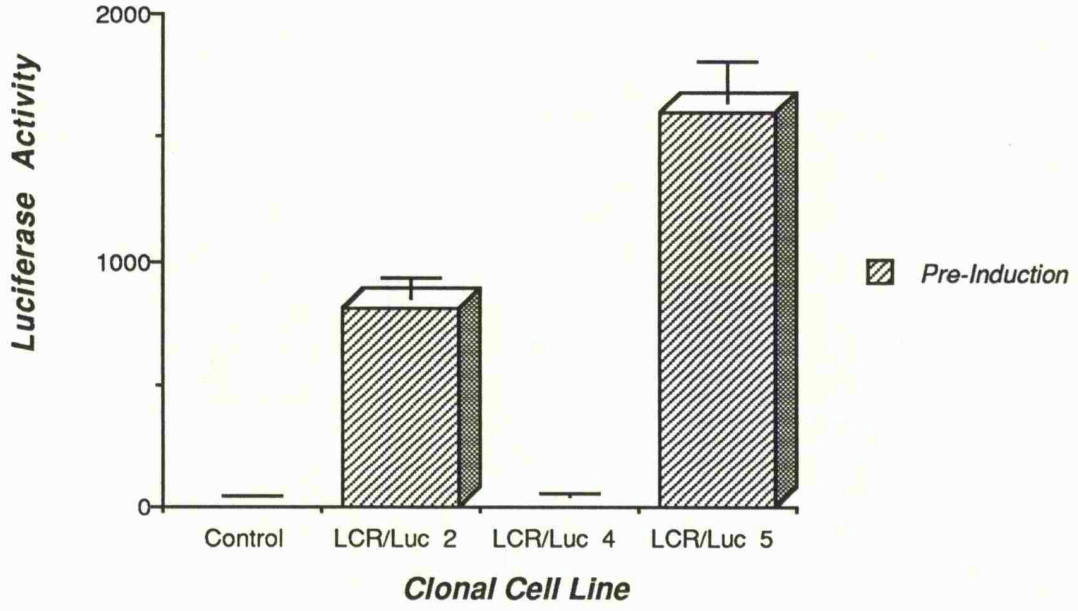

(b) *Luciferase Activity Pre- and Post-Induction (2%(v/v) DMSO)*

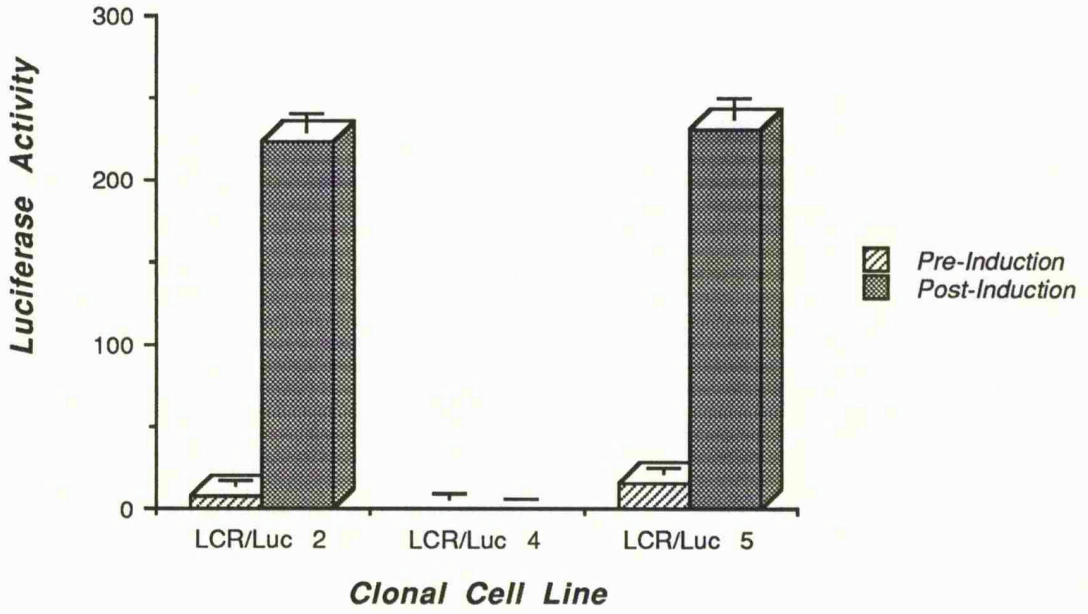

Figure 6.2 Luciferase activity of clonal cell lines μLCR/*luc* 2 ,3, and 5 pre-(a) and post-(b) 4 day 2% DMSO (v/v) induction.

In (a) luciferase activity has been measured as total counts per minute (cpm) x $10^4/10^6$ MEL cells whereas in (b) as cpm $10^6/10^6$ MEL cells. In addition a 1:10 serial dilution has been made for post-induced samples in (b). The control sample in (a) represents a mock-transfected MEL cell population.
Mean and standard deviations of triplicate luciferase determinations are shown.

6.2.1 *Production of cAMP-responsive luciferase pADneo2-C6-BGL/MEL clonal cell lines*

The vector pADneo2-C6-BGL, was kindly provided by Dr. A. Himmler (Ernst Boehringer Institut, Vienna. Austria). The 6.5 kb vector contains six heterologous CRE sequences (derived from bovine leukaemia virus LTR, vasoactive intestinal peptide, somatostatin and cytomegalovirus), upstream of a minimal β-globin promoter driving the expression of the luciferase reporter gene (Figure 6.3).

Following a large scale preparation, 20 μg of Qiagen purified pADneo2-C6-BGL plasmid, were digested to completion with *Sca*I prior to electroporation into MEL cells, and selection of stable G418-resistant clonal cell lines.

6.2.2 *Characterisation of clonal cell lines for cAMP-induction of luciferase expression*

Stably transfected clonal cell lines containing a functional reporter plasmid integrated in their genome were characterised for cAMP-induction of luciferase expression by using forskolin, a constitutive activator of adenylyl cyclase. Of five clonal cell lines analysed, only pAD 2 and 3 showed luciferase activity above basal levels in response to 20 μM forskolin (Figure 6.4). Forskolin resulted in a 2 to 3-fold induction of luciferase activity in these clonal MEL cell lines. These levels of induction were considerably lower than those previously reported in CHO cells, which exhibited 20 to 30-fold induction of luciferase activity upon stimulation of adenylyl cyclase with forskolin [Himmler *et al.*, 1993]. Whether this poor response in MEL cells was dependent on their differentiation state, is discussed later (Section 6.5). A comparative analysis in the induction of luciferase activity within MEL cells (Figure 6.2(b) and 6.4), demonstrates that activation by CRE of the minimal β-globin promoter in the vector pADneo2-C6-BGL, was considerably lower (by a factor of 10^3) than activation of the RSV promoter by the microlocus LCR gene-activation elements.

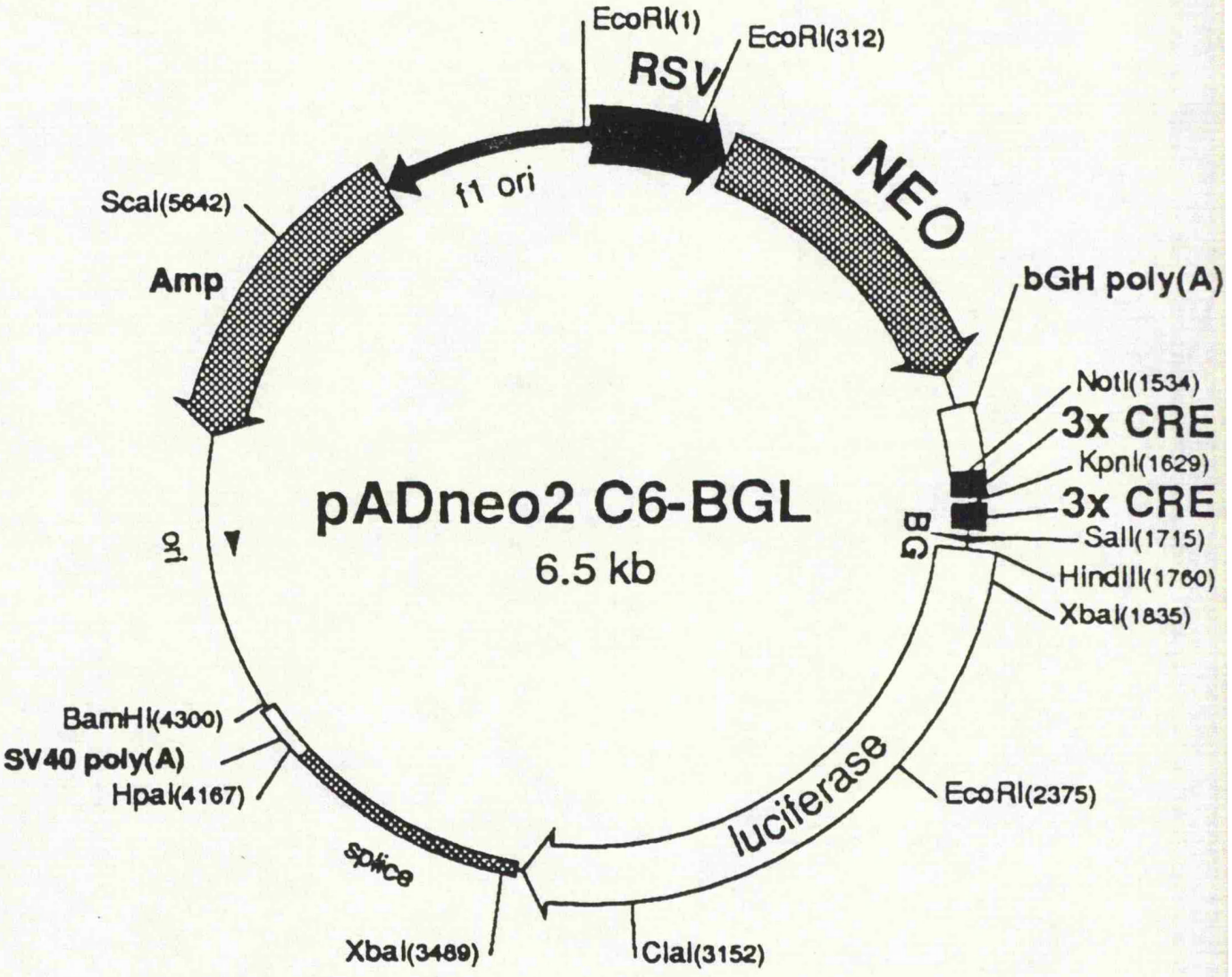

Figure 6.3 Schematic representation of the cAMP responsive luciferase reporter plasmid pADneo2-C6-BGL.

The luciferase gene is driven from the minimal b-globin promoter (BG) and terminated with a SV40 poly (A) region by 6 upstream cAMP-response elements (CRE). The neomycin gene (NEO) conferring G-418 resistance is driven from the Rous sarcoma virus long terminal repeat promoter (RSV) and terminated with a bovine growth hormone (bGH) poly (A) region. Locations of restriction enzyme sites are indicated.
Abbreviations: Amp: b-lactamase; f1: intergenic region of bacteriophage f1; ori: origin of replication.

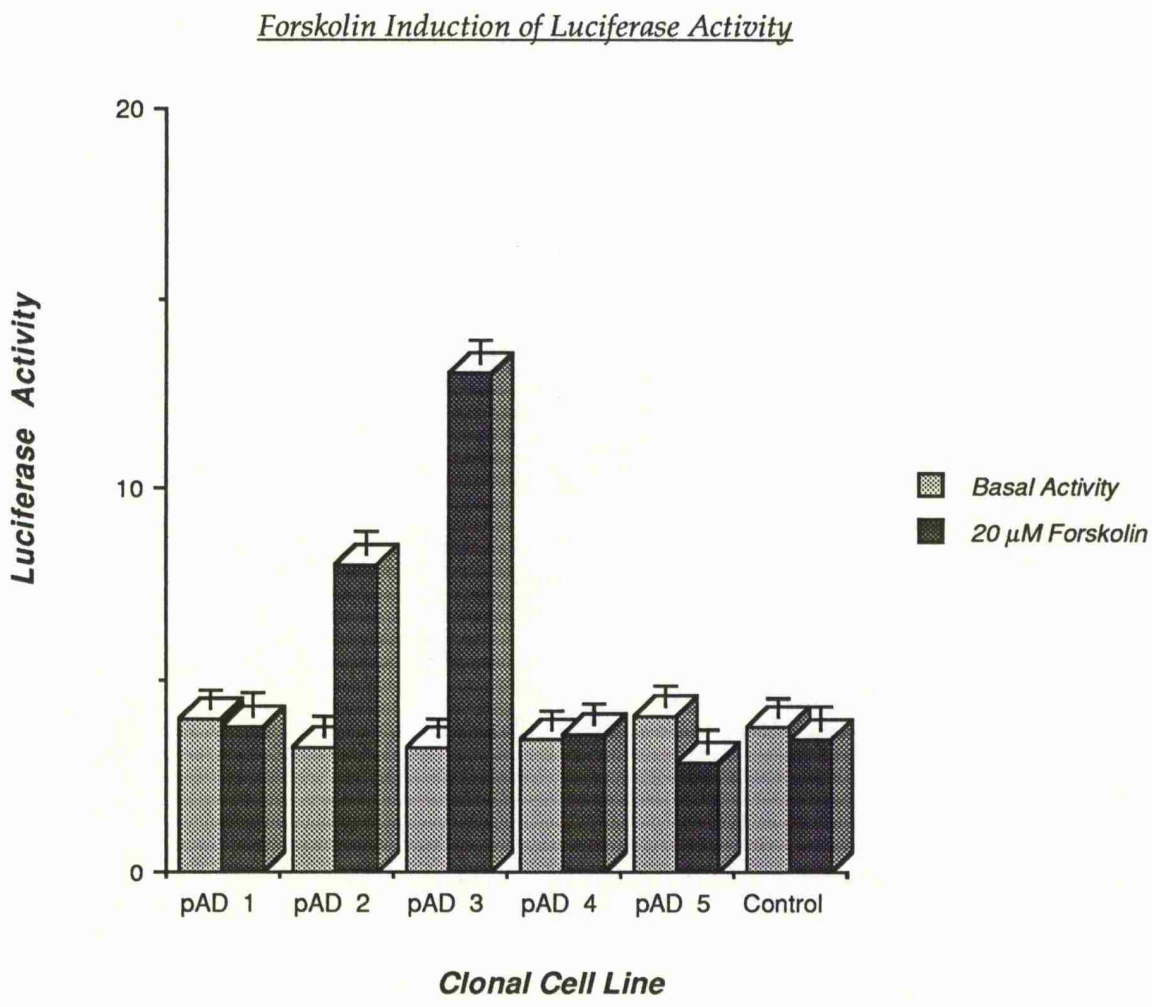

Figure 6.4 Characterisation of reporter pADneo2-C6-BGL/MEL clonal cell lines for forskolin induction of luciferase expression.

3×10^5 MEL cells from each clonal cell line were incubated with either 10% DMSO (v/v) (basal activity) or 20μM forskolin in 10% DMSO (v/v) for 4 hours prior to luciferase assays. Control represents a mock-transfected MEL cell population. Luciferase activity measured as total counts per minute x 10^4 / 3×10^5 MEL cells. Mean and standard deviations of triplicate luciferase determinations are shown.

So called 'position-effects' may have accounted for the lack of demonstrable forskolin induction of luciferase activity in the clonal cell lines pAD 1, 4 and 5. In which 'local' DNA sequences surrounding the site of insertion of the transfected DNA construct, may have had an inhibitory effect on the ability of the CRE to drive expression of the heterologous gene.

6.3 Functional characterisation of endogenous receptors positively coupled to adenylyl cyclase in stable cAMP-responsive luciferase/MEL clonal cell lines pAD 2 and 3

The clonal MEL cell lines pAD 2 and 3 exhibiting luciferase activation in response to forskolin, were chosen as reporter cell lines for characterisation of endogenous G protein-coupled receptors.

Agonists were chosen for receptor molecules which are known to be positively coupled to adenylyl cyclase eliciting cAMP production. The presence of endogenous receptors of the adrenergic, purinergic, serotonin, peptidic, muscarinic and histaminergic type positively coupled to adenylyl cyclase, was determined by stimulation of non-induced cells with the corresponding agonists isoproterenol. adenosine, serotonin, calcitonin gene-related peptide (CGRP), carbachol and histamine. None of the above receptor agonists led to an increase in luciferase activity above basal levels (Figure 6.5). A 2-fold induction of luciferase activity upon stimulation of adenylyl cyclase with 20 μM forskolin, demonstrated that the integrity of the cAMP gene regulatory pathway, (subsequent to receptor activation) had been maintained within the sampled clonal cell populations. This pharmacological screening technique suggested that non-induced MEL cells lacked *functional* endogenous G protein-coupled receptors for a range of distinct agonists.

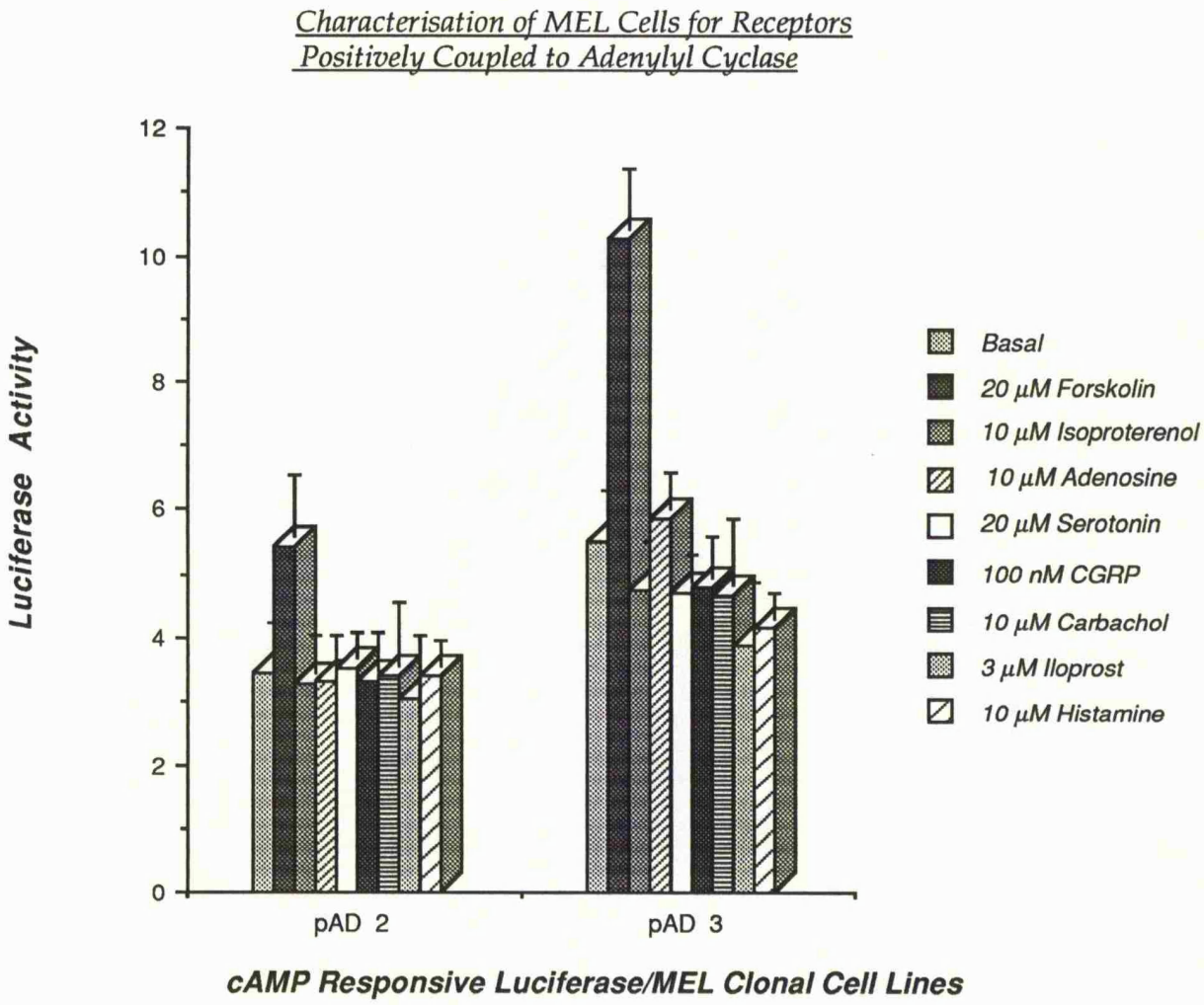

Figure 6.5 Functional characteristion of cAMP responsive luciferase/MEL clonal cell lines pAD 2 and 3 for endogenous receptors positively coupled to adenylyl cyclase

10^6 MEL cells from each clonal cell line were stimulated for 4 hours with the above concentrations of agonists. Basal refers to stimulation with 10 % DMSO (v/v). Luciferase activity measured as total counts per minute x $10^4/10^6$ MEL cells. Mean and standard deviation of triplicate luciferase determinations are shown.

6.4 Characterisation of the stable cAMP-responsive luciferase/MEL clonal cell lines pAD 2 and 3, for the expression of a functional adenosine A_2 receptor subtype

6.4.1 MEL cells may express an adenosine receptor subtype

Adenosine receptors can be divided into two families (A_1 and A_2) based on their differential coupling to adenylate cyclase and on their relative affinities for adenosine analogs. A_2 receptors activate adenylyl cyclase in platelets and cause vasodilation by relaxing vascular smooth muscle, the mechanism of which is unknown [Linden, 1991]. Feoktistov and Biaggioni (1993), demonstrated that adenosine agonists produced an accumulation of cAMP in human erythroleukaemia (HEL) cells, implying the presence of functional A_2 receptors. However the presence of different subtypes of A_2 receptors has been suggested based on the differences in their pharmacological profiles. The adenosine receptor present in HEL cells was tentatively classified as an A_{2b} receptor subtype based on the response of cells to various adenosine agonists.

20 μM adenosine failed to induce luciferase expression in the clonal MEL cell lines pAD 2 and 3. However, the specific adenosine analog 5'-*N*-ethylcarboxamidoadenosine (NECA) is a more potent agonist of the tentative A_{2b} receptor subtype found in HEL cells and at a concentration of 10 μM, NECA was shown to produce 75% of its maximal effect [Feoktistov and Biaggioni, (1993)].

6.4.2 Characterisation of MEL cells for functional A_2 receptor subtypes by pharmacological and molecular techniques

Both pharmacological and molecular techniques were used to determine; i) whether the absence of luciferase induction in response to adenosine in the MEL clonal cell lines pAD 2 and 3 was due to the use of an inappropriate agonist, and ii) the effect of DMSO-induced differentiation on the expression and functional state of adenosine A_2 receptor subtypes.

The response of both pre- and post-induced MEL clonal cell lines pAD 2 and 3, to the agonists adenosine, NECA, and forskolin (positive control)

were investigated. Both the pre- and post-induced cell lines failed to show an increase in luciferase activity following stimulation with the A_{2b} receptor subtype-specific agonist NECA (Figure 6.6). Similar responses were seen with the agonists adenosine and isoproterenol. However, the induction of luciferase activity upon stimulation of adenylyl cyclase with 20 μM forskolin, demonstrated that the integrity of the cAMP gene regulatory pathway within both pre- and post-induced clonal cell populations had been maintained. It was reasoned therefore that pre- and post-induced MEL cells lacked functional A_{2b} adenosine receptor subtypes.

DMSO-induced terminal differentiation of MEL cells resulted in a 6-fold increase in the induction of luciferase activity following forskolin stimulation (Figure 6.6: compare pre- and post-induced MEL clonal cell lines). This suggested that following DMSO-induced MEL cell differentiation, the activity of components within the cAMP gene regulatory cascade — 'downstream' of adenylyl cyclase activation, are increased. Indeed the resulting 20-30 fold increase in luciferase activity above basal levels in response to forskolin within terminally-differentiated MEL cells, are similar to levels reported in other cell lines [Himmler *et al.*, 1993].

To determine whether the absence of reporter gene expression within MEL cells in response to A_2 agonists was a consequence of; (i) inefficient coupling of receptor bound ligand complexes to intracellular effector systems or (ii) a lack of expression of A_2 receptor subtypes — RT-PCR studies were conducted to assay for receptor messenger RNA.

An A_2 receptor cDNA had been retrieved from a canine thyroid library by PCR using degenerate primers designed to consensus sequences in the third and sixth transmembrane segments of G protein-coupled receptors [Libert *et al.*, 1989]. Following expression in Cos 7 cells, the receptor exhibited binding characteristics of an adenosine A_{2a} receptor subtype [Maenhaut *et al.*, 1990]. A 25 bp antisense oligonucleotide (A_{2a}-1) to prime first strand cDNA synthesis, and a pair of 22 bp primers for PCR amplification were designed to the published A_2 receptor cDNA sequence (see Materials and Methods for sequences). The PCR primer pair A_{2a}-2 and 3 were designed to sequences within the third cytoplasmic and extracellular loop regions, found to be unique to the A_2 receptor. First-

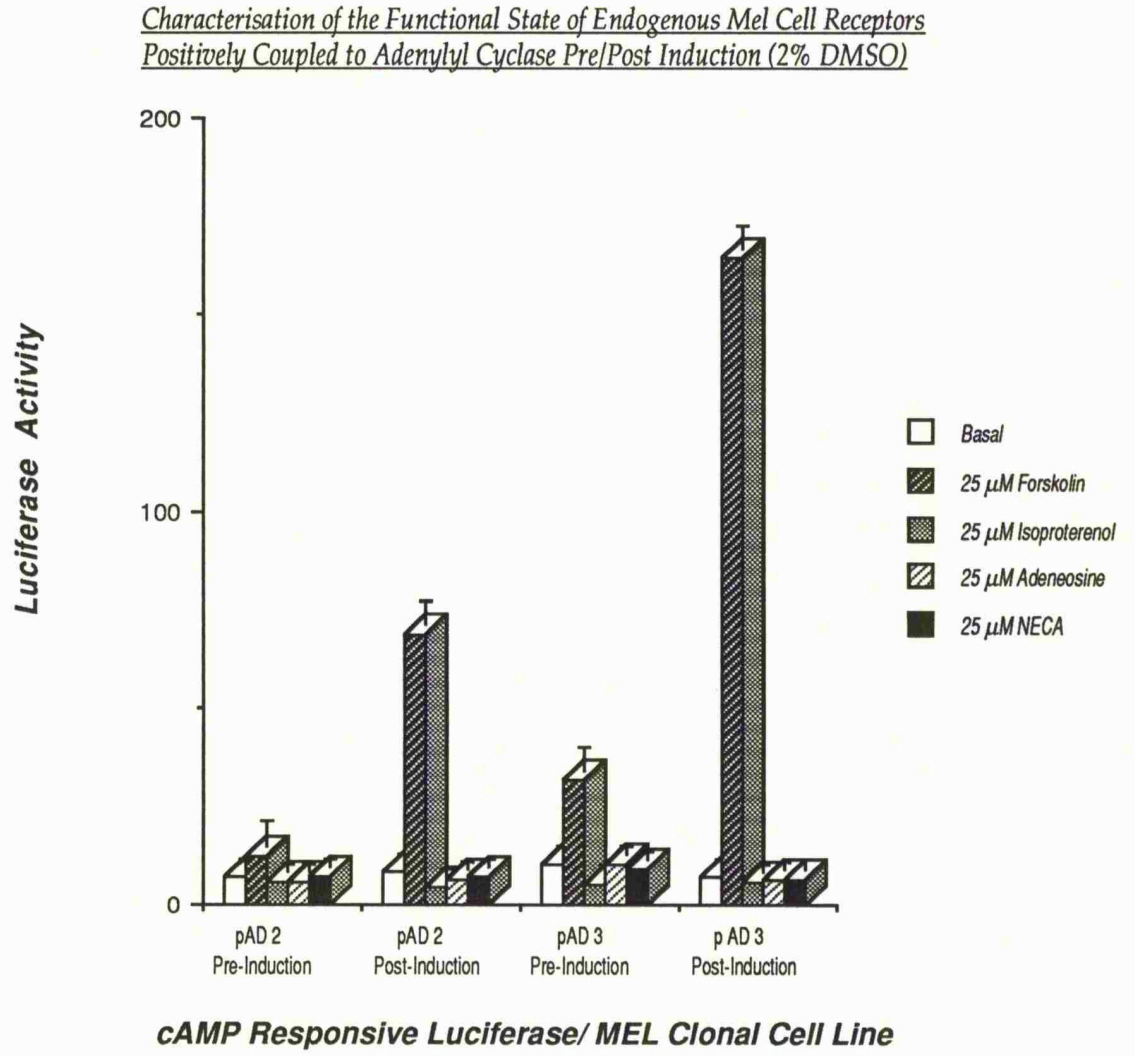

Figure 6.6 Characterisation of cAMP responsive luciferase/MEL clonal cell lines pAD 2 and 3 for functional A_{2b} adenosine receptor subtypes.

10^6 MEL cells from each clonal cell line were stimulated for 4 hours with the above concentrations of agonists. Differentiated clonal cell lines assayed 4 days post 2% (v/v) DMSO induction. Basal represented clonal cell lines stimulated with 10% (v/v) DMSO. Luciferase activity measured as total counts per minute x $10^4/10^6$ MEL cells. Mean and standard deviations of triplicate luciferase determinations shown.

strand cDNA was prepared from 3 μg of total RNA extracted from uninduced MEL cells. A subsequent 30 cycle amplification at a series of annealing temperatures (54-60°C) failed to produce PCR products. This demonstrated that MEL cells do not functionally express A_2 receptor subtypes.

6.5 Heterologous expression of a cDNA encoding the bovine olfactory cAMP-gated ion channel using LCR/MEL

Although the previous results had demonstrated an absence of endogenous receptors of the adrenergic and purinergic type positively coupled to adenylyl cyclase within MEL cells, it was still of interest to determine whether the LCR/MEL expression system could support the electrophysiological characterisation of a heterologously expressed cNG channel molecule. It was demonstrated by a PCR fingerprint that the sino-atrial node cDNA library contained a homologue of the cAMP-gated ion channel (Section 5.1), previously shown to be expressed in olfactory neurons [Dhallan *et al.*, 1990; Ludwig *et al.*, 1990]. Subsequently, it was shown that the coding region for this channel gene contained no introns (E.C Conley, unpublished). It was reasoned therefore, that the cAMP-gated ion channel expressed in nodal tissue would be of a similar structure to the cDNA clone retrieved from olfactory epithelium. Thus a cDNA clone representing an olfactory cAMP-gated ion channel was used for expression studies in the LCR/MEL system.

6.5.1 Production of stable cNG channel/MEL clonal cell lines

The cDNA clone OLF102a encoding for the bovine olfactory cAMP-gated ion channel, was kindly provided by Dr. U.B Kaupp (Institut fur Biologische Informationsverarbeitung, Forschungszentrum, Julich. FRG). Functional expression of this cDNA had already been established in *Xenopus* oocytes (Altenhoffen *et al.*, 1991). The 2.75 kb cDNA was provided as a plasmid pOLF102a in the vector pT7T3. The cDNA had been cloned into the *Eco*RV site of this vector, such that the initiating methionine of the cDNA was downstream of a T3 promoter. The LCR plasmid vector pEV3 (Figure 6.7), kindly provided by Dr. M. Needham

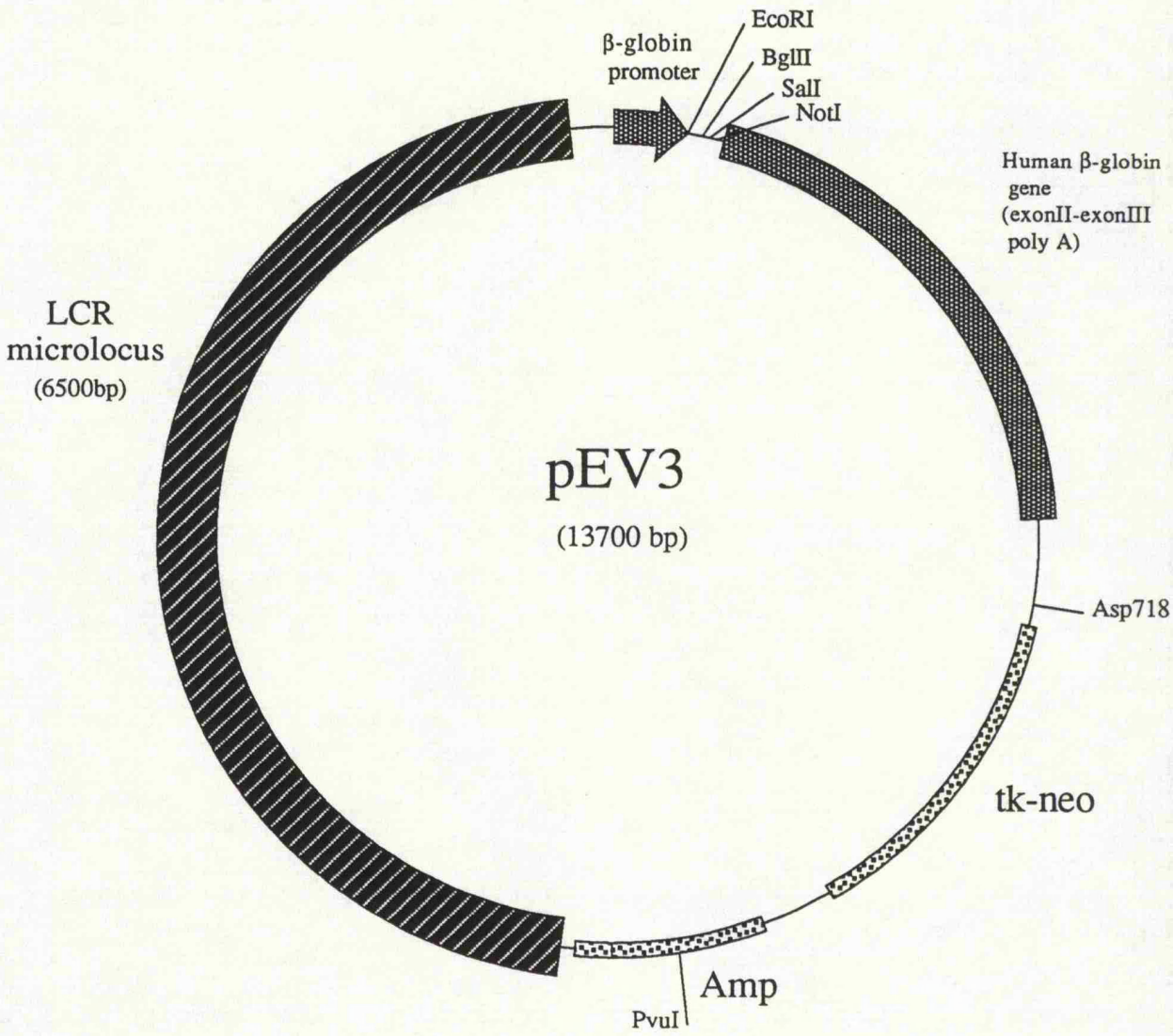

Figure 6.7 Schematic representation of pEV3

The 13.7 kb vector pEV3 contains a LCR micolocus 6.5 kb in size encompassing four erythroid cell-specific DNase I hypersensitive sites [Talbot *et al.*, 1989] upstream of a human β-globin promoter. The polylinker contains unique sites for 4 restriction enzymes which are indicated on the plasmid map. Downstream of the polylinker is found a 2.8 kb fragment representing exonII-exonIII and the polyadenylation recognition sequences of the human β-globin gene. A partial *Nar*I-thymidine kinase-neomycin resistance (tk-neo) and ampicillin resistance genes (amp), confer G418 and ampicillin resistance upon transformation of MEL and bacterial cells. The 2.8 kb fragment of the β-globin gene provides mRNA processing and maturation signals which has been shown to increase both the stability of the final RNA transcript and the overall expression levels of heterologous cDNA molecules in induced cells [Needham *et al.*, 1992].

(Zeneca Pharmaceuticals, Alderley Edge, U.K), was used to produce a pOLF102a construct for expression using the LCR/MEL system.

The pEV3-OLF102a expression vector was constructed as follows. Following a large scale preparation, 5 µg of pEV3 was digested to completion with *Sal*I and treated with alkaline phosphatase prior to purification. The 2.74 kb OLF102a cDNA was removed from the 2.9 kb T7T3 vector by digesting 10 µg of the recombinant plasmid with *Sal*I and *Xho*I, followed by separation by agarose gel electrophoresis and purification by electroelution. 100 ng of the gel purified *Sal*I/*Xho*I OLF102a fragment was ligated into 50 ng of the phosphatased pEV3/*Sal*I vector. After transformation of *E.coli* SURE competent cells, 12 ampicillin-resistant clones were propagated and recombinants containing the OLF102a cDNA in the correct orientation with respect to the β–globin promoter of pEV3 were identified by a diagnostic *Eco*RI digest. The OLF102a cDNA contained a single internal *Eco*RI site, 760 bp from the 3' end of the cDNA. Therefore, OLF102a cDNA inserts in the same orientation as that of the β–globin promoter produced DNA fragments of 1.9 kb in size following *Eco*RI digestion. A recombinant in the correct orientation was propagated. The final pEV3-OLF102a construct is shown in Figure 6.8. Following a large scale preparation, 50µg samples of the pEV3-OLF102a recombinant were digested to completion with *Pvu*I before electroporation into MEL cells, and selection of stable G418-resistant clonal cell lines.

6.5.2 RT-PCR screen of stable cNG/MEL clonal cell lines for the heterologous expression of cAMP-gated channels

RT-PCR amplification was used prior to patch-clamp analysis to screen cNG/MEL clonal cell lines for expression of the cAMP-gated ion channel. Oligonucleotide primers employed were those designed to the cyclic nucleotide-binding domain of the rat olfactory neuron cAMP-gated channel (described in Section 5.1). The complementary 'target' sequences for these primers are well conserved within the bovine cAMP-gated channel cDNA sequence. Oligonucleotide cA-Pr6 was used to prime first strand cDNA from 3 µg of total RNA (DNase I treated), extracted from six stable cNG/MEL clonal cell lines. A 30 cycle amplification at an annealing temperature of 52°C with primer pair cA-Pr 1 and 5, produced a PCR product of 213 bp in all clonal cell lines apart from cNG/MEL 4 (Figure 6.9).

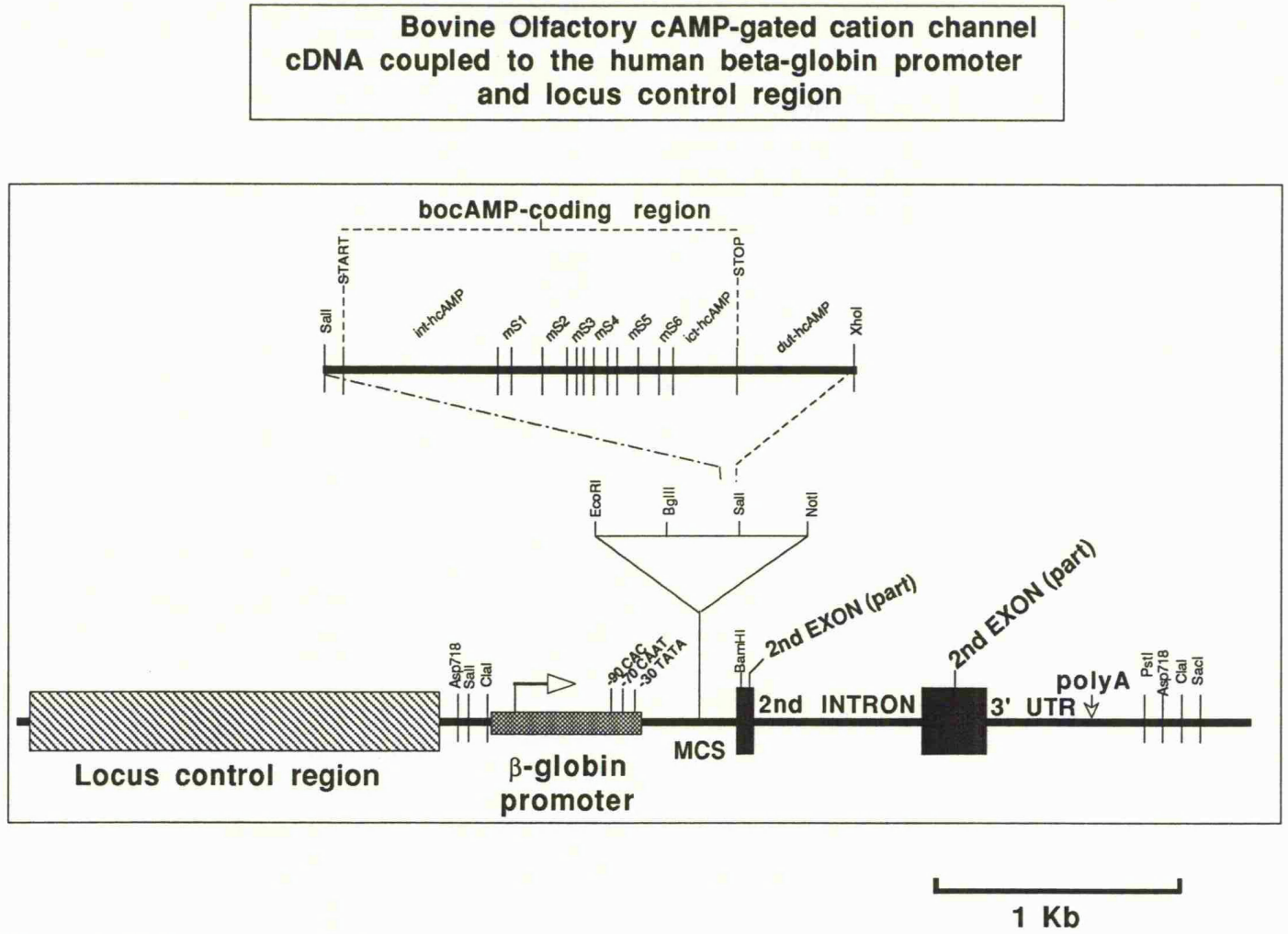

Figure 6.8 pEV3-OLF102a expression construct.

The 2.74 kb *Sal*1/*Xho*1 fragment representing the bovine olfactory cAMP-gated channel (bocAMP) cDNA was subcloned into the unique *Sal*I site of the multiple cloning site (MCS) of pEV3. This is located downstream of the minimal β-globin promoter which is driven by LCR region. Other features of the plasmid pEV3 have been described in Figure 6.7.
The bocAMP channel cDNA has been subdivided into functional subregions according to the following prefix nomenclature: uut-, upstream untranslated region 5' to the start codon; int-, encoding an intracellular N-terminus; ms1-6, encoding the putative transmembrane domains; ict-, encoding an intracellular C-terminal domain; dut-, downstream untranslated region, 3' to the stop codon.

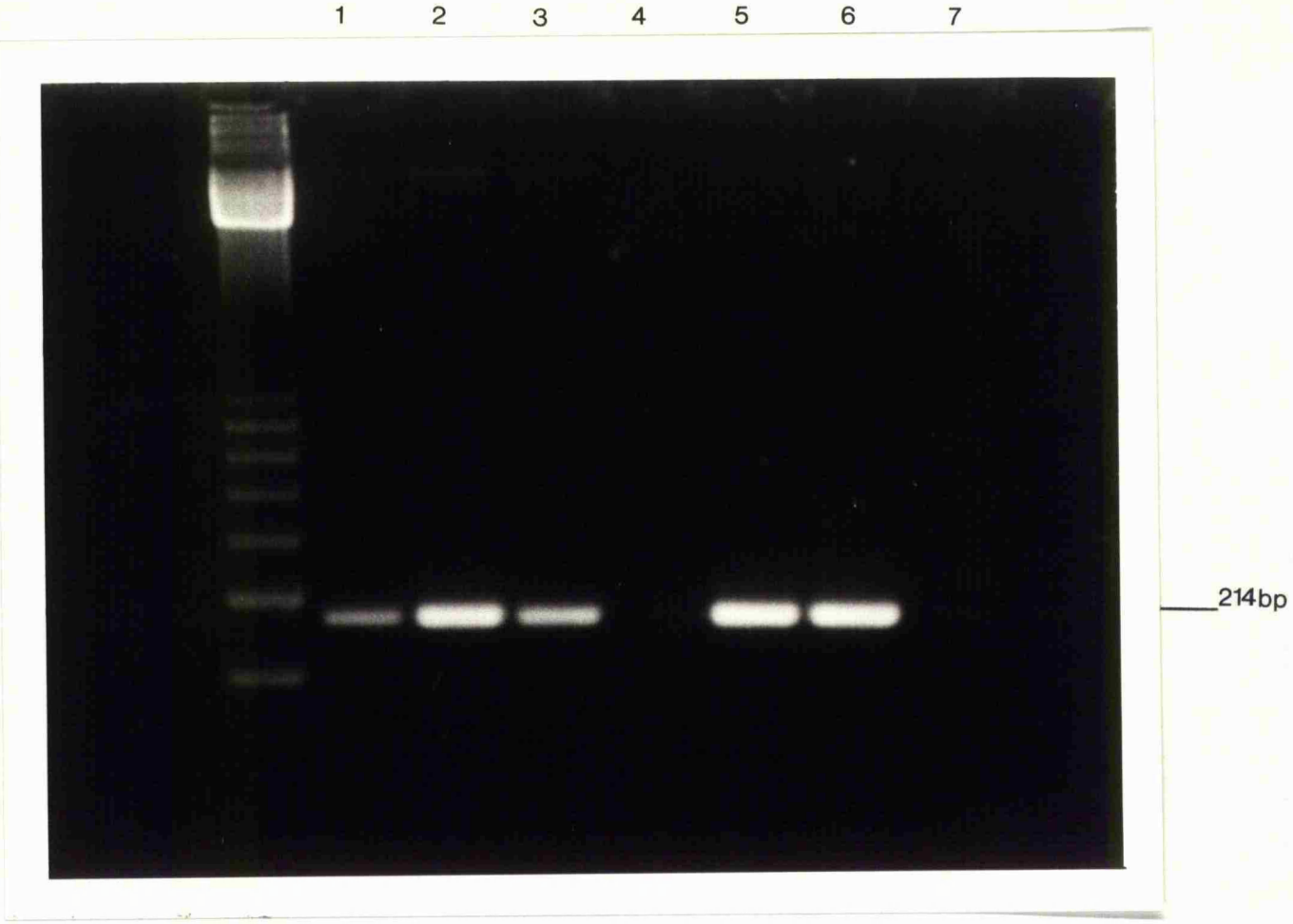

Figure 6.9 RT-PCR demonstration that stable cNG/MEL clonal cell lines heterologously expressed cAMP-gated channels.

PCR Molecular size ladder (50-1000 bp). Lanes 1-6: cA-Pr 6 primed first-strand cDNA from 3 μg of total RNA extracted from cNG/MEL clonal lines 1-6, amplified with primers cA-Pr 1 and 5. Lane 7: Control. cA-Pr 6 primed first-strand cDNA from total RNA extracted from mock-transfected MEL cells, amplified with primers cA-Pr 1 and 5.

Samples were amplified for 30 cycles at an annealing temperature of 52°C, and a portion of the reaction product was electrophoresed on a 1.2% ethidium bromide-stained agarose gel.

The size of the amplified product was as expected from the bovine cAMP-gated channel cDNA sequence. Similar sized products were not obtained from total RNA extracted from mock-transfected MEL cells. Thus 5 out of the 6 cNG/MEL clonal cell lines propagated, expressed RNA transcripts for the heterologous cAMP-gated ion channel.

6.5.3 Assaying for cAMP-activated currents within cNG/MEL clonal cell lines using electrophysiological methods

Both whole cell and excised inside-out configurations of the patch-clamp technique (discussed in Section 1.1), were used to assay the cNG/MEL clonal cell lines for cAMP-stimulated cation selective currents.

6.5.3.1 Electrophysiological measurements using the whole cell configuration

In these experiments the ionic conditions were arranged (extracellular and intracellular solutions contained 70 mM and 140 mM of potassium respectively), such that cation selective currents would have a reversal potential of -21 mV. Solutions were designed in this manner to distinguish the current through cAMP-gated ion channels from potential 'leakage' currents. These would not be selective for cations and would therefore have a reversal potential of around -6 mV (a point between the reversal potential for cations and anions). Application of 1 mM cAMP to the intracellular solution repeatedly produced ionic currents which were found to have a reversal potential close to 0 mV, indicating that the current did not pass through cation selective cAMP-gated channels. These non-selective or leakage currents were large, and would therefore have obscured current flow through expressed cAMP-gated ion channels.

6.5.3.2 Electrophysiological measurements using the inside-out excised patch configuration

1 mM cAMP was directly applied to the intracellular membrane of the excised patch. This resulted in the generation of conductances with single-channel properties distinct from those of cAMP-gated channels. This approach was technically more difficult than the whole cell approach

because the small single channel amplitude of cAMP-gated channels were at the limits of resolution of the patch clamp technique.

Both whole cell and excised inside-out configurations of the patch-clamp technique, because of the problem of large non-selective or leakage currents in response to 1 mM cAMP, were unable to detect *functional* cAMP-gated channels within the cNG/MEL clonal cell lines.

Discussion

The demonstration that two distinct cNG ion channels are expressed within sino-atrial nodal tissue, raised the issue of what receptor-mediated second messenger systems are coupled to the channel molecules *in situ*? The aim of the present work was to reconstitute and study within a heterologous system a defined cNG channel interaction with a receptor-mediated second messenger pathway. Such a model is an essential first step in understanding the functional role of cNG channels in diverse signal transduction pathways. The MEL cell was chosen as the heterologous system because it had been previously shown to support both the expression and electrophysiological characterisation of voltage and G protein-gated K^+ channels.

Of particular interest was the functional reconstitution of a cytoplasmic second messenger pathway coupling adenosine A_2 receptors to a heterologously expressed cAMP-gated channel. Both components have been shown to be expressed in vasculature [Ijzerman and Van Galen, 1990; Biel *et al.*, 1993], where adenosine has been shown to regulate vascular smooth muscle resistance [Linden, 1991]. Such a pathway may be of physiological importance within native mammalian SAN.

MEL cells were characterised for the presence of functional receptors coupled to the cAMP signal transduction pathway by transcriptional activation of a luciferase reporter gene under the control of multiple CRE. These studies demonstrated the absence of endogenous receptors of the adrenergic, muscarinic, serotonin, histamine and purinergic (adenosine) type. The use of an additional adenosine agonist, NECA shown to be more

specific to the pharmacological 'low affinity' A_{2b} receptor subtype also failed to induce expression of the reporter gene. A major difficulty in studying adenosine A_2 receptors via pharmacological techniques lies in part in their relatively low affinity for currently known agonists and antagonists. Therefore, molecular methods were additionally employed in characterisation of MEL cells for purinergic A_2 receptors. RT-PCR studies demonstrated that MEL cells did not express endogenous A_2 receptors of the pharmacological 'high affinity' A_{2a} receptor subtype. Although the observed diversity of recognised pharmacological subtypes of the adenosine A_2 receptor is probably matched by differing mRNAs, the combination of both pharmacological and molecular techniques indicated that MEL cells did not express either A_{2a}or A_{2b} receptor subtypes. A possible reason for observed differences in expression of A_2 receptor subtypes between MEL and HEL cells could be that the two cell types are at differing stages of erythroid development. This has been shown to affect expression of membrane-bound receptors [Murray *et al.*, 1989].

DMSO-induction of terminal MEL cell differentiation, resulted in a 6-fold increase in forskolin stimulation of luciferase expression. This suggests that the induction of terminal differentiation within MEL cells leads to an increase in expression of one or more components involved in the cAMP gene regulatory pathway. Consistent with this is the observation that cAMP-dependent protein kinase (PKA) activity increases following chemically-induced differentiation of MEL cells [Pilz *et al.*, 1992]. Infact such differentiation was shown to be severely impaired in PKA-deficient cells. Changes have also been shown to occur in the expression of various nuclear factors, indeed down-regulation of the *c-myc* and *c-myb* proto-oncogenes is a prerequisite for MEL cell differentiation [Dmitrovsky *et al.*, 1986].

Although RT-PCR methods demonstrated the expression of RNA transcripts of the cAMP-gated channel in five out of six cNG/MEL clonal cell lines, two variations of the patch-clamp technique were unable to characterise functional cAMP-stimulated cation selective currents, following addition of 1 mM cAMP to intracellular patch solutions. The main technical difficulty was the presence of large non-selective or leakage currents within MEL-C88 cells following differentiation, which obscured any possible current flow through the cAMP-gated channels. Possibly

suggesting that DMSO-induced terminal differentiation of MEL cells, results in *de novo* expression of plasma membrane channel components leading to the generation of such large non-selective currents. This needs to be addressed by further electrophysiological characterisation of induced MEL cells. The situation is in direct contrast to the electrophysiological characterisation of heterologous K^+ channels within MEL C-88 cells. Such voltage-activated channels can be studied in isolation since the cell differentiation protocol does not produce any endogenous voltage-dependent currents which may interfere with measurements of the heterologous channels [Shelton *et al.*, 1993].

Suitability of MEL cells for reconstitution of receptor-cNG coupling

These studies have demonstrated the *inappropriateness* of the MEL cell as a heterologous system for studying by traditional electrophysiological techniques, the functional reconstitution of a second messenger pathway mediating receptor-cNG channel coupling. Studying functional coupling by alternative techniques, such as calcium-imaging may also prove technically difficult within MEL cells. As studies have shown that calcium influx is an early event associated with chemically-induced differentiation [Gillo *et al.*, 1993]. These and other changes in the calcium permeability of differentiated MEL cells, could mask any second-messenger mediated calcium influx through activated cNG channels.

The absence of many endogenous receptor types coupled to the cAMP signal transduction pathway, does make the MEL cell a potential system for studying the pathways involved in the coupling of reconstituted receptor-voltage-gated channel components. It is expected that such heterologously expressed components would be able to interact with the *appropriate* coupling molecules, particularly G proteins. This is because erythroid cells have been rich sources of isolated, purified G protein subunits for the use in patch 'reconstitution' studies, which have demonstrated direct pathways of ion channel activation [reviewed by Birnbaumer *et al.*, 1990].

Chapter 7

General Discussion

Précis

An objective of the work presented within this thesis was to clone and functionally characterise cyclic nucleotide-*sensitive* ion channel genes expressed within the sino-atrial node (SAN) region of heart. Prior to this study, the only reported cardiac channel within this class was the one underlying the cardiac 'pacemaker' current I_f [DiFrancesco and Tortora, 1991]. Based on the known cyclic nucleotide modulation of I_f channel gating, a prepared SAN specific cDNA library was screened with a PCR-generated probe representing a cAMP-gated channel. As described in Chapter 3, characterisation of inserts to six putative positive isolates revealed a partial cDNA (clone rscNGC 1) which represented a cGMP-gated channel homologue, previously undescribed in heart. Clone rscNGC 1 belonged to the family of cyclic nucleotide-*gated* (cNG) channels which unlike the I_f channel are *oligatorily* gated by cyclic nucleotides.

The retrieval of a full protein-coding sequence and subsequent heterologous expression in *Xenopus* oocytes as described in Chapter 4, demonstrated that rscNGC 1 exhibited both structural and functional properties identical to those previously described for an α-subunit of the vertebrate rod photoreceptor cGMP-gated channel [Kaupp *et al.*, 1989]. Following the demonstration that the photoreceptor channel existed as a heteromultimer *in situ* [Chen *et al.*, 1993], studies focused on i) possible regions of rscNGC 1 mediating subunit interactions, as described in Chapter 4 this led to the creation of a mutated Δ92-rscNGC 1 construct, and ii) additional cNG channel subunits within the SAN which may co-assemble with rscNGC 1 giving rise to heteromultimeric channels with distinct properties. Employing PCR methods it was demonstrated in Chapter 5 that a cAMP-gated channel homologue was also present within amplified stocks of the library. Thus at least two distinct cNG ion channel genes were expressed within SAN tissue. A subsequent primary library screen also identified a *potential* distantly-related member of the superfamily of second-messenger gated channels.

Because cNG channels are *obligatorily* coupled to receptor-second messenger systems for their activation, it was important to study such

channel-receptor interactions within a heterologous system. As described in Chapter 6 murine erythroleukaemia (MEL) cells were used to reconstitute coupling of endogenous receptor components to heterologously expressed cAMP-gated channels. Employment of a cellular screening system that measured receptor coupling to the cAMP signal transduction pathway via transcriptional activation of a reporter gene, demonstrated the absence of a range of *functional* G protein-coupled receptor types within MEL cells. Additionally, electrophysiological characterisation of the heterologously expressed cAMP-gated channel by the patch-clamp technique, failed to characterise a cyclic nucleotide-activated cation selective current amongst 'masking' non-selective conductances. These studies demonstrated the difficulty in employing the MEL cell as a heterologous system, for studying specific receptor-mediated second messenger coupling to cNG channels.

The molecular identity of I_f remains unresolved

Successive low stringency screens of both amplified and primary SAN cDNA libraries with cNG channel probes, failed to isolate sequence variants of the broader class of cyclic nucleotide-sensitive channels, which encompass I_f. Recently, I_f has been suggested in purely electrophysiological terms, to be behave as an *inward-rectifier* class of ion channel [DiFrancesco, personal comm.]. The cloning of mammalian members of this superfamily [Ho *et al.*, 1993; Kubo *et al.*, 1993] raises the possibility that future studies may isolate I_f from *preprocessed* cDNA libraries, by a cross-hybridisation approach based on sequence similarities to inward-rectifier channels.

Structure and Composition of SAN cNG channels

Characterisation of the two cNG channel genes expressed within the SAN demonstrated that they represented nodal *homologues* of genes previously shown to be expressed in mammalian rod photoreceptor cells [Kaupp *et al.*, 1989] and olfactory neurons [Dhallan *et al.*, 1990]. It is anticipated that future studies in understanding these SAN cNG channels at the molecular level, will attempt to relate functional properties to their

overall structure. Of particular functional interest is the N-terminal polypeptide of rscNGC 1, which has been shown to be specifically processed amongst homologues of rod photoreceptor channels within native cells [Molday *et al.*, 1991]. Whether the processed N-terminus is essential for mediating and determining both homo- and heteromeric subunit interactions, awaits functional studies with the Δ92-rscNGC 1 construct. Additional functional questions concern the role of the residual S4 motif within rscNGC 1. It is possible that by interacting with the cyclic nucleotide-binding domain thereby 'sensing' bound ligand, the S4 motif may act as general 'gating-motif' within cNG channels. It is expected that future engineered modifications in the coding sequence, will allow detailed analyses of the contribution of such polypeptide regions to rscNGC 1 biological activity.

The question of whether the two characterised SAN cNG channels, if expressed within the same cell type, could co-assemble to form functional heteromultimers was raised in Chapter 5. Such co-assembly might be expected to *increase* the functional heterogeneity of cNG channels. However, in common with subunits from different *Drosophila* K^+ channel subfamilies [Covarrubias *et al.*, 1991], it is unlikely that these monomers from *distinct* cNG subfamilies will co-assemble. Whether these distinct cNG channels exist as separate heteromultimeric complexes *in situ* awaits the cloning of new nodal subunits. It is tacitly assumed that such homo and heteromultimeric cNG channels will exhibit a tetrameric structure based on both electrophysiological data and analogy to other members of the superfamily of voltage and second messenger-gated ion channels. However, high resolution structural information is not yet available to support such a quaternary structure.

Electrophysiological characterisation of 'native' and heterologously-expressed SAN cNG channels

Since the establishment of the expression of two distinct cNG channels within SAN tissue, a systematic patch-clamp study characterising native heart tissues for such cyclic nucleotide-activated conductances has yet to be undertaken. It is essential to identify and characterise the properties of these native conductances, and to compare these with their cloned

counterparts. Only then will it be possible to determine the functional roles and likely effects of cNG channels on SAN physiology.

The cyclic nucleotide dependence of gating and small unitary conductance, makes cNG channels difficult to analyse using traditional patch-clamp techniques. As was demonstrated in Chapter 6, cAMP-activated cation-selective currents could not be resolved from the 'masking' effects of large non-selective currents in MEL clonal cell lines heterologously expressing the cAMP-gated channel. Additionally, as discussed in Chapter 4 the small maximal current amplitudes and low success rate of detecting rscNGC 1 activity following heterologous expression in *Xenopus* oocytes, hampered full characterisation by patch-clamp. These heterologous expression studies demonstrated a necessity to assay for cyclic nucleotide-activated currents by additional techniques. Due to their high permeability to calcium (Ca^{2+}) ions, cNG channels can be functionally characterised both *in situ* and *in vitro* by fluorescence imaging of cyclic nucleotide-induced calcium influxes [Brüggemann *et al.*, 1993; Weyand *et al.*, 1994]. These techniques rely on increases in the fluorescence of Ca^{2+} sensitive dyes such as Fluo-3 and Fura-2. Both rscNGC 1 and Δ92-rscNGC 1 cDNAs have been successfully re-cloned into the eukaryotic expression vector pcDNA3 (Invitrogen) and are awaiting transfection into human embryonic kidney 293 cells. This *stable* heterologous expression system offers the additional opportunity to assay for functional expression by calcium imaging techniques. It is expected that a combination of traditional patch-clamp and calcium imaging techniques will improve functional characterisation of these SAN cNG channels.

Functional reconstitution of receptor-cNG channel coupling

An important step in understanding the functional roles of cNG channels in SAN tissue is to reconstitute a defined receptor-mediated second messenger-channel interaction. The reconstitution of a heterologously expressed cAMP-gated channel shown to be expressed in SAN tissue, to endogenous intracellular signalling components generating cAMP was attempted within MEL cells. As discussed in Chapter 6 such a heterolgous system proved to be unsuitable for studying such channel coupling.

It remains of great importance to reconstitute such heterologous coupling as this will provide an excellent model for fundamental studies on the precise mechanism and kinetics of channel activation. In addition a heterologous system incorporating functional coupling may be employed as a *biosensor* for detecting intracellular fluctuations in cyclic nucleotide molecules in response to extracellular agonists [Kramer, 1990]. cNG channels represent exquisite 'detector' molecules because their *direct* activation by cyclic nucleotides provides a mechanism for *rapid* stimulation of electrical signalling (which can be assayed by both electrophysiological and fluorescence imaging techniques), in response to *small* changes in the intracellular concentration of second messengers. Other qualities suitable for such a role include; (i) their high sensitivity and specificity for cyclic nucleotides, (ii) rapid activation and deactivation kinetics, (iii) lack of agonist-induced desensitisation, and (iv) a dose-response relationship of activation within the physiological range of intracellular cyclic nucleotide concentrations.

What are the possible functional roles of cNG channels in SAN?

As discussed in Chapters 1 and 5, molecular cloning techniques have identified additional, distinct cNG channels in other non-sensory tissues, such as the kidney, testis and vasculature. It is true to say that the functions of these cNG channels in tissues other than the retina and the olfactory epithelium remain unresolved.

In examining the possible biological roles of cNG channels, one has to consider; i) to which second messenger-mediated systems are they functionally coupled, and ii) the physiological consequences of channel activation. By their very nature cNG channels affect the responsiveness of excitable cells, by changes in both the membrane potential and the intracellular concentration of ions, particularly Ca^{2+}. As such they represent second messenger-operated Ca^{2+} channels, providing a regulated pathway for Ca^{2+} influx at a wide range of membrane potentials. By acting as a cytoplasmic messenger, Ca^{2+} is ultimately able to control cell physiology.

SAN cNG channels are likely to be coupled to cGMP-generating systems

Both of the characterised homologues of the SAN cNG channels have been shown to be more sensitive to cGMP than to cAMP agonists [reviewed by Eismann *et al.*, 1993]. Specifically, the photoreceptor homologue of rscNGC 1 is approximately 30- to 40-fold more sensitive to cGMP than to cAMP *in situ* [Haynes *et al.*, 1986]. Thus within SAN tissue, rscNGC 1 is more likely to be functionally coupled to molecular components involved in the generation of intracellular cGMP. From the literature to date, cGMP has been shown to be an integral component involved in; i) the negative chronotrophic response (decrease in beat rate) of myocytes to cholinergic agonists, and ii) smooth muscle relaxation, mediating vasodilation in vasculature. cGMP can *modulate* the activity of ion channels through *indirect* pathways, mediated by cGMP-dependent protein kinase (G kinase) phosphorylation. However, the *direct* activation by cGMP of cNG channels provides a mechanism for *rapid* electrical signalling, which may control such diverse functions as chronotropy and vasodilation.

Could a cGMP-stimulated electrical signal underlie in part, the negative chronotropic response of cardiac myocytes to cholinergic agonists?

Chronotropic actions of β–adrenergic agents are mediated by cAMP, which as discussed in Chapter 1 can cause a direct, phosphorylation-independent activation of the pacemaker channel I_f in SAN cells. A similar 'depolarising' response mediating an increase in myocyte beat frequency, is also possible following activation of the cAMP-gated channel homologue shown to be expressed within SAN tissue. While more sensitive to cGMP, the channel can be activated by cAMP concentrations well within those controlled under normal physiological concentrations by adenylyl cyclase [Nakamura and Gold, 1987]. However SAN cNG channels, particularly rscNGC 1 homologues, if involved in the mediation of chronotropic effects, are more likely to underlie the negative chronotropic response to muscarinic cholinergic agonists.

As discussed in Chapter 1 the negative chronotropic response of cardiac myocytes to cholinergic agonists is mediated through direct G protein activation of an inwardly-rectifying potassium current, $I_{k,ACh}$ [Sakmann *et al.*, 1983], and reduction of $I_{Ca,L}$ [Brown and Denyer, 1988] and I_f [DiFrancesco and Tromba, 1988(a)]. As well as reducing intracellular cAMP concentrations through the inhibition of adenylyl cyclase, cholinergic agonists are known to elevate intracellular levels of cGMP in cardiac muscle [George *et al.*, 1970]. cGMP analogs have also been shown to produce a negative chronotropic effect in cultured ventricular myocytes [Krause *et al.*, 1972]. This has led to the suggestion that the action of muscarinic cholinergic agonists on heart rate is mediated, in part by cGMP [reviewed by Lohmann *et al.*, 1991]. Recently, it was demonstrated that cholinergic agonists elevated cGMP by an endogenous nitric oxide (NO*) signalling system, constitutively present within myocytes [Balliigand *et al.*, 1993] as shown in Figure 7.1. The NO*-mediated response of cultured ventricular myocytes to the muscarinic agonist carbachol was very rapid, as is characteristic of NO* release by constitutive, Ca^{2+}/calmodulin responsive isoforms of nitric oxide synthase (NOS). By acting as an intracellular second messenger, NO* is known to increase cytoplasmic concentrations of cGMP by activation of the soluble form of guanylyl cyclase (sGC) [Feelisch and Noack, 1987]

Importantly, the *rapid* nature of the negative chronotropic response of cardiac myocytes to cGMP analogs is suggestive of a fast modulation of an electrical signal. Electrophysiological studies on isolated cardiac myocytes, have revealed that while cAMP can increase the activity of a L-type calcium channel current (I_{Ca}) (which plays a predominant role in the initiation and regulation of cardiac excitability) by cAMP-dependent protein kinase phosphorylation [Kameyama *et al*, 1985], cGMP can decrease the activity of I_{Ca} by two *indirect* mechanisms (Figure 7.1); i) cAMP hydrolysis via cGMP-stimulated cAMP-phosphodiesterase, in frog ventricle [Hartzell and Fischmeister, 1986], and ii) cGMP-dependent protein kinase (G kinase) phosphorylation, in mammalian heart [Méry *et al.*, 1991]. However the possibility of a phosphorylation-independent pathway, mediated by *direct* cGMP activation of cardiac cNG channels, has not been specifically investigated. Such a pathway would provide a mechanism for *rapid* changes in membrane potential in response to humoral-mediated fluxes in the intracellular concentration of cGMP.

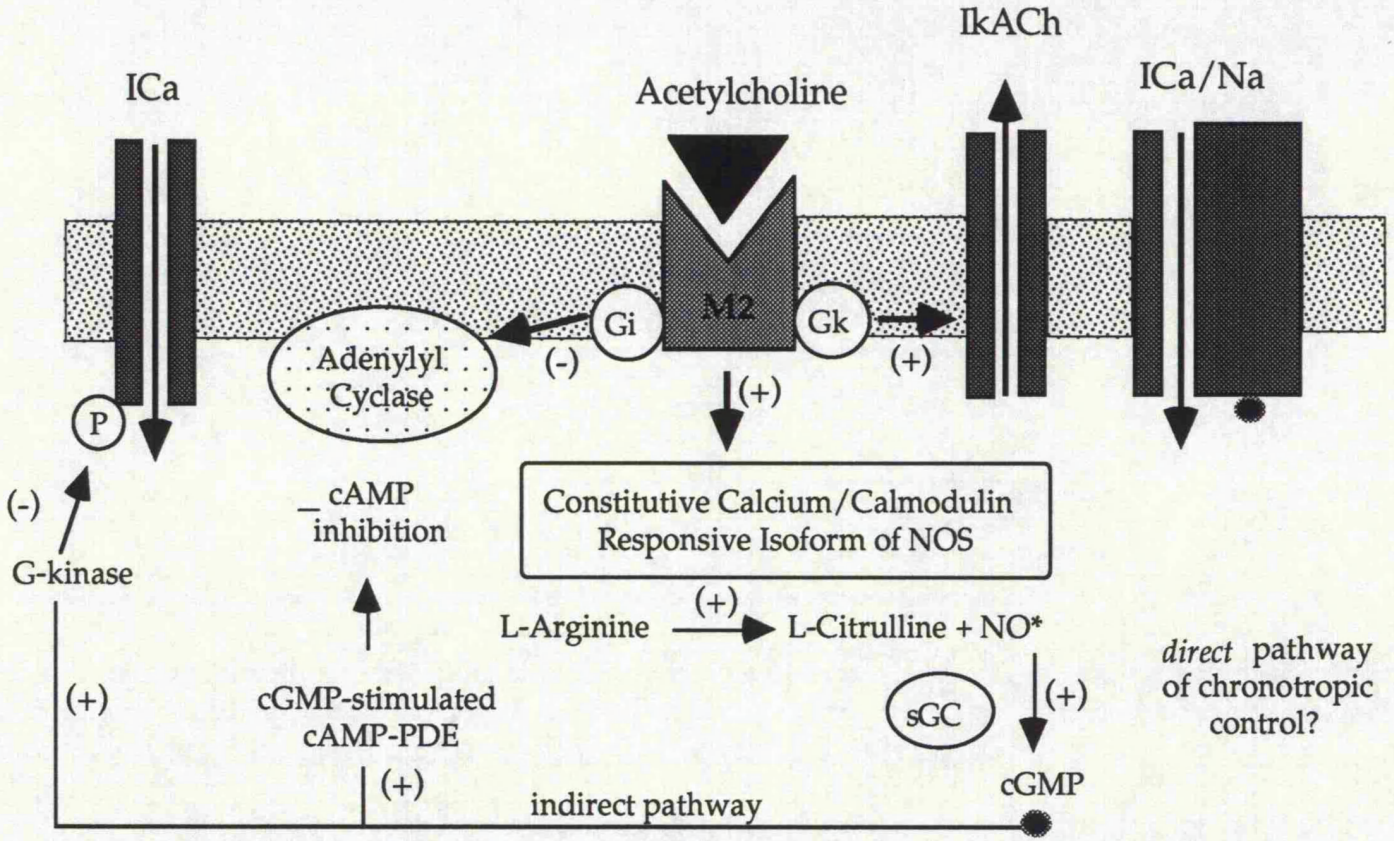

Figure 7.1 Schematic diagram outlining the 'possible' role of cyclic nucleotide-gated ion channels in the negative chronotrophic response of cardiac myocytes to cholinergic agonists. Additional M_2 coupling leading to the direct activation of I_{kACh} by G_k, and inhibition of adenylyl cyclase by G_s are also shown.

Abbreviations: Cyclic nucleotide-gated channel ($I_{Ca/Na}$), L-type voltage-gated calcium channel (I_{Ca}), G protein-gated potassium inward-rectifier channel (I_{kACh}), muscarinic cholinergic receptor (M_2), guanine nucleotide-binding proteins (G_s and G_k), cGMP-dependent protein kinase (G-kinase), cGMP-stimulated cAMP phosphodiesterase (cGMP-stimulated cAMP-PDE), nitric oxide synthase (NOS), nitric oxide (NO*) and soluble guanylyl cyclase (sGC). Activation and inhibition represented by (+) and (-) respectively.

Could a cGMP-stimulated electrical signal underlie vascular smooth muscle relaxation?

Recent molecular and electrophysiological evidence supports the supposition, that the characterised cNG channels expressed in SAN tissue are likely to be components of *direct* second messenger pathways, mediating vascular tone in response to humoral agents — mammalian SAN tissue is richly innervated by the coronary circulation. A cNG channel homologous to the cAMP-gated channel shown to be expressed in SAN tissue, has been cloned and functionally expressed from aorta [Biel *et al.*, 1993]. The absence of signals in Northern hybridisation studies suggested that the channel may be expressed only in specific cells of the aorta. In addition RT-PCR studies, following preliminary evidence for the existence of a previously-undescribed cNG conductance in porcine coronary arterial smooth muscle, has demonstrated the expression of a homologue of rscNGC 1 [J Boyle and C.F Ratcliffe, unpublished]. Electrophysiological experiments have also demonstrated the existence of a cGMP-stimulated conductance within cultured coronary endothelial cells [Seiss-Geuder *et al.*, 1993], however it is still to be determined whether cGMP was directly activating a channel-independently of G kinase.

It is known that a wide variety of humoral agents such as acetylcholine, bradykinin, substance P, atrial naturetic peptides (ANP) by acting on vascular endothelial cells can synthesize the labile chemical messenger NO^*, which as part of a signal transduction pathway activates a soluble guanylyl cyclase in the underlying smooth muscle. The subsequent rise in the intracellular concentration of cGMP is responsible for vascular smooth muscle relaxation and thereby vasodilation [reviewed by Knowles and Moncada, 1992]. The precise mechanisms of cGMP-induced relaxation remain largely unresolved but are thought to involve G-kinase reduction of cytosolic calcium [reviewed by Lincoln and Cornwell, 1993].

What could be the functional role of cNG channels in vasculature? The demonstration that ANP depolarises confluent monolayers of cultured coronary endothelium [Seiss-Geuder *et al.*, 1993] raises the possibility that receptors for naturetic peptides may be *directly* coupled to cNG channels within endothelial cells (Figure 7.2(a)). Naturetic membrane receptors

contain a transmembrane domain contiguous with a carboxy-terminal intracellular guanylyl cyclase [reviewed by Yuen and Garbers, 1992], leading to agonist-induced cGMP synthesis. Direct ANP receptor-cNG channel coupling would result in an influx of calcium ions through activated cNG channels. Such coupling within endothelial cells may have a physiological role in the formation of NO* by NOS, whose activity is entirely dependent on intracellular calcium concentrations within the range of 100-500 nM — this calcium-dependence appears to be mediated by calmodulin [Pollock *et al.*, 1991]. Thus cNG channels may be integral components in ANP-induced synthesis of the intercellular second messenger NO* within the endothelium (Figure 7.2(a)), leading to the subsequent relaxation of the underlying smooth muscle.

Recent data have indicated that modulation of smooth muscle channel components represented a key physiological mechanism by which cGMP causes smooth muscle relaxation. This raises the possibility that cNG channels may also represent end effector molecules for NO*-induced cGMP within smooth muscle cells. An *indirect* G kinase-dependent phosphorylation pathway has been shown to stimulate Ca^{2+}-activated K^+ channels (K^+_{Ca}) in coronary arterial smooth muscle cells [Taniguchi *et al.*, 1993]. Additionally, NO has been demonstrated to directly activate K^+_{Ca} independently of cGMP [Bolotina *et al.*, 1994] (Figure 7.2(b)). It is reasoned that the resulting membrane hyperpolarisation, by inhibiting Ca^{2+} influx through the closure of voltage-dependent calcium channels results in smooth muscle relaxation.

The mechanism(s) by which direct activation of cNG channels within smooth muscle may control relaxation remain speculative. Excessive activation of the NO* signal transduction pathway within vasculature can result in life-threatening vasodilation of endotoxic shock [Nathan, 1992]. A possible functional role of a cNG channel in smooth muscle cells could be in cellular processes controlling the sensitivity and response kinetics of the NO* signal transduction pathway (Figure 7.2(b)). Such 'adaptation' mediated by calcium influx through activated cNG channels, may be able to inhibit sGC activity by a mechanism analogous to rod photoreceptor cells, where calcium by binding to a regulatory protein, recoverin [Dizhoor *et al.*, 1991] is able to inhibit sGC activity [Koch and Stryer, 1988]. This 'negative' feedback pathway could form an important physiological

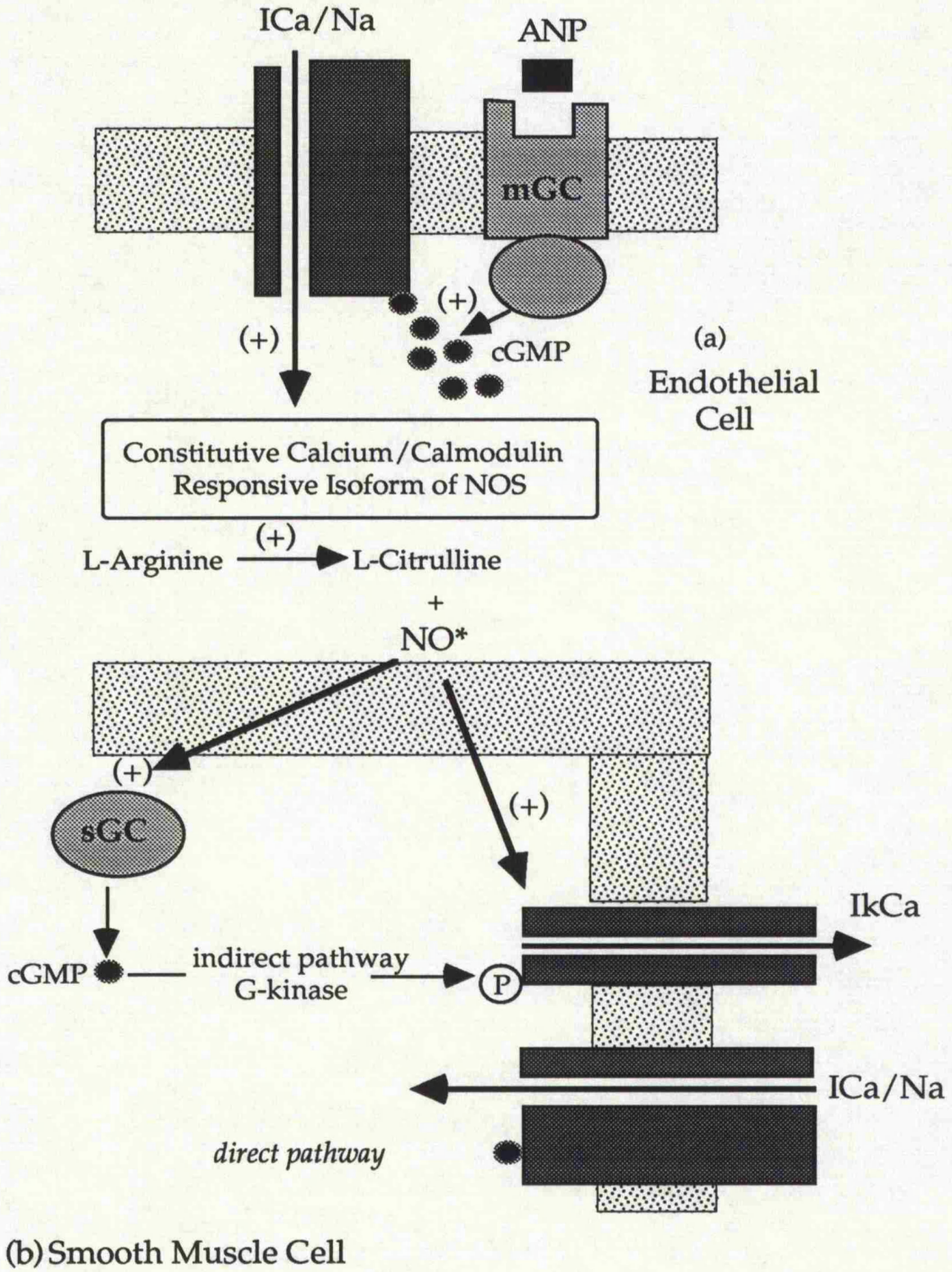

Figure 7.2 Schematic diagram outlining the 'possible' role of cyclic nucleotide-gated ic channels in processes governing vasodilation in (a) endothelial and (b) smooth muscle cells.

Abbreviations: Cyclic nucleotide-gated channel ($I_{Ca/Na}$), calcium-activated potassium channel (I_{kCa}), atrial naturetic peptide (ANP), cGMP-dependent protein kinase (G-kinas nitric oxide synthase (NOS), nitric oxide (NO*), membrane-bound guanylyl cyclase (mG(and soluble guanylyl cyclase (sGC). Activation and inhibition represented by (+) and (-) respectively.

mechanism by which cNG channels prevent chronic vasodilation. Whether such an adaptive mechanism consisting of molecular components found in photoreceptor cells is conserved within smooth muscle awaits further molecular studies.

It is expected that the future employment of immunocytochemical techniques, in parallel with electrophysiological studies on isolated cells from native SAN tissue will determine the specific cellular location of cNG channels. Such studies particularly within vasculature, are essential in the elucidation of the function of SAN cNG channels.

Perspective

The results presented within this thesis have demonstrated the expression of a class of ion channels within the pacemaker region of the heart, which were previously thought to be solely expressed within mammalian sensory tissues. Over the course of this thesis molecular cloning has demonstrated the expression of distinct cNG channel genes in additional non-sensory tissues. It is expected that new family members await cloning and characterisation from further non-sensory tissues. However, answers to questions concerning the regulation of tissue-specific expression, and more fundamentally the functional roles of these channels in non-sensory tissues, have lagged behind their cloning. It is hoped that future molecular and electrophysiological studies will address the precise interactions that co-ordinate the diverse functions of cNG channels in cell physiology.

Bibliography

Adams, M. D., Kelley, J.M., Gocayne, J.D., Dubnick, M., Polymeropoulos, M.H, Hong, X., Merril, C.R., Wu, A., Olde, B., Moreno, R.F., Kerlavage, A.R., McCombie, R.W., and Venter, J.C. (1991). Complementary DNA sequencing: expressed sequence tags and human genome project. Science *252*, 1651-1656.

Ahmad, I., Korbmacher, C., Segal, A.S, Cheung, P., Boulpaep, E.L. and Barnstable, C.J. (1992). Mouse cortical collecting duct cells show non-selective cation channel activity and express a gene related to the cGMP-gated rod photoreceptor channel. Proc. Natl. Acad. Sci. USA *89*, 10262-10266.

Ahmad, I., Leinders-Zufall, T., Kocsis, J.D., Shepherd, G.M, Zufall, F and Barnstable, C.J. (1994). Retinal ganglion cells express a cGMP-gated cation conductance activatable by nitric oxide donors. Neuron *12*, 155-165.

Altenhoffen, W., Ludwig, J., Eismann, E., Kraus, W., Bonigk, W., and Kaupp, U.B. (1991). Control of ligand specificity in cyclic nucleotide-gated channels from rod photoreceptors and olfactory epithelium. Proc. Natl. Acad. Sci. USA *88*, 9868-9872.

Anderson, J. A., Best, L.A and Gaber, R.F. (1991). Structural and functional conservation between the high-affinity K^+ transporters of *Saccharomyces uvarum* and *Sacchaomyces cerevisiae*. Gene *99*, 39-46.

Anderson, J. A., Huprikar, S.S., Kochian L.V., Lucas, W.J and Gaber, R.F. (1992). Functional expression of a probable *Arabidopsis thaliana* potassium channel in *Saccharomyces cerevisiae*. Proc. Natl. Acad. Sci. USA *89*, 3736-3740.

Atkinson, N. S., Robertson, G.A., and Ganetzky, B. (1991). A component of calcium-activated potassium channels encoded by the *Drosophila slo* locus. Science *253*, 551-555.

Bahnson, T. D., Pandol, S.J., and Dionne, V.E. (1993). Cyclic GMP modulates depletion-activated Ca^{2+} entry in pancreatic acinar celis. J. Biol. Chem. *268*, 10808-10812.

Balligand, J.-L., Kelly, R,A., Marsden, P.A., Smith, T.W., and Michei, T. (1993). Control of cardiac muscle cell function by an endogenous nitric oxide signalling system. Proc. Nati. Acad. Sci. USA *90*, 347-351.

Barnard, E. A. (1992). Receptor classes and the transmitter-gated ion channels. Trends Biol. Sci. *17*, 368-373.

Biel, M., Altenhfen, W., Hullin, R., Ludwig, J., Freichel, M., Flockerzi, V., Dascal, D., Kaupp, B.U. and Hofmann, F. (1993). Primary structure and functional expression of a cyclic nucleotide-gated channel from rabbit aorta. FEBS Lett. *329*, 134-138.

Biel, M., Zong, X., Distler, M., Bosse, E., Klugbauer, N., Murakami, M., Flockerzi, V., and Hofmann, F. (1994). Another member of the cyclic nucleotide-gated channel family, expressed in testis, kidney, and heart. Proc. Natl. Acad. Sci. USA *91*, 3505-3509.

Birnbaumer, L., Abramowitz, J., and Brown, A.M. (1990). Receptor-effector coupling by G proteins. Biochim. Biophys. Acta. *1031*, 163-224.

Blom van Assendelft, G., Hanscombe, O., Grosveld, F., and Greaves, D.R. (1989). The β-globin dominant control region activates homologous and heterologous promoters in a tissue-specific manner. Cell *56*, 969-977.

Bolotina, V. M., Najibi, S., Palacino, J.J., Pagano., and Cohen, R.A. (1994). Nitric oxide directly activates calcium-dependent potassium channels in vascular smooth muscle. Nature *368*, 850-853.

Bonigk, W., Altenhofen, W., Muller, F., Dose, A., Illing, M,. Molday, R.S. and Kaupp, B.U. (1993). Rod and cone photoreceptor cells express distinct genes for cGMP-gated channels. Neuron *10*, 865-877.

Bonner, T. I., Buckley, N.J., Young, A.C., and Brann, M.R. (1987). Identification of a family of muscarinic acetylcholine receptor genes. Science *237*, 527-532.

Brown, A. M., and Birnbaumer, L. (1988). Direct G protein gating of ion channels. Amer. J. Physiol. *252*, H1235-42.

Brown, H. F., and Denyer, J.C. (1988). Low-dose acetylcholine reduces calcium current in isolated sino-atrial node cells of rabbit. J. Physioi. *410*, 65P.

Brown, A. M. (1990). Regulation of heartbeat by G protein-coupled ion channels. Amer. J. Physiol. *259*, H1621-H1628.

Brown, A. M. (1991). A cellular logic for G protein-coupled ion channel pathways. FASEB J. *5*, 2175-2179.

Brown, A. M. (1991). Membrane-delimited cell signalling complexes: direct ion channel regulation by G proteins. J. Membrane Bioi. *131*, 93-104.

Bruggemann, A., Pardo, L.A., Stuhmer, W. and Pongs, O. (1993). *Ether-a-go-go* encodes a voltage-gated channel permeable to K^+ and Ca^+ and modulated by cAMP. Nature *365*, 445-448.

Campbell, D. L., and Giles, W.R. (1990). Calcium currents. New York: Raven.

Campbell, D. L., Rasmusson, R.L., and Strauss, H.C. (1991). Ionic and cellular mechanisms underlying primary cardiac pacemaker activity. New York: Dekker.

Campbell, D. L., Rasmusson, R.L., and Strauss, H.C. (1992). Ionic current mechanisms generating vertebrate primary cardiac pacemaker activity at the single cell level: an integrative view. Annu. Rev. Physiol. *54*, 279-302.

Casey, J., and Davidson, N. (1977). Rates of formation and thermal stabilities of RNA:DNA and DNA:DNA duplexes at high concentrations of formamide. Nucleic Acids Res. *4*, 1539.

Catterall, W. A. (1988). Structure and function of voltage-sensing ion channels. Science *242*, 50-61.

Chang, F., Gao, J., Tromba, C., Cohen, I.S., and DiFrancesco, D. (1990). Acetylcholine reverses effects on β-agonists on pacemaker current in canine Purkinje fibers but has no direct action. A difference between primary and secondary pacemakers. Circulation Res. *66*, 633-636.

Chang, F., Cohen, I.S., DiFrancesco, D., Rosen, M.R., and Tromba, C. (1991). Effects of protein kinase inhibitors on canine Purkinje fiber pacemaker depolarization and the pacemaker current I_f. J. Physioi. *440*, 367-384.

Chang, F., and Cohen, i.S. (1992). Mechanism of acetylcholine action on pacemaker current (I_f) in canine Purkinje fibers. Pflugers Arch. *420*, 389-392.

Chen, T.-Y., Peng, T-W., Dhallan, R.S., Reed, R.R., and Yau, K-W. (1993). A new subunit of the cyclic nucleotide-gated cation channel in retinal rods. Nature *362*, 764-767.

Church, G. M. a. G., W. (1984). Genomic sequencing. Proc. Natl. Acad. Sci. USA *81*, 1991-1995.

Collis, P., Antoniou, M., and Grosveld, F. (1990). Definition of the minimal requirements within the human β–globin gene and the dominant control region for high level expression. EMBO J. *9*, 233-240.

Cook, N. J., Hanke, W., and Kaupp, U.B. (1987). Identification, purification, and functional reconstitution of the cyclic GMP-dependent channel from rod photoreceptors. Proc. Natl. Acad. Sci. USA *84*, 585-589.

Cook, N. J., Moiday, L.L., Reid, D., Kaupp, B.U., and Molday, R.S. (1989). The cGMP-gated channel of bovine rod photoreceptors is localized exclusively in the plasma membrane. J. Biol. Chem. *264*, 6996-6999.

Covarrubias, M., Wei, A.A., and Salkoff, L. (1991). *Shaker, Shal, Shab,* and *Shaw* express independent K^+ current systems. Neuron *7*, 763-773.

De Wet, J. R., Wood, K,V., DeLuca, M., Helinski, D.R., and Subramani, S. (1987). Firefiy iuciferase gene: structure and expression in mammalian cells. Mol. Cell. Biol. *7*, 725-737.

Delgado, R., Hidalgo, P., Diaz, F., Latorre, R., and Labarca, P. (1991). A cyclic AMP-activated K+ channel in *Drosophila* larval muscle is persistentiy activated in *dunce*. Proc. Natl. Acad. Sci. USA *88*, 557-560.

Denyer, J. C., and Brown, H.F. (1990). Pacemaking in rabbit isolated sino-atrial node cells during Cs^+ block of the hyperpolarization-activated current I_f. J. Physiol. *429*, 401-409.

Dhallan, R. S., Yau, K., Schrader, K., and Reed, R. (1990). Primary structure and

functional expression of a cyclic nucleotide-activated channel from olfactory neurons. Nature *347*, 184-187.

Dhallan, R. S., Macke, J.P, Eddy, R.L, Shows, T.B, Reed, R.R, Yau, K-W. and Nathans, J. (1992). Human rod photoreceptor cGMP-gated channel: amino-acid sequence, gene structure, and functional expression. J Neurosci. *12*, 3248-3256.

DiFrancesco, D. (1985). The cardiac hyperpolarizing-activated current, I_f: origins and develoments. Prog. Biophys. Molec. Bioi. *46*, 163-183.

DiFrancesco, D. (1986(b)). Characterization of singie pacemaker channels in cardiac sino-atrial node cells. Nature *324*, 470-473.

DiFrancesco, D., Ferroni, A., Mazzanti, M., and Tromba, C. (1986(b)). Properties of the hyperpolarization-activated current (I_f) in cells isolated from the rabbit sino-atrial node. J. Physiol. *377*, 61-88.

DiFrancesco, D., and Tromba, C. (1988). Muscarinic control of the hyperpolarization-activated current (i_f) in rabbit sino-atrial node myocytes. J. Physiol. *405*, 493-510.

DiFrancesco, D., and Tromba, C. (1988(a)). Inhibition of the hyperpolarization-activated current (I_f) induced by acetylcholine in rabbit sino-atrial node myocytes. J. Physiol. *405*, 477-491.

DiFrancesco, D., Ducouret, P., and Robinson, R.B. (1989). Muscarinic modulation of cardiac rate at low acetylcholine concentrations. Science *243*, 669-671.

DiFrancesco, D., and Noble, D. (1989). Current I_f and its contribution to cardiac pacemaking. New York: Dekker New York.

DiFrancesco, D., and Tortora, P. (1991). Direct activation of cardiac pacemaker channels by intracellular cyclic AMP. Nature *351*, 145-147.

DiFrancesco, D. (1991). Generation and control of cardiac pacing-the pacemaker current. Trends Cardiovasc. Med. *1*, 250-255.

Dizhoor, A. M., Ray, S., Kumar, S., Niemi, G., and Spencer, M. (1991). Recoverin: A calcium sensitive activator of retinal rod guanylate cyclase. Science *251*, 915-918.

Dmitrovsky, E., Kuehl, W.M., Hollis, G.F., Kirsch, I.R., Bender, T.P., and Segal, S. (1986). Nature *322*, 748-750.

Doerr, T., and Trautwein, W. (1990). On the mechanism of the "specific bradycardic action" of the verapamil derivative UL-FS 49. Arch. Pharmacoi. *341*, 331-340.

Dryer, S. E., and Henderson, D. (1991). A cyclic GMP-activated channel in dissociated cells

of the chick pineal gland. Nature *353*, 756-758.

Dumas, J. B., Edwards, M., Delort, J., and Mallet, J. (1991). Nucleic Acids. Res. *19*, 5227-5232.

Egan, T. M., Noble, D., Noble, S. J., Powell, T. and Twist, V. W. (1987). An isoprenaline activated sodium-dependent inward current in ventricular myocytes. Nature *328*, 634-7.

Eismann, E., Bonigk, W., and Kaupp, B.U. (1993). Structural features of cyclic nucleotide-gated channels. Cell Physiol. Biochem. *3*, 332-351.

Feelish, M., and Noack, E.A. (1987). Correlation between nitric oxide formation during degradation of organic nitrates and activation of guanylate cyclase. Eur. J. Pharmacol. *139*, 19-30.

Feinberg, A. P., and Vogelstein, B. (1983). A technique for radiolabelling DNA restriction endonuclease fragments to high specific activity. Anal. Biochem. *132*, 6.

Feoktistov, I., and Biaggioni, I. (1993). Characterisation of adenosine receptors in human erythroleukaemia cells and platelets; further evidence for heterogeneity of adenosine A_2 receptor subtypes. Mol. Pharm. *43*, 909-914.

Frielle, T., Collins, S., Daniel, K.W., Caron, M.G., Lefkowitz, R.J., Kobilka, B.K. (1987). Cloning of the cDNA for the human β_1-adrenergic receptor. Proc. Natl. Acad. Sci. USA *84*, 7920-7924.

Friend, C., Scher, W., Holland, J.G., and Sako, T. (1971). Haemoglobin synthesis in murine virus-induced leukaemic cells *in vitro*: stimulation of erythroid differentiaton by dimethyl sulphoxide. Proc. Natl. Acad. Sci. USA *68*, 377-382.

Frohmam, M. A., Dush, M.K., and Martin, G.R. (1988). Rapid production of full-iength cDNAs from rare transcripts: Amplification using a single gene-specific oligonucleotide primer. Proc. Natl. Acad. Sci. USA *85*, 8998-9002.

George, W. J., Polson, J.B., O'Toole, A.G., and Goldberg, N. (1970). Elevation of 3', 5'-cyclic phosphate in rat heart after perfusion with acetylcholine. Proc. Natl. Acad. Sci. USA *66*, 398-403.

Giies, W. R., van Ginneken, A.C.G., and Shibata, E.F. (1986). ionic currents underlying pacemaker activity: A summary of voltage clamp data from single cells. Academic.

Gillo, B., Ma, Y-S., and Marks, A.R. (1993). Calcium influx in induced differentiation of murine erythroleukaemia cells. Blood *81*, 783-792.

Gilman, A. (1987). G proteins: transducers of receptor-generated signals. Annu. Rev. Biochem. *56*, 615-649.

Gocayne, J., Robinson, D.A., FitzGerald, M.G., Chung, F-Z., Kerlavage, A.R., Lentes, K-U., Lai, J., Wang, C-D., Fraser, C.M., and Venter, J.C. (1987). Primary structure of rat

cardiac β-adrenergic and muscarinic cholinergic receptors obtained by automated DNA sequence analysis: Further evidence for a multigene family. Proc. Natl. Acad. Sci. USA *84*, 8296-8300.

Gordon, S. E., Brautigan, D.L., and Zimmerman A.L. (1992). Protein phosphatases modulate the apparent agonist affinity of the light-regulated ion channel in retinal rods. Neuron *9*, 739-748.

Grosveld, F. G., Van Assendelft, G.B., Greaves, D.R., and Kollias, G. (1987). Position-independent, high-level expression of the human β-globin gene in transgenic mice. Cell *51*, 975-985.

Gubler, U., and Hoffman, B.J. (1983). A simple and very efficient method for generating cDNA libraries. Gene *25*, 263-269.

Guy, R. H., and Dureii, S.R. (1991). Similarities in amino acid sequences of *Drosophila eag* and cyclic nucleotide-gated channels. Science *252*, 730.

Hames, B. D., and Higgens, S.J. (1985). Nucleic acid hybridisation. (Oxford, England: IRL Press Limited).

Hamill, O. P., Marty, A., Neher, E., Sakmann, B., and Sigworth, F.J. (1981). Improved patch clamp techniques for high-resolution current recording from cell and cell-free membrane patches. Pflugers Arch. *391*, 85-100.

Hanke, W., Cook, N.J., and Kaupp, B.U. (1988). cGMP-dependent channel protein from photoreceptor membranes: single-channel activity of the purified and reconstituted protein. Proc. Natl. Acad. Sci. USA *85*, 94-98.

Hardie, R. C., and Minke, B. (1992). The *trp* gene is essential for a light-activated Ca^{2+} channel in *Drosophila* photoreceptors. Neuron *8*, 643-651.

Hartley, D. A., Preiss, A., and Artavanis-Tsakonas, S. (1990). A deduced gene product from the Drosophila neurogenic locus, *Enhancer of split*, shows homology to mammalian G-protein β-subunit. Cell *55*, 785-795.

Hartmann, H. A., Kirsch, G.E., Drewe, J.A., Tagliatela, M., Joho, R.H., and Brown, A.M. (1991). Exchange of conduction pathways between two related K^+ channels. Science *251*, 942-944.

Hartzell, C. H., and Fischmeister, R. (1986). Opposite effects of cyclic GMP and cyclic AMP on Ca^{2+} current in single heart cells. Nature *323*, 273-275.

Hartzell, H. C. (1988). Regulation of cardiac ion channels by catecholamines, acetylcholine and second messenger systems. Prog. Biophys. Moiec. Biol. *52*, 165-247.

Hartzell, C. H., Mery, P-F., Fischmeister, R., and Szabo., G. (1991). Sympathetic regulation of cardiac calcium current is due exclusively to cAMP-dependent

phosphorylation. Nature *351*, 573-576.

Haskill, S., Berg, A.A., Tompkins, S.M., Morris, J.S., Yurochko, A.D., Sampson-Johannes, A., Mondal, K., Ralph, P., and Baldwin, A.S. (1991). Characterisation of an immediate-early gene induced in adherent monocytes that encodes IκB-like activity. Cell *65*, 1281-1289.

Haynes, L. W., Kay, A.R., and Yau, K-W. (1986). Single cyclic GMP-activated channel activity patches of rod outer segment membranes. Nature *321*, 66-70.

Haynes, L. W. (1992). Block of the cyclic GMP-gated channel of vertebrate rod and cone photoreceptors by *l-cis*-diltiazem. J. Gen. Physiol. *100*, 783-801.

Heginbotham, L., Abramson, T., and MacKinnon, R.A. (1992). A functional connection between the pores of distantly related ion channels as revealed by mutant potassium channels. Science *251*, 1152-1155.

Hille, B. (1991). Ionic Channels of Excitable Membranes. Sunderland, Massachusettes: Sinauer Associates.

Himmler, A., Stratowa, C., and Czernilofsky, A.P. (1993). Functional testing of human dopamine D1 and D5 receptors expressed in stable cAMP-responsive luciferase reporter ceii lines. Journal of Receptor Research *13*, 79-94.

Ho, K., Nichols, C.G., Lederer, W.J., Lytton, J., Vassilev, P.M., Kanazirska, M.V., and Hebert, S.C. (1993). Cloning and expression of an inwardly rectifying ATP-regulated potassium channel. Nature *362*, 31-38.

Hoshi, T., Zagotta, W.N., and Aldrich, R.W. (1990). Biophysical and molecular mechanisms of shaker potassium channel inactivation. Science *250*, 533-538.

Hoshi, T., and Zagotta, W.N. (1993). Recent advances in the understanding of potassium channel function. Current Opinion in Neurobiology *3*, 283-290.

Hsu, Y.-T., and Molday, R.S. (1993). Modulation of the cGMP-gated channel of rod photoreceptor cells by calmodulin. Nature *361*, 76-79.

Hubbard, S., and Ivatt, R. (1981). Synthesis and processing of asparagine-linked oligosaccharides. Annu. Rev. Biochem. *50*, 555-583.

Hundal, S. P. S., DiFrancesco, D., Mangoni, M., Brammar, W.J., and Conley, E.C. (1993). An isoform of the cGMP-gated retinal photoreceptor channel gene expressed in the sino-atrial node (pacemaker) region of rabbit heart. Biochemical Society Transactions *21*, 119.

Hutter, O. F., and Trautwein, W. (1956). Vagal and sympathetic effects on the pacemaker fibers in the sinus venosus of the heart. J. Gen. Physiol. *39*, 715-733.

Ijzerman, A., and Van Galen, P. (1990). Pharmacology of purinergic receptors: implications for drug design. Trends Pharm. Sci. *11*, 342-343.

Imoto, K. (1993). Ion channels: molecular basis of ion selectivity. FEBS Lett. *325*, 100-103.

Irisawa, H. (1987). Membrane currents in cardiac pacemaker tissue. Experientia *43*, 1131-1140.

Irisawa, H., and Hagiwara, N. (1991). ionic current in sinoatrial node cells. J. Cardiovasc. Electrophysiol. *2*, 531-540.

irisawa, H., Brown, H.F., and Giles, W. (1993). Cardiac pacemaking in the sinoatrial node. Physiological Reviews *73*, 197-225.

Jan, L. Y., and Jan, Y.N. (1990). A superfamily of ion channels. Nature *345*, 672.

Jan, L., and Jan, Y N. (1992). Tracing the roots of ion channels. Cell *69*, 715-718.

Kabat, D., Sherton, C.C., Evans, L.H., Bigley, R., and Koler, R.D. (1975). Synthesis of erythrocyte-specific proteins in cultured Friend leukaemia cells. Cell *5*, 331-338.

Kamb, A., Tseng-Crank, J., and Tanouye, M.A. (1988). Multiple products of the *Drosophila Shaker* gene may contribute to potassium channel diversity. Neuron *1*, 421-430.

Kameyama, M., Hofmann, F., and Trautwein, W. (1985). On the mechanisms of β-adrenergic regulation of the Ca channel in the guinea-pig heart. Pflugers Arch. *407*, 123-128.

Kaupp, B. U., Niidome, T., Tanabe, T., Terada, S., Bonigk, W., Suhmer, W., Cook, N., Kangawa, K., Matsuo, H., Hirose, T., and Numa, S. (1989). Primary structure and functional expression from complementary DNA of the rod photoreceptor cyclic GMP-gated channel. Nature *342*, 762-766.

Kaupp, U. B. (1991). The cyclic nucleotide-gated channels of vertebrate photoreceptors and olfactory epithelium. Trends Neuro. Sci. *14*, 150-157.

Kaupp, U. B., and Koch, K.W. (1992). Role of cGMP and calcium in vertebrate photoreceptor excitation and adaptation. Annu. Rev. Physiol. *54*, 153-175.

Khan, A. S., Wilcox, A.S., Polymeroopoulos, M.H., Hopkins, J.A., Stevens, T.J., Robinson, M., Orpana, A.K., and Sikeia, J.M. (1992). Single pass sequencing and physical and genetic mapping of hunam brain cDNAs. Nature Genetics *2*, 180-186.

Kirsch, G. E., and Brown, A.M. (1989). Trypsin activation of atrial muscarinic K^+ channels. Am. J. Physiol. *257*, H334-H338.

Knowles, R. G., and Moncada, S. (1992). Nitric oxide as a signal in blood vessels. Trends Biol. Sci. *17*, 399-402.

Koch, K.-W., and Stryer, L. (1988). Highly cooperative feedback control of retinal rod

guanylate cyclase by calcium ions. Nature *334*, 64-66.

Kolesnikov, S. S., Rebrik, T.I., Zhinazarov, A.B., Tavartkiladze, G.A., and Kalamkarov, G.R. (1991). A cyclic-AMP-gated conductance in cochlear hair cells. FEBS Lett. *290*, 167-170.

Koob, R., Zimmermann, M., Schoner, W., and Drenckhahn, D. (1988). Eur. J. Cell Biol. *45*, 230-237.

Kozak, M. (1991). Structural features in eukaryotic mRNAs that modulate the initiation of translation. J. Biol. Chem. *266*, 19867-19870.

Kramer, R. H. (1990). Patch cramming: monitoring intracelluar messengers in intact cells with membrane patches containing detector ion channels. Neuron *2*, 335-341.

Krebs, E., and Beavo, J. (1979). Phosphorylation-dephosphorylation of enzymes. Annu. Rev. Biochem. *48*, 923-959.

Kubo, Y., Baldwin, T.J., Jan, Y.N., and Jan, L.Y. (1993). Primary structure and functional expression of a mouse inward rectifier potassium channel. Nature *362*, 127-133.

Kumar, V. D., and Weber, I.T. (1992). Molecular model of the cyclic GMP-binding domain of the cyclic GMP-gated ion channel. Biochemistry, 4643-4669.

Lefkowitz, R. J., and Caron, M.G. (1988). Adrenergic receptors: models for the study of receptors coupled to guanine nucleotide regulatory proteins. J. Bioi. Chem. *263*, 4993-4996.

Lester, H. A. (1988). Heterologous expression of excitability proteins: route to more specific drugs? Science *241*, 1057-1063.

Li, M., Jan, Y.N., and Jan, L.Y. (1992). Specification of subunit assembly by the hydrophobic amino-terminal domain of the *Shaker* potassium channel. Science *267*, 1225-1230.

Libert, F., Parmentier, M., Lefort, A., Dinsart, C., Van Sande, J., Maenhaut, C., Simons, M-J., Dumont, J.E., and Vassart, G. (1989). Selective amplification and cloning of four new members of the G protein-coupled receptor family. Science *244*, 569-572.

Light, D. B., Crbi, J.D., and Stanton, B.A. (1990). Dual ion-channel regulation by cyclic GMP and cyclic GMP-dependent protein kinase. Nature *344*, 336-339.

Lincoln, T. M., and Cornwell, T.L. (1993). FASEB J. *7*, 328-338.

Linden, J. (1991). Structure and function of A1 adenosine receptors. FASEB J. *5*, 2668-2676.

Lipman, D. J., and Pearson, W.R. (1985). Rapid and sensitive protein similarity searches. Science *227*, 1435-1440.

Lohmann, S. R., Fischmeister, R., and Walter, U. (1991). Signal transduction by cGMP in heart. Basic Res. Cardiol. *86*, 503-514.

Loveland, B. E., Wang, C.-R., Yonekawa, H., Hermal, E., and Fischer-Lindahl, K. (1990). Maternally transmitted histocompatibility antigen of mice: A hydrophobic peptide of a mitochondrially encoded protein. Cell *60*, 971-980.

Ludwig, J., Marglit, T., Eismann, E., Lancet, D., and Kaupp, B. (1990). Primary structure of a cAMP-gated channel from bovine olfactory epithelium. FEBS Lett. *270*, 24-29.

Lux, S. E., John, K.M., and Bennett, V. (1990). Analysis of cDNA for human erythrocyte ankyrin indicates a repeated structure with homology to tissue-differentiation and cell-cycle control proteins. Nature *344*, 36-42.

MacKinnon, R., and Yellen, G. (1990). Mutations affecting TEA blockade and ion permeation in voltage-activated K channels. Science *250*, 276-279.

MacKinnon, R. (1991). Determination of the subunit stoichiometry of a voltage-activated potassium channel. Nature *350*, 232-235.

Maenhaut, C., Van Sande, J., Libert, F., Abramowicz, M., Parmentier, M., Vanderhaegen, J-J., Dumont, J.E., Vassart, G., and Schiffman, S. (1990). RDC8 codes for an adenosine A2 receptor with physiological constitutive activity. Biochem. Biophys. Res. Comm. *173*, 1169-1178.

Maniatis, T., Fritsch, E.F., and Sambrook, J. (1982). Molecular Cloning: A Laboratory Manual. Cold Spring Harbor, New York: Cold Spring Harbor Laboratory. .

Matthews, G., and Watanabe, S-I. (1987). Properties of ion channels closed by light and opened by guanosine 3,5-cyclic monophosphate in toad retinal rods. J. Physiol. *389*, 691-715.

Mazzanti, M., and DiFrancesco, D. (1989). Intracellular Ca modulates K-inward rectification in cardiac myocytes [published erratum appears in Pflugers Arch 1989 Apr;413(6):688]. Pflugers Arch *413*, 322-4.

McKay, D. B., and Steitz, T.A. (1981). Structure of catabolite gene activator protein at 2.9 A resolution suggests binding to left-handed B-DNA. Nature *290*, 744-749.

Melton, D. A., Krieg, P.A., Rebagliati, M.R., Maniatis T., Zinn, K., and Green M.R. (1984). Efficient in vitro synthesis of biologically active RNA and RNA hybridisation probes from plasmids containing a bacteriophage SP6 promoter. Nucleic Acids Res. *12*, 7035.

Mery, P.-F., Lohmann, S.W., Walter, U., and Fischmeister, R. (1991). Ca^{2+} current is regulated by cyclic GMP-dependent protein kinase in mammalian cardiac myocytes. Proc. Natl. Acad. Sci. USA *88*, 1197-1201.

Mileham, K. A., Northover, B.J., Winter, A.W., Hundal, S.P.S., Brammar, W.J., and Conley, E.C. (1994). Competitive titration for probing low-abundance ion channel mRNA molecules

in normal and regionally-ischaemic heart tissue. Molecular and Cellular Probes *8*, 161-176.

Miller, C. (1992). Hunting for the pore of voltage-gated channels. Curr. Opin. Biol. *2*, 573-575.

Molday, L. L., Cook, N.J., kaupp, B.U., and Molday, R.S. (1990). The cGMP-gated cation channel of bovine rod photoreceptor cells is associated with a 240-kDa protein exhibiting immunochemical cross-reactivity with spectrin. J. Biol. Chem *265*, 18690-18695.

Molday, R. S., Molday, L.L., Dose, A., Clark-Lewis, I., Illing, M., Cook, N.J., Eismann, E., and Kaupp B.U. (1991). The cGMP-gated channel of the rod photoreceptor cell characterisation and orientation of the amino terminus. J. Biol. Chem. *266*, 21917-21922.

Montminy, M. R., Gonzalez, G.A., and Yamamoto., K.K. (1990). Regulation of cAMP-inducible genes by CREB. Trends Neuro. Sci. *13*, 184-188.

Murray, R., Furci, L., and FitzGerald, G.A. (1989). Induction of prostacyclin receptor expression in human erythroleukeamia cells. FEBS Lett. *255*, 172-174.

Nakamura, T., and Gold, G.H. (1987). A cyclic nucleotide-gated conductance in olfactory receptor cilia. Nature *325*, 342-344.

Nathan, R. D. (1986). Two electrophysiologically distinct types of cultured pacemaker cells from rabbit sinoatrial mode. Am. J. Physiol. *250*, H325-329.

Nathan, C. (1992). FASEB J. *6*, 3051-3064.

Nathanson, N. M. (1987). Molecular properties of the muscarinic receptor. Annu. Rev. Neurosci. *10*, 195-236.

Nawy, S., and Jahr, C.E. (1990). Suppression by glutamate of cGMP-activated conductance in retinal bipolar cells. Nature *346*, 269-271.

Needham, M., Gooding, C., Hudson, K., Antoniou, M., Grosveld, F., and Hollis, M. (1992). LCR/MEL: A versatile system for the high-level expression of heterologous proteins in erythroid cells. Nucl. Acids. Res. *20*, 997-1003.

Nizzari, M., Sesti, F., Giraudo, M.T., Virginio, C., Cattanaeo, A., and Torre,V. (1993). Single-channel properties of cloned cGMP-activated channels from retinal rods. Proc. R. Soc. Lond. B *254*, 69-74.

Noda, M., Furutani, Y., Takahashi, H., Toyosato, M., Tanabe, T., Shimizu, S., Kikyotani, S., Kayano, T., Hirose, T., Inayama, S., and Numa, S. (1983). Cloning and sequence analysis of calf cDNA and human genomic DNA encoding α-subunit precursor of muscle acetylcholine receptor. Nature *305*, 818-823.

Noma, A. (1983). ATP-reguiated K^+ channels in cardiac muscle. Nature *305*, 147-148.

Numa, S. (1989). A molecular view of neurotransmitter receptors and ionic channels. Harvey Lect. *83*, 121-165.

Papazian, D. M., Schwartz, T.L., Tempel, B.L., Jan, Y.N., and Jan, L.Y. (1987). Cloning of genomic and complementary DNA from *Shaker,* a putative potassium channel gene from *Drosophila*. Science *237*, 749-753.

Papazian, D. M., Timpe, L.C., Han, Y.N., and Jan, L.Y. (1991). Alteration of voltage-dependence of *Shaker* potassium channel by mutations in the S4 sequence. Nature *349*, 305-310.

Partridge, L. D., and Swandulla, D. (1988). Calcium-activated non-specific cation channels. Trends Neuro. Sci *11*, 69-72.

Peralta, E. G., Winslow, J.W., Peterson, G.L., Smith, D.H., Ashkenazi, A., Ramachandran. J., Schimerlik, M.i., and Capon, D.J. (1987). Primary structure and biochemical properties of an M2 muscarinic receptor. Science *236*, 600-605.

Phillips, A. M., Bull, A., and Kelly, L.E. (1992). Identification of a *Drosophila* gene encoding a caimodulin-binding protein with homology to the *trp* phototransduction gene. Neuron *8*, 631-642.

Pilz, R. B., Eigenthaler, M., and Boss, G.R. (1992). Chemically induced murine erythroleukaemia ceii differentiation is severely impaired when cAMP-dependent protein kinase activity is repressed by transfected genes. J. Biol. Chem. *267*, 16161-16167.

Pittler, S. J., Lee, A.K., Altherr, M.R., Howard, T.A., Seldin, M.F., Hurwitz, R.L., Wasmuth, J.J., and Baehr, W. (1992). Primary structure and chromosomal location of human and mouse rod photoreceptor cGMP-gated cation channel. J. Biol. Chem. *267*, 6257-6262.

Pollack, J. S., Forstermann, U., Mitchell, J.A., Warner, T.D., Schmidt, H.W., Nakane, M., and Murad, F. (1991). Proc. Natl. Acad. Sci. USA *88*, 10480-10484.

Pongs, O., Kecskemethy, N., Müiier, R., Krah-Jentgens, I., Baumann, A., Klitz, H.H., Canal, I., Llamazares, S., and Ferrus, A. (1988). *Shaker* encodes a family of putative potassium channel proteins in the nervous system of *Drosophila*. Embo J *7*, 1087-1096.

Ranganathan, R. (1994). Evolutionary origins of ion channels. Proc. Natl. Acad. Sci. USA *91*, 3484-3486.

Rasmusson, R. L., Clark, J.W., Giles, W.R., Robinson, K., and Clark, R.B. (1990). A mathematical model of electrophysiological activity in a bullforg atrial cell. Am. J. Physiol. *259*, H370-H389.

Rasmusson, R. L., Clark, J.W., Giles, W.R., Shibata, E.F., and Campbell, D.L. (1990). A mathematical model of a bull-frog cardiac pacemaker ceii. Am. J. Physioi. *259*, H352-H369.

Rettig, J., Wunder, F., Stocker, M., Lichtinghagen, R., Mastiaux, F., Beckh, S., Kues, W., Pedarzani, P., Schroter, K.H., Ruppersberg, J.P., Veh, R., and Pongs, O. (1992). Characterisation of a *Shaw*-related potassium channel family in rat brain. Embo. J. *11*, 2473-2486.

Root, M., and Mackinnon, R. (1993). Divalent cation block is affected by mutations of an acidic residue in the pore region of cGMP-gated channels (abstract). Biophys. J. *64*, A16.

Rosen, M. R., Janse, M.J., and Wit, A.L. (Ed.). (1990). Cardiac Electrophysiology: A Textbook. Mount Kisco, New York: Futura.

Ruiz, M. L., London, B., Logothetis, D., and Nadal-Ginard, B. (1993). Molecular cloning of a cyclic-nucleotide gated channel from mouse heart. Biophys. J. *64*, A208.

Sackmann, B., Noma, A., and Trautwein, W. (1983). Acetylcholine activation of singie muscarinic K channels in isolated pacemaker cells of the mammalian heart. Nature *303*, 250-253.

Sanguinetti, M. C., and Jurkiewicz, A. (1990). Two components of cardiac delayed rectifier K^+ current. Differential sensitivity to block by class III anti-arrhythmic agents. J. Gen. Physiol. *96*, 195-215.

Schachtman, D. P., Schroeder, J.I, Lucas, W.J., Anderson, J.A., and Gaber, R.F. (1992). Expression of an inward-rectifying potassium channei by the *Arabidopsis* KAT1 cDNA. Science *258*, 1654-1657.

Schubert, B., VanDongen, A.M.J., Kirsch, G.E., and Brown, A.M. (1989). β-adrenergic inhibition of cardiac sodium channeis by dual G protein pathways. Science *245*, 516-519.

Schubert, B., VanDongen, A.M.J., Kirsch, G.E., and Brown, A.M. (1990). Inhibition of cardiac Na^+ currents by isoproterenol. Am. J. Physiol. *258*, H977-H982.

Schwarz, T. L., Tempel, D.M., Papazian, D.M., Jan, Y.N., and Jan, L.Y. (1988). Multiple potassium-channel components are produced by alternative splicing at the *Shaker* locus in *Drosophila*. Nature *331*, 137-142.

Seiss-Geuder, M., Mehrke, G and Daut, J. (1993). Atrial natriuretic peptide depoiarises confluent monolayers of cultured coronary endothelium. Pfluggers Arch. *422 Suppl. 1*, R118.

Sentenac, H., Bonneaud, N., Minet, M., Lacroute, F., Salmon, J-M., Gaymard, F., and Grigon, C. (1992). Cloning and expression in yeast of a plant potasssium ion transport system. Science *256*, 663-665.

Shabb, J. B., and Corbin, J.D. (1992). Cyciic nucleotide-binding domains in proteins having diverse functions. J. Biol. Chem. *267*, 5723-5726.

Shelton, P. A., Davies, N.W., Antoniou, M., Grosveld, F., Needham, M., Hollis, M., Brammar, W.J., and Coniey, E.C. (1993). Regulated expression of K+ channel genes in electrically

silent mammalian cells by linkage to β-globin gene-activation elements. Receptors and Channels. *1*, 25-37.

Shibasaki, T. (1987). Conductance and kinetics of delayed rectifier potassium channels in nodal cells of the rabbit heart. J. Physiol. *387*, 227-250.

Shibata, E. F., Giles, W., Nakajima, T., and Ono, K. (1985). Modulation of the delayed rectifier K+ current by isoprenaline in buii-frog atrial myocytes. J Physiol Lond *415*, 233-49.

Shimomura, H., and Terada, A. (1990). Primary structure of the rat beta-1 adrenergic receptor gene. Nucleic Acids. Res. *18*, 4591.

Soreq, H., and Seidman, S. (1992). Xenopus oocyte microinjection: from gene to protein. Methods in Enzymoiogy *207*, 225-266.

Srinivasan, Y., Elmer, L., Davis, J., Bennett, V., and Angelides, K. (1988). Ankyrin and spectrin associate with voltage-dependent sodium channeis in brain. Nature *333*, 177-180.

Starr, T. V. B., Prystay, W., and Snutch, T.P. (1991). Primary structure of a calcium channei that is highly expressed in the rat cerebellum. Proc. Natl. Acad. Sci. USA *88*, 5621-5625.

Sumikawa, K., and Miledi, R. (1989). Mol. Brian Res. *5*, 183.

Sussman, M. R. (1992). Shaking *Arabidopsis* thaiiana. Science *256*, 619-620.

Swanson, R., and Folander, K. (1992). In vitro synthesis of RNA for expression of ion channels in xenopus oocytes. Methods in Enzymology *207*, 310-317.

Takio, K., Wade, R.D., Smith, S.B., Krebs, E.G., Walsh, K.A., and Titani, K. (1984). Biochemistry *23*, 4207-4218.

Taibot, D., Collis, P., Antoniou, M., Vidal, M., Grosveld, F., and Greaves, G.R. (1989). A dominant control region from the human β-globin locus conferring integration site-independent gene expression. Nature *338*, 352-355.

Taniguchi, J., Furukawa, K-I., and Shigekawa, M. (1993). Maxi K^+ channeis are stimulated by cyclic guanosine monophosphate-dependent protein kinase in canine coronary artery smooth muscie ceils. Pflugers Arch. *423*, 167-172.

Teresaki, W. L., and Brooker, G. (1977). J. Biol. Chem. *250*, 1041-1050.

Torre, V., Straforini, M., Sesti, F., and Lamb, T.D. (1992). Different channel-gating properties of two ciasses of cyclic GMP-activated channel in vertebrate photoreceptors. Proc. R. Soc. Lond. B. *250*, 209-215.

Trautwein, W., Noma, A., and Peper, K. (1981). Ref for IKACh in pacemaker cells slowing the heartbeat. Pflügers Arch Ges Physiol *381*, 255-262.

Trautwein, W., and Hescheler, J. (1990). Regulation of cardiac L-type calcium current by phosphorylation and G proteins. Annu. Rev. Physiol. *52*, 257-274.

Van Boagaert, P., Goethals, M., and Simoens, C. (1990). Use-and frequency-dependent blockade by UL FS 49 of the I_f pacemaker current in sheep cardiac Purkinje fibres. Eur. J. Pharmacol. *187*, 241-256.

Walsh, K. B. a. K., R. S. (1988). Regulation of a heart potassium channel by protein kinase A and C. Science *242*, 67-9.

Warmke, J., Drysdale, R., and Ganetzky B. (1991). A distinct potassium channel polypeptide encoded by the *Drosophila eag* locus. Science *252*, 1560-1562.

Weber, I. T., and Steitz, T.A. (1987). Structure of a complex of catabolite gene activator protein and cyclic AMP refined at 2.5 A resolution. J. Mol. Biol. *198*, 311-326.

Weber, I. T., Steitz, T.A., Bubis, J., and Taylor, S.S. (1987). Predicted structures of cAMP binding domains of type I and II regulatory cAMP-dependent protein kinase. Biochemistry *26*, 343-351.

Weber, I. T., Shabb, J.B., and Corbin, J.D. (1989). Predicted structures of the cGMP binding domains of the cGMP-dependent protein kinase; A key alanine/threonine difference in evolutionary divergence of cAMP and cGMP binding sites. Biochemistry *28*, 6122-6127.

Weyand, I., Godde, M., Frings, S., Weiner, J., Muller, F., Altenhofen, W., Hatt, H., and Kaupp B.U. (1994). Cloning and functional expression of a cyclic nucleotide-gated channel from mammalian sperm. Nature *368*, 859-863.

Wilbur, W. J., and Lipman, D.J. (1983). Rapid similarity searches of nucleic acid and protein databanks. Proc. Natl. Acad. Sci. USA *80*, 726-730.

Wohlfart, P., Muller, H., and Cook, N.J. (1989). J. Biol. Chem. *264*, 20934-20939.

Woodcock, D. M. (1989). Nucleic Acids. Res. *17*, 3469-3478.

Yatani, A., Codina, J., Imoto, Y., Reeves, J.P., Birnbaumer, L., and Brown, A.M. (1987). A G protein direcetly regulates mammalian cardiac calcium channels. Science *238*, 1288-1292.

Yatani, A., and Brown, A.M. (1989). Rapid β-adrenergic modulation of cardiac calcium channel currents by a fast G protein pathway. Science *245*, 71-74.

Yatani, A., Okabe, K., Codina, J., Birnbaumer, L., and Brown, A.M. (1990). Heart rate regulation by G proteins acting on the cardiac pacemaker channel. Science *249*, 1163-1166.

Yatani, A., and Brown, A.M. (1990). Regulation of cardiac pacemaker current I_f in excised membranes from sinoatrial node cells. Am. J. Physiol. *258*, H1947-H1951.

Yau, K.-W., and Baylor, D.A. (1989). Cyclic GMP-activated conductance of retinal photoreceptor cells. Annu. Rev. Neurosci. *12*, 289-327.

Yau, K.-W. (1994). Cyclic nucleotide-gated channels: An expanding new family of ion channels. Proc. Natl. Acad. Sci. USA *91*, 3481-3483.

Yellen, G., Jurman, M.E., Abramson, T., and MacKinnon, R. (1991). Mutations affecting internal TEA blockage identify the probable pore-forming region of a K channel. Science *251*, 939-944.

Yooi, A. J., and Schwarz, T.L. (1991). Alteration of ionic selectivity of a K^+ channel by mutation of the H5 region. Nature *349*, 700-704.

Yuen, P. S. T., and Garbers, D.L. (1992). Guanylyl cyclase-linked receptors. Annu. Rev. Neurosci. *15*, 193-225.